Luděk Berec

Mathematical modeling
in ecology and epidemiology

Habilitation thesis

Masaryk University, Faculty of Science, Brno

České Budějovice, July 2011

Typeset using the Springer svmono LaTeX class

Contents

Part III Infectious diseases and pest control

Chapter 1
Introduction

This thesis is about mathematical modeling of mostly animal populations. Therefore, it dwells at the interface of two fields: mathematics and biology (or more specifically population ecology). Coupled together, these fields provide the basis for the scientific discipline of mathematical biology (Murray, 1993; Case, 2000; Kot, 2001; Mangel, 2006). The primary aim of model development in population ecology is not to predict change of specific populations, but rather to provide general insight into how biological processes, often driven by individual behavior, affect population change over time. Information on these processes, or on behavior of individual population members, is collected through observations and carefully planned experiments. Mathematical models of population dynamics build on this empirical knowledge, attempt at linking such lower-level individual phenomena to upper-level population dynamics, help formulate ecological theories, and generate falsifiable hypotheses to be tested in the next round of empirical work (for a recent example, see Vercken et al, 2011). For a real progress to be made, empirical and mathematical approaches in biology have to be used complementarily.

The wealth of mathematical biology can also be seen on the journal market. A great many of articles published in biological journals use mathematics to help address their focal questions (e.g. Vercken et al, 2011). Conversely, a plenty of articles published in journals on applied mathematics use biology as a source of challenging nonlinear problems to solve (e.g. Sun and Saker, 2005). These two types of articles often meet in specialized journals on mathematical biology, such as Journal of Theoretical Biology, Bulletin of Mathematical Biology, Journal of Mathematical Biology, Ecological Modelling, Theoretical Population Biology, Mathematical Biosciences, Mathematical Medicine and Biology, and a recent newbie Theoretical Ecology. In addition, mathematically oriented biological papers are commonly accepted by general biological journals such as Ecology, Evolution, American Naturalist, and Oikos, and at times even by such world-leading scientific journals as Nature, Science, and PNAS. This only strengthens the role mathematics plays in current biology, not to speak of many textbooks and monographs on mathematical biology published by such world-leading scientific publishing houses as Oxford

University Press, Cambridge University Press, Springer, and Princeton University Press.

Mathematical models of population dynamics are often expressed in terms of differential or difference equations, which describe how populations change with time, space, or stage of development (Murray, 1993; Case, 2000; Kot, 2001; Mangel, 2006). Biological processes are, however, inherently complex. Given that mathematical models disconnected from biological reality are of a little use, this complexity has to show up in the models. Unfortunately, this is paid by the fact that although it is often not that complicated to write down an adequate system of dynamical equations, frequently it is virtually impossible to analyze such equations by standard mathematical methods, or at least not for the most part. Thus, formal analysis needs to often be complemented with numerical simulations or use of a numerical bifurcation tool that exemplify and often even reveal interesting, analytically intractable system behavior. Simulations can thus be incredibly helpful, allowing the reader to see what the equations predict and allowing the author to obtain results from even very complex models. On top of that, many models in current mathematical biology are by definition simulation models, consisting of a set of rules of how individuals behave and interact. This is in part because current ecology increasingly recognizes impacts of individual variability on population dynamics. These rules are repeatedly simulated for an ensemble of individuals with the aim to come up with dynamics of the population as a whole. Such models are often referred to as *individual-based models* (IBMs; e.g. Grimm and Railsback, 2005). Due to substantial complexity of IBMs, techniques have been developed that allow for approximating IBM dynamics by differential or difference equations, thus providing further insight into the systems under study (e.g. Dieckmann et al, 2000).

Inherent interdisciplinarity of mathematical biology necessarily brings about two contrasting approaches. On one hand, there are mathematicians that have a taste for biology and develop analytically tractable models for the sake of the analysis itself (e.g. Sun and Saker, 2005). On the other hand, there are theoretically inclined biologists who use relatively simple models in support of their empirical findings (e.g. Johnson et al, 2006) or develop very complex models, not only IBMs but also systems of dozens of differential equations, to simulate complex biological systems (e.g. Novák and Tyson, 2004). The niche in between these two worlds is the playground for mathematical biologists or biomathematicians who develop and analyze and/or numerically simulate relatively sophisticated mathematical models to primarily address a biological question, yet with the attendant aim to get from these models as much as possible also mathematically. I believe I belong to this latter type of researchers.

This thesis consists of three major parts, all linked by the question of how processes at the individual level affect the population as a whole.

Part I: Predator-prey theory and optimal foraging

Although work in the field of population dynamics, traditionally the dominant field of mathematical ecology, can be traced back to the end of 18th century, a milestone of its establishment as a scientific discipline and its subsequent upswing are the works of Alfred J. Lotka and Vito Volterra. A U.S. chemist and an Italian mathematician, respectively, these scientists independently developed a dynamical model of predator-prey interactions (Lotka, 1926; Volterra, 1926), now known as the Lotka-Volterra predator-prey model and taught in virtually any course on population ecology. The model is as follows:

$$
\frac{dN}{dt} = rN - \lambda NP
$$
$$
\frac{dP}{dt} = e\lambda NP - mP
$$

$$(1.1)$$

where N and P stand for prey and predator density, respectively, r is the per capita prey growth rate (births minus deaths per unit time) in the absence of predators, m is the per capita predator death rate in the absence of prey, λ scales the predator encounter rate with prey, and e is the efficiency with which consumed prey are transformed into new predators. This model has a unique interior (i.e. coexistence) equilibrium $N^* = m/(e\lambda)$ and $P^* = r/\lambda$ which is neutrally stable; for any initial state $N(0)$ and $P(0)$ there exists a periodic solution that circles the equilibrium in the phase plane, the amplitude and period of which being functions of the initial state (Fig. 1.1). This follows from two facts: first, eigenvalues of the linearized version of the model (1.1) are purely imaginary, $\pm i\sqrt{rm}$, and second, the first integral of the model (1.1) is of the form

$$
e\lambda N + \lambda P - m \ln N - r \ln P = C
$$

$$(1.2)$$

where a constant C is given by the initial state (Kot, 2001).

Beyond its structural instability, the model (1.1) is largely phenomenological, combining simple 'laws' of exponential growth of populations not limited by resources and of mass action kinetics borrowed from chemistry and describing an interaction of two reactants (Murray, 1993). From this perspective, it can hardly be considered mechanistic in that it comprises terms based on real animal behavior. First real instances of individual behavior come with the concept of functional response, defined as the rate at which an individual predator consumes prey as a function of prey density. This concept dates back to a Russian ecologist Georgii F. Gause (Křivan, 2011, and references therein) and was getting fame with a Canadian ecologist Crawford S. Holling (Holling, 1959). Holling's type II functional response,

$$
\frac{\lambda N}{1 + \lambda h N}
$$

$$(1.3)$$
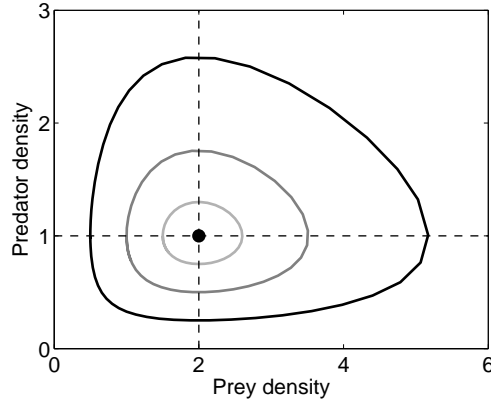
Fig. 1.1 Dynamics of the Lotka-Volterra predator-prey model (1.1). The predator-prey coexistence equilibrium (dot) is neutrally stable. Model solutions are periodic trajectories that circle the equilibrium and their amplitude and period are functions of the initial state. Dashed lines represent the model isoclines

is based on the assumption that upon a successful attack, each predator needs a 'handling' time h to subdue, eat and digest that prey item (Holling, 1959). The type II functional response has since become a prototype for functional response that has been elaborated upon many times (Jeschke et al, 2002) and, more importantly, has been observed to apparently be the most widespread functional response in nature (Hassell et al, 1976; Jeschke et al, 2002). With the type II functional response (1.3), the predator-prey model (1.1) changes to

$$
\begin{aligned}
\frac{dN}{dt} &= rN - \frac{\lambda N}{1 + \lambda h N} P \\
\frac{dP}{dt} &= e \frac{\lambda N}{1 + \lambda h N} P - mP
\end{aligned}
\tag{1.4}
$$

Another milestone in further development of predator-prey theory was the formulation of optimal foraging theory (Charnov, 1976; Stephens and Krebs, 1986). This theory considers predators facing several types (e.g. species) of prey of which they may compose theit diet. By tracking foraging energetics, optimal foraging theory prescribes what is the optimal predator diet composition. The result is critical prey densities at which predators should instantly change their foraging behavior, in order to maximize their food intake rate. As an example, in a homogeneous environment with two prey types, assuming that prey 1 is more profitable than prey 2 ($e_1/h_1 > e_2/h_2$) and that at most one prey type can be encountered at any time instant, prey 1 is always attacked upon encounter, whereas prey 2 is attacked upon encounter only if

$$
N_1 < N_c = \frac{e_2 + \alpha h_2}{\lambda_1 (e_1 h_2 - e_2 h_1)}
\tag{1.5}
$$

and ignored upon encounter if $N_1 > N_c$; α is the average rate at which predators loose energy when searching (Křivan, 1996; Berec and Křivan, 2000). Note that in this case, the optimal predator diet does not depend on the parameter λ_2 scaling the encounter rate with the less profitable prey 2.

This and other optimal foraging rules have subsequently been incorporated into two-prey variants of several predator-prey models like (1.4), to see how adaptivity in predator foraging decisions with respect to changes in prey densities affects predator-prey dynamics, showing that it can sometimes destabilize them, but mostly it has a stabilizing effect (Křivan, 1996; Fryxell and Lundberg, 1998). Note that due to the instant switches of diet composition by predators, the resulting model becomes a set of ordinary differential equations with discontinuous right-hand sides, yet allowing for some formal analysis (Křivan, 1996, 2011). This 'technical difficulty', and more importantly the actual observation of gradual rather than instant diet shifts in a number of species led to the replacement of instant switches by smooth transitions between any two diet composition states (Fryxell and Lundberg, 1998). Mathematically, ordinary differential equations with continuous (and even smooth) right-hand sides are recovered, albeit now the model becomes analytically intractable. Biologically, this has stimulated a quest for mechanisms responsible for such gradual diet shifts. A variety of mechanisms have been proposed, ranging from incorrect classification of prey by predators to limited memory capacity of predators, including perceptual constraints of predators that result in prey densities being assessed only locally, not globally (Berec, 2000; Berec and Křivan, 2000). This latter mechanism forms the topic of the first part of this thesis. Specifically, we ask how perceptual constraints of predators in their ability to assess prey densities and the possibility that predators encounter prey sequentially (one prey type at a time) and/or simultaneously (more prey types at a time) may affect predator attack decisions, diet composition and functional response.

Part II: Allee effects and population extinction

A few years later than Lotka and Volterra formulated their predator-prey model, a U.S. ecologist Warder C. Allee published his initial studies on undercrowding dynamics, more specifically on factors leading to the formation and maintenance of animal aggregations (Allee, 1931; Allee and Bowen, 1932). At that time, it was already acknowledged that the exponential model of single species population growth,

$$\frac{dN}{dt} = rN \tag{1.6}$$

holds true only where populations are not limited by resources, such as at early stages of an outbreak or invasion. Population ecologists have also been aware for some time of the logistic model of single species population dynamics, due to a Belgian mathematician Pierre F. Verhulst and a U.S. biologist Raymond Pearl,

$$\frac{dN}{dt} = rN\left(1 - \frac{N}{K}\right) \tag{1.7}$$

where K is the carrying capacity of the environment, i.e. the maximum population density the environment can sustain. Unlike the exponential model (1.6) for which the per capita population growth rate, $(dN/dt)/N$, does not depend on population density, the logistic model (1.7) states that this rate and population density are negatively correlated (Fig. 1.2). The logistic model thus accounts for resource limitations and decreased individual fitness at higher population densities. For high enough population densities the per capita population growth rate becomes negative. The logistic model thus has a unique, globally stable positive equilibrium at the carrying capacity K.

The logistic model (1.7) has become a flagship of the concept of *negative density dependence*, or overcrowding, the concept that has always dominated research on population dynamics – as populations grow resources decline so that fitness of any population member is negatively correlated to population density. Contrary to that, Allee demonstrated that at least in some populations opposite forces might be at work – at low population densities, individuals can benefit from the presence of conspecifics (Allee and Bowen, 1932; Allee and Wilder, 1938). This phenomenon has later been given the name *Allee effect*. As we understand it now, an Allee effect occurs whenever fitness of an individual in a small or sparse population decreases as the population size or density declines (Stephens et al, 1999; Berec et al, 2007).

For many decades, the concept of Allee effects lingered on the outskirts of population ecology, considered by many as a curiosity and not much worth of consideration for general ecological theory. An interest in Allee effects was revived some 40 years ago by such works as Dennis (1989) and Widén (1993). Since then, the number of studies on Allee effects has grown virtually exponentially, identifying many mechanisms behind this phenomenon and showing that Allee effects are ubiquitous rather than curious, occur in plants, both marine and terrestrial invertebrates, fish, mammals, birds, and even parasites; the most recent stocktaking is carried out in Kramer et al (2009). Likewise, many mathematical models of population dynamics involving Allee effects have been developed, demonstrating substantial impact of the phenomenon on many aspects of population ecology, including applied issues of conserving threatened species (Courchamp et al, 2000), controling invasive pest species (Boukal and Berec, 2009), and harvesting economically important species (Dennis, 1989) – nearly all about Allee effects is summarized in a marvelous book by Courchamp et al (2008).

One of the simplest extensions of the logistic model (1.7) that accounts for the Allee effect is (Boukal and Berec, 2002; Boukal et al, 2007)

$$\frac{dN}{dt} = rN\left(1 - \frac{N}{K}\right)\left(1 - \frac{A+C}{N+C}\right) \tag{1.8}$$

For $A > 0$ and $C > -A$, the model exhibits a critical population density $N = A$ below which the population is doomed to extinction and above which it persists and attains the carrying capacity of the environment K (Fig. 1.2). If this is the case,

such Allee effects are referred to as *strong Allee effects* and the critical population density A is termed the *Allee threshold* (Berec et al, 2007). For $A \leq 0$ and $C > -A$, the per capita population growth rate still declines with declining density in rare populations, but stays positive for any $N > 0$. As a consequence, there is no Allee threshold in this case; one then speaks of *weak Allee effects* (Berec et al, 2007). In both cases, C is an auxiliary parameter, affecting the overall shape of the per capita population growth rate curve. As C increases, the curve becomes increasingly 'flatter' and reaches lower maximum values (Boukal and Berec, 2002; Boukal et al, 2007).
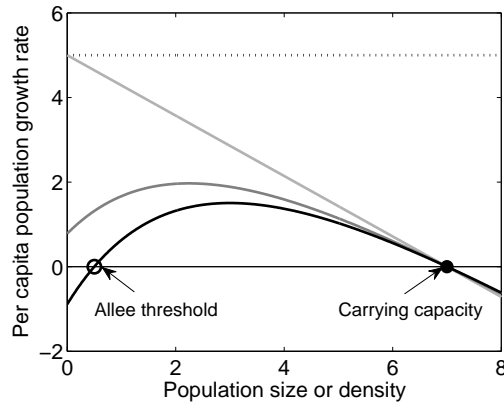
Fig. 1.2 Relationships between the per capita population growth rate and either population size or density for exponential growth (dotted), negative density dependence (light gray), and weak (mid gray) and strong (black) Allee effects. For weak or strong Allee effects, the relationship is positive at low population sizes or densities, where positive density-dependent (Allee effect) mechanisms overpower negative density-dependent (intraspecific competition) ones. It is negative at high population sizes or densities, where the converse is true

However, many population models involving Allee effects are more complex than the model (1.8). In particular, the above model is phenomenological and does not enable one to study how the Allee threshold responds to life history details of a species. To allow for this, one needs to develop mechanistic models in which Allee effects will reflect mechanisms responsible for these effects. For example, a simple population model involving an Allee effect due to enhanced difficulty of finding mates at low population densities (Gascoigne et al, 2009) can be as follows:

$$\frac{dN}{dt} = bNP(N) - (d + d_1 N)N \tag{1.9}$$

Here b and d are intrinsic per capita birth and death rate, respectively, d_1 scales the strength of negative density dependence in the overall per capita death rate $d + d_1 N$ (as N increases so does the probability per unit time of each individual to die), and

$P(N)$ is a function standing for the probability that a female mates with a male when population density equals N. Quite naturally, $P(0) = 0$ (no mating in no population), $dP/dN > 0$ (the more males the higher the chance for any female to mate), and $\lim_{N \to +\infty} P(N) = 1$ (mating virtually assured at high densities) (Courchamp et al, 2008); commonly used forms for $P(N)$ include

$$P(N) = 1 - \exp(-N/\theta) \quad \text{and} \quad P(N) = \frac{N}{N + \theta} \tag{1.10}$$

for a positive parameter θ (Boukal and Berec, 2002). Once $b > d$ and θ is less than a critical value θ_c, the model (1.9) demonstrates a strong Allee effect; the Allee threshold increases and the carrying capacity decreases as θ increases, and the two merge and disappear in a saddle-node bifurcation when $\theta = \theta_c$. Although the per capita population growth rate defined by the model (1.10) still resembles the black curve in Fig. 1.2, both the Allee threshold and the carrying capacity for this and many similar models are now functions of model parameters, here b, d, d_1 and θ, rather than independent parameters as in the phenomenological model (1.8).

But the world is still not that simple. Real populations are structured to various extent, by age, developmental stage, size, sex, or space, and these often need to be incorporated into population models. It turns out that the Allee threshold, a single number in unstructured population models as in the model (1.9), is manifested differently in variously structured population models. In the second part of this thesis, we are interested in how. In addition, we explore the role Allee effects play in predator-prey systems, whether present in prey or in predators, coming around to predator-prey models discussed above. This latter issue is actually one of the most quickly evolving topics in the theory on Allee effects.

Part III: Infectious diseases and pest control

Population dynamics overlap with another active area of research in mathematical biology: mathematical epidemiology, the study of infectious diseases affecting populations. Parasites appear responsible for many aspects of population ecology, including population regulation, sexual selection, evolution of mating systems, and maintenance of sex (e.g. Boots and Knell, 2002; Kokko et al, 2002; Knell and Webberley, 2004). A great many mathematical models of infectious disease dynamics have been proposed and analyzed (Keeling and Rohani, 2008, and references therein), which provide invaluable results that are increasingly incorporated into health policy decisions (e.g. Riley et al, 2003).

The field of mathematical epidemiology is generally thought to prosper following the work of Sir Ronald Ross, a British doctor, on models of malaria, a vector-borne disease (Ross, 1911), and the series of papers by William O. Kermack, a Scottish mathematician, and Anderson G. McKendrick, a Scottish physician and epidemiologist, in 1920-1930's (Kermack and McKendrick, 1927, 1932, 1933). Interestingly, Sir Ronald Ross received the Nobel Prize for Physiology or Medicine in 1902 for

his work on malaria, discovering that malaria was transmitted by the *Anopheles* mosquitoes.

Early motivation for modeling infectious disease dynamics was human epidemiology in developed countries. That is why the two basic and notoriously known epidemiological models taught today, the epidemic SIR model and the endemic SIR model, assume constant host population size. The endemic SIR model is as follows:

$$\frac{dS}{dt} = bN - \beta(N)\frac{SI}{N} - dS$$

$$\frac{dI}{dt} = \beta(N)\frac{SI}{N} - \gamma I - dI \tag{1.11}$$

$$\frac{dR}{dt} = \gamma I - dR$$

It assumes that there is no mortality due to the disease and the birth rate b and the death rate d are equal, $b = d$; this implies that the total population size $N = S + I + R$ obeys $dN/dt = 0$, hence is constant. Further, $\beta(N)$ is the disease transmission factor comprising both the rate at which the susceptible (S) and infectious (I) individuals meet each other and the probability the disease is transmitted upon such encounter, γ is the rate at which infectious individuals recover (R). Trajectories of this model attain a unique, globally stable, disease-free equilibrium $(S^*, I^*, R^*) = (N, 0, 0)$ provided that $R_0 = \beta(N)/(\gamma + d)$, the *basic reproduction number*, is less than 1, and a globally stable, endemic equilibrium

$$(S, I, R) = N\left(\frac{1}{R_0}, \frac{d(R_0 - 1)}{\beta(N)}, \frac{\gamma(R_0 - 1)}{\beta(N)}\right) \tag{1.12}$$

provided that $R_0 > 1$; the disease-free equilibrium is in the latter case unstable (Fig. 1.3; e.g. Keeling and Rohani, 2008).

Later on, the focus has widened to cover animal infections, at first the zoonoses (diseases that have the potential to be transmitted from animals to humans) and the wildlife diseases that can be transmitted to domesticated animals. With the upswing of conservation biology, an emphasis extended to study infections (both natural and those spilled over from domesticated animals) that threatened already endangered wildlife populations (e.g. Kat et al, 1995). Finally, pathogens have recently started to be considered potential regulating agents of invasive pest populations, with the advantage of their self-spreading and thus relative cost-effectiveness of such a control technique (e.g. Deredec et al, 2008, and references therein). In the final part of this thesis, we are going to present and analyze a mathematical model of infectious disease dynamics that considers a pathogen as a potential regulating agent. In particular, given that non-reproducing animals might live longer than the reproducing ones, we explore whether and to what extent does such a life expectancy prolongation due to sterilizing pathogens affect dynamics of the host population. This study thus characterizes pathogens that are promising candidates for an effective pest control and that might possibly be engineered if not present naturally.
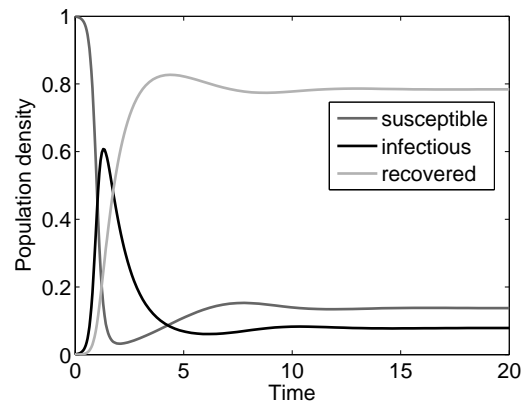
Fig. 1.3 Sample trajectories of the model (1.11). The transmission factor $\beta(N)$ is here assumed constant, hence independent of population density; this is commonly referred to as *standard incidence*. Parameter values were set such that $R_0 > 1$

Relationship to the author's work

This thesis is based on the author's past, recent, and ongoing scientific work. The following list presents the papers the corresponding parts of this thesis are based upon. Although many of them co-authored, these are papers based on the author's idea and with the author's major contribution, both as regards model development and its subsequent analysis. The list also contains further author's work related to the corresponding topics. In these latter papers, the author's contribution was not major and/or the papers were of a predominantly biological character.

Part I: Predator-prey theory and optimal foraging

Author's work the text of this thesis is based upon:

Berec, L., Krivan, V. 2000. A mechanistic model for partial preferences. Theoretical Population Biology 58:279-289

Berec, L. 2000. Mixed encounters, limited perception and optimal foraging. Bulletin of Mathematical Biology 62:849-868

Further author's work related to this topic:

Berec, M., Krivan, V., Berec, L. 2003. Are great tits (*Parus major*) really optimal foragers? Canadian Journal of Zoology 81:780-788

Berec, L. 2003. Simultaneous prey encounters by optimally foraging predators: theory and experiments. Comments on Theoretical Biology 8:1-36

Berec, M., Krivan, V., Berec, L. 2006. Asymmetric competition, body size and foraging tactics: testing the ideal free distribution in two competing species. Evolutionary Ecology Research 8:929-942

Berec, L., Eisner, J., Krivan, V. 2010. Adaptive foraging does not always lead to more complex food webs. Journal of Theoretical Biology 266:211-218

Part II: Allee effects and population extinction

Author's work the text of this thesis is based upon:

Berec, L., Boukal, D. S., Berec, M. 2001. Linking the Allee effect, sexual reproduction and temperature-dependent sex determination via spatial dynamics. American Naturalist 157:217-230

Berec, L., Boukal, D. S. 2004. Implications of mate search, mate choice and divorce rate for population dynamics of sexually reproducing species. Oikos 104:122-132

Berec, L., Angulo, E., Courchamp, F. 2007. Multiple Allee effects and population management. Trends in Ecology & Evolution 22:185-191

Boukal, D. S., Berec, L., Krivan, V. 2008. Does sex-selective predation stabilize or destabilize predator-prey dynamics? PloS ONE 3(7): e2687

Courchamp, F., Berec, L., Gascoigne, J. 2008. Allee effects in ecology and conservation. Oxford University Press

Pavlova, V., Berec, L., Boukal, D. S. 2010. Caught between two Allee effects: trade-off between reproduction and predation risk. Journal of Theoretical Biology 264:787-798

Berec, L. 2010. Impacts of foraging facilitation among predators on predator-prey dynamics. Bulletin of Mathematical Biology 72:94-121

Pavlova, V. Berec, L. In review (Theoretical Ecology). Impacts of predation on dynamics of age-structured prey: Allee effects and multi-stability.

Further author's work related to this topic:

Boukal, D. S., Berec, L. 2002. Single-species models of the Allee effect: extinction boundaries, sex ratios and mate encounters. Journal of Theoretical Biology 218:375-394

Boukal, D. S., Sabelis, M. W., Berec, L. 2007. How predator functional responses and Allee effects in prey affect the paradox of enrichment and population collapses. Theoretical Population Biology 72:136-147

Angulo, E., Roemer, G. W., Berec, L., Gascoigne, J., Courchamp, F. 2007. Double Allee effects and extinction in the island fox. Conservation Biology 21:1082-1091

Berec, L. 2008. Models of Allee effects and their implications for population and community dynamics. Biophysical Reviews and Letters 3:157-181

Berec, L. 2008. Models of Allee effects and their implications for population and community dynamics. Pages 179-207 in R. P. Mondaini and R. Dilao, eds. BIOMAT 2007: International Symposium on Mathematical and Computational Biology. World Scientific, Singapore

Gascoigne, J., Berec, L., Gregory, S., Courchamp, F. 2009. Dangerously few liaisons: a review of mate-finding Allee effects. Population Ecology 51:355-372

Boukal, D. S., Berec, L. 2009. Modelling mate-finding Allee effects and populations dynamics, with applications in pest control. Population Ecology 51:445-458

Tobin, P. C., Berec, L., Liebhold, A. M. 2011. Exploiting Allee effects for managing biological invasions. Ecology Letters 14:615-624

Part III: Infectious diseases and pest control

Author's work the text of this thesis is based upon:

Berec, L., Maxin, D. 2011. Double impact of sterilizing pathogens: added value of increased life expectancy on pest control effectiveness. Journal of Mathematical Biology, doi: 10.1007/s00285-011-0449-x

Further author's work related to this topic:

Deredec, A., Berec, L., Boukal, D. S., Courchamp, F. 2008. Are non-sexual models appropriate for predicting the impact of virus-vectored immunocontraception? Journal of Theoretical Biology 250:281-290

Part I
Predator-prey theory and optimal foraging

Chapter 2

Predator-prey encounters, limited perception and optimal foraging

All animals need food to live and reproduce. Foraging behavior thus forms a substantial component of individual fitness. Beginning with Emlen (1966) and MacArthur and Pianka (1966), optimal foraging theory has aimed at formalizing such behavior in mathematical terms and at explaining the observed foraging behavior from the perspective of fitness maximization (Schoener, 1971; Pulliam, 1974; Werner and Hall, 1974; Charnov, 1976; Krebs and McCleery, 1984; Stephens and Krebs, 1986; Krebs and Davies, 1987; Schmitz, 1997). Since the 1960's, the theory has grown to cover plenty of aspects of foraging behavior and many experiments have been carried out to test for its predictions. Still, the empirical support is limited and the scientific community is split between proponents of the optimal foraging theory and its opponents; see, e.g. Pierce and Ollason (1987) for a criticism.

Although it is naïve to expect complete congruence between relatively simple theoretical models and real observations on imperfect and variable individuals, the fact is that little has often been done to reconcile the two. On one hand, theoretical predictions have often been based on assumptions that are difficult to test for (e.g. assumptions on animal capability to collect and process information) or rather simple to hold in reality (e.g. assumptions on random prey encounters). On the other hand, experimental settings have not often adhered to many assumptions of the specific optimal foraging models and the experimental results have often been presented in qualitative rather than quantitative terms and/or all relevant data have not always been collected or presented.

As a way out of this dilemma, a number of mechanisms thought to better reflect reality have been proposed and incorporated into those simple models of optimal foraging[1]. As an example, a class of optimal foraging models assume that individual predators are globally omniscient, that is, they have exact knowledge of prey population densities in the environment. In reality, however, individual predators are presumably able to assess prey population densities only in a neighborhood of their actual spatial location. As a consequence, because of local variations in prey densities, different predators may estimate global prey densities differently. Local

---

[1] See the next section for many specific examples.

omniscience of real predators can be due to limited abilities in their perception, e.g. a limited detection range of volatile substances released by prey, or limited visual or auditory ranges of predators (Rice, 1983; Kindvall et al, 1998).

In this chapter, we show how perceptual constraints of predators and the possibility that predators encounter their prey sequentially (one prey type at a time) and/or simultaneously (more prey types at a time) affect predator attack decisions, diet composition and functional response with respect to their prey. The work on sequential encounters is based on Berec and Křivan (2000), while that on simultaneous and mixed encounters on Berec (2000).

2.1 Predator-prey encounters and classical theory of optimal foraging

Prey models of optimal foraging theory are based on the assumption that the environment in which predators search for and choose their prey is spatially homogeneous, i.e. not patchy. We study only prey models here, and will thus refer to 'prey models' simply as 'models'; other types of optimal foraging models can be found, e.g. in Stephens and Krebs (1986) and Krebs and Davies (1987). Assumptions of the classical models of optimal foraging theory are as follows (Stephens and Krebs, 1986): prey value is measured as its net energy or another equivalent quantity that does not vary with time, each prey type has an associated fixed handling time, searching for prey and handling prey are mutually exclusive activities, prey are recognized instantaneously and with no errors, prey are encountered randomly at a rate known to predators, and predators have evolved to maximize the net energy intake rate during foraging. These models may differ in the way predator-prey encounters are treated – these can be sequential, simultaneous, or mixed.

Sequential encounters

The first optimal foraging models assumed that predators encountered their prey sequentially, i.e. at most one prey type at a time (Pulliam, 1975; Charnov, 1976; Hughes, 1979; Gleeson and Wilson, 1986; McNamara and Houston, 1987; Fryxell and Lundberg, 1994; Křivan, 1996). Just imagine a great tit sitting on a perch and accepting or rejecting single mealworm pieces that pass by on a conveyor belt (Krebs et al, 1977; Berec et al, 2003). Upon each prey encounter, predators have to decide whether to attack that prey and invest some time in its handling or to ignore it and go on searching for another prey that might be more valuable. Whatever the predator strategy, its net energy intake rate is (Stephens and Charnov, 1982)

$$R(p_1, \ldots, p_n) = \frac{E}{T_s + T_h} = \frac{\sum_{i=1}^n p_i \Lambda_i e_i - \alpha}{1 + \sum_{i=1}^n p_i \Lambda_i h_i} \qquad (2.1)$$

where T_s is the total time spent searching for prey, T_h is the total time spent handling prey, and E is the net amount of energy gained by the predator during the total foraging time $T_s + T_h$. In addition, n is the number of prey types, Λ_i is the encounter rate of predators with prey $i = 1, \ldots, n$ when searching, e_i is the expected net energy gained from handling prey i, h_i is the expected handling time spent to subdue, eat and digest prey i, p_i is the probability that predators will attack prey i upon encounter, and α is the average rate at which predators loose energy when searching.

For two prey types ($n = 2$), maximization of (2.1) with respect to the decision probabilities p_i gives the classical *zero-one rule* (Krebs and Davies, 1987): assuming, without loss of generality, that prey 1 is *more profitable* than prey 2, i.e. $e_1/h_1 > e_2/h_2$, prey 1 is always attacked upon encounter ($p_1 = 1$), whereas prey 2 is attacked upon encounter ($p_2 = 1$) only if

$$\Lambda_1 < \Lambda_c^{seq} = \frac{e_2 + \alpha h_2}{e_1 h_2 - e_2 h_1} \tag{2.2}$$

and ignored upon encounter ($p_2 = 0$) if $\Lambda_1 > \Lambda_c^{seq}$. Note that the zero-one rule does not depend on the encounter rate Λ_2 with the less profitable prey 2; prey 2 is thus attacked upon (each) encounter with a predator only if the predator encounters with prey 1 are sufficiently rare. The theorem specifying the zero-one foraging strategy for any number of prey types ($n \geq 2$) does not provide any detailed insight into the optimal predator behavior, and we refer to Charnov (1976) and McNamara and Houston (1987) for its precise formulation and corollaries.

Among other things, the classical sequential-encounter model predicts that any prey type is either always attacked or always ignored upon encounter with a predator. Yet partial preferences (prey type is sometimes attacked and sometimes ignored when encountered) are rather a rule than an exception in both field and laboratory studies (McNamara and Houston, 1987, and references therein). Partial preferences may be seen by instantly observing food decisions of a group of predators (partial preferences of a population of individuals) and/or by observing foraging behavior of a single predator in a series of food decisions (partial preferences of individuals).

A variety of mechanisms have been proposed to account for this discrepancy and make the model more realistic. In particular, all assumptions underlying the classical sequential-encounter model have been questioned: net energy content and handling time of prey were assumed random variables by Stephens and Charnov (1982), searching for prey and handling prey were not mutually exclusive activities in Farnsworth and Illius (1998), non-negligible recognition time was introduced by Hughes (1979) and Houston et al (1980), errors in recognizing prey types were discussed by Hughes (1979) and Rechten et al (1983), non-random prey encounters appeared in McNair (1979) and Rechten et al (1981), encounter rates with prey types were not known to predators but rather estimated in McNamara and Houston (1987) and Hirvonen et al (1999), and predators were supposed to optimize alternative currencies in Schoener (1971) and even multiple currencies simultaneously in Schmitz et al (1998). Other mechanisms include nutrient constraints (Pulliam, 1975), learning and crypsis (Hughes, 1979), sampling (Rechten et al, 1983), limited memory

capacity of predators (Bélisle and Cresswell, 1997), and perceptual constraints of predators (Mangel and Roitberg, 1989; Berec, 2000; Berec and Křivan, 2000); see McNamara and Houston (1987), Mitchell (1989), and Bélisle and Cresswell (1997) for more detailed lists.

Mixed encounters

Waddington and Holden (1979) argued that simultaneous encounters, i.e. encounters with more prey types at a time, are quite common in nature due to, for example, visual capabilities of foragers. Upon a simultaneous encounter, predators have to decide which prey type to attack, if any; the alternatives are assumed to be mutually exclusive choices. Just imagine bees flying over a meadow or fish hunting in a plankton bloom. The idea of simultaneous encounters has been elaborated upon in several studies (Waddington and Holden, 1979; Engen and Stenseth, 1984a; Stephens et al, 1986; Barkan and Withiam, 1989).

However, it is hard to imagine an animal that would strictly follow only simultaneous prey encounters. Rather, the most natural scenario seems to include possibility of encounters with various subsets of the available prey types, thus including sequential and simultaneous encounters as special cases. Engen and Stenseth (1984b) were probably the first to consider this scenario. They proposed a generalized version of the classical sequential-encounter model and derived qualitative corollaries that were markedly distinct from those of the classical sequential-encounter model. Generality of the Engen and Stenseth (1984b)'s model is paid, however, by the loss of detailed quantitative insight into specific model instances, such as for two prey types only.

For two prey types, the net energy intake rate under mixed encounters is (Berec, 2003)

$$R(p_1, p_2, p_{31}, p_{32}) = \frac{p_1 \Lambda_1 e_1 + p_2 \Lambda_2 e_2 + p_{31} \Lambda e_1 + p_{32} \Lambda e_2 - \alpha}{1 + p_1 \Lambda_1 h_1 + p_2 \Lambda_2 h_2 + p_{31} \Lambda h_1 + p_{32} \Lambda h_2} \quad (2.3)$$

where p_i is the probability that predators will attack prey $i = 1, 2$ when encountered alone, while p_{3i} is the probability that predators will attack prey i when encountered together with the other prey type; hence, $p_{31} + p_{32} \leq 1$. Maximization of (2.3) with respect to these decision probabilities gives the following prediction (Box 2.1): assuming that $e_1/h_1 > e_2/h_2$, prey 1 is always attacked when encountered alone ($p_1 = 1$). In addition,

$$\begin{array}{ll} p_2 = 1 & \text{if } \Lambda_1 + \Lambda < \Lambda_c^{seq} \\ p_2 = 0 & \text{if } \Lambda_1 + \Lambda > \Lambda_c^{seq} \\ p_{31} = 0, p_{32} = 1 & \text{if } \Lambda_1 + \Lambda_2 + \Lambda < \Lambda_c^{sim} \\ p_{31} = 1, p_{32} = 0 & \text{if } \Lambda_1 + \Lambda_2 + \Lambda > \Lambda_c^{sim} \end{array} \quad (2.4)$$

where Λ_c^{seq} is given by the formula (2.2) and

$$\Lambda_c^{sim} = \frac{(e_2 + \alpha h_2) - (e_1 + \alpha h_1)}{e_1 h_2 - e_2 h_1} \tag{2.5}$$

Note that $\Lambda_1 + \Lambda$ is the total encounter rate of a predator with prey 1, while $\Lambda_1 + \Lambda_2 + \Lambda$ is the total encounter rate of a predator with prey regardless of its type and type of encounter. Note also that

$$\Lambda_c^{sim} = \Lambda_c^{seq} - \frac{e_1 + \alpha h_1}{e_1 h_2 - e_2 h_1} < \Lambda_c^{seq}$$

Box 2.1 Optimal diet composition under mixed encounters

Here we derive the optimal diet composition under mixed encounters, by maximizing the net energy intake rate (2.3),

$$R(p_1, p_2, p_{31}, p_{32}) = \frac{p_1 \Lambda_1 e_1 + p_2 \Lambda_2 e_2 + p_{31} \Lambda e_1 + p_{32} \Lambda e_2 - \alpha}{1 + p_1 \Lambda_1 h_1 + p_2 \Lambda_2 h_2 + p_{31} \Lambda h_1 + p_{32} \Lambda h_2}$$

over the decision probabilities p_1, p_2, p_{31} and p_{32}. First note that although $p_{31} + p_{32} \leq 1$, optimality requires $p_{31} + p_{32} = 1$. This is because when a predator encounters a pair of (different) prey, it has nothing to gain by neglecting that pair and searching for another prey (alone or in pair)[2]. Since

$$\frac{\partial R}{\partial p_1} = \frac{\Lambda_1 (e_1 + \alpha h_1 + (e_1 h_2 - e_2 h_1)(\Lambda_2 p_2 + \Lambda p_{32}))}{(1 + p_1 \Lambda_1 h_1 + p_2 \Lambda_2 h_2 + p_{31} \Lambda h_1 + p_{32} \Lambda h_2)^2} > 0$$

R is an increasing function of p_1 and hence reaches its maximum at $p_1 = 1$. Hence, prey 1 is therefore always attacked when encountered alone. Furthermore,

$$\frac{\partial R}{\partial p_2} = \frac{\Lambda_2 (e_2 + \alpha h_2 - (e_1 h_2 - e_2 h_1)(\Lambda_1 p_1 + \Lambda p_{31}))}{(1 + p_1 \Lambda_1 h_1 + p_2 \Lambda_2 h_2 + p_{31} \Lambda h_1 + p_{32} \Lambda h_2)^2}$$

Since $p_1 = 1$, this implies that $\partial R / \partial p_2$ is positive if and only if

$$\Lambda_1 + \Lambda p_{31} < \Lambda_c^{seq}$$

and negative if the reverse inequality holds; Λ_c^{seq} is given by (2.2). Finally, substituting $p_{32} = 1 - p_{31}$ into R,

$$\frac{\partial R}{\partial p_{31}} = \frac{\Lambda \left((e_1 + \alpha h_1) - (e_2 + \alpha h_2) + (e_1 h_2 - e_2 h_1)(\Lambda + \Lambda_1 p_1 + \Lambda_2 p_2) \right)}{(1 + p_1 \Lambda_1 h_1 + p_2 \Lambda_2 h_2 + p_{31} \Lambda h_1 + (1 - p_{31}) \Lambda h_2)^2}$$

Since $p_1 = 1$, this implies that $\partial R / \partial p_{31}$ is positive if and only if

$$\Lambda + \Lambda_1 + \Lambda_2 p_2 > \Lambda_c^{sim}$$

and negative if the reverse inequality holds; Λ_c^{sim} is given by (2.5).

Consider now the following three cases:

1. $\Lambda_1 + \Lambda < \Lambda_c^{seq}$. This implies $p_2 = 1$ and hence $p_{31} = 1$ if and only if $\Lambda + \Lambda_1 + \Lambda_2 > \Lambda_c^{sim}$ and $p_{31} = 0$ if and only if $\Lambda + \Lambda_1 + \Lambda_2 < \Lambda_c^{sim}$
2. $\Lambda_1 < \Lambda_c^{seq}$ and $\Lambda_1 + \Lambda > \Lambda_c^{seq}$. Since $\Lambda_c^{seq} > \Lambda_c^{sim}$ then $\Lambda + \Lambda_1 + \Lambda_2 p_2 > \Lambda_c^{sim}$. This implies $p_{31} = 1$ and hence $p_2 = 0$, as $\Lambda_1 + \Lambda p_{31} = \Lambda_1 + \Lambda > \Lambda_c^{seq}$
3. $\Lambda_1 > \Lambda_c^{seq}$ (which implies $\Lambda_1 + \Lambda > \Lambda_c^{seq}$). Again, since $\Lambda_c^{seq} > \Lambda_c^{sim}$ then $\Lambda + \Lambda_1 + \Lambda_2 p_2 > \Lambda_c^{sim}$. This implies $p_{31} = 1$ and hence $p_2 = 0$, as $\Lambda_1 + \Lambda p_{31} = \Lambda_1 + \Lambda > \Lambda_1 > \Lambda_c^{seq}$

The latter two cases can be coupled together as if $\Lambda_1 + \Lambda > \Lambda_c^{seq}$ then $p_{31} = 1$ and $p_2 = 0$. We thus get the optimal decision probabilities (2.4). In addition, since $\Lambda_1 + \Lambda > \Lambda_c^{seq}$ implies $\Lambda_1 + \Lambda > \Lambda_c^{sim}$ and hence $\Lambda + \Lambda_1 + \Lambda_2 > \Lambda_c^{sim}$ we cannot have simultaneously $p_2 = 0$ and $p_{31} = 0$. In biological terms, when the predator does not attack prey 2 when encountered alone, it neither attacks it when encountered together with prey 1.

Under mixed encounters, preferences are partial in a wide range of prey encounter rates. Indeed, denoting the total decision probability of a predator to attack prey i as

$$\pi_i = \frac{\Lambda_i}{\Lambda_i + \Lambda} p_i + \frac{\Lambda}{\Lambda_i + \Lambda} p_{3i} \qquad (2.6)$$

partial preferences do occur quite frequently (Fig. 2.1). Still, transitions from full to partial preferences in any of the prey types are abrupt rather than gradual. We show below that perceptual constraints of predators, limiting their knowledge of prey densities to a neighborhood of their actual spatial location, make these transitions gradual.

Interestingly, the predator decision rules (2.4) show that a prey type may become rarer in the optimal predator diet as a consequence of being more abundant in the environment; this has been termed the "paradox of self-reduction" by Engen and Stenseth (1984a,b). For example, in Fig. 2.1b, π_2 drops to a lower value as soon as Λ_2 exceeds $\Lambda_c^{sim} - \Lambda_1 - \Lambda$. A necessary condition for this paradox to occur is that a prey type is sometimes encountered alone and sometimes together with other prey types (Engen and Stenseth, 1984a,b).

2.2 Limited perception: models and results

In this section, we develop a spatially explicit, individual-based model (IBM) of a one-predator two-prey system. We then re-derive the above-given classical prey choice rules within the IBM framework and derive new prey choice rules that incorporate a mechanism of limited perception by predators. The main advantage of
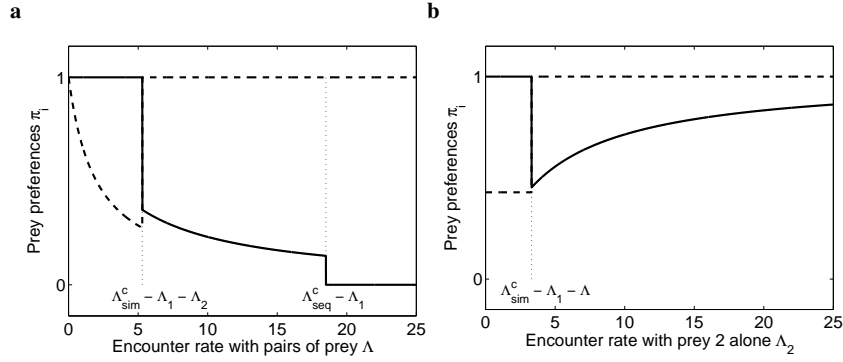
Fig. 2.1 Partial preferences in the classical mixed-encounter model (2.3). Parameter values: $e_1 = 0.1$, $h_1 = 0.2$, $e_2 = 0.2$, $h_2 = 0.5$, $\alpha = 0.01$. Dashed lines show π_1, while solid lines delimit π_2. (a) Encounter rates $\Lambda_1 = 2$ and $\Lambda_2 = 3$ are fixed, while Λ is an independent variable. (b) Encounter rates $\Lambda_1 = 3$ and $\Lambda = 4$ are fixed, while Λ_2 is an independent variable

the spatially explicit IBM is that it allows for tracking every single individual in the environment, thus enabling us to delimit perception neighborhoods readily for individual predators.

The spatially homogeneous environment is modeled as a lattice of square sites. Population densities are limited by the lattice size as we allow for at most one prey individual of one or any type and one predator individual to occupy any single site. Let time run in discrete steps. We assume that the numbers of prey 1 individuals (x_1), prey 2 individuals (x_2), and predators (y) do not change with time. This is the standard assumption "when we want to look at the instantaneous behavior under a range of conditions" (Murdoch and Oaten, 1975). In addition, we assume that prey are randomly distributed across the lattice at each time step.

Sequential encounters

At most one prey individual (regardless of its type) can occupy a single site. At each time step, any single predator may find itself in one of three situations: it can share the site with a prey 1 individual or with a prey 2 individual or the site can be free of prey. For either of the first two cases, the predator attacks a prey $i = 1, 2$ individual with probability p_i. If the predator decides to attack prey i, the attack is successful with probability P_a^i. Following a successful attack, the predator handles prey i for T_h^i time steps. When handling a prey, the predator cannot attack another prey individual. Also, the handled prey cannot be attacked by any other predator. No interference is assumed to take place between any two predators; for an instance of predator interference, see Stillman et al (1997). To keep prey numbers fixed, the

handled prey is instantly replaced by a new individual of the same type, located randomly in any prey-free site.

Consider a single predator in a long series of searching time steps. The proportion of prey i individuals from all prey the predator captures in the series can be well approximated by the formula

$$\frac{\frac{x_i}{S}p_iP_a^i}{\frac{x_1}{S}p_1P_a^1 + \frac{x_2}{S}p_2P_a^2} \tag{2.7}$$

where S is the number of lattice sites (Box 2.2). Similarly, the formula (2.7) will approximate the proportion of prey i individuals of all prey items that are captured by a number y_s of searching predators in a single time step if y_s (and hence S and x_i such that x_i/S stay constant) tends to infinity (Box 2.2).

Box 2.2 Derivation of the diet composition formula (2.7)

Given that both prey types are randomly distributed across the lattice at each time step, with each site occupied by at most one prey individual (regardless of its type), the probability that a searching predator shares a site with a prey i individual is $w_i = x_i/S$. In turn, the probability that the searching predator will successfully attack that prey is $P_s = w_ip_iP_a^i$, that is, the probability of encountering the prey times the probability of attacking it times the probability of attacking it successfully. After T_s searching time steps, we will thus have

$$\mathrm{E}\left[\text{number of successful attacks} \mid T_s\right] = P_sT_s$$

$$\mathrm{Var}\left[\text{number of successful attacks} \mid T_s\right] = P_s(1 - P_s)T_s$$

Using V = number of successful attacks$/T_s$ to denote the proportion of successful attacks out of T_s possibilities, we have

$$\mathrm{E}\left[V \mid T_s\right] = P_s$$

$$\mathrm{Var}\left[V \mid T_s\right] = \frac{P_s(1 - P_s)}{T_s}$$

According to the law of large numbers,

$$\frac{S - P_sT_s}{\sqrt{P_s(1 - P_s)T_s}} \to N(0, 1)$$

in distribution as T_s grows large, where $N(0, 1)$ is the normalized Gaussian distribution with zero mean and unit variance, and hence

$$\frac{V - P_s}{\sqrt{P_s(1 - P_s)/T_s}} \to N(0, 1)$$

in distribution as T_s grows large. Thus, for sufficiently large T_s,

$$V \approx P_s + \sqrt{\frac{P_s(1-P_s)}{T_s}}\varepsilon$$

where $\varepsilon \sim N(0,1)$. This all implies that, given constant prey densities, $w_i p_i P_a^i$ will reasonably approximate the proportion of successful attacks on prey i by a single predator as the number of searching time steps tends to infinity. Similarly, given constant prey densities, the proportion of searching predators that successfully attack prey i in a fixed time step will approach $w_i p_i P_a^i$ as the number of searching predators y_s (and, in turn, the lattice size S and prey numbers x_i such that prey densities w_i stay constant) tends to infinity, given no interference between predators. Hence, the proportion of prey i individuals of all prey items that are captured by a single predator within its searching time or by a number of searching predators in a single time step, is well approximated by the formula (2.7).

The predator functional response to prey i, defined here as the number of captured prey i individuals per predator per time step, can be analogously shown to approach

$$\frac{y_s \frac{x_i}{S} p_i P_a^i}{y} \tag{2.8}$$

as y_s (and hence S and x_i such that x_i/S stay constant) tends to infinity. Let T_s and T_h be the total time an individual predator devotes to searching for prey and handling prey, respectively, and let $T = T_s + T_h$ be the total foraging time. Obviously,

$$T_h = T_s \left(T_h^1 \frac{x_1}{S} p_1 P_a^1 + T_h^2 \frac{x_2}{S} p_2 P_a^2 \right) \tag{2.9}$$

Inserting this expression to $T = T_s + T_h$ and rearranging, we have

$$\frac{T_s}{T} = \frac{1}{1 + T_h^1 \frac{x_1}{S} p_1 P_a^1 + T_h^2 \frac{x_2}{S} p_2 P_a^2} \tag{2.10}$$

If the time steps in which a predator searches for prey or handles prey are randomly distributed within the total foraging time T, then the mean number of actually searching predators would be $y_s = yT_s/T$. If the handling times T_h^1 and T_h^2 of individual prey are small relative to the total handling time T_h, we may assume this formula to approximately hold, too. Hence, y_s/y is close to T_s/T and the (approximate) predator functional response to prey $i = 1, 2$ is

$$\frac{\frac{x_i}{S} p_i P_a^i}{1 + T_h^1 \frac{x_1}{S} p_1 P_a^1 + T_h^2 \frac{x_2}{S} p_2 P_a^2} \tag{2.11}$$

In what follows, the optimal values for the decision probabilities p_i are derived.

Omniscient predators

Classical optimal foraging theory assumes that predator fitness is proportional to the average rate of net energy gain during foraging,

$$\frac{E}{T_s + T_h} \tag{2.12}$$

In the context of our IBM formulation, T_s is the number of time steps a predator individual spent searching for prey, T_h is the number of time steps it spent handling prey, and E is the net amount of energy it gained during the total foraging time $T_s + T_h$. Because of the stochastic character of the IBM, the rate (2.12) is a random variable. For a sufficiently long foraging time and a sufficiently large lattice size, the mean value of (2.12) approaches

$$R(p_1, p_2) = \frac{E_1 \frac{x_1}{S} p_1 P_a^1 + E_2 \frac{x_2}{S} p_2 P_a^2}{1 + T_h^1 \frac{x_1}{S} p_1 P_a^1 + T_h^2 \frac{x_2}{S} p_2 P_a^2} \tag{2.13}$$

whereas its variance tends to zero (Stephens and Charnov, 1982; Stephens and Krebs, 1986); E_i is the net amount of energy predators gain from consuming one prey $i = 1, 2$ item. Assuming that prey 1 is more profitable than prey 2 ($E_1/T_h^1 > E_2/T_h^2$), then by maximizing the function (2.13) with respect to the decision probabilities p_1 and p_2 we have that the optimal strategy of a predator is to always attack prey 1 upon encounter ($p_1 = 1$) and to decide as

$$p_2(x_1) = \begin{cases} 1 \text{ if } x_1 < L_1 \\ 0 \text{ if } x_1 > L_1 \end{cases} \tag{2.14}$$

upon encounter with prey 2, where

$$L_1 = S \frac{E_2}{P_a^1 (E_1 T_h^2 - E_2 T_h^1)} \tag{2.15}$$

(see Stephens and Krebs (1986) or Křivan (1996) for a detailed derivation). The case $x_1 = L_1$ is not considered here as the prey 1 abundance x_1 can take only non-negative integer values within the IBM framework; consequently, we can always make the threshold value L_1 different from all the admissible values of x_1 by a negligible change of parameter values[3].

The effects of this optimal foraging strategy on the predator diet composition (2.7) and the functional response (2.11) are summarized in Fig. 2.2a-c. Three observations are worth noting. First, both the prey 1 proportion in the predator diet and the

---

[3] Within the framework of ordinary differential equations, however, population densities may acquire any non-negative value and such a case has to be treated properly (Křivan, 1996).

prey 1 consumption rate increase with prey 1 abundance x_1 but decrease with prey 2 abundance x_2. Also, the abrupt changes of these quantities do appear around the prey 1 threshold abundance L_1 at which the predator diet changes abruptly. Finally, magnitudes of these abrupt changes do increase with increasing prey 2 abundance x_2.

Numerical IBM simulations are in agreement with our above-derived approximate formulas (Fig. 2.3)a-c. The simulation results were obtained by counting and processing analogously the actual numbers of successfully attacked prey $i = 1, 2$ individuals, for various values of prey 1 abundance. More rigorously, 100 time steps were simulated for each prey 1 abundance (prey 2 numbers were kept constant across these simulations) and the numbers of successfully attacked prey in the last time step, when the number of searching predators had relatively stabilized, were processed. We observe that the predator consumes disproportionately more prey 2 items below the prey 1 abundance threshold $x_1 = L_1$, due to higher probability $P_a^2 > P_a^1$ used in the figure to successfully attack prey 2 individuals upon encounter (Fig. 2.3b). The prey 1 proportion in the diet would coincide with the oblique line below L_1 for $P_a^1 = P_a^2$.

Predators with limited perception

McNamara and Houston (1987) and Hirvonen et al (1999) explained partial preferences by letting predators estimate prey densities on the basis of actual encounters with prey. This is one possibility of how to incorporate limited knowledge of the environment by predators. Alternatively, we suppose here that predators know the exact numbers of individuals of each prey type, but only within a restricted neighborhood of their spatial locations (for example, a square of 5×5 lattice sites with the predator in its center), rather than in the environment as a whole.

Let the perception neighborhood have the same number N of sites for every predator individual; we refer to it as an N-neighborhood further on. Let individuals of both prey be randomly distributed across the lattice at each time step. This assumption implies, among other things, that the actual form of the N-neighborhood is not important and may vary with different predators, because the probability that a site is occupied by a prey i individual is the same for each site. The question now is how a predator should decide upon encountering a prey if it perceives $\tilde{x}_i$ prey i individuals in its N-neighborhood. Obviously, these numbers vary with different predators and may also vary for a single predator with time if the predators and/or prey are allowed to move over the lattice.

Let us suppose that there are $\tilde{x}_i$ prey i individuals in the N-neighborhood of a predator. If we consider this neighborhood as the *effective* environment of the predator, then the above derived optimal foraging rule predicts that the predator should always attack prey 1 upon encounter ($p_1 = 1$), whereas its decision to attack prey 2 upon encounter depends on the relation between the local abundance $\tilde{x}_1$ of prey 1 within the N-neighborhood and the local threshold abundance
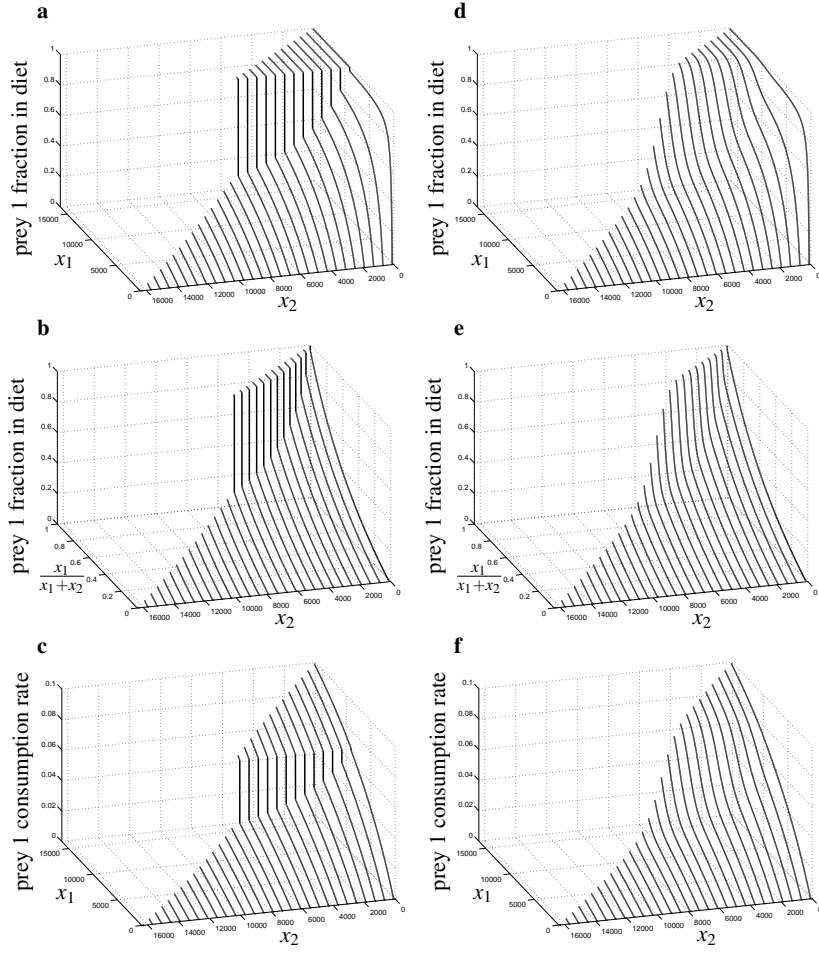
Fig. 2.2 Effects of the optimal foraging strategy on the predator foraging behavior. The proportion of prey 1 individuals from all prey captured by the optimally foraging predators in a single time step (or by a single predator in a series of searching time steps) (2.7) against the prey population abundances (panels (a) and (d)), the same quantity plotted against the proportion of prey 1 in the environment and prey 2 abundance (panels (b) and (f)), and the functional response of optimally foraging predators to prey 1 (the mean number of successfully attacked prey 1 individuals per predator per time step) (2.11) against the prey population abundances (panels (c) and (f)). Panels (a) to (c) correspond to omniscient predators, while panels (d) to (f) are for predators with limited perception ($N = 7 \times 7 = 49$). Common parameter values: $S = 16384\,(128 \times 128)$, $P_a^1 = 0.2$, $E_1 = 0.06$, $T_h^1 = 5$, $P_a^2 = 0.42$, $E_2 = 0.05$, $T_h^2 = 12$

$$L_1' = N \frac{E_2}{P_a^1 \left(E_1 T_h^2 - E_2 T_h^1 \right)} \tag{2.16}$$
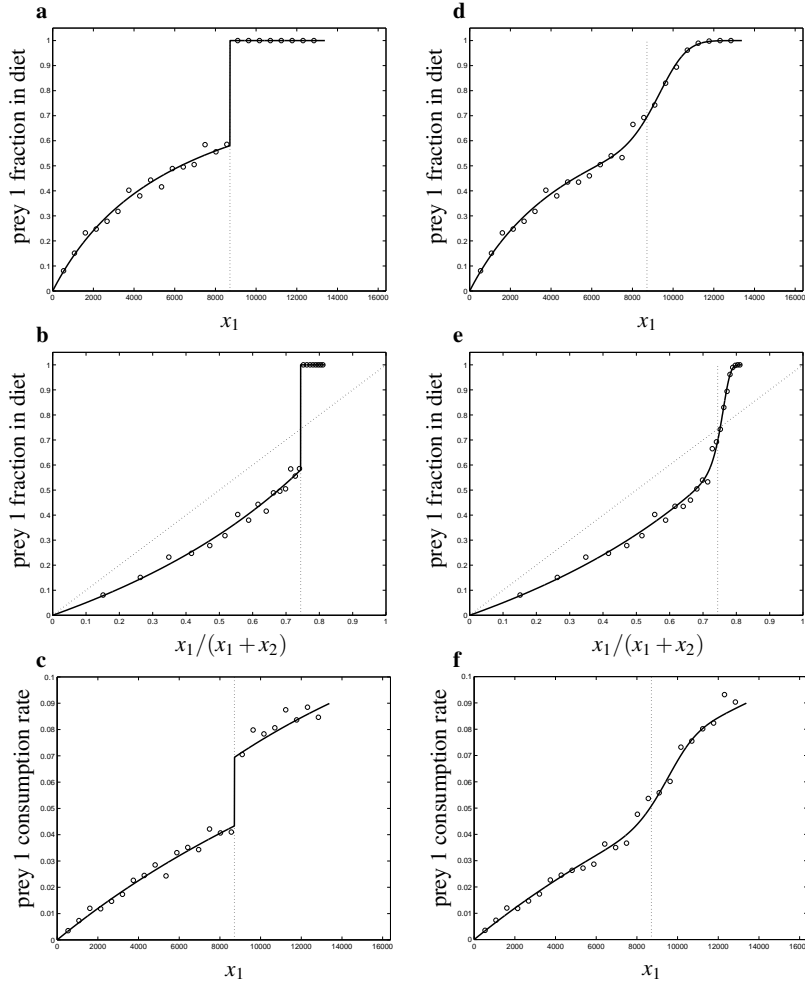
Fig. 2.3 Effects of the optimal foraging strategy on the predator foraging behavior when the prey 2 abundance is fixed at the value $x_2 = 3000$. The circles represent the results of numerical IBM simulations when prey are randomly distributed across the lattice at each time step, the solid lines are the approximate predictions (2.7) and (2.11). Parameter values are as in Fig. 2.2, $y = 6000$. For a comparison, the dotted oblique line in panels (b) and (e) indicates behavior of an opportunistic predator consuming prey types at the proportion equal to their proportion in the environment. All predators were initially in the searching state. As in Fig. 2.2, panels (a) to (c) correspond to omniscient predators, while panels (d) to (f) are for predators with limited perception ($N = 7 \times 7 = 49$). Dotted lines mark location of the threshold prey 1 abundance L_1

This is the threshold abundance (2.15) with the size S of the whole environment replaced by the size N of the effective environment. The predator should attack prey 2 if $\tilde{x}_1 < L'_1$ and ignore it if $\tilde{x}_1 > L'_1$. Note that $L'_1/N = L_1/S$: the threshold *densities* do not change with the transition from global to local scale.

We have already noted that the local prey 1 abundance $\tilde{x}_1$ need not be the same for every predator individual nor for the same individual under different spatial prey distributions[4]. Let a single predator share a site with a prey 2 individual. Then, the decision probability p_2 that the predator will attack that prey equals the probability that the number of prey 1 individuals $\tilde{x}_1$ in the N-neighborhood of this predator is less than L'_1. Given $0 < x_i < S$ for $i = 1, 2$ and $x_1 + x_2 \leq S$, there are

$$D_{\text{total}} = \binom{S-1}{x_1} \binom{S-1-x_1}{x_2-1} \tag{2.17}$$

possibilities for the distribution of prey on the lattice, provided that the focal site is occupied by a prey 2 individual and the predator. The number of possibilities by which $\tilde{x}_1$ prey 1 individuals can be located within the N-neighborhood is then

$$D_{\text{admissible}}(\tilde{x}_1) = \binom{S-N}{x_1-\tilde{x}_1} \binom{N-1}{\tilde{x}_1} \binom{S-1-x_1}{x_2-1} \tag{2.18}$$

provided that this expression is defined, i.e. $\max(0, x_1 - S + N) \leq \tilde{x}_1 \leq \min(x_1, N - 1)$, and $D_{\text{admissible}}(\tilde{x}_1) = 0$ otherwise. Hence, the probability that the number of prey 1 individuals in the neighborhood of size N is lower than the threshold value L'_1 is

$$p_2(x_1) = \sum_{\tilde{x}_1=0}^{[L'_1]} \frac{D_{\text{admissible}}(\tilde{x}_1)}{D_{\text{total}}} \tag{2.19}$$

where $[L'_1]$ denotes the largest integer less than L'_1 (i.e. the whole part of L'_1). Note that the expression (2.19) does not depend on the prey 2 abundance x_2, as the respective terms in (2.17) and (2.18) cancel out. Figure 2.4 shows the decision probability p_2 as a function of prey 1 abundance x_1. The zero-one step function of the omniscient predators changes to a gradually decreasing, sigmoid-like function (2.14). Therefore, $0 < p_2(x_1) < 1$ for a range of prey 1 numbers. As N approaches S, the decision probability (2.19) approaches the zero-one step function. Indeed, for $N = S$, it is $L'_1 = L_1$ and $D_{\text{admissible}}(\tilde{x}_1) = 0$ for any $\tilde{x}_1 \neq x_1$. This implies $p_2(x_1) = 1$ if $x_1 < L_1$ and $p_2(x_1) = 0$ if $x_1 > L_1$, that is, the formula (2.14).

We claim that the decision probability p_2 given by the expression (2.19) and based on temporal and/or spatial variability in $\tilde{x}_1$ gives rise to partial preferences on both the individual and population levels. To see the former, consider a single predator in the course of time and observe its food decisions. As x_1 is kept constant, after m encounters with prey 2, the number of prey 2 items it has actually consumed is binomially distributed with parameters m and $p_2(x_1)$. Hence, the mean proportion of prey 2 items the predator has consumed of those encountered is $p_2(x_1)$, which is neither 0 nor 1 for such x_1 for which $0 < p_2(x_1) < 1$. The actual proportion of prey 2 items the predator has attacked after m encounters with prey 2 approaches $p_2(x_1)$ as m (that is, the number of food decisions) tends to infinity. To elucidate the existence of partial preferences on the population level, consider a fixed time

---

[4] Which may arise due to prey and/or predator movement.
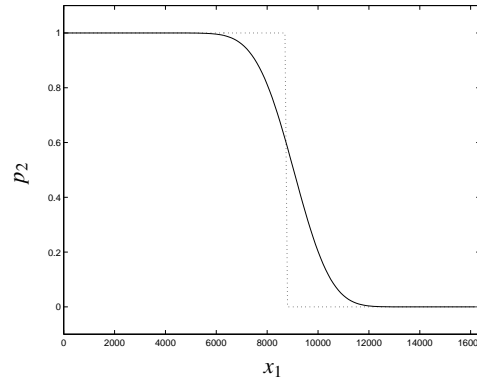
Fig. 2.4 The decision probability p_2 as a function of the prey 1 population abundance x_1, for omniscient predators (dotted line) and predators with limited perception (solid line). Parameter values are as in Fig. 2.2, $x_2 = 3000$, $N = 49 \, (7 \times 7)$. Dotted lines mark location of the threshold prey 1 abundance L_1

step and a number of predators on the lattice. Let m out of a number of searching predators encounter prey 2 in that time step. Then the actual number of predators that attack prey 2 is also binomially distributed with parameters m and $p_2(x_1)$. Hence, the mean proportion of predators that attack prey 2 is $p_2(x_1)$, whereas the actual proportion approaches $p_2(x_1)$ as m (that is, predator numbers and, in turn, lattice size) tends to infinity.

Figures 2.2d-f and 2.3d-f are respectively analogous to Figs. 2.2a-c and 2.3a-c. They show the effects of perceptual limitations of predators on their diet composition [Eq. (2.7)] and functional response to prey 1 [Eq. (2.11)], for $p_1 = 1$ and p_2 specified by the formula (2.19). The fundamental distinction in these characteristics between omniscient predators and predators with limited perception is the shift from abrupt changes around L_1 characteristic of the former to gradual transitions over this threshold value for the latter (Figs. 2.2 and 2.3). As a consequence, the predator functional response to prey 1 takes a sigmoidal form (Fig. 2.3f) which may in turn have implications for long-term dynamics of the whole predator–prey system (Murdoch and Oaten, 1975).

Mixed encounters

Under mixed encounters, the philosophy of calculating the optimal foraging behavior for both omniscient predators and predators with limited perception is analogous to that under sequential encounters. Obviously, things become a bit more complicated technically due to more possibilities that may occur, but conceptually everything stays the same and our treatment will thus be more concise here. At most one individual of each type (prey 1, prey 2, predator) is allowed to occupy each site

at any one time; one may think, for example, of territorial, monogamous birds in which at most one male (prey 1) and one female (prey 2) occupy a single territory (site). As a consequence, any predator may encounter either a prey individual alone (sequential encounter) or a pair of individuals of different prey types (simultaneous encounter).

Every time step, any single predator may find itself in one of four situations: it can share the lattice site with a prey 1 individual alone, a prey 2 individual alone, with a pair of different prey individuals, or the site is free of prey. If the predator shares the site with a prey $i = 1, 2$ individual alone, it decides to attack that prey with probability p_i. If the predator encounters individuals of both prey types, it decides to attack the prey 1 individual with probability p_{31}, whereas it strikes the prey 2 individual with probability p_{32}; we assume that at most one individual may be attacked at a time so that $p_{31} + p_{32} \leq 1$.

Before we derive optimal values for the decision probabilities p_i and p_{3i}, we give formulas for the predator diet composition and the functional response. Consider a single predator, making decisions in a series of time steps. For a sufficiently long foraging time, the proportion of prey i individuals from those it captures is well approximated by the expression (Box 2.3)

$$\frac{\frac{x_i}{S} \pi_i P_a^i}{\frac{x_1}{S} \pi_1 P_a^1 + \frac{x_2}{S} \pi_2 P_a^2} \tag{2.20}$$

where

$$\pi_1 = \left(1 - \frac{x_2}{S}\right) p_1 + \frac{x_2}{S} p_{31} \tag{2.21}$$

$$\pi_2 = \left(1 - \frac{x_1}{S}\right) p_2 + \frac{x_1}{S} p_{32} \tag{2.22}$$

For a sufficiently large lattice size S, the formula (2.20) can also be derived by observing all predators searching for prey i in a single time step (Box 2.3). Similarly, if we define the predator functional response to prey i as the number of captured prey i individuals per predator per time step, we (approximately) get

$$\frac{y_s \frac{x_i}{S} \pi_i P_a^i}{y} \tag{2.23}$$

where y_s is the number of searching predators and y the total (fixed) number of predators. Analogously to the case of sequential encounters, the term y_s/y can be well approximated by the expression $1/(1 + T_h^1 \frac{x_1}{S} \pi_1 P_a^1 + T_h^2 \frac{x_2}{S} \pi_2 P_a^2)$. The (approximate) predator functional response to prey i is thus

$$\frac{\frac{x_i}{S} \pi_i P_a^i}{1 + T_h^1 \frac{x_1}{S} \pi_1 P_a^1 + T_h^2 \frac{x_2}{S} \pi_2 P_a^2} \tag{2.24}$$

The *total* decision probabilities π_i, given by the expressions (2.21) and (2.22), are the probabilities that a predator will attack prey i upon encounter, averaged over the frequencies with which prey i is encountered alone or together with the alternative.

These probabilities are just the ones that are estimated from experimental observations. Recall that the expressions formalizing the predator diet composition and the functional response in the case of sequential encounters, (2.7) and (2.11), have the same form as derived here, with π_i replaced by p_i.

Box 2.3 Derivation of the diet composition formula (2.20)

Consider a fixed time step and a searching predator. Provided that both prey types are randomly distributed across the lattice, with each site occupied by at most one item of each prey type, the probability that the predator shares its site with a prey 1 item alone is $w_1(1-w_2)$, where we denote by $w_i = x_i/S$ the prey i population density. As a consequence, the probability that the predator attacks that prey successfully is $w_1(1-w_2)p_1P_a^1$, that is, the probability to encounter the prey times the probability to decide to attack it times the probability to attack it successfully. Hence, using the analogous arguments as in Box 2.2, the proportion of time steps spent searching in which the predator encounters prey 1 alone and attacks it successfully approaches $w_1(1-w_2)p_1P_a^1$ as the total searching time T_s goes to infinity. Likewise, in a single time step, the proportion of searching predators that encounter prey 1 alone and attack it successfully approaches $w_1(1-w_2)p_1P_a^1$ as the number of predators and hence the lattice size approach infinity.

The probability that the predator shares its site with both prey types is w_1w_2. Therefore, the probability that the predator encounters a pair of prey and successfully attacks prey 1 out of it is $w_1w_2p_{31}P_a^1$. Analogous expressions can be derived for prey 2. Under the assumption $T_s \to \infty$ or $y_s \to \infty$ (and so $S \to \infty$), the same arguments as above are valid to these subcases. Altogether, the expected proportion of prey $i = 1,2$ individuals of all prey captured by a single predator in a series of searching time steps (or by a number of searching predators in a single time step) is given by the expression (2.20).

Omniscient predators

Following Stephens and Krebs (1986), and assuming a sufficiently long foraging time or a sufficiently large lattice size, fitness maximization is equivalent to maximization of the expression

$$R(p_1, p_2, p_{31}, p_{32}) = \frac{E}{T_s + T_h} = \frac{E_1 \frac{x_1}{S} \pi_1(p_1, p_{31})P_a^1 + E_2 \frac{x_2}{S} \pi_2(p_2, p_{32})P_a^2 - \alpha}{1 + T_h^1 \frac{x_1}{S} \pi_1(p_1, p_{31})P_a^1 + T_h^2 \frac{x_2}{S} \pi_2(p_2, p_{32})P_a^2} \tag{2.25}$$

where the total decision probabilities π_i are given by the expressions (2.21) and (2.22), E_i is the net energy gained from consuming prey $i = 1,2$, and α is the amount of energy lost by a predator per one time step searching. The expression (2.25) is maximized over the *partial* decision probabilities p_i and p_{3i}, subject to the

constraints $0 \leq p_i \leq 1$, $0 \leq p_{3i} \leq 1$, $p_{31} + p_{32} \leq 1$. Assuming, without loss of generality, that prey 1 is more profitable than prey 2 ($E_1/T_h^1 > E_2/T_h^2$), prey 1 is predicted to be always attacked by predators when encountered alone ($p_1 = 1$), whereas

$$
\begin{aligned}
&p_2 = 1 \ \text{if} \ x_1 < L_1 \\
&p_2 = 0 \ \text{if} \ x_1 > L_1 \\
&p_{31} = 0, \, p_{32} = 1 \ \text{if} \ x_1 + x_2 - x_1 x_2/S < L_2 \\
&p_{31} = 1, \, p_{32} = 0 \ \text{if} \ x_1 + x_2 - x_1 x_2/S > L_2
\end{aligned}
\tag{2.26}
$$

where

$$
L_1 = S \frac{E_2 + \alpha T_h^2}{P_a^1 (E_1 T_h^2 - E_2 T_h^1)}
\tag{2.27}
$$

and

$$
L_2 = S \frac{(E_2 + \alpha T_h^2) - \frac{P_a^1}{P_a^2}(E_1 + \alpha T_h^1)}{P_a^1 (E_1 T_h^2 - E_2 T_h^1)} < L_1
\tag{2.28}
$$

These expressions can be derived by analogous reasoning as used in Box 2.1. Also here, we do not consider the singular cases $x_1 = L_1$ and $x_1 + x_2 - x_1 x_2/S = L_2$ because the prey abundances x_i can take only non-negative integer values (bounded from above by S) within our IBM framework; therefore, one can always make the threshold values L_1 and L_2 different from the values of x_1 and $x_1 + x_2 - x_1 x_2/S$, respectively, by a negligible change of parameter values. The values L_1 and L_2 are in units of individuals; dividing them by S gives them the meaning of densities.

We make a remark concerning the formulas (2.27) and (2.28). The net energy gained from consuming prey i can be expressed as $E_i = E_g^i - \alpha_h^i T_h^i$, where E_g^i is the gross energy gained from prey i and α_h^i is the energy a forager looses per one time step spent handling prey i. Let $\alpha = \alpha_h^1 = \alpha_h^2$. In other words, let searching for prey and handling prey be equally energy-consuming activities, and let $E_g^2 = c E_g^1$ for a constant value $c > 0$, i.e. let the prey types be perfect substitutes (the gross energy gained from consuming an individual of prey 2 is proportional to that gained from consuming an individual of prey 1). Then,

$$
L_1 = S \frac{c}{P_a^1 (T_h^2 - c T_h^1)}
\tag{2.29}
$$

$$
L_2 = S \frac{c - P_a^1/P_a^2}{P_a^1 (T_h^2 - c T_h^1)} < L_1
\tag{2.30}
$$

The same simplifications could be achieved if the rate α of energy loss during searching is assumed to be negligible with respect to the other terms in the numerator of (2.25), and $E_2 = c E_1$ for a $c > 0$. These assumptions are rather standard in the optimal foraging literature (Krebs et al, 1977; Houston et al, 1980; Stephens et al, 1986; Schmidt, 1998), since measurements of energy gains and losses are very difficult to perform. We use these simplified expressions further on. We also note that the inequality $E_1/T_h^1 > E_2/T_h^2$ now implies $T_h^2 > c T_h^1$.

Now, consider the prey 2 abundance fixed at a value $0 < x_2 < S$. The abundances of prey 1 at which predators change their diet are then $x_1^* \equiv L_1$ and $x_1^{**} \equiv (L_2 - x_2)/(1 - x_2/S)$. A necessary and sufficient condition for the inequality $x_1^{**} \geq x_1^*$ to hold is $L_1 > S$, $L_2 > S$ and $x_2 \geq (L_1 - L_2)/(L_1/S - 1)$ which implies $x_1^{**} \geq x_1^* > S$. Hence, both prey 1 thresholds x_1^* and x_1^{**} are greater than the lattice size which makes this case behaviorally uninteresting. If $x_1^{**} \geq S$, $p_{32} = 1$ for all $0 < x_1 < S$. If $x_1^{**} \leq 0$, on the other hand, $p_{31} = 1$ for all the admissible values of x_1, and similarly for x_1^*. The most interesting case occurs when both of the prey 1 thresholds are 'active', that is, when $x_1^{**} > 0$ and $x_1^* < S$. Figure 2.5 gives an idea of how the space of prey population sizes is divided into regions with different predator foraging strategies.
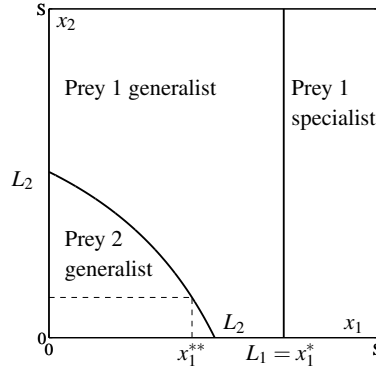
Fig. 2.5 Division of the space of prey population sizes into regions with different optimal foraging strategies of omniscient predators. Parameter values: $S = 128 \times 128$, $P_a^1 = 0.3$, $T_h^1 = 2$, $P_a^2 = 0.85$, $T_h^2 = 8$, $c = 1.2$. Prey 1 generalist: $p_1 = p_{31} = p_2 = 1$, $p_{32} = 0$; prey 2 generalist: $p_1 = p_{32} = p_2 = 1$, $p_{31} = 0$; prey 1 specialist: $p_1 = p_{31} = 1$, $p_2 = p_{32} = 0$

The expression

$$x_1 + x_2 - x_1 x_2/S = S \left[\frac{x_1}{S} \left(1 - \frac{x_2}{S}\right) + \frac{x_2}{S} \left(1 - \frac{x_1}{S}\right) + \frac{x_1}{S} \frac{x_2}{S} \right] \tag{2.31}$$

used to decide which prey out of the pair encountered should be attacked [Eq. (2.26)], is the mean number of sites occupied by prey, given that x_i individuals of prey $i = 1, 2$ are randomly distributed on the lattice. Moreover, by rewriting this expression as

$$x_1 + x_2 - x_1 x_2/S = x_1 + x_2 \left(1 - \frac{x_1}{S}\right) \tag{2.32}$$

the paradox of self-reduction (Engen and Stenseth, 1984a,b) can be demonstrated via increasing the prey 2 abundance x_2, for a fixed prey 1 abundance x_1: if the prey abundances are initially such that $p_2 = 1$, $p_{31} = 0$, $p_{32} = 1$, then an increase in the prey 2 abundance x_2 makes this prey rarer in the predator diet if conditions change for $p_2 = 1$, $p_{31} = 1$, $p_{32} = 0$ to be optimal [Eq. (2.26)]. These expressions also imply that when a predator encounters a pair of (different) prey individuals it does not

necessarily attack the more profitable one. Instead, somewhat counterintuitively at a glance, it may attack the less profitable prey; see also Stephens et al (1986) and Barkan and Withiam (1989).

Figure 2.6a shows the total decision probabilities π_1 (2.21) and π_2 (2.22) for the optimally foraging predators, as functions of prey 1 abundance x_1, for a fixed prey 2 abundance x_2 and for a particular set of parameters ensuring that both the prey 1 thresholds x_1^* and x_1^{**} are active. The interesting observation is not only an appearance of partial preferences for (less profitable) prey 2 when prey 1 abundance lies in between the values x_1^{**} and x_1^*, but also an appearance of partial preferences for (more profitable) prey 1 when its abundance is below the value x_1^{**}. Moreover, since x_1^{**} is a function of x_2, the optimal diet choice depends on the prey 2 abundance, too. These facts, first qualitatively recognized by Engen and Stenseth (1984a), were made quantitative for a system with two prey types here. The effects of the optimal foraging strategy on the predator diet composition and the functional response, for a fixed prey 2 abundance x_2, are summarized in Fig. 2.7a-c.
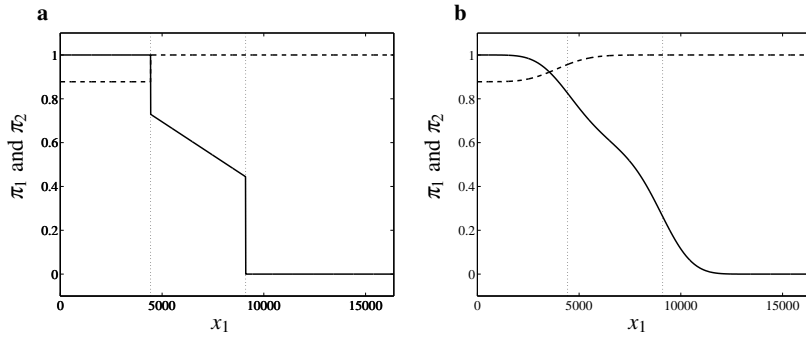
Fig. 2.6 Total decision probabilities for (more profitable) prey 1 (dashed line) and (less profitable) prey 2 (solid line) for (a) omniscient predators and (b) predators with limited perception, experiencing mixed encounters, as functions of prey 1 abundance x_1. Prey 2 abundance is fixed at the value $x_2 = 2000$. Other parameter values: $S = 16384 (128 \times 128)$, $P_a^1 = 0.3$, $T_h^1 = 2$, $P_a^2 = 0.85$, $T_h^2 = 8$, $c = 1$, for limited perception $N = 49 (7 \times 7)$. In each panel, dotted lines mark location of the threshold prey 1 abundances x_1^{**} and x_1^*, with $x_1^{**} < x_1^*$

Predators with limited perception

Although we observe partial preferences for both prey types, the predator diet composition and the functional response change abruptly around the prey 1 thresholds x_1^* and x_1^{**}, since all predators change their diet at the same moment (Fig. 2.7a-c). Such synchrony is unlikely to occur in natural systems; moreover, the assumption on predator omniscience does not seem entirely realistic, particularly when the lattice size is large.
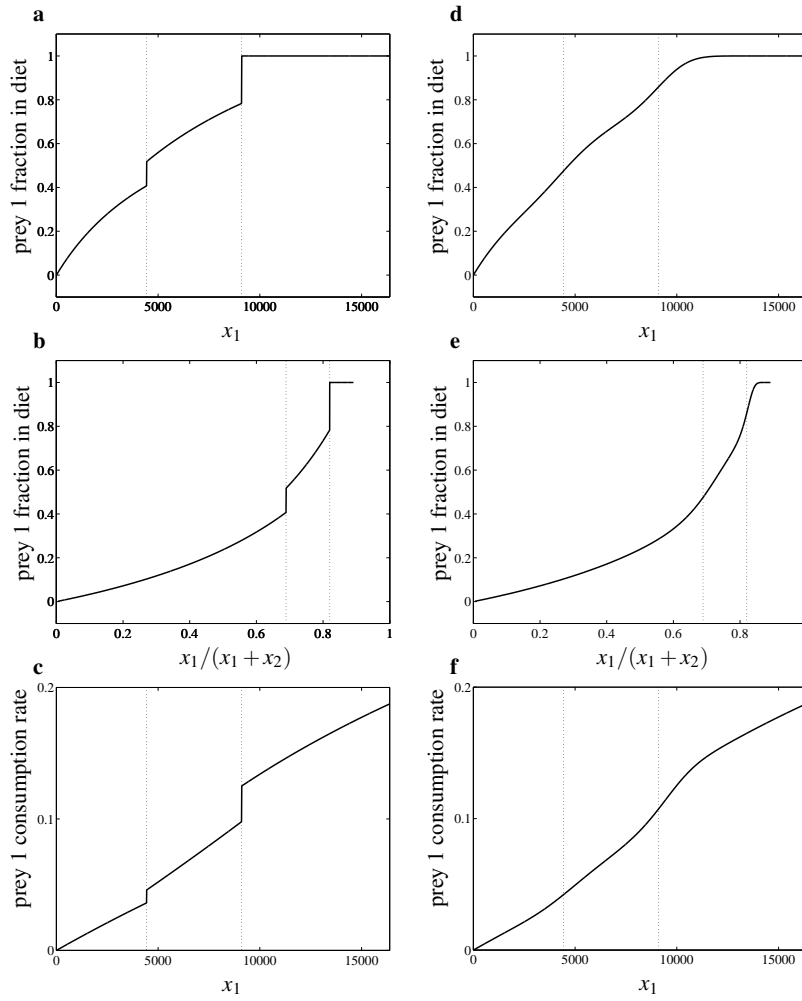
Fig. 2.7 Effects of the optimal foraging strategy under mixed encounters on the predator diet composition and the functional response. The proportion of prey 1 individuals from all prey captured by an optimally foraging predator in a series of time steps (or by more predators in a single time step) against the prey 1 population abundance (panels (a) and (d)), the same quantity plotted against the proportion of prey 1 in the environment (panels (b) and (e)), and the functional response of optimally foraging predators to prey 1 (the mean number of successfully attacked prey 1 individuals per predator per time step) against the prey 1 population abundance (panels (c) and (f)). Panels (a) to (c) correspond to omniscient predators, while (d) to (f) to predators with limited perception. Prey 2 abundance is fixed at the value $x_2 = 2000$. Parameter values are as in Fig. 2.6. In each panel, dotted lines mark location of the threshold prey 1 abundances x_1^{**} and x_1^*, with $x_1^{**} < x_1^*$

As we have already mentioned above, McNamara and Houston (1987) and Hirvonen et al (1999) removed the assumption on predator omniscience by letting predators estimate prey densities on the basis of actual time sequence of encounters with

prey. Bélisle and Cresswell (1997) assumed that the forager could memorize only a number of recently consumed prey items; if all these items are of the same type the forager forgets the relative values of the prey types and consumes prey indiscriminately, until both prey types are again present in the predator memory window. In the models with sequential prey encounters, both these mechanisms predicted partial preferences for the less profitable prey. Although they could possibly be extended to the models with mixed encounters, we instead assume that predators know exact numbers of individuals of each prey type only within a neighborhood of their actual spatial location.

Again, let us consider the N-neighborhood of a predator. The optimal foraging rule (2.26) predicts that the predator should always attack prey 1 encountered alone. Moreover, the predator decision to attack prey 2 encountered alone depends on the threshold value (2.29) with the size S of the whole environment replaced by the local (or effective) environment size N, i.e. always attack prey 2 if $\tilde{x}_1 < L_1'$ and always ignore it if the reverse inequality holds, where $\tilde{x}_1$ is the prey 1 abundance in the N-neighborhood, and

$$L_1' = N \frac{c}{P_a^1 (T_h^2 - c T_h^1)} \tag{2.33}$$

In addition, the predator decision of which prey to attack when encountered in a pair of different types should depend on the threshold value (2.30) with S replaced by N, i.e. always attack prey 2 if $\tilde{x}_1 + \tilde{x}_2 - \tilde{x}_1 \tilde{x}_2 / N < L_2'$ and always attack prey 1 if the reverse inequality holds, where $\tilde{x}_2$ is the prey 2 abundance in the N-neighborhood, and

$$L_2' = N \frac{c - P_a^1/P_a^2}{P_a^1 (T_h^2 - c T_h^1)} \tag{2.34}$$

Since $L_i'/N = L_i/S$, the critical densities do not change upon the transition from global to local scale.

Now, recalling that even for fixed total prey $i = 1, 2$ densities x_i, the local abundances $\tilde{x}_i$ need not be the same for every predator individual, nor for the same individual in different time steps (as the spatial distribution of prey may change with time and/or the predator may move to another site), consider a single predator individual that shares its site with a prey 2 individual alone, and compute the (partial) decision probability p_2 that the predator will attack that prey. Clearly, p_2 is the probability that the number $\tilde{x}_1$ of prey 1 individuals in the predator N-neighborhood is below the threshold value L_1'. Let the total prey abundances on the lattice be fixed at $0 < x_i < S$. There are

$$\binom{S-1}{x_1} \binom{S-1}{x_2 - 1} \tag{2.35}$$

possibilities for the distribution of prey individuals on the lattice composed of S sites, conditioned on the event that the focal site is occupied by a prey 2 individual, no prey 1 individual, and the predator. The number of ways in which $\tilde{x}_1$ prey 1 individuals can be arranged in the N-neighborhood is

$$\binom{N-1}{\tilde{x}_1}\binom{S-N}{x_1-\tilde{x}_1}\binom{S-1}{x_2-1} \tag{2.36}$$

provided that $x_1 - (S-N) \leq \tilde{x}_1 \leq \min\{x_1, N-1\}$; it is zero otherwise. As a consequence, the probability $P_2(\tilde{x}_1, x_1)$ that $\tilde{x}_1$ out of x_1 prey 1 individuals are located within the N-neighborhood of the predator, sharing the lattice site with a prey 2 individual alone, defines the hypergeometric distribution

$$P_2(\tilde{x}_1, x_1) = \begin{cases} \dfrac{\binom{N-1}{\tilde{x}_1}\binom{S-N}{x_1-\tilde{x}_1}}{\binom{S-1}{x_1}} & \text{if } x_1 - (S-N) \leq \tilde{x}_1 \leq \min\{x_1, N-1\} \\ 0 & \text{otherwise} \end{cases} \tag{2.37}$$

Finally, the required probability p_2 that the number of (more profitable) prey 1 individuals within the N-neighborhood is lower than the threshold value L_1' is

$$p_2(x_1) = \sum_{\tilde{x}_1=0}^{[L_1']} P_2(\tilde{x}_1, x_1) \tag{2.38}$$

where $[L_1']$ denotes the largest integer less than L_1' [5]. As N approaches S, so $p_2(x_1)$ approaches the zero-one step function (2.26); indeed, $N = S$ implies $L_1' = L_1$, $P_2(\tilde{x}_1, x_1) = 1$ if $\tilde{x}_1 = x_1$, and zero otherwise. In turn, $p_2(x_1) = 1$ if $x_1 < L_1$, and $p_2(x_1) = 0$ if $x_1 > L_1$.

Analogously, consider a single predator individual that shares its site with a pair of (different) prey individuals, and compute the partial decision probability p_{32} of attacking prey 2 out of this pair. Obviously, p_{32} is the probability that the condition $\tilde{x}_1 + \tilde{x}_2 - \tilde{x}_1\tilde{x}_2/N < L_2'$ is satisfied. For fixed total prey abundances $0 < x_i < S$, there are

$$\binom{S-1}{x_1-1}\binom{S-1}{x_2-1} \tag{2.39}$$

possibilities for the distribution of prey individuals on the lattice containing S sites, conditioned on the event that the focal site is occupied by one prey 1 individual, one prey 2 individual, and the predator. The number of ways in which $\tilde{x}_1$ prey 1 individuals and $\tilde{x}_2$ prey 2 individuals can be arranged in the N-neighborhood is

$$\binom{N-1}{\tilde{x}_1-1}\binom{S-N}{x_1-\tilde{x}_1}\binom{N-1}{\tilde{x}_2-1}\binom{S-N}{x_2-\tilde{x}_2} \tag{2.40}$$

if $\max\{1, x_i - (S-N)\} \leq \tilde{x}_i \leq \min\{x_i, N\}$, $i = 1, 2$; it is zero otherwise. The probability $P_{32}(\tilde{x}_1, \tilde{x}_2, x_1, x_2)$ that $\tilde{x}_1$ prey 1 individuals and $\tilde{x}_2$ prey 2 individuals are located in the predator N-neighborhood thus defines the multihypergeometric distribution

---

[5] Analogously to L_1, we assume that neither L_1' takes an integer value.

$$P_{32}(\tilde{x}_1, \tilde{x}_2, x_1, x_2) = \begin{cases} \dfrac{\binom{N-1}{\tilde{x}_1-1}\binom{S-N}{x_1-\tilde{x}_1}\binom{N-1}{\tilde{x}_2-1}\binom{S-N}{x_2-\tilde{x}_2}}{\binom{S-1}{x_1-1}\binom{S-1}{x_2-1}} \\ \qquad \text{if } \max\{1, x_i - (S-N)\} \leq \tilde{x}_i \leq \min\{x_i, N\} \\ 0 \qquad \text{otherwise} \end{cases} \tag{2.41}$$

Finally, the probability p_{32} that $\tilde{x}_1 + \tilde{x}_2 - \tilde{x}_1\tilde{x}_2/N < L_2'$ is

$$p_{32}(x_1, x_2) = \sum_A P_{32}(\tilde{x}_1, \tilde{x}_2, x_1, x_2) \tag{2.42}$$

where the summation is performed over the set $A = \{\tilde{x}_1, \tilde{x}_2 : \tilde{x}_1 + \tilde{x}_2 - \tilde{x}_1\tilde{x}_2/N < L_2'\}$. Moreover,

$$p_{31}(x_1, x_2) = 1 - p_{32}(x_1, x_2) \tag{2.43}$$

As N approaches S, $p_{32}(x_1, x_2)$ approaches the zero-one step function; indeed, for $N = S$, it is $L_2' = L_2$, $P_{32}(\tilde{x}_1, \tilde{x}_2, x_1, x_2) = 1$ if $\tilde{x}_1 = x_1$ and $\tilde{x}_2 = x_2$, and zero otherwise. In turn, $p_{32}(x_1, x_2) = 1$ if $x_1 + x_2 - x_1x_2/S < L_2$, and $p_{32}(x_1, x_2) = 0$ if $x_1 + x_2 - x_1x_2/S > L_2$.

Figure 2.6b shows the total decision probabilities π_1 (2.21) and π_2 (2.22) as functions of x_1, for a fixed value of x_2 and for predators with limited perception, i.e. for the partial decision probabilities $p_1 = 1$, p_2 given by the expression (2.38), $p_{31} = 1 - p_{32}$, and p_{32} given by the expression (2.42). The abrupt changes observed in Fig. 2.6a are now replaced by gradual transitions over the prey 1 threshold values x_1^* and x_1^{**} in Fig. 2.6b, and the range of x_1 in which partial preferences appear has increased a bit. Panels (d) to (f) of Fig. 2.7 are analogous to Fig. 2.7a-c, with the total decision probabilities of Fig. 2.6a replaced by those of Fig. 2.6b. Also here, the abrupt changes observed in Fig. 2.7a-c were replaced by gradual transitions over the prey 1 threshold values x_1^* and x_1^{**} in Fig. 2.7d-f.

2.3 Conclusions and further research

In this chapter, we have developed a spatially explicit, individual-based model for one predator population feeding on two prey types, and used it to search for the optimal predator behavior with respect to the type of predator-prey encounters (sequential vs. mixed) and degree of predator omniscience (omniscient predators vs. predators with limited perception). We have shown that:

1. Because of local variations in prey densities, probability of acceptance of the less profitable prey under sequential encounters shifts from the zero-one rule to a gradually decreasing function (for which an explicit formula has been derived) giving rise to partial preferences. The corresponding predator functional response to the more profitable prey has a sigmoid-like form.

	Omniscient predators	Predators with limited perception (local rule)	Predators with limited perception (average rule)
Sequential encounters	$p_1 = 1$ $p_2(x_1) = 1$ if $x_1 < L_1$ $p_2(x_1) = 0$ if $x_1 > L_1$ $L_1 = S \dfrac{E_n^2 + \alpha T_h^2}{p_a^1(E_n^1 T_h^2 - E_n^2 T_h^1)}$	Rules for omniscience with $x_1 \mapsto \tilde{x}_1$ $L_1' = (N/S)L_1$	$p_1 = 1, \; p_2(x_1) = \sum_{\tilde{x}_1=0}^{[L_1']} P_2(\tilde{x}_1, x_1)$ $P_2(\tilde{x}_1, x_1) = \begin{cases} \binom{N-1}{\tilde{x}_1}\binom{S-N}{x_1-\tilde{x}_1} \big/ \binom{S-1}{x_1} & \text{if } \max\{0, x_1 - (S-N)\} \le \tilde{x}_1 \le \min\{x_1, N-1\} \\ 0 & \text{otherwise} \end{cases}$ $L_1' = (N/S)L_1$
Mixed encounters	$p_1 = 1$ $p_2 = 1$ if $x_1 < L_1$ $p_2 = 0$ if $x_1 > L_1$ $p_{31} = 0, \, p_{32} = 1$ if $x_1 + x_2 - x_1 x_2/S < L_2$ $p_{31} = 1, \, p_{32} = 0$ if $x_1 + x_2 - x_1 x_2/S > L_2$ $L_1 = S \dfrac{E_n^2 + \alpha T_h^2}{p_a^1(E_n^1 T_h^2 - E_n^2 T_h^1)}$ $L_2 = S \dfrac{(E_n^2 + \alpha T_h^2) - (p_a^1/p_a^2)(E_n^1 + \alpha T_h^1)}{p_a^1(E_n^1 T_h^2 - E_n^2 T_h^1)}$	Rules for omniscience with $x_i \mapsto \tilde{x}_i$ $S \mapsto N$ $L_i' = (N/S)L_i$	$p_1 = 1, \; p_2(x_1) = \sum_{\tilde{x}_1=0}^{[L_1']} P_2(\tilde{x}_1, x_1)$ $P_2(\tilde{x}_1, x_1) = \begin{cases} \binom{N-1}{\tilde{x}_1}\binom{S-N}{x_1-\tilde{x}_1} \big/ \binom{S-1}{x_1} & \text{if } \max\{0, x_1 - (S-N)\} \le \tilde{x}_1 \le \min\{x_1, N-1\} \\ 0 & \text{otherwise} \end{cases}$ $p_{31}(x_1, x_2) = 1 - p_{32}(x_1, x_2); \; p_{32}(x_1, x_2) = \sum_A P_{32}(\tilde{x}_1, \tilde{x}_2, x_1, x_2)$ $A = \{\tilde{x}_1, \tilde{x}_2 : \tilde{x}_1 + \tilde{x}_2 - \tilde{x}_1 \tilde{x}_2/N < L_2'\}$ $P_{32}(\tilde{x}_1, \tilde{x}_2, x_1, x_2) = \begin{cases} \binom{N-1}{\tilde{x}_1-1}\binom{S-N}{x_1-\tilde{x}_1}\binom{N-1}{\tilde{x}_2-1}\binom{S-N}{x_2-\tilde{x}_2} \big/ \binom{S-1}{x_1-1}\binom{S-1}{x_2-1} & \text{if } \max\{1, x_i - (S-N)\} \le \tilde{x}_i \le \min\{x_i, N\} \\ 0 & \text{otherwise} \end{cases}$ $L_i' = (N/S)L_i$

Table 2.1 Summary of the optimal predator behavior with respect to the type of encounters (sequential vs. mixed) and degree of predator omniscience (omniscient predators vs. predators with limited perception). *Note*. From Berec (2000) and Berec and Křivan (2000). See the main text for a detailed explanation. The symbol $A \mapsto B$ means here that A is replaced by B, and $[z]$ stands for the whole part of a real number z.

2. For omniscient predators, the zero-one rule optimal under sequential encounters shifts to abruptly changing partial preferences for both prey types when encounters become mixed.
3. The latter, in turn, become gradually changing partial preferences when predators are limited in their perception. Predators demonstrate gradually changing partial preferences for both prey types. In addition, these partial preferences depend on the population densities of both prey.

The corresponding formulas are summarized in Table 2.1. Note the distinction between the 'local' vs. 'average' rule: any predator considered in our article behaves optimally within its *local* perception range, whereas it behaves suboptimally when seen from the perspective of *average* predator behavior over the whole lattice where the zero-one rule is the optimal one. Our results thus contribute to the optimal foraging theory, as the majority of its models assume sequential encounters of omniscient predators with their prey (Schoener, 1971; Pulliam, 1974; Werner and Hall, 1974; Charnov, 1976).

Whether animals are omniscient or not may depend on the spatial scale. On the scale which corresponds to the range of animal perception, the assumption of omniscience is reasonable. As the spatial scale increases, predators rather become limited by their perception capabilities. Due to a variation in prey distribution across time and the environment, individual predators will face different prey densities in their respective perception ranges. Although all predators still change their diet at the same threshold abundances (formulas (2.16), and (2.27) and (2.28) for sequential and mixed encounters, respectively), these changes are no longer synchronized.

Another mechanism accounting for incomplete knowledge of predators on prey densities was presented by McNamara and Houston (1987) and Hirvonen et al (1999). These authors assumed that predators perceive their environment through encounters with prey, and also derived an analytical formula for partial preferences. These partial preferences were due to a variation in estimates of the encounter rate with more profitable prey. Both these studies and our work replace the assumption of predator omniscience by a weaker one, and reveal partial preferences within the classical optimal foraging framework. That said, and recognizing ubiquity of partial preferences in nature, perceptual limitations of predators achieve an appreciable increase in the realism of system description.

Consideration of a spatially explicit, individual-based model proves to be a good tool for our purposes, as it allows us to treat each individual separately and naturally define and work with its perception neighborhood. Within this IBM framework, our predator decision rule can be further extended to situations in which the neighborhood size varies with different predators. This would make the threshold values L'_1 and L'_2 individual-dependent. These threshold values and also L_1 and L_2 may also be made individual-dependent by separating the predator population into a number of groups, each having different parameters, e.g. the probability of successfully attacking more profitable prey, P^1_a. Both these extensions may be motivated by and made dependent on, e.g. predator age (gaining experience when aging), sex or variability in predator body size.

The predator decision rule based on local prey abundances $\tilde{x}_1$ and $\tilde{x}_2$ and specified by the quantities L_1' and L_2', though derived for a homogeneous system in which prey individuals are randomly distributed across the lattice, seems to be justified for prey individuals that disperse at a limited rate, too. For individual-based models involving demographic processes (i.e. births and deaths), spatial patterns occur on the lattice at low dispersal rates (de Roos et al, 1991; McCauley et al, 1993; Wilson et al, 1993). Yet there is a so-called characteristic spatial scale such that if one observes such a system in a window of a smaller scale, its dynamics are reminiscent of those of the system in which individuals are randomly distributed across the lattice. The characteristic spatial scale depends on the lattice size and the population dispersal rates, and is closely related to the area visited by individuals during their lifetime (de Roos et al, 1991). Hence, the limited-perception-based decision rule might be used even when prey individuals disperse at a limited rate, provided that the size of predator N-neighborhood is smaller than the characteristic spatial scale.

Predator-prey dynamics with mixed prey encounters

Population dynamical implications of mixed encounters of predators with their prey have not been explored yet. Rather, all the existing population dynamical studies coupled the classical predator–prey models with the classical sequential-encounter prey model of optimal foraging. Recall that for two prey types, the latter model predicts that either only more profitable prey is always attacked by predators upon encounter, or both prey types (always) are, with an abrupt change between these two strategies at a critical density of the more profitable prey. Empirical observations largely falsified these predictions and suggested that if these pure strategies exist at all, transition between them is rather gradual than abrupt. Whereas Křivan (1996) and Křivan and Sikder (1999) explored population dynamical implications of the abrupt change, Fryxell and Lundberg (1994), Fryxell and Lundberg (1998), and van Baalen et al (2001) focused on the effects of gradual transition. Gleeson and Wilson (1986) also considered the abrupt change, with an additional effect of inter-prey competition.

The generic model used by all the authors is

$$\dot{x}_1 = x_1 g_1(x_1, x_2) - \frac{p_1 \lambda_1 x_1}{1 + p_1 h_1 \lambda_1 x_1 + p_2 h_2 \lambda_2 x_2} y$$
$$\dot{x}_2 = x_2 g_2(x_1, x_2) - \frac{p_2 \lambda_2 x_2}{1 + p_1 h_1 \lambda_1 x_1 + p_2 h_2 \lambda_2 x_2} y \qquad (2.44)$$
$$\dot{y} = -my + \frac{e_1 p_1 \lambda_1 x_1 + e_2 p_2 \lambda_2 x_2}{1 + p_1 h_1 \lambda_1 x_1 + p_2 h_2 \lambda_2 x_2} y$$

In addition to the symbols introduced earlier, $g_i(x_1, x_2)$ is the prey i per capita growth rate in the absence of predation and m is the predator per capita death rate. Exponential, logistic, as well as Lotka-Volterra competition growth rates were used for g_i. Note that because of the ordinary differential equations framework, as opposed

to the IBMs studied above, x_i and y cannot be here interpreted as numbers of prey i and predator individuals, respectively, but rather as densities (numbers per area) of these populations. In this formulation, the critical prey 1 density for changing predator diet is $x_1^* = e_2/[\lambda_1(e_1h_2 - e_2h_1)]$. The formulas used to approximate gradually decreasing partial preferences for prey 2 were

$$p_2 = \frac{x_1^{*z}}{x_1^z + x_1^{*z}} \quad \text{and} \quad p_2 = \frac{1}{1 + e^{z(x_1 - x_1^*)}} \tag{2.45}$$

where z is a positive parameter.

The big picture emerging from these studies is as follows. Optimal diet choice of predators may both (partially) stabilize and destabilize dynamics of predator-prey systems, when compared to systems in which predators specialize on the more profitable prey type or have fixed preferences for both. Also, optimal foraging behavior of predators may promote coexistence of predators and prey as well as of competing prey types provided that superior competitor is at the same time more profitable. 'Suboptimal' predators with gradual changes in their diet have been shown to stabilize predator-prey systems to a larger extent than those with the abrupt change scenario. Moreover, these population dynamical studies demonstrated that the more gradual is the change, the larger is the region in parameter space in which stabilization is observed. This is due to the fact that the Holling type II functional response used in the population models and the gradually changing diet preferences of predators combine to give a sigmoid (Holling type III) functional response, which is known to have stabilizing effects in predator-prey models (Murdoch and Oaten, 1975). However, as the range of parameter values for which these stabilizing effects are observed is relatively narrow, optimal diet choice is unlikely to be the only stabilizing factor in trophic interactions.

Given the distinction between the diet choice rules derived under sequential and mixed predator-prey encounters, an interesting question is whether this distinction projects itself into dynamics of predator-prey systems. Whether proper consideration of mixed encounters in a model parallel to (2.44) modifies the predictions listed in the previous paragraph thus remains an open question. No doubt worth of further exploration, given that mixed encounters are likely to be much more common in nature than the sequential ones.

Food webs

A predator and a bunch of its prey is rarely an isolated unit. Rather, it is just a piece in a complex ecological network describing, in the simplest case, who eats whom in a species community. Such network is commonly referred to as a *food web*. Recently, Berec et al (2010) have shown that stability of such food webs, defined as the number or proportion of species surviving in the food web in a long run, can be significantly affected by the way predators choose their diet. Moreover, adaptive foraging was shown not to always lead to more complex food webs, contrary to

invariable predictions of recent modeling studies exploring the effect of consumer adaptivity in diet composition on food web complexity that adaptivity in foraging decisions of consumers makes food webs more complex (Berec et al, 2010, and references therein). Of the diet choice rules explored in this chapter, the considered food web model used only sequential encounters of predators with their prey. Not aware of whether mixed encounters enhance stability of predator-prey systems relative to sequential encounters (see the previous paragraph), we cannot say anything about how mixed encounters could affect complex food webs. So, addressing successfully the question posed in the previous paragraph is a necessary first step in throwing more light onto some more subtle issues of food web dynamics.

Part II
Allee effects and population extinction

When a population is small, or at low density, the classical view of population dynamics is that individuals are released from the constraints of intraspecific competition (Case, 2000). The fewer we are, the more each of us has, and the better we will prosper. However, this view, termed *negative density dependence*, lacks a crucial component: cooperation. Individuals of many species join forces to hunt, repel predators, survive unfavorable abiotic conditions, or overcome host defence mechanisms (Berec et al, 2007). Also, at higher densities, they have a better chance to locate or attract mates (Gascoigne et al, 2009). When there are too few of them, it may be that the individuals will each benefit from more resources, but in many cases they will also suffer from a lack of conspecifics. If the costs of being rare exceed the benefits, then the individuals may be less likely to reproduce and/or survive when rare – their fitness may be reduced. If this happens, we have an *Allee effect* (Courchamp et al, 2008).

Conceptually, we distinguish component-demographic and weak-strong Allee effects. *Component Allee effects* designate a positive relationship between any measurable component of individual fitness and either numbers or density of conspecifics (Stephens et al, 1999; Berec et al, 2007). For example, plants occurring at low densities can receive a reduced amount of pollen and hence suffer a lowered seed set, as observed in many plant taxa ranging from herbaceous temperate plants to tropical trees (Courchamp et al, 1999). By contrast, *demographic Allee effects* refer to a *positive density dependence* at the overall fitness level, traditionally measured by the per capita population growth rate (Stephens et al, 1999; Berec et al, 2007). For example, rare populations of the Glanville fritillary butterfly *Melitaea cinxia* grow at a reduced rate owing to reduced ability of females to find mates (Kuussaari et al, 1988). Although component Allee effects need not always result in demographic Allee effects, due to strong negative density dependence, observation of a demographic Allee effect is, by definition, always evidence of an underlying component Allee effect, though often hard to identify.

Whether a demographic Allee effect is weak or strong depends on the opposing strengths of positive density dependence (i.e. an Allee effect mechanism) and negative density dependence (i.e. intraspecific competition). As we have already accentuated in the introductory chapter, demographic Allee effects are characterized by a hump-shaped relationship between the per capita population growth rate and population size or density (Fig. 1.2). Provided that the growth rate gets negative when the population becomes rare, we speak of a *strong Allee effect*. The population size or density at which this happens is termed the *Allee threshold*; populations that drop below this threshold are declining and eventually go extinct. Allee thresholds have been observed in a number of species, including the gypsy moth *Lymantria dispar*, an invasive pest causing extensive defoliation of North American forests (Tobin et al, 2009). When the per capita population growth rate remains positive in rare populations (yet still hump-shaped) we say the *Allee effect is weak*, and there is no Allee threshold. A weak Allee effect was reported, e.g. for the wind-pollinated smooth cordgrass *Spartina alterniflora*, a plant species invading estuaries of the U.S. Pacific coast (Davis et al, 2004; Taylor et al, 2004). A comprehensive review of

the available evidence for Allee effects and their causative mechanisms has recently been conducted (Kramer et al, 2009).

Since demographic Allee effects (especially the strong ones) negatively affect rare populations, they have broad ramifications for applied ecology, be it conservation of endangered species, management of invasive pest species, or harvesting of economically important species (Berec et al, 2007; Courchamp et al, 2008). While a nightmare for conservation biologists, demographic Allee effects are a daydream for pest managers. Allee threshold is always a threat to endangered species. For example, a rescue operation of a population supposedly subject to an Allee effect was successfully attempted for the Hawaiian goose *Branta sandvicensis*, where nearly all scattered living individuals were collected and bred in captivity until the population had again reached a viable size (Kear and Berger, 1980). Conservation biologists thus attempt to minimize impacts of Allee effects so that extinctions are less likely. On the contrary, pest managers should consider Allee effects as a benefit in limiting establishment success or subsequent spread of an invasive species. For example, Liebhold and Bascompte (2003) suggested, using a mathematical model and data collected on the gypsy moth, that to eradicate its isolated populations it would suffice to remove slightly more than 80% of individuals as long as populations were relatively small; the nature does the rest. Allee effects are also discussed in relation to animal (re)introductions (Deredec and Courchamp, 2007), including releases of pest biocontrol agents (Hopper and Roush, 1993; Grevstad, 1999), for similar reasons. As regards harvesting of economically important species, mathematical models have convincingly demonstrated that species subject to strong demographic Allee effects might easily come to troubles and be easily extirpated if harvesting tactics do not take these Allee effects into account (Dennis, 1989; Kot, 2001). Examples of overharvesting abound, characterized by a lack of population recovery when harvesting is banned, and include species which presumably have an Allee effect, such as the Atlantic cod *Gadus morhua* (Hutchings, 2001; Courchamp et al, 2008).

This part consists of two chapters. In the first one, we study how Allee thresholds look like in models that incorporate diverse population structure. This endeavor is motivated by the prolific view and presentation of Allee thresholds as one-dimensional quantities (i.e. single-number population sizes or densities), obvious even from a swift fly over the existing literature on Allee effects and discussions with many researchers. This markedly deficient view stems from an overuse of unstructured population models, models that have also become an essence of the Allee effects theory. In the second chapter of this part, we explore various ways in which Allee effects in prey or predator populations may affect predator-prey dynamics. This latter issue is actually one of the most quickly evolving topics in the theory on Allee effects (Boukal et al, 2007; van Voorn et al, 2007; Boukal et al, 2008; Aguirrea et al, 2009; Berec, 2010; Pavlova et al, 2010; Verdy, 2010; McLellan et al, 2010; Wang et al, 2011)

Chapter 3
Allee threshold

Strong demographic Allee effects, triggered by sufficiently strong component Allee effects, give rise to a threshold population size or density, below which the population is most likely doomed to extinction and above which it most likely persists and approaches a system attractor. This threshold population size or density is commonly referred to as the *Allee threshold*. View and presentation of Allee thresholds as one-dimensional quantities (i.e. single-number population sizes or densities), almost exclusive in the literature on Allee effects, is deficient and stems from an overuse of unstructured population models, models that have also become an essence of the Allee effects theory. In this chapter, we are going to dispel this view and show how Allee thresholds look like in models that incorporate diverse population structure. We are also interested in what implications for population management this may have.

3.1 From sameness to age to sex: Allee thresholds and population structure

When attempting to model dynamics of any population, one of the first decisions we need to make is what structure the model population should have. Should we structure it by age, developmental stage, sex, space, genotype, or anything else, if any? The answer obviously depends on the system we are to model, scientific questions being asked, available information on the system, and the detail we require for the answers. Here we mainly focus on continuous-time deterministic population models, first the unstructured ones, and then population models structured by age and/or sex. Allee thresholds in some discrete-time deterministic population models, stochastic population models and models structured with respect to some other criteria are briefly discussed at the end of this chapter.

Unstructured population models

The simplest (and classical) situation arises when we assume that the only state variable of interest is the total population density. Models of this kind are often referred to as *unstructured*, since the population is not structured in any obvious way. Assuming the population to grow logistically when large and decline due to a mate-finding Allee effect when small, a population model that fits these assumptions might be as follows:

$$\frac{dN}{dt} = bN\frac{N}{N+\theta} - (d+d_1N)N \tag{3.1}$$

Here b and d are intrinsic per capita birth and death rate, respectively, and θ and d_1 scale the strength of mate-finding Allee effect and negative density dependence, respectively. Indeed, with all parameters positive, the per capita birth rate $bN/(N+\theta)$ declines with decreasing population density N (mate-finding Allee effect = positive density dependence in reproduction due to enhanced difficulty to find mates at low population densities) while the per capita mortality rate $d + d_1N$ increases with increasing population density N (negative density dependence in survival due to overcrowding), with the overall per capita population growth rate demonstrating a hump-shaped form on the interval $(-\theta,\infty)$; see Box 3.1. Although the per capita birth rate $bN/(N+\theta)$ can be thought of as a phenomenological model of a mate-finding Allee effect, there is a clear mechanistic rationale behind it (Box 3.2).

Box 3.1 Shape of the per capita growth rate of the model (3.1)

Denoting

$$g(N) = \frac{1}{N}\left(\frac{dN}{dt}\right) = b\frac{N}{N+\theta} - d - d_1N$$

we have $g''(N) < 0$ on the interval $(-\theta,\infty)$, and

$$\lim_{N\to-\theta+} g(N) = \lim_{N\to\infty} g(N) = -\infty$$

So the per capita population growth rate of the model (3.1) is hump-shaped on the interval $(-\theta,\infty)$. In addition, on this interval, it attains its maximum at

$$N_{\max} = -\theta + \sqrt{\frac{b\theta}{d_1}}$$

The model (3.1) has no or two positive equilibria if $\theta > 0$. These two cases correspond to population extinction from any initial density and to a strong demographic Allee effect, respectively. Indeed, positive equilibria are solutions of the quadratic equation

$$N^2 - \left(\frac{b-d}{d_1} - \theta\right)N + \frac{d\theta}{d_1} = 0 \tag{3.2}$$

As $d\theta/d_1 > 0$, the situation with one positive and one negative solution cannot occur. Standard phase-line analysis shows that the extinction equilibrium $N^* = 0$ is locally stable if $\theta > 0$, and if the two positive equilibria exist, the low-density equilibrium

$$N^* \equiv A = \frac{(b - d - d_1\theta) - \sqrt{(b - d - d_1\theta)^2 - 4d_1 d\theta}}{2d_1} \tag{3.3}$$

is unstable and the high-density equilibrium

$$N^* \equiv K = \frac{(b - d - d_1\theta) + \sqrt{(b - d - d_1\theta)^2 - 4d_1 d\theta}}{2d_1} \tag{3.4}$$

is locally stable. Moreover, the low-density equilibrium A divides the phase-line into the areas of attraction of the extinction equilibrium (below A) and the high-density equilibrium K (above A). Thus, the low-density equilibrium A corresponds to the Allee threshold of the model (3.1) and the high-density equilibrium K corresponds to the environmental carrying capacity of the model (3.1). In unstructured population models, Allee thresholds are thus single numbers.

Box 3.2 A mechanistic derivation of the per capita birth rate $bN/(N + \theta)$

Mate-finding Allee effects concern the core process of sexual reproduction – mating, and so it is only natural to consider mate-finding Allee effects within the context of two-sex population models. Consider the following age- and sex-structured population, with a simplified reproduction phase: juveniles have to mature to become adults and mate, males and females that are ready to mate have to search for each other, form a pair and, upon successful mating, split and rest for some time, to give birth (females), and search again. We note that appropriate models can be developed for more complex life histories, too. We distinguish six state variables: juveniles J, searching male M_s and female F_s adults, mating couples C, and resting male M_r and female F_r adults. These may change dynamically as follows:

$$\begin{aligned}
\frac{dJ}{dt} &= b\frac{1}{t_F}F_r - d_J J - mJ \\
\frac{dM_s}{dt} &= -\alpha M_s F_s - d_M M_s + d_F C + \frac{1}{t_M}M_r + \mu m J \\
\frac{dF_s}{dt} &= -\alpha M_s F_s - d_F F_s + d_M C + \frac{1}{t_F}F_r + (1 - \mu)mJ \\
\frac{dC}{dt} &= \alpha M_s F_s - d_M C - d_F C - \frac{1}{t_C}C \\
\frac{dM_r}{dt} &= \frac{1}{t_C}C - \frac{1}{t_M}M_r - d_M M_r \\
\frac{dF_r}{dt} &= \frac{1}{t_C}C - \frac{1}{t_F}F_r - d_F F_r
\end{aligned} \tag{3.5}$$

Model parameters are summarized in the following table:

Parameter	Meaning
b	Clutch size
d_J	Mortality rate of juveniles
d_M	Mortality rate of adult males
d_F	Mortality rate of adult females
α	Rate at which a male and a female meet and mate
m	Maturation rate of juveniles
μ	Sex ratio at birth (proportion males)
t_C	Mean time spent in a couple
t_M	Mean time spent as resting male
t_F	Mean time spent as resting female

Let us now assume that maturation is very fast relative to the mortality rate d_J of juveniles. Introducing the dimensionless time τ, $\tau = d_J t$, and dividing the first equation of the model (3.5) by the maturation rate m, we obtain

$$\varepsilon \frac{dJ}{d\tau} = \frac{b}{mt_F}F_r - \varepsilon J - J$$

where we have denoted $\varepsilon = d_J/m$. Our assumption can now be rephrased as $m \gg d_J$ or $0 < \varepsilon \ll 1$. Setting $\varepsilon = 0$ and solving for J, we get

$$J = \frac{b}{mt_F}F_r$$

Substituting this into the model (3.5) and returning to the unscaled time, we obtain the following reduced system

$$\frac{dM_s}{dt} = -\alpha M_s F_s - d_M M_s + d_F C + \frac{1}{t_M}M_r + \mu b \frac{1}{t_F}F_r$$

$$\frac{dF_s}{dt} = -\alpha M_s F_s - d_F F_s + d_M C + \frac{1}{t_F}F_r + (1-\mu)b \frac{1}{t_F}F_r$$

$$\frac{dC}{dt} = \alpha M_s F_s - d_M C - d_F C - \frac{1}{t_C}C \qquad (3.6)$$

$$\frac{dM_r}{dt} = \frac{1}{t_C}C - \frac{1}{t_M}M_r - d_M M_r$$

$$\frac{dF_r}{dt} = \frac{1}{t_C}C - \frac{1}{t_F}F_r - d_F F_r$$

solutions of which approximate those of the original system (3.5). This technique of multiple (slow and fast) time scales is based on singular perturbation theory (Hoppensteadt, 1974; O'Malley, 1991; Kooi et al, 2002, and references therein).

Similarly, assuming fast mating implies $C/t_C = \alpha M_s F_s$ and the system (3.6) reduces to four equations:

$$\frac{dM_s}{dt} = -\alpha M_s F_s - d_M M_s + \frac{1}{t_M} M_r + \mu b \frac{1}{t_F} F_r$$

$$\frac{dF_s}{dt} = -\alpha M_s F_s - d_F F_s + \frac{1}{t_F} F_r + (1-\mu) b \frac{1}{t_F} F_r$$

$$\frac{dM_r}{dt} = \alpha M_s F_s - \frac{1}{t_M} M_r - d_M M_r$$

$$\frac{dF_r}{dt} = \alpha M_s F_s - \frac{1}{t_F} F_r - d_F F_r$$

(3.7)

Adding equations for males ($M = M_s + M_r$) and for females ($F = F_s + F_r$), one gets two equations:

$$\frac{dM}{dt} = \mu b \frac{1}{t_F} F_r - d_M M$$

$$\frac{dF}{dt} = (1-\mu) b \frac{1}{t_F} F_r - d_F F$$

(3.8)

To close the system (3.8), we need to express F_r as a function of M and F. To do that, we assume that females divide their reproductive time T into time for searching for males T_s and time for resting T_r (which includes pregnancy, oviposition, etc.). Then, the number of matings ϕ_T per T per female can be expressed as

$$\phi_T = \alpha M_s (T - T_r) = \alpha M_s (T - \phi_T t_F)$$

where αM_s is the rate at which a female meets males, and $T_r = \phi_T t_F$. Solving this equation for ϕ_T/T, the female mating rate or the number of matings per unit time, gives

$$\frac{\phi_T}{T} = \frac{\alpha M_s}{1 + \alpha M_s t_F}$$

If the female mean resting time t_F is small relative to the total resting time T_r, the probability that an average female is currently in its resting stage can be approximated as T_r/T. Hence, approximately, $F_r = F T_r/T = F t_F \phi_F/T$ which in turn implies

$$\frac{F_r}{t_F} = F \frac{\phi_T}{T} = F \frac{\alpha M_s}{1 + \alpha M_s t_F}$$

In addition, if we assume virtually no resting time for males, then $M \approx M_s$ and we have

$$\frac{F_r}{t_F} = F \frac{\alpha M}{1 + \alpha M t_F} = \frac{1}{t_F} F \frac{M}{M + \theta}$$

(3.9)

where we denoted $\theta = 1/(\alpha t_F)$. Incorporating the formula (3.9) into the model (3.8), we get

$$\frac{dM}{dt} = \mu\tilde{b}F\frac{M}{M+\theta} - d_M M$$
$$\frac{dF}{dt} = (1-\mu)\tilde{b}F\frac{M}{M+\theta} - d_F F \tag{3.10}$$

where we assigned $\tilde{b} = b/t_F$. Interestingly and correctly, $\tilde{b}$ has units of clutch size / mean resting time of a female and hence has the meaning of the maximum birth rate the female can achieve (when permanently mated).

Finally, assuming $\mu = 0.5$, $d_M = d_F = d$, and $M(0) = F(0)$, it is $M(t) = F(t)$ for any $t > 0$, since

$$\frac{d(M-F)}{dt} = -d(M-F) \tag{3.11}$$

and hence

$$M(t) - F(t) = [M(0) - F(0)]e^{-dt}, \, t > 0 \tag{3.12}$$

This implies that $M = F = N/2$ where $N = M + F$, and the model (3.10) eventually reduces to a single equation

$$\frac{dN}{dt} = \bar{b}N\frac{N}{N+\bar{\theta}} - dN \tag{3.13}$$

where we denoted $\bar{b} = \tilde{b}/2$ and $\bar{\theta} = 2\theta$. We note that we did not consider any negative density dependence in mortality rate in this derivation, but by replacing d_X, $X = M$ or F, with $d_X + d_1 N$ in any relevant above equation we eventually get the model (3.1).

The two positive equilibria A and K merge and cease to exist in a saddle-node bifurcation when the discriminant of the quadratic equation (3.2) equals zero, which happens at

$$\theta_c = \frac{(\sqrt{b} - \sqrt{d})^2}{d_1} \tag{3.14}$$

The extinction equilibrium $N^* = 0$ becomes globally stable beyond this critical mate-finding Allee effect strength, i.e. for $\theta > \theta_c$. For $\theta < \theta_c$, as θ increases in the model (3.1), the Allee threshold increases since $\partial A/\partial\theta > 0$, the environmental carrying capacity decreases since $\partial K/\partial\theta < 0$, and the population resilience (maximum perturbation from the locally stable equilibrium K that subsequently vanishes, here distance between K and A) thus declines (see also Fig. 3.1). This paragraph thus suggests that Allee effects destabilize population dynamics.

Our choice of the model (3.1) as a tool to explore Allee thresholds in unstructured population models is just one of the many that can be developed for the same purpose. But even though alternative model formulations can be structurally quite different and involve component Allee effects other than those due to mate finding (Courchamp et al, 2008), their properties remain analogous to what we present here.
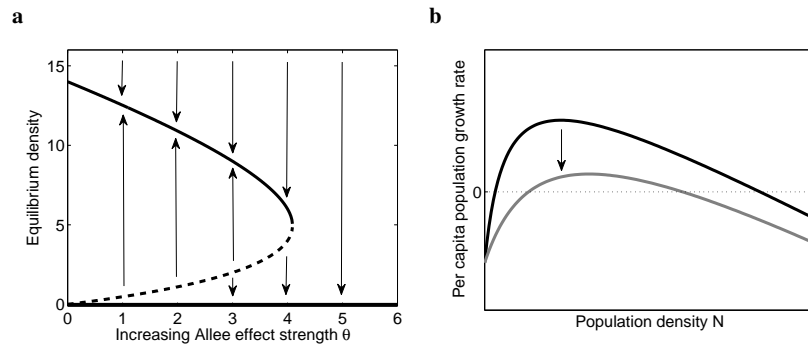
Fig. 3.1 Many unstructured population models with a strong demographic Allee effect share the property that changes in the Allee threshold and the environmental carrying capacity implied by changes in a model parameter are negatively correlated (a; arrows indicate how population densities dynamically change in time). This is because in those models an increase in the component Allee effect strength results in a decrease in the per capita population growth rate over the whole range of population densities (b; component Allee effect strength increases in the arrow direction). Parameter values of the model (3.1): $b = 2$, $d = 0.6$, $d_1 = 0.1$, hence $\theta_c = 4.09$; in panel (b), $\theta = 1$ (black line) and $\theta = 3$ (gray line)

In addition, although our model (3.1) demonstrated a strong demographic Allee effect for any positive value of θ, unstructured population models have been formulated that produce weak demographic Allee effects once the underlying component Allee effect is relatively weak and strong demographic Allee effects once it is strong enough; for an example, see Berec et al (2007). Still, the absence of any population structure in these models is quite a simplification and we now consider some more detailed population models to see what other forms the Allee threshold might adopt.

Age

Age is presumably the first structural element ever considered in population models, largely as a consequence of human demography and its early interest in life tables, recognizing that both the per capita birth and death rates are more often than not age-dependent (Caswell, 2001; Iannelli et al, 2005, and references therein). If an age-structured model contains a finite number of groups and these groups rather correspond to some well-defined developmental stages of an individual, such as eggs, larvae, pupae, and adults, we sometimes speak of stage-structured models.

We consider here the simplest extension of the model (3.1) that considers an age structure, namely two age (or stage) classes corresponding to juveniles and adults:

$$\frac{dJ}{dt} = bA\frac{A}{A+\theta} - mJ - (d + d_1 N)J$$

$$\frac{dA}{dt} = mJ - (d + d_1 N)A$$

(3.15)

Here A is the density of adults, J is the density of juveniles, and m is the maturation rate; $N = J + A$ is the total population density. Again, we assume a mate-finding Allee effect and a negative density dependence in survival. We note that the model (3.15) can be further modified in a number of ways, including age-specific mortality rates, density dependence in the maturation rate, etc.

Standard analysis of the model (3.15) reveals that the extinction equilibrium $A^* = J^* = 0$ is locally stable for any $\theta > 0$. In addition, extensive numerical simulations show that if $\theta > 0$ is not too large, there are two positive equilibria, of which the one closer to the extinction equilibrium is unstable (saddle point) and the more distant one is locally stable. As θ increases, the two positive equilibria approach one another, merge and cease to exist in a saddle-node bifurcation at a critical value θ_c. The Poincaré-Bendixson theorem can be used to show that the extinction equilibrium becomes globally stable as soon as $\theta > \theta_c$.

So up to now no real difference from the unstructured model (3.1). But whereas the locally stable positive equilibrium (if it exists) is an attractor (corresponding to the environmental carrying capacity) for any sufficiently large population, the concept of Allee threshold is not that straightforward here as it was for the unstructured model (3.1). As the state space is now two-dimensional, we cannot speak of what lies below the unstable positive equilibrium and what lies above it. But the unstable equilibrium of the age-structured model (3.15) is a saddle point. So a promising candidate for the Allee threshold might here be its stable manifold. If it divides the state space into an attraction area for the extinction equilibrium and an attraction area for the locally stable positive equilibrium, and the union of these areas and the stable manifold equals the whole state space, then the stable manifold is a natural way of how to define the Allee threshold for the age-structured model (3.15). This is indeed the case (Fig. 3.2 and Box 3.3).

What does this Allee threshold imply for the risk of population extinction? Note first that it is compact, i.e. closed and bounded (see also Fig. 3.3). This implies that a sufficiently high density of juveniles or adults (one can even be zero) ensures population persistence. On the other hand, too low densities of both juveniles and adults bring about population extinction. As Figs. 3.2 and 3.3 suggest, the population can go extinct even if either the juvenile density or the adult density lies above the respective component of the unstable positive equilibrium, provided that the other density is well below the other component.

The existence and compactness of the Allee threshold has been rigorously proven for a wide class of structured population models with any finite number of compartments (Schreiber, 2004). Writing a generic continuous-time population model as $dx/dt = xG(x)$ where $G(x)$ are $k \times k$ matrices, one requires, among other things, that $\exp(G(0))$ is primitive and that any entry $g_{ij}(x)$ of $G(x)$ is either density-independent or positively density-dependent, i.e. that no negative density depen-
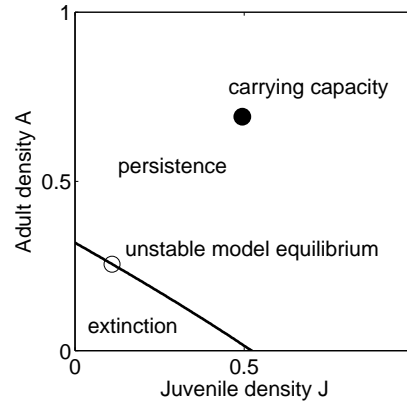
Fig. 3.2 Allee threshold in an age-structured population. A compact extinction boundary delimits the areas of population extinction (below) and persistence (above) in the state space of juvenile and adult densities in the age-structured population model (3.15) with a mate-finding Allee effect. Parameter values: $b = 3$, $d = 0.3$, $\theta = 1$, $d_1 = 0.35$, $m = 1$

dence acts and the system is subject to at least one component Allee effect. Schreiber (2004) applied his theorem to a model of an age-structured population preyed upon by a generalist predator with a type II functional response. This type of predation creates a component Allee effect in prey survival (Gascoigne and Lipcius, 2004; Berec et al, 2007, see also Chapter 4). Interestingly, for our model (3.16) with a mate-finding Allee effect the matrix $\exp(G(0))$ is not primitive (Box 3.3). Leaving out negative density dependence, this suggests that the class of structured population models for which the Allee threshold exists and is compact can be much wider.

Box 3.3 Analysis of a density-independent version of the model (3.15)

The model (3.15) is hardly tractable analytically. Therefore, we analyze here its density-independent version

$$\frac{dJ}{dt} = bA\frac{A}{A + \theta} - mJ - d_J J$$
$$\frac{dA}{dt} = mJ - d_A A \tag{3.16}$$

in which we moreover consider age-dependent mortality rates. Denoting $D = d_A(1 + d_J/m)$, the model (3.16) has a unique interior equilibrium

$$A^* = \frac{D\theta}{b - D} \quad \text{and} \quad J^* = \frac{d_A}{m}A^* \tag{3.17}$$

provided that $b > D$. The Jacobian $\mathbf{J}$ of the model (3.16), evaluated at the extinction equilibrium $J = A = 0$ (which always exists), is

$$\mathbf{J} = \begin{pmatrix} -m - d_J & 0 \\ m & -d_A \end{pmatrix} \tag{3.18}$$

Hence the extinction equilibrium is always locally stable, due to the mate-finding Allee effect. For the interior equilibrium (J^*, A^*), we have

$$\mathbf{J} = \begin{pmatrix} -m - d_J & D(2 - D/b) \\ m & -d_A \end{pmatrix} \tag{3.19}$$

Since $\det \mathbf{J} = mD(D/b - 1) < 0$, the interior equilibrium, if it exists, is a saddle point – both eigenvalues of $\mathbf{J}$ are real, one positive,

$$\lambda_1 = \frac{1}{2} \left[-(m + d_J + d_A) + \sqrt{(m + d_J + d_A)^2 - 4mD(D/b - 1)} \right] \tag{3.20}$$

and one negative,

$$\lambda_2 = \frac{1}{2} \left[-(m + d_J + d_A) - \sqrt{(m + d_J + d_A)^2 - 4mD(D/b - 1)} \right] \tag{3.21}$$

The right eigenvector corresponding to the eigenvalue λ_i $(i = 1, 2)$ is

$$v_i = \begin{pmatrix} 1 \\ \dfrac{m}{d_A + \lambda_i} \end{pmatrix} \tag{3.22}$$

Since the eigenvectors v_1 and v_2 are respectively tangent to the unstable and stable manifolds of the interior equilibrium (J^*, A^*) at this equilibrium, they can be used to approximate these manifolds, e.g. using the technique proposed by van Voorn et al (2007): for a small $\varepsilon > 0$, the model (3.16) is run forward in time from $(J^*, A^*) \pm \varepsilon v_1$ to get an approximation of the unstable manifold and backward in time from $(J^*, A^*) \pm \varepsilon v_2$ to get an approximation of the stable manifold. Figure 3.3 exemplifies this, for the same parameter values as in Fig. 3.2.

Numerical simulations show that these results stay unchanged once a negative density dependence is added, as is the case of our model (3.15).

Finally, writing the model (3.16) as $dx/dt = xG(x)$, where $x = (J, A)$, the matrix G becomes

$$G(J, A) = \begin{pmatrix} -m - d_J & bA/(A + \theta) \\ m & -d_A \end{pmatrix} \tag{3.23}$$
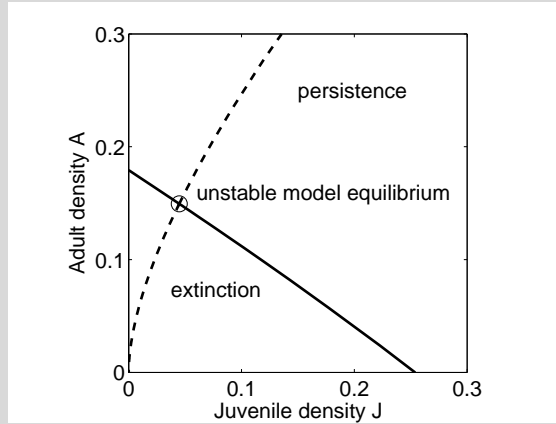
Fig. 3.3 Allee threshold in an age-structured population. The stable manifold of the unstable equilibrium (solid line) delimits the areas of population extinction (below) and persistence (above) in the state space of juvenile and adult densities in the age-structured population model (3.16) with a mate-finding Allee effect; dashed line is the unstable manifold of the unstable equilibrium. Parameter values: $b = 3$, $d_J = d_A = 0.3$, $\theta = 1$, $m = 1$

For this matrix,

$$\exp(G(0,0)) = \exp\left(\begin{pmatrix} -m - d_J & 0 \\ m & -d_A \end{pmatrix}\right) =$$

$$= \begin{pmatrix} \exp(-m - d_J) & 0 \\ m\dfrac{\exp(-m - d_J) - \exp(-d_A)}{(-m - d_J) - (-d_A)} & \exp(-d_A) \end{pmatrix} \qquad (3.24)$$

Although $\exp(G(0,0))$ is non-negative, there is no integer n for which $[\exp(G(0,0))]^n$ is positive. This implies that $\exp(G(0,0))$ is not primitive, as required by the Schreiber (2004)'s theorem to hold.

Sex

Sex is ubiquitous – virtually all higher organisms, as well as many lower organisms, reproduce sexually. Since sex brings about a variety of dimorphisms in behavior and demography (often related to mate-finding via sexual selection) that might profoundly affect population dynamics, it needs to be considered when appropriate. These dimorphisms include differences between males and females in survivorship (Miller et al, 2007; Boukal et al, 2008) and dispersal (Wickman and Rutowski, 1999;

Perrin and Mazalov, 2000), and biases in the sex ratio at birth (Ewen et al, 2001). In addition, males and females have to seek for one another to mate, in the sea of diverse mating systems (Shuster and Wade, 2003), so mate-finding Allee effects are intimately tied to mating (Gascoigne et al, 2009).

Here we examine the simplest extension of the model (3.1) that accounts for sex structure and considers male and female populations only. The core of this model goes back to Kendall (1949) and Goodman (1953), and the model we are going to present is derived in Box 3.2:

$$\frac{dM}{dt} = \mu b F \frac{M}{M+\theta} - (d+d_1 N)M$$
$$\frac{dF}{dt} = (1-\mu)bF \frac{M}{M+\theta} - (d+d_1 N)F$$

$$(3.25)$$

Here M is the density of males, F is the density of females, and μ is the sex ratio at birth (proportion males); $N = M + F$ is the total population density. Again, we assume a mate-finding Allee effect and a negative density dependence in survival. We note that the model (3.25) can further be modified in a number of ways, including sex-specific mortality, density dependence in μ, etc.

As in the previous two cases, standard analysis of the model (3.25) shows that the extinction equilibrium $M^* = F^* = 0$ is locally stable for any $\theta > 0$. In addition, extensive numerical simulations show that if $\theta > 0$ is not too large, there are two positive equilibria, of which the one closer to the extinction equilibrium is unstable (saddle point) and the more distant one is locally stable. As θ increases, the two positive equilibria approach one another, merge and cease to exist in a saddle-node bifurcation at a critical value θ_c. The Poincaré-Bendixson theorem can be used to show that the extinction equilibrium becomes globally stable as soon as $\theta > \theta_c$.

Whereas the locally stable positive equilibrium is again an attractor (corresponding to the environmental carrying capacity) for any population comprising sufficiently large numbers of males and females, the concept of Allee threshold can in principle be explored here in the same way as in the case of age-structured models, that is, via exploring the stable manifold of the unstable positive equilibrium. Numerical simulations suggest that the stable manifold is not compact here (Fig. 3.4). This makes perfect sense as zero density of males or females necessarily means no mating and hence inevitable extinction of the other sex. Note that the hyperbolic Allee threshold contrasts with the straight line that arises if the Allee threshold of the corresponding unstructured model

$$\frac{dN}{dt} = \frac{b}{2} N \frac{N}{N+2\theta} - (d+d_1 N)N \qquad (3.26)$$

is projected on the male-female state space (Fig. 3.4). This unstructured model has been gained by adding two equations of the model (3.25), assuming $\mu = 0.5$ and $M(0) = F(0)$ and hence $M = F = N/2$ for any $t > 0$. The Allee threshold of the unstructured model (3.26) is

$$A_u = \frac{(b/2 - d - 2d_1\theta) - \sqrt{(b - d - 2d_1\theta)^2 - 8d_1 d\theta}}{2d_1} \tag{3.27}$$
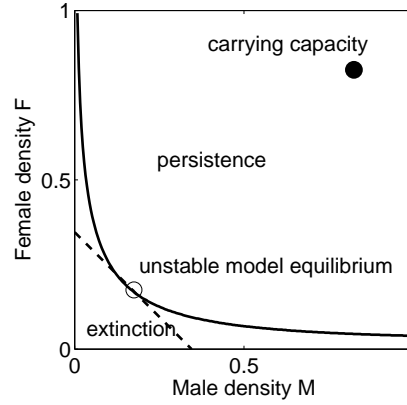
Fig. 3.4 Allee threshold in a sex-structured population. A hyperbolic extinction boundary delimits the areas of population extinction (below) and persistence (above) in the state space of male and female densities in the sex-structured population model (3.25) with a mate-finding Allee effect. The dashed line corresponds to the Allee threshold of the unstructured model (3.26), projected on the male-female state space; it is the straight line $M + F = A_u$ connecting points $(0, A_u)$ and $(A_u, 0)$, where A_u is the Allee threshold of the unstructured model (3.26). Common parameter values: $\mu = 0.5$, $b = 3$, $d = 0.1$, $\theta = 1$, $d_1 = 0.35$

There is currently no result equivalent to that of the Schreiber (2004)'s theorem for non-compact Allee thresholds. So the question of how the Allee threshold generally looks like in sex-structured models is still open. But before any such attempt is made, one needs to think of what constitutes here more than two model classes, the question of no difficulty in age-structured models. We show in Section 3.2 how the Allee threshold (hyperbolic boundary) in the male-female state space varies with diverse mate-finding strategies; although qualitatively the same as here, its location varies. Also, we show in Section 3.3 how the Allee threshold looks like when males and females are allowed to form long-time pair bonds, the situation not considered here as here males and females are just assumed to meet, mate, and say goodbye. But none of these extensions addresses the question of more than two sex classes.

Box 3.4 Analysis of a density-independent version of the model (3.25)

The model (3.25) is hardly tractable analytically. Therefore, we analyze here its density-independent version

$$\frac{dM}{dt} = \mu b F \frac{M}{M+\theta} - d_M M$$
$$\frac{dF}{dt} = (1-\mu) b F \frac{M}{M+\theta} - d_F F \tag{3.28}$$

in which we moreover consider sex-dependent mortality rates. Denoting $D = d_F/[(1-\mu)b]$, the model (3.28) has a unique interior equilibrium

$$M^* = \frac{D\theta}{1-D} \quad \text{and} \quad F^* = \frac{(1-\mu)d_M}{\mu d_F} M^* \tag{3.29}$$

provided that $D < 1$, i.e. $(1-\mu)b > d_F$. The Jacobian $\mathbf{J}$ of the model (3.28), evaluated at the extinction equilibrium $M = F = 0$ (which always exists), is

$$\mathbf{J} = \begin{pmatrix} -d_M & 0 \\ 0 & -d_F \end{pmatrix} \tag{3.30}$$

Hence the extinction equilibrium is always locally stable, due to the mate-finding Allee effect. For the interior equilibrium (M^*, F^*), we have

$$\mathbf{J} = \begin{pmatrix} -d_M + d_M b^2 (1-D) & d_F \mu/(1-\mu) \\ d_M b^2 (1-D)(1-\mu)/\mu & 0 \end{pmatrix} \tag{3.31}$$

Since $\det \mathbf{J} = -d_F d_M b^2 (1-D) < 0$, the interior equilibrium, if it exists, is a saddle point – both eigenvalues of $\mathbf{J}$ are real, one positive,

$$\lambda_1 = \frac{1}{2} \left[-d_M + d_M b^2 (1-D) + \sqrt{(-d_M + d_M b^2 (1-D))^2 + 4 d_F d_M b^2 (1-D)} \right] \tag{3.32}$$

and one negative,

$$\lambda_2 = \frac{1}{2} \left[-d_M + d_M b^2 (1-D) - \sqrt{(-d_M + d_M b^2 (1-D))^2 + 4 d_F d_M b^2 (1-D)} \right] \tag{3.33}$$

The right eigenvector corresponding to the eigenvalue λ_i $(i = 1,2)$ is

$$v_i = \begin{pmatrix} 1 \\ \dfrac{d_M b^2 (1-D)(1-\mu)/\mu}{\lambda_i} \end{pmatrix} \tag{3.34}$$

Since the eigenvectors v_1 and v_2 are respectively tangent to the unstable and stable manifolds of the interior equilibrium (M^*, F^*) at this equilibrium, they can be used to approximate these manifolds, e.g. using the technique proposed by van Voorn et al (2007): for a small $\varepsilon > 0$, the model (3.28) is run forward in time from $(M^*, F^*) \pm \varepsilon v_1$ to get an approximation of the unstable

manifold and backward in time from $(M^*, F^*) \pm \varepsilon v_2$ to get an approximation of the stable manifold. Figure 3.5 exemplifies this, for the same parameter values as in Fig. 3.4.

Numerical simulations show that these results stay unchanged once a negative density dependence is added, as is the case of our model (3.25).
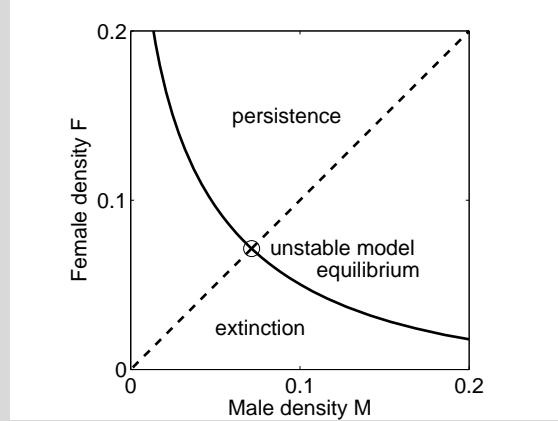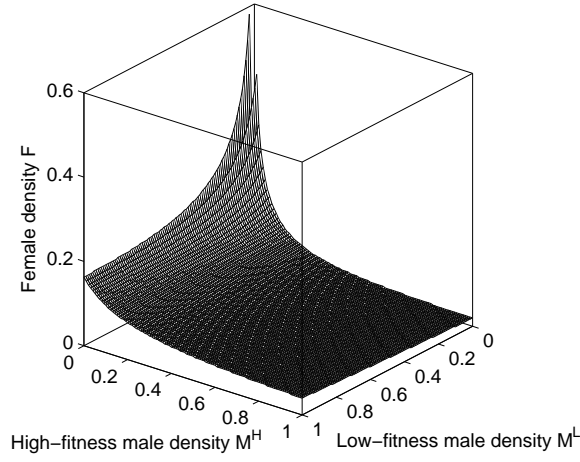

Fig. 3.5 Allee threshold in a sex-structured population. The stable manifold of the unstable equilibrium (solid line) delimits the areas of population extinction (below) and persistence (above) in the state space of male and female densities in the sex-structured population model (3.25) with a mate-finding Allee effect; dashed line is the unstable manifold. Parameter values: $\mu = 0.5$, $b = 3$, $d_M = d_F = 0.1$, $\theta = 1$

A really simple extension in this direction is to consider two male types, a low-fitness one and a high-fitness one, and only one female type. Low-fitness males and high-fitness males are assumed to die at rates d_M^L and d_M^H, respectively, with $d_M^L > d_M^H$; females are assumed to die at rate d_F. Upon mating, females give birth at rates b^L and b^H, depending on the male type. Any offspring becomes male or female with probability μ and $1 - \mu$, respectively. If a low-fitness male fathers the offspring, male offspring become of the low-fitness type with probability β and of high-fitness type with probability $1 - \beta$; the converse probabilities are applied to male progeny fathered by high-fitness males. The population model is then as follows:

$$\frac{dM^L}{dt} = \mu \left(\beta b^L \frac{M^L}{M^L + M^H + \theta} + (1-\beta)b^H \frac{M^H}{M^L + M^H + \theta} \right) F - (d_M^L + d_1 N)M^L$$

$$\frac{dM^H}{dt} = \mu \left(\beta b^H \frac{M^H}{M^L + M^H + \theta} + (1-\beta)b^L \frac{M^L}{M^L + M^H + \theta} \right) F - (d_M^H + d_1 N)M^H$$

$$\frac{dF}{dt} = (1-\mu) \left(b^H \frac{M^H}{M^L + M^H + \theta} + b^L \frac{M^L}{M^L + M^H + \theta} \right) F - (d_F + d_1 N)F$$

$$\tag{3.35}$$

where $N = M^L + M^H + F$ and d_1 denotes the strength of negative density dependence, for simplicity the same for all three model classes. We do not carry out any detailed analysis of this model here. Instead, we just exemplify the resulting Allee threshold in Fig. 3.6. As might be expected, this Allee threshold is just a 3D extension of the 2D case studied above; indeed, both the side projections with one or the other male type absent correspond to Fig. 3.4.

Fig. 3.6 Allee threshold in a sex-structured population. A hypersurface delimits the areas of population extinction (below) and persistence (above) in the three-dimensional space of densities of two male types and one female type in the sex-structured population model (3.35) with a mate-finding Allee effect. Parameter values: $\mu = 0.5$, $b^L = 1.5$, $b^H = 2$, $d_M^L = 0.12$, $d_M^H = 0.1$, $d_F = 0.1$, $\theta = 0.5$, $d_1 = 0.35$, $\beta = 0.95$

The model (3.25) can also be used to show that it is impossible to rank pest control tactics in any absolute manner (i.e. dependent only on the total population density); rather, pest control tactics can be tailored to the actual (ratio of) male and female densities (Boukal and Berec, 2009). To see this, consider the following two-sex model:

$$\frac{dM}{dt} = \mu bF \frac{M}{M+S+\theta} - (d_M + d_C)M$$

$$\frac{dF}{dt} = (1-\mu)bF \frac{M}{M+S+\theta} - d_F F \qquad (3.36)$$

Here d_C denotes an additional male mortality rate due to a density-independent culling, such as when sex pheromone-baited traps are deployed en mass to attract and kill males of some insect species (Yamanaka, 2007). In addition, S represents a constant level of sterile males released into the population, assuming that they are as competitive as the fertile males in the mating process. Proposed many decades ago (Knipling, 1955), the tactic of releasing sterile individuals is a classic among all tactics that exploit the presence of and accentuate the mate-finding Allee effect (Krafsur, 1998; Boukal and Berec, 2009); it even creates an additional component Allee effect in the controlled population (Barclay and Mackauer, 1980; Boukal and Berec, 2009) and its efficiency has frequently been assessed via mathematical models (Lewis and van den Driessche, 1993; Maiti et al, 2006). Figure 3.7 shows that, economical and practical aspects notwithstanding, the release of sterile males might be a better strategy if the pest sex ratio is female-biased, while increasing the male mortality should be preferred in pest populations with an excess of males (Boukal and Berec, 2009). In addition, the two tactics act in synergy (we assume here that the extra mortality does not affect the sterile males, e.g. sterile males are kept at the fixed level S irrespectively of d_C), i.e. the effect of their co-occurrence is much stronger than a 'sum' of their effects when they act in isolation; see also Berec et al (2007).

Finally, the risk of suffering from mate-finding Allee effects might have been a significant evolutionary driver for different mate-finding adaptations and even mating systems. Adaptations for finding a mate are widespread, ranging from sex pheromones to bird songs, to ability to move faster or more efficiently. A common mechanism behind these adaptations is to allow mate-finding at low density (e.g., long-distance attractants such as calling and sex pheromones). These need to be distinguished from adaptations which reduce the likelihood of low density per se (e.g., mass spawning or reproductive aggregations). Although both types of adaptation may have a similar purpose, in the context of populations reduced by anthropogenic impacts their effects can be diametrically opposed. Species with the former types of adaptation are less likely to suffer from mate-finding Allee effects, since they are already adapted to cope with low density – see Gascoigne et al (2009) for a deeper discussion on this issue and a number of specific examples.

One of the mechanisms that may mitigate mate-finding Allee effects (although it could evolve due to other selection pressures) is haplodiploidy, a mating system whereby mated females produce offspring of both sexes while unmated female produce just sons. The simplest model of this system may look like

$$\frac{dM}{dt} = \mu bF \frac{M}{M+\theta} + bF \left(1 - \frac{M}{M+\theta}\right) - d_M M$$

$$\frac{dF}{dt} = (1-\mu)bF \frac{M}{M+\theta} - d_F F \qquad (3.37)$$
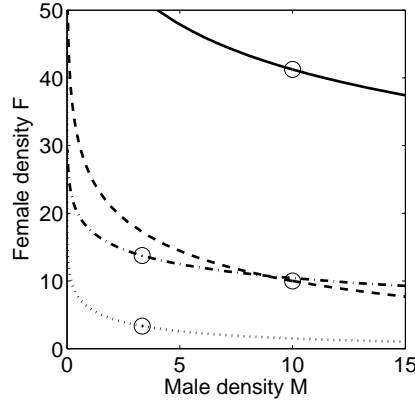
Fig. 3.7 Unstable equilibria (circles) and Allee thresholds (lines) corresponding to the sex-structured population model (3.36) with a mate-finding Allee effect and two control tactics. Population before control: $S = 0$ and $d_C = 0$ (dotted line); only sterile male released: $S = 10$ and $d_C = 0$ (dashed line); only culling applied: $S = 0$ and $d_C = 0.625$ (dash-dot line); both sterile male released and culling applied: $S = 10$ and $d_C = 0.625$ (solid line). Both tactics have the same relative efficiency, i.e. the same ratio of the distances of the control-affected and original unstable equilibria from the origin. Parameter values common to all three scenarios: $\mu = 0.5$, $b = 1$, $d_M = d_F = 0.2$, $\theta = 5$

Standard analysis of the model (3.37) shows that a unique interior equilibrium occurs at

$$M^* = \frac{\theta D}{1 - D} \quad \text{and} \quad F^* = \frac{\theta D}{1 - D} \frac{d_M}{b - d_F} \tag{3.38}$$

where $D = d_F / [(1 - \mu)b]$. Obviously, this equilibrium is feasible provided that $D < 1$, which translates to $(1 - \mu)b > d_F$, and it is quite natural to assume this condition to hold as otherwise the population would go extinct from any density even in the absence of Allee effects (i.e. for $\theta = 0$). Also, it is easy to show that both eigenvalues of the Jacobian of the model (3.37) evaluated at the extinction equilibrium are negative (they equal $-d_M$ and $-d_F$); hence, the extinction equilibrium is always locally stable. This implies that haplodiploidy cannot by itself remove the mate-finding Allee effect. Actually, keeping the same parameter values for the diploid model (3.28) studied in Box 3.4 and for the haplodiploid model (3.37) analyzed here, the equilibrium male density stays the same, but the equilibrium female density is higher for the diploid model for which it is

$$F^* = \frac{\theta D}{1 - D} \frac{(1 - \mu)d_M}{\mu d_F}$$

In addition, the stable manifold of the interior equilibrium corresponding to the haplodiploid model (3.37) lies below that of the diploid model (3.28) (Fig. 3.8). Moreover, starting with only females need not lead to population extinction as they

produce just males and hence partners for themselves in the next round of matings – hence the Allee threshold is no more a hyperbolic curve as for the diploid species. But beware, this is because we assume populations with overlapping generations. For populations with non-overlapping generations this cannot happen as males produced by such females have no one to mate in the next generation; hence the Allee threshold is again in this case a hyperbolic curve. In any case, haplodiploidy mitigates the mate-finding Allee effect relative to diploidy (provided that both models have the same parameter values).
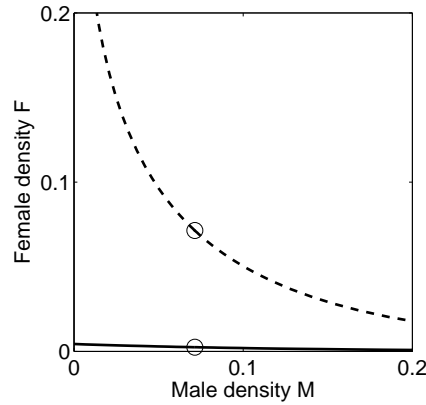
Fig. 3.8 Unstable equilibria (circles) and Allee thresholds (lines) corresponding to the sex-structured population model with a mate-finding Allee effect and haplodiploidy (solid line) or diploidy (dashed line). Parameter values common to both models: $\mu = 0.5$, $b = 3$, $d_M = d_F = 0.1$, $\theta = 1$

Age and sex

Finally, we combine the models (3.15) and (3.25) so as to explore how is the Allee threshold represented in models that combine both age and sex structure. Of the many ways of how to combine these models, a straightforward one is as follows (see also Box 3.2):

$$\frac{dJ}{dt} = bF\frac{M}{M+\theta} - mJ - (d+d_1N)J$$

$$\frac{dM}{dt} = \mu mJ - (d+d_1N)M \tag{3.39}$$

$$\frac{dF}{dt} = (1-\mu)mJ - (d+d_1N)F$$

Note that as the maturation rate becomes very high, $m \to \infty$, the model (3.39) reduces to the sex-structured model (3.25), while for $\mu = 0.5$ (balanced sex ratio at birth) and $M(0) = F(0)$ (identical initial densities of males and females), it reduces to the age-structured model (3.15).

Again, the model (3.39) has two interior equilibria for not too large $\theta > 0$ (and no interior equilibrium for too large $\theta > 0$), of which the one closer to the origin is again unstable (saddle point) and the other one is again locally stable. In addition, the extinction equilibrium is always locally stable for $\theta > 0$. Whereas the upper interior equilibrium is again an attractor (corresponding to the environmental carrying capacity) for any population composed of sufficiently large numbers of (adult) males and females, or of juveniles, the concept of Allee threshold can in principle be explored here in the same way as in the case of age- or sex-structured models, that is, via examination of the stable manifold of the unstable interior equilibrium. Numerical simulations suggest that the stable manifold is not compact here (Fig. 3.9). This makes perfect sense, as zero density of males or females necessarily means no mating and hence inevitable extinction of the other sex. On the other hand, there is a critical density of juveniles, above which the population persists no matter how large the adult population is (it need not even exist at that time) – adults are in this case soon replenished (Fig. 3.9). We do not carry out any formal analysis of the model (3.39) here.
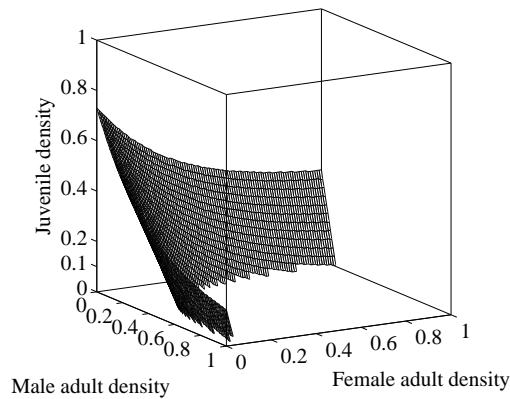
Fig. 3.9 Allee threshold in an age- and sex-structured population. An extinction boundary delimits the areas of population extinction (below) and persistence (above) in the state space of juvenile, male and female densities in the age-structured, two-sex population model (3.39) with a mate-finding Allee effect. Parameter values: $\mu = 0.5$, $b = 4$, $d = 0.1$, $\theta = 1$, $d_1 = 0.35$, $m = 1$

3.2 Linking the Allee effect, sexual reproduction and temperature-dependent sex determination via spatial dynamics

Population models like (3.25) are non-spatial, that is, they assume that all population members mix homogeneously and any individual can equally interact with any other. This also applies to the mate-finding Allee effect – the decisive quantity for any female to find a mate and get fertilized is the total male density. A corollary of this is that individuals can perceive any mating partner however far it is and can instantly mate with it, thus dispersing at virtually an infinite rate. Real mate search strategies may differ, however. Rather than with all members of the population individuals usually interact only with their close neighbors, and rather than dispersing infinitely quickly they disperse only locally.

In what follows, we are going to explore Allee thresholds under such more realistic dispersal strategies, including local diffusive movement (i.e. passive search) and active (but still local) search. We show that for both strategies there is still a hyperbolic extinction boundary in the male-female state space, and examine in detail how the position of this extinction boundary (i.e. Allee threshold) responds to population demography and adopted mate search strategies. We do that by developing and analyzing a spatially explicit, individual-based model in which males and females search one for another explicitly.

To demonstrate a potential application of the developed models, we predict the impact of environmental temperature changes on two turtle species with temperature-dependent sex determination (TSD). The sex ratio at birth depends on the incubation temperature of eggs in a number of reptiles (Paukstis and Janzen, 1990; Janzen and Paukstis, 1991; Girondot, 1999). Environmental temperature changes could thus profoundly affect reptile populations subject to a combination of the mate-finding Allee effect and TSD.

Model development

Consideration of mate search strategies requires explicit modeling of both sex and space. We thus develop a spatially explicit, individual-based model that keeps track of every single male and female in a spatial habitat during their entire lifetime. We also derive its spatially homogeneous counterpart that permits a more detailed analysis and comparison with known models. Parameters used in the developed models are summarized in Table 3.1 and explained below.

Parameter	Meaning
S	Lattice size (128×128 sites)
p_r	Probability of reproduction per reproductive event
μ	Sex ratio at birth
p_m^M (p_m^F)	Probability that a male (female) dies in a time step
d_M (d_F)	Neighborhood size of males (females) with diffusive movement
s_M (s_F)	Size of perception neighborhood of males (females) actively searching for mates
n_M (n_F)	Number of males (females) on the lattice in a time step
x_M (x_F)	Male (female) density in a time step
x'_M (x'_F)	Male (female) density in the next time step with respect to x_M (x_F)

Table 3.1 Parameters used in the developed models

Two-sex spatially explicit, individual-based model

A square lattice of 128×128 uniform sites approximates the homogeneous spatial habitat, with each site occupied by at most one male and one female. Periodic boundary conditions are used to mimic an unbounded environment so that the left and right edges and the top and bottom edges of the lattice are joined together. Time runs in discrete steps in which all sites are simultaneously updated. Initially, individuals are (uniformly) randomly scattered over the lattice, with males and females distributed independently. Two sorts of processes are repeatedly applied in a sequential way: demographic processes (reproduction and mortality) and mate search.

Reproduction. At every time step, each pair (male and female sharing a site) gives birth to one offspring with non-zero probability p_r. The conceived offspring becomes a male with probability $0 < \mu < 1$ (primary sex-ratio) and a female with probability $1 - \mu$. It is placed into a randomly selected nearest neighbor of its parents' site (north, west, south, east) if the selected site is free of an adult of the same sex. If two or more offspring of the same sex attempt to recruit to the same site at the same time step, one of them is randomly chosen and allowed to do it, and the rest is discarded. Thus, reproduction is density-dependent. Maturation time of each offspring is one time step.

Mortality. At every time step, each male and female die with probability p_m^M and p_m^F, respectively (background mortality). No other components of mortality are assumed, so that we may concentrate solely on the effects of mate search.

Reproduction and mortality act concurrently (McCauley et al, 1993). This means that newborns cannot die in the same time step and adults that are marked as dead have the full opportunity to reproduce in that step. Once the demographic processes are accomplished, mate search is initiated. We consider two mate search strategies.

Diffusive movement. An individual with this strategy moves independently of the others to a randomly selected site in a square neighborhood of side $2d + 1$, $d = 0, 1, 2, \ldots$ ($d = 0$ models sedentary individuals), centered on its location; if it is occupied by the same sex, the individual does not move. The neighborhood size may differ for males (d_M) and females (d_F) to allow for a range of movement rates.

Active mate search. Any searching individual is assumed to have a square perception neighborhood of side $2s+1$, $s=1,2,\ldots$, around its location due to, e.g. detection of pheromones (insects, reptiles, rodents), advertisement calls (amphibians), or songs (birds) by the other sex. Let us consider a particular, actively searching male (the same rules apply to females). If a sole and partner-free female is present in his perception neighborhood, the male moves to her site. If he locates two or more unmated females, one of them is randomly selected. If no such female is found, the male moves to a randomly selected site inside his perception neighborhood unless it is occupied by another male, and does not move otherwise. The perception neighborhood size may differ for males (s_M) and females (s_F).

If a pair is formed during the mate search process, individuals of that pair no longer move in that time step. Moreover, males and females paired in the previous time step move independently, and irrespectively of their previous reproductive success or failure. This rule corresponds to a monogamous mating system with no fidelity. To apply any of the two mate search rules, all individuals are randomly ordered and move one by one. As a consequence, contests for mates do not occur. The reader is referred to McCauley et al (1993) and Berec (2002) for further technical issues on discrete-time, discrete-space, individual-based models.

Non-spatial model

The spatially homogeneous counterpart of the above-defined individual-based model, also known as the *mean-field approximation*, is derived under the assumption that individuals of each sex are randomly distributed on a sufficiently large lattice at each time step (among other things, this assumption implies random mating). With this assumption, system dynamics are sufficiently approximated by the following system of coupled difference equations (see Box 3.5 for its derivation),

$$
\begin{aligned}
x'_M &= x_M(1-p_m^M) + \mu p_r x_M x_F(1-x_M) \\
x'_F &= x_F(1-p_m^F) + (1-\mu)p_r x_F x_M(1-x_F)
\end{aligned}
\tag{3.40}
$$

In this model, x_M (x_F) and x'_M (x'_F) denote mean male (female) density in a time step and the time step next to it, respectively. We will refer to the model (3.40) as the *non-spatial* model further on.

Box 3.5 Derivation of the non-spatial model (3.40)

Assume that individuals are randomly distributed on a sufficiently large lattice in each time step. The probability that a male survives to the next time step is $1-p_m^M$; hence, the proportion of males that survive to the next time step approaches $1-p_m^M$ for the lattice size S tending to infinity and the male density $x_M = n_M/S$ kept constant. Reproduction and mortality are independent events due to their concurrent ordering. There are $S-n_M$ male-free sites

at the beginning of a time step. The probability that a particular male-free site will become occupied by a male offspring coming from a given nearest neighbor equals the probability that the neighbor contains both male and female ($n_M/S \times n_F/S$) times the probability that the pair gives birth to a male offspring ($\mu \times p_r$) times the probability that this offspring is placed to this particular male-free site ($1/4$). Reproductive events from various neighbors are independent; hence, the probability that the male-free site remains empty at the end of the time step is

$$\left(1 - \mu \frac{n_M}{S} \frac{n_F}{S} \frac{p_r}{4}\right)^4$$

The proportion of currently male-free sites that is occupied by males in the next time step thus tends to

$$1 - \left(1 - \mu \frac{n_M}{S} \frac{n_F}{S} \frac{p_r}{4}\right)^4$$

for S going to infinity and the male and female densities kept constant. Analogous expressions hold for females. The mean number of males and females in the next time step may thus be approximated as

$$n_M(1 - p_m^M) + (S - n_M)\left[1 - \left(1 - \mu \frac{n_M}{S} \frac{n_F}{S} \frac{p_r}{4}\right)^4\right]$$

and

$$n_F(1 - p_m^F) + (S - n_F)\left[1 - \left(1 - (1-\mu) \frac{n_F}{S} \frac{n_M}{S} \frac{p_r}{4}\right)^4\right]$$

respectively. Given that $(1 - w)^4 \approx 1 - 4w$ for sufficiently small w, then after dividing both expressions by S and setting $x_{M(F)} = n_{M(F)}/S$ we have for the mean male and female densities in the next time step that

$$\begin{aligned} x_M' &= x_M(1 - p_m^M) + \mu p_r x_M x_F(1 - x_M) \\ x_F' &= x_F(1 - p_m^F) + (1 - \mu) p_r x_F x_M(1 - x_F) \end{aligned} \tag{3.41}$$

These equations guarantee $0 \leq x_M', x_F' \leq 1$ provided that x_M and x_F satisfy the same constraint. The neglected higher-order terms could become significant only when the population approaches the environmental carrying capacity. As we are primarily interested in what happens at lower population densities, it is sufficient to analyze the model (3.41).

Model results

Non-spatial model

We start by examining the non-spatial model (3.40). Results are derived analytically unless stated otherwise (details on the underlying analysis are given in Boxes 3.6 and 3.7).

For all parameter combinations, populations with sufficiently small initial male and female densities go extinct. Moreover, there are either zero, one, or two interior steady states. To map parameter regions corresponding to each of these three cases (Fig. 3.10), we introduce compound, dimensionless parameters

$$A_M = \frac{p_m^M}{\mu p_r} \ \text{ and } \ A_F = \frac{p_m^F}{(1-\mu)p_r}$$
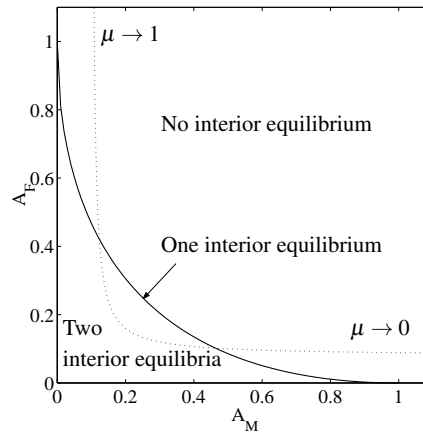
Fig. 3.10 Compound-parameter space with regions of zero, one, and two interior equilibria of the non-spatial model (3.40). The dashed line corresponds to the compound parameters A_M and A_F with $p_r = 0.1$, $p_m^M = 0.01$, $p_m^F = 0.008$, and primary sex-ratio μ varying from zero to one. Points on the bold line satisfy $\sqrt{A_M} + \sqrt{A_F} = 1$

If $\sqrt{A_M} + \sqrt{A_F} > 1$, there are no interior steady states. On the other hand, if $\sqrt{A_M} + \sqrt{A_F} < 1$, two distinct interior equilibria exist. As we were unable to resolve stability of the interior equilibria analytically, we performed extensive numerical simulations of the non-spatial model (3.40) for $0 < A_M, A_F < 1$. We also varied demographic parameters for some fixed values of A_M and A_F. For each set of parameters, we chose a set of initial conditions that sufficiently covered the male-female state space. These simulations suggest that if no interior steady state exists, the origin E^0 is globally stable and the population always dies out regardless of ini-

tial male and female population densities. If two interior equilibria exist, we claim that the equilibrium closer to the origin, denoted $E^u = (x_M^u, x_F^u)$, is unstable (saddle point), and that the more distant steady state $E^s = (x_M^s, x_F^s)$ is locally stable. Numerical simulations also showed that the system either approaches E^0 or E^s depending on initial conditions. Hence, we observe the bistable regime typical of the Allee effect, and recover the hyperbolic Allee threshold typical of the dioecious species (Fig. 3.11). Note that a sharp decline in one sex or even in the total population size may not necessarily mean an ultimate population extinction.

Box 3.6 Analysis of the non-spatial model (3.40)

The eigenvalues of the non-spatial model (3.40) linearized at E^0 are $\lambda_1 = 1 - p_m^M$ and $\lambda_2 = 1 - p_m^F$, and E^0 is thus locally asymptotically stable. Two distinct interior equilibria,

$$E^u = (x_M^u, x_F^u) = \left(\tfrac{1}{2}(1 - A_M + A_F - \sqrt{D}), \tfrac{1}{2}(1 + A_M - A_F - \sqrt{D})\right)$$

$$E^s = (x_M^s, x_F^s) = \left(\tfrac{1}{2}(1 - A_M + A_F + \sqrt{D}), \tfrac{1}{2}(1 + A_M - A_F + \sqrt{D})\right)$$

where $D = (1 - A_M + A_F)^2 - 4A_F$, exist if and only if $D > 0$. Note that for $A_M \geq 1$ or $A_F \geq 1$, the population driven by the model (3.41) goes extinct, as $x_M' < x_M$ or $x_F' < x_F$, respectively. Assume now that $A_M < 1$ and $A_F < 1$. Under these conditions, $D > 0$ is equivalent to $\sqrt{A_M} + \sqrt{A_F} < 1$. The model (3.41) thus has two distinct interior equilibria if and only if

$$\sqrt{A_M} + \sqrt{A_F} < 1$$

and no interior equilibrium once the opposite inequality holds. Note that $\sqrt{A_M} + \sqrt{A_F} < 1$ implies $A_M + A_F < 1$. The singular case of one interior equilibrium $E^\star = (x_M^\star, x_F^\star) = (1 - \sqrt{A_M}, \sqrt{A_M})$ occurs if and only if $D = 0 \Leftrightarrow \sqrt{A_M} + \sqrt{A_F} = 1$. It is structurally unstable and thus biologically irrelevant.

Although the number and location of equilibria are fully described by the compound parameters A_M and A_F, we would have to take all demographic parameters into account if we needed to (numerically) locate the extinction boundary and to study transient dynamics of the non-spatial model (3.40). Despite that, the areas of initial conditions leading to extinction and persistence can be partially characterized by the distance of E^u from the other two equilibria. The extinction (persistence) area is positively related to the distance of E^u from E^0 (E^s) and enlarges (shrinks) with increasing A_M and/or A_F.

What are the effects of changing the primary sex-ratio μ on the system dynamics when mortality and reproduction parameters p_m^M, p_m^F and p_r are kept fixed? Such a dependence may play a crucial role in species for which changing environmental conditions affect sex determination much more than other life history characteristics (Charnov and Bull, 1977). If reproductive rates are relatively low,
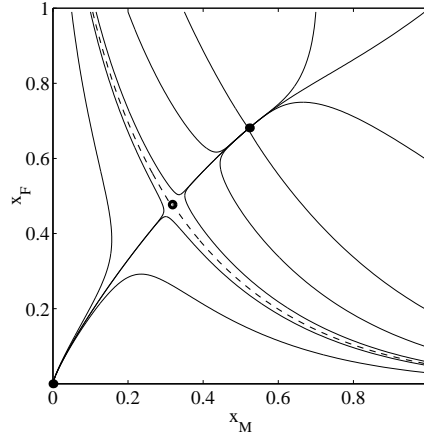
Fig. 3.11 Sample trajectories of the non-spatial model (3.40) in the male-female state space, showing equilibria (filled circles = stable, empty circle = unstable) and extinction boundary (Allee threshold; dashed line). All trajectories starting below (above) the Allee threshold approach the extinction equilibrium (carrying capacity) as time goes to infinity. Parameter values: $\mu = 0.4$, $p_r = 0.1$, $p_m^M = 0.013$, $p_m^F = 0.01$

$$\sqrt[3]{p_m^M} + \sqrt[3]{p_m^F} > \sqrt[3]{p_r} \tag{3.42}$$

then all trajectories of the non-spatial model (3.40) approach the extinction equilibrium E^0 for all $\mu \in (0,1)$; different values of μ can only slow down or speed up the inevitable population extinction. For high reproductive rates,

$$\sqrt[3]{p_m^M} + \sqrt[3]{p_m^F} < \sqrt[3]{p_r} \tag{3.43}$$

critical values $0 < \mu_1 < \mu_2 < 1$ exist such that extreme values of μ lying outside the interval (μ_1, μ_2) drive the system to extinction whereas $\mu \in (\mu_1, \mu_2)$ induce a strong Allee effect.

If male and female mortalities are equal ($p_m^M = p_m^F$), the conditions (3.42) and (3.43) reduce to $P > 1/8$ and $P < 1/8$, respectively, where $P = p_m^M/p_r = p_m^F/p_r$ and the critical values μ_1 and μ_2 can be derived analytically. They are symmetric with respect to the unbiased primary sex-ratio $\mu = 0.5$,

$$\mu_{1,2} = \frac{1}{2} \pm \frac{1}{2} \sqrt{1 - 4P - 8P^2 - 8P\sqrt{P(1+P)}} \tag{3.44}$$

The interval (μ_1, μ_2) becomes larger with decreasing P, i.e. with increasing reproduction p_r and/or decreasing mortality $p_m^M = p_m^F$. We observed analogous qualitative dependence also for different male and female mortalities $p_m^M \neq p_m^F$.

Box 3.7 Role of the primary sex-ratio

The sum $\sqrt{A_M} + \sqrt{A_F}$ is a convex function of μ as $\partial^2\left(\sqrt{A_M} + \sqrt{A_F}\right)/\partial\mu^2 > 0$. Moreover, $\sqrt{A_M} + \sqrt{A_F} \to \infty$ for $\mu \to 0$ or 1. The sum attains its global minimum

$$\min_{0<\mu<1}\left(\sqrt{A_M} + \sqrt{A_F}\right) = \left(\frac{\sqrt[3]{p_m^M} + \sqrt[3]{p_m^F}}{\sqrt[3]{p_r}}\right)^{\frac{3}{2}}$$

at

$$\mu = \mu^\star = \frac{\sqrt[3]{p_m^M}}{\sqrt[3]{p_m^M} + \sqrt[3]{p_m^F}}$$

If the inequality (3.43) holds, then the primary sex-ratios $\mu_1 < \mu^\star < \mu_2$ exist such that $\sqrt{A_M} + \sqrt{A_F} = 1$ for $\mu = \mu_1$ and $\mu = \mu_2$. the non-spatial model (3.40) thus possesses two distinct interior equilibria for $\mu \in (\mu_1, \mu_2)$, one interior equilibrium for $\mu = \mu_1$ or $\mu = \mu_2$, and only the extinction equilibrium E^0 for $\mu < \mu_1$ or $\mu > \mu_2$. In addition, E^0 is the only steady state of the non-spatial model (3.40) for all $\mu \in (0,1)$ if the inequality (3.42) holds, as then $\sqrt{A_M} + \sqrt{A_F} > 1$ for all $\mu \in (0,1)$. For $\sqrt[3]{p_m^M} + \sqrt[3]{p_m^F} = \sqrt[3]{p_r}$, the non-spatial model (3.40) possesses a unique interior equilibrium for $\mu = \mu^\star$, due to $\sqrt{A_M} + \sqrt{A_F} = 1$, but the system is in this singular case structurally unstable.

Solving the equality $\sqrt{A_M} + \sqrt{A_F} = 1$ with respect to μ in the special case $p_m^M = p_m^F$, we get the formula (3.44); the distance $\mu_2 - \mu_1 = \sqrt{1 - 4P - 8P^2 - 8P\sqrt{P(1+P)}}$ increases with decreasing ratio $P = p_m^M/p_r = p_m^F/p_r$ because

$$\frac{\partial(\mu_2 - \mu_1)}{\partial P} = -\frac{2\left(\sqrt{1+P}(1+4P) + \sqrt{P}(3+4P)\right)}{(\mu_2 - \mu_1)\sqrt{1+P}} < 0$$

Application to temperature-dependent sex determination (TSD)

We now use the non-spatial model (3.40) and available data to predict the combined impact of TSD and the mate-finding Allee effect on the snapping turtle *Chelydra serpentina* and the European pond turtle *Emys orbicularis*. For both species, demographic characteristics have been quantitatively studied (Christiansen and Burken, 1979; Obst, 1986; Paukstis and Janzen, 1990; Iverson, 1991; Girondot and Pieau, 1993). In *Ch. serpentina*, only females are produced at low as well as high egg incubation temperatures and only males are produced at intermediate temperatures, with two transitional ranges between these extremes; we found the original polynomial fit in Janzen and Paukstis (1991) unsatisfactory and replaced it by an exponential function (Table 3.2 and Fig. 3.12a). In *E. orbicularis*, only males are produced at low egg

incubation temperatures and only females at high temperatures, with a transitional range in which both sexes are produced; Girondot (1999) gives the exponential fit (Table 3.2 and Fig. 3.12b).

We transform the field data (Table 3.2) to fit our model using several compromising assumptions. The number of eggs per year is multiplied by the fraction of individuals achieving maturity to get the number of new adults each year, and this number is then divided into "single-individual reproductive events" by rescaling the time step (i.e. we assume that each female gives birth to one offspring per reproductive event with probability $p_r = 1$ and this offspring matures in one time step). Both assumptions in fact mean that we neglect possible effects of time lags in population dynamics; similar arguments have been adopted by Veit and Lewis (1996). The annual adult mortality is recomputed to the per time step adult mortality; as there is no distinction in the literature between male and female adult mortalities, we use $p_m^M = p_m^F$.

Species	Annual adult mortality	Clutches (eggs)	Fraction (~number) achieving maturity	p_r	$p_m^M = p_m^F$	μ_1	μ_2
Chelydra serpentina	0.04	1 (30)	0.133 (~4)	1.0	0.01	0.01	0.99
Emys orbicularis	0.10	2 (6)	0.206 (~2.5)	1.0	0.033	0.05	0.95

Table 3.2 Demographic data, reproduction and mortality probabilities, and critical values of the primary sex-ratio for the snapping turtle *Ch. serpentina* and the European pond turtle *E. orbicularis*

The last two columns of Table 3.2 give the critical values μ_1 and μ_2 of the primary sex-ratio that are evaluated by the formula (3.44). Figure 3.12 shows the dependence of the primary sex-ratio on incubation temperature together with the temperature intervals leading to strong Allee effects. It follows that for *Ch. serpentina* (*E. orbicularis*), hatchling sex ratios as biased as 1:99 (1:19) can prevent inevitable population extinction. This translates into two egg incubation temperature intervals of about 2°C width and a single, about 1°C wide interval that enable persistence of *Ch. serpentina* and *E. orbicularis*, respectively.

We apply our non-spatial model (3.40) to the two turtle species not to provide reliable quantitative predictions but to illustrate the potential strategic use of models developed in this section. The fundamental message is that the Allee effect further narrows temperature ranges under which population persistence is possible. However, knowledge of appropriate spatial and temporal scales, mate search strategies, variations in the egg incubation temperature between nesting sites and years, and further life history details of the examined species would be instrumental in adopting any control measure.
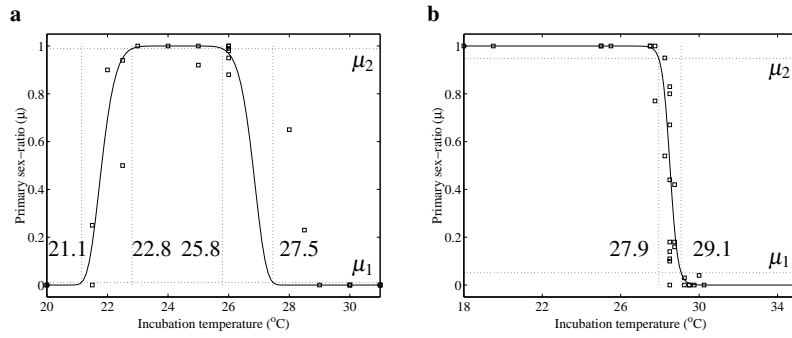
Fig. 3.12 Dependence of the primary sex-ratio μ on the egg incubation temperature for (a) the snapping turtle *Chelydra serpentina* and (b) the European pond turtle *Emys orbicularis*, combined with the primary sex-ratio interval (μ_1, μ_2) for which the non-spatial model (3.40) induces a strong Allee effect. Solid lines denote the best fits of the original data (squares) taken from Paukstis and Janzen (1990). Parameter values and data fits: *Ch. serpentina*: $p_r = 1.0$, $p_m^M = p_m^F = 0.01$, $\mu = \exp(-(t - 24.3)^8/2177.3)$, fitted by the MATLAB procedure *lsqcurvefit*; *E. orbicularis*: $p_r = 1.0$, $p_m^M = p_m^F = 0.033$, $\mu = 1/(1 + \exp(-(28.51 - t)/0.196))$, taken from Girondot (1999). Values of μ_1 and μ_2 are given in Table 3.2

Mate search strategies

In nature, many organisms do not mate at random but rely on more or less elaborate mate search strategies. What consequences do they have for population persistence and resistance to adverse conditions? To shed more light on this issue, we use the above-defined individual-based model to explore some consequences of the diffusive movement and active mate search defined above.

Both males and females move diffusively. Among all combinations of d_M and d_F, the case $d_M = d_F = 1$ deviates most from the non-spatial model (3.40). On the other hand, the non-spatial model and the individual-based model with diffusive movement and high enough values of d virtually coincide. Figure 3.13 demonstrates a shift of the Allee threshold towards lower population densities; all Allee thresholds corresponding to higher values of d lie in between the one for the non-spatial model and the one for the individual-based model with $d_M = d_F = 1$.

Both males and females use active mate search strategy. Individual-based model simulations show that mutual active mate search lowers extinction thresholds even more. Figure 3.14 shows an extinction/persistence diagram for a population (with the same initial number of males and females) with various sizes of perception neighborhoods (equal for both sexes). We note that the minimum viable population size decreases non-linearly with increasing the perception neighborhood.

As the individual-based model is inherently stochastic, there is always a non-zero probability that a population of any size will go extinct in a finite time. This stochasticity is due to both demography (variation in numbers of births and deaths over various realizations) and environment (variation in spatial distribution of individuals on the lattice over various realizations). For each combination of the initial population
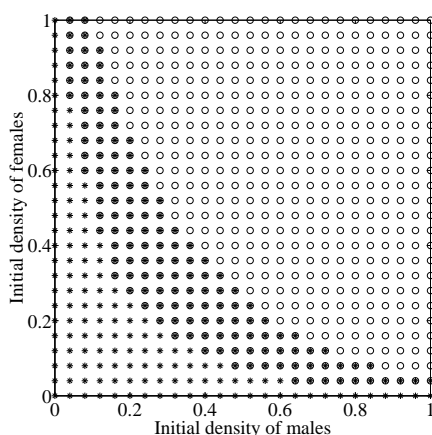
Fig. 3.13 Space of initial male and female population densities divided into the persistence (circles) and extinction (asterisks) parts as determined by the individual-based model with diffusive movement, $d_M = d_F = 1$. Circles filled by asterisks show the area where the non-spatial model (3.40) predicts extinction whereas the individual-based model with $d_M = d_F = 1$ predicts persistence. Other parameter values: $\mu = 0.4$, $p_r = 0.1$, $p_m^M = 0.013$, $p_m^F = 0.01$
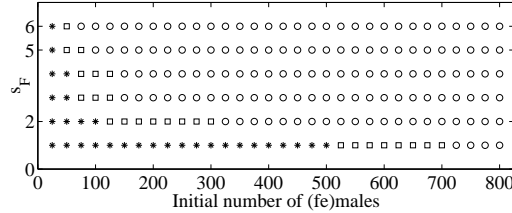
size and size of the perception neighborhood, we performed ten simulation replicates. While some combinations gave only extinction (asterisks) or persistence (circles), some led to both extinction and persistence within the ten runs (squares): the squares thus estimate the "region of strong stochasticity," defined here as a range of initial conditions for which the probability of extinction lies in the interval $[0.1, 0.9]$. Clearly, this probability decreases with increasing initial population size.
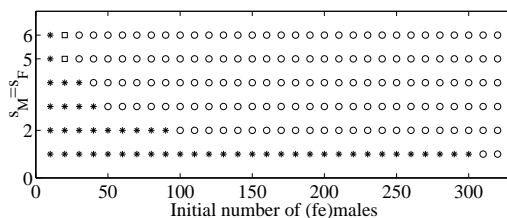
Fig. 3.14 Division of space formed by the initial population size and size of the perception neighborhood into the persistence (circles) and extinction (asterisks) parts as determined by the individual-based model with active mate search strategy. Squares show the region of strong stochasticity where at least one out of ten simulation replicates leads to persistence and at least one to extinction. Other parameter values: $\mu = 0.4$, $p_r = 0.1$, $p_m^M = 0.013$, $p_m^F = 0.01$

Sedentary males and actively searching females. In many frogs, males are territorial, do not move during the mating period, and attract females by advertisement

calls (Duellman and Trueb, 1986). We model the immobility of males by the diffusive strategy with $d_M = 0$ and let the distance s_F for females to hear the male calls vary; we use the same initial number of males and females (Fig. 3.15). Two principal changes occur compared to Fig. 3.14: the extinction boundary shifts towards higher population sizes and the region of strong stochasticity widens.


Fig. 3.15 Division of space formed by the initial population size and size of the perception neighborhood of females into the persistence (circles) and extinction (asterisks) parts as determined by the individual-based model with sedentary males ($d_M = 0$) and actively searching females. Squares show the region of strong stochasticity where at least one out of ten simulation replicates leads to persistence and at least one to extinction. Other parameter values: $\mu = 0.4$, $p_r = 0.1$, $p_m^M = 0.013$, $p_m^F = 0.01$

Three generic phases of population dynamics are observed around the region of strong stochasticity (Fig. 3.16). Starting from a random distribution of individuals on the lattice, abundances of both sexes first decrease since male-female encounters are rare and mortality outnumbers reproductive events. This phase is the real demonstration of scarcity in reproductive possibilities and, if too long, may result in population extinction; this is what happens when we start well below the region of strong stochasticity. During the second phase, males and females start to meet each other with a greater frequency as clusters of individuals begin to form. This increase in pair formation more or less balances mortality and keeps the population relatively constant. Finally, when the clusters become more pronounced, the probability of finding a mate after a recent encounter steadily increases. The population starts to grow, clusters expand radially and fill the lattice, and densities approach the environmental carrying capacity. The first two phases are negligible if the initial numbers of both sexes are high.

Summary

We show in this section that the initial numbers of males and females sufficing for the population persistence may decrease significantly when changing the mate search strategy from random mating to diffusive movement of both sexes to one actively searching sex to both sexes active in searching for mates (Figs. 3.13, 3.14 and 3.15). The Allee threshold preserves its hyperbolic shape; its shift towards the
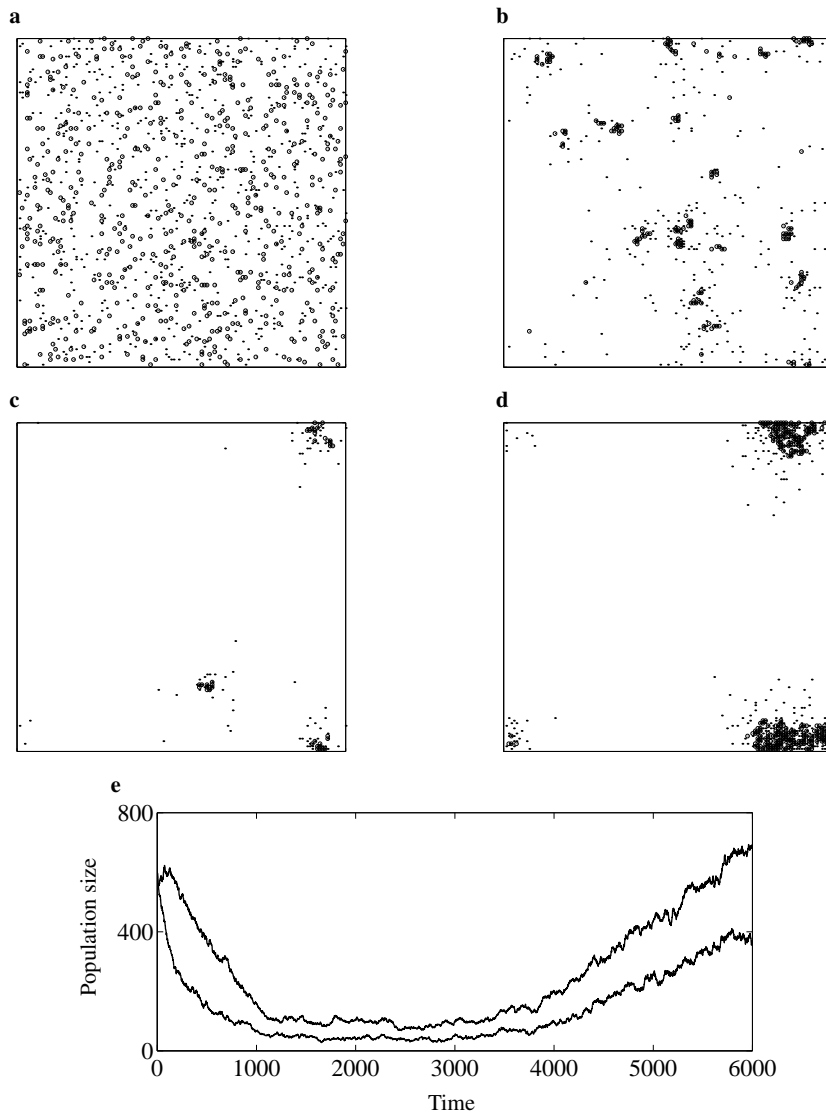
Fig. 3.16 Typical spatio-temporal dynamics of the individual-based model around the region of strong stochasticity: snapshots of the spatial pattern of males (empty circles) and females (full circles) at times 0 (a), 500 (b), 2000 (c), and 5000 (d), and corresponding temporal evolution (e; lower curve = number of males, upper curve = number of females). Parameter values: sedentary males ($d_M = 0$), actively searching females ($s_F = 1$), $\mu = 0.4$, $p_r = 0.1$, $p_m^M = 0.013$, $p_m^F = 0.01$

origin may be explained as follows. If random mating is replaced by diffusive movement, successful pair formation enhances mating probability of the paired individuals in the next time step due to cluster formation. The probability that a successfully

mated individual encounters the same or another partner (e.g. a recent newborn) in the next time step increases – for the same population sizes – with decreasing diffusion range, and is higher than the probability n_M/S (n_F/S) of encountering a male (female) in the non-spatial model. Hence, the increase in pair formation compensates for mortality in at least some populations that become extinct according to the non-spatial model. If at least one sex uses active mate search, the formation of successfully breeding clusters is further enhanced by the ability of individuals to much more effectively find their mates. If both sexes actively search for partners, an individual without a partner may incidentally approach an individual of the opposite sex that still has the possibility to move and mate with it in the same time step. On the other hand, if the other sex is sedentary, they cannot meet before the next time step. This results in a narrower region of strong stochasticity and lower Allee thresholds if both sexes use active search relative to when males are sedentary and females active. Some of our results were later corroborated by Preece and Mao (2009).

If one or both sexes actively search for mates, an increased perception neighborhood facilitates population persistence. Using an example with equal initial abundances of both sexes, we show that the Allee threshold is more or less inversely dependent on size of the perception neighborhood (Figs. 3.14 and 3.15). This result agrees well with predictions of the reaction-diffusion model of a sexually reproducing population studied by Hopper and Roush (1993). Indirect experimental evidence of this dependence is provided by Kindvall et al (1998) in their field study of the bush cricket *Metrioptera roeseli*. They found that the crickets tend to move more at lower population densities and thus probably increase size of the effective perception neighborhood. Such behavior could be an adaptive response of organisms to alleviate Allee effects at low population sizes or densities; see also Gascoigne et al (2009).

Both reaction-diffusion models and observations of real populations suggest that Allee effects impose slower rates of spread and growth of populations in the early stages of invasion or (re)introduction which is followed by a rapid expansion through the environment (Hopper and Roush, 1993; Lewis and Kareiva, 1993; Kot et al, 1996; Veit and Lewis, 1996). We observed similar behavior in individual-based model simulations – before successful establishment, populations starting at lower densities invariably passed through three successive stages (Fig. 3.16). Knowledge of these stages may help to better understand mechanisms regulating spread or extinction of natural populations. Also, it emphasizes differences between local and global densities and shows the importance of scale when assessing the impact of Allee effect.

3.3 Implications of mate search, mate choice and divorce rate for population dynamics of sexually reproducing species

In this section, we consider yet another aspect of sexual reproduction: formation of long-time male-female pairs. The pairs are created when a male and a female meet and choose to establish a bond and cease to exist by death of one member of a pair or by divorce. In many animals, successful reproduction requires paired individuals and there exist numerous ways pairs are being formed and maintained. Three major processes play a significant role in pair dynamics: mate search, mate choice, and breakup of established pairs. Different taxa use different ways to locate mates; in this section we use random search, local passive (i.e. diffusive) search, and local active search as three generic examples (that is, the same mate search strategies as in the previous section). Many animals are known to avoid or reduce reproduction with mates belonging to incompatible or non-preferred phenotypes; this phenomenon is known as *mate choice* (Andersson, 1994; Møller and Legendre, 2001). Also, animals vary widely in their fidelity (i.e. pair bond duration; Choudhury, 1995; Dubois et al, 1998). In some species, such as the wandering albatross *Diomedea exulans*, individuals tend to maintain life-long pair bonds, whereas in others, such as the grey heron *Ardea cinerea*, birds experience many partners during their reproductive lifespan.

Mate search, mate choice and divorce behavior are apparently intertwined. It is now believed and partly supported by observational evidence that divorce is an adaptive strategy of an individual to improve its reproductive success; "divorce may simply be an extension of the mate-choice process, where birds continue to sample mates and improve on their breeding situation after initial pairing" (Choudhury, 1995). Mate choice is also tightly related to mate search efficiency. For example, actively searching individuals may locate many more potential mates than passive or random searchers in a given time interval, and thus secure a better mate. Last but not least, intuition suggests that the lower is divorce rate of an individual, i.e. the fewer partners it has during its lifetime, the more carefully it should choose these partners in order to secure that its genes pass to the future generations. Needless to say, these processes have certainly evolved together and strongly shaped the currently observed mating strategies.

Tightly coupled with these processes, there is an ongoing debate in the literature about the relationship between longevity and mate fidelity (Saether, 1986; Choudhury, 1995; McNamara and Forslund, 1996). So far the evidence provided by theoretical models is ambivalent and competing hypotheses do exist: some authors have argued that selection may not favor mate fidelity in species with high mortality rates, yet the others have suggested that divorce should be expected mainly in long-lived species, since they gain more in terms of improving lifetime reproductive success (Choudhury, 1995). Recently, Jeschke and Kokko (2008) have demonstrated that among birds, species with a high divorce rate tend to have a high mortality rate.

Model development

We study population dynamics of sexually reproducing species by means of a spatially explicit, individual-based model and its mean-field (i.e. spatially homogeneous) approximation (further referred to as the non-spatial model). We represent two-dimensional, physically homogeneous environment as a regular lattice of 200×200 identical square sites, with periodic boundary conditions. Time runs continuously. At any time instant, each site represents a 'territory' that can be vacant or occupied by a single (i.e. unpaired) individual or pair, i.e. the environment can host up to $80,000$ individuals. Simulations are initialized with a given number of single males, single females, and pairs, all randomly distributed over the lattice. The following life history processes determine the fate of each individual. Due to continuous time, process ordering is determined by the actual occurrence of particular events. Further technicalities of this approach are discussed in Box 3.8 and Berec (2002).

Males and females die at rates d_m and d_f, respectively, regardless of their paired status. Dead individuals are instantly removed from the lattice. Pairs give birth to one offspring at rate b. The offspring becomes male or female with probability μ or $1 - \mu$, respectively. Respecting boundary conditions, it instantly and equiprobably disperses to a parents' nearest neighbor site and becomes an adult capable of reproduction. If the chosen site is already occupied, the offspring dies. If the chosen site is vacant, the offspring settles there. Pairs separate at rate m_p, and we assume that divorce (i.e. the act of leaving the pair) is pursued by males and females equally. The terminal site of the leaving individual is determined by a mate search strategy described below. Divorce is withdrawn if the leaving individual would step on a site with a pair or a same-sex single. As a consequence, contests for mates do not occur. If it would step on a site occupied by a single of the other sex, there is probability p_s of a successful pair formation; this probability may quantify, e.g. female choosiness with respect to males. If the new pair is not formed divorce is also withdrawn.

Single males and females move at rates m_m and m_f, respectively. Again, the terminal site of the disperser is determined by its mate search strategy. Dispersal is discarded if a pair or individual of the same sex occupies the site to which the disperser intends to move. Upon male and female encounter, a pair is formed with probability p_s. If the pair formation is not successful, the disperser does not move. We distinguish two local mate search strategies which may differ for males and females, identical to those of the previous section. First, single individuals are expected to search for their mates passively by moving or leaving divorcing pairs equiprobably to any site in a square neighborhood of side length $2r + 1$ sites, $r = 0, 1, 2, \ldots$ ($r = 0$ models sedentary individuals), centered on their current location. Side length of the neighborhood may differ for males (r_m) and females (r_f). Second, individuals are assumed to be active searchers through perceiving other conspecifics in a square neighborhood of side length $2s + 1$ sites, $s = 1, 2, \ldots$, centered on their current location. A male perceiving only one single female moves directly to her site. If two or more unpaired females are perceived, one is chosen equiprobably. If no single female is detected, the male moves to a randomly chosen site in the neighborhood

unless it is occupied by a single male or pair, and stays in the current site otherwise. Analogous rules apply to females. Neighborhood side length may differ for males (s_m) and females (s_f).

The non-spatial model is extracted from the above spatially explicit, individual-based model by assuming an infinite lattice, random initial condition, and random search strategy (i.e. dispersal of all individuals, including offspring, equiprobably to any site on the lattice). Then, densities of single males (v_m), single females (v_f), and pairs (v_p) obey the following system of ordinary differential equations (Box 3.8 and Berec (2002)):

$$\frac{dv_m}{dt} = -d_m v_m - p_s(m_m + m_f)v_m v_f + d_f v_p + (m_p + b\mu)(1 - v_m - v_f - v_p)v_p \,,$$

$$\frac{dv_f}{dt} = -d_f v_f - p_s(m_m + m_f)v_m v_f + d_m v_p + [m_p + b(1 - \mu)](1 - v_m - v_f - v_p)v_p \,,$$

$$\frac{dv_p}{dt} = p_s(m_m + m_f)v_m v_f - (d_m + d_f)v_p - m_p(1 - v_m - v_f - v_p)v_p \,.$$

$$(3.45)$$

The male and female equations consist of five terms. From left to right, these correspond to the death of a single individual, formation of a pair when two singles meet, death of a paired individual, divorce, and birth of an offspring. Pair dynamics are driven by formations of new pairs, deaths of pair members, and divorces.

Box 3.8 Derivation of the non-spatial model (3.45)

To understand how model rules describing individual behavior translate into the non-spatial model (3.45), we give a brief outline of how simulations of the individual-based model formally run; see also Berec (2002). Events are said to occur at rate a if the event occurrence times are described by a Poisson process with the parameter a. The model rules require that a number of Poisson processes run for each individual (mortality, reproduction, divorce, and dispersal). Fortunately, a 'thinning' technique exists that keeps one background Poisson process only (Durrett, 1995). This single process generates time instants at which events may occur. Let S be the number of lattice sites and let the background Poisson process generate time instants at rate cS, with $c \geq \max\{d_m + m_m, d_f + m_f, d_m + d_f + m_p + b\}$. Upon each generated time instant, a site is randomly chosen. Thus, each site is independently trying to change at rate c, as $cS \times 1/S = c$, with $1/S$ being the probability that a particular site is randomly chosen. If the chosen site is occupied by a single male [female], the male [female] dies with probability d_m/c [d_f/c] and attempts to move with probability m_m/c [m_f/c]. If the chosen site is occupied by a pair, a pair member dies with probability $(d_m + d_f)/c$, divorce is initiated with probability m_p/c, and birth takes place with probability b/c.

To derive a mean-field approximation of the spatially explicit, individual-based model, we assume an infinite lattice, random initial conditions, and dis-

persal of all individuals, including offspring, equiprobably into any site on the lattice (these conditions are often referred to as the mass action law or the homogeneous mixing conditions). Now, we need to consider one by one all processes corresponding to single males, single females, and pairs, and calculate how they affect current population size. As an example, consider single male population. Its size may be decreased by death of a single male or formation of a new pair, and increased by death of a paired female, divorce or production of a male offspring. Consider a sufficiently small time interval h, and let x_m, x_f, and x_p denote current numbers of males, females, and pairs, respectively. By definition, probability that just one event time is generated within h is $cSh + o(h)$ as $h \to 0$, while probability that two or more event times are generated within h is negligible (it is $o(h)$ as $h \to 0$). Probability that a single-male-occupied site is randomly chosen is x_m/S. The event of death of that male takes place with probability d_m/c, while a new pair is formed due to movement of that male with probability $(m_m/c)(x_f/S)p_s$ – the male has to move, step on a single-female-occupied site, and be accepted by that female. Probability that a single-female-occupied site is randomly chosen is x_f/S. A new pair is formed due to movement of this female with probability $(m_f/c)(x_m/S)p_s$. A pair is chosen with probability x_p/S. Female of that pair dies with probability d_f/c, and divorce with the leaving individual ending up in a vacant site takes place with probability $(m_p/c)(x_0/S)$, where $x_0 = S - x_m - x_f - x_p$ is the number of currently vacant sites. Finally, birth and consequent successful establishment of a male offspring by that pair occurs with probability $\mu(b/c)(x_0/S)$. Other events do not affect single male population size. To sum up, the mean change in the number of single males in a small time interval h is

$$\mathrm{E}[X_m(t+h)|X_m(t) = x_m, X_f(t) = x_f, X_p(t) = x_p] - x_m =$$

$$= \mathrm{E}[X_m(t+h) - x_m|X_m(t) = x_m, X_f(t) = x_f, X_p(t) = x_p] =$$

$$= (-1) \times \left[cSh\frac{x_m}{S}\left(\frac{d_m}{c} + \frac{m_m}{c}\frac{x_f}{S}p_s \right) \right] + (-1) \times \left[cSh\frac{x_f}{S}\left(\frac{m_f}{c}\frac{x_m}{S}p_s \right) \right] +$$

$$+ (+1) \times \left[cSh\frac{x_p}{S}\left(\frac{d_f}{c} + \frac{m_p}{c}\frac{x_0}{S} + \mu\frac{b}{c}\frac{x_0}{S} \right) \right] +$$

$$+ 0 \times (\text{terms due to the other events}) + o(h) =$$

$$= \left(-d_m x_m - p_s m_m \frac{x_f}{S}x_m - p_s m_f \frac{x_m}{S}x_f + d_f x_p + (m_p + \mu b)\frac{x_0}{S}x_p \right) h + o(h)$$
(3.46)

as $h \to 0$. For the single male population density, denoting $V[v]_\bullet = X[x]_\bullet/S$ ($\bullet$ stands for m, f, or p), we thus have

$$\mathrm{E}[V_m(t+h)|V_m(t)=v_m,V_f(t)=v_f,V_p(t)=v_p]-v_m =$$

$$= \frac{1}{S}\left(\mathrm{E}[X_m(t+h)|X_m(t)=x_m,X_f(t)=x_f,X_p(t)=x_p]-x_m\right)=$$

$$\left[-d_m v_m - p_s(m_m+m_f)v_m v_f + d_f v_p + (m_p+b\mu)(1-v_m-v_f-v_p)v_p\right]h + o(h)$$
$$(3.47)$$

Letting $S \to \infty$ and $x_\bullet \to \infty$ so that $v_\bullet = x_\bullet/S$ is constant ($\bullet$ also here stands for m, f, or p), it is a straightforward but tedious exercise to show that variance in the single male density $\mathrm{Var}[V_m(t+h)|V_m(t)=v_m,V_f(t)=v_f,V_p(t)=v_p]$ tends to zero as $h \to 0$. As a consequence, as $h \to 0$, dynamics of the single male density v_m converge to the solution of the ordinary differential equation

$$\frac{dv_m}{dt} = -d_m v_m - p_s(m_m+m_f)v_m v_f + d_f v_p + (m_p+b\mu)(1-v_m-v_f-v_p)v_p$$
$$(3.48)$$

Equations for single female and pair densities follow an analogous derivation.

The non-spatial model (3.45) was analysed using the software package Content (Kuznetsov, 1998). We examined a number of scenarios differing in values of pair divorce rate m_p and probability of successful pair formation p_s. For stochastic simulations of the spatially explicit, individual-based model, one replicate run (5,000 time units) was conducted for each parameter combination, with densities during the last 200 time units averaged to get an equilibrium estimate. For each parameter combination, population dynamics were summarized into three single numbers: total population sizes in the two interior equilibria (or 0 if the equilibria did not exist), and time to extinction (time at which the total population density falls below a small predefined value ε). We could not locate the interior unstable equilibria in simulations of the spatially explicit model; hence, we compared these simulations to the behavior of the model (3.45), using only total population sizes in the interior locally stable equilibria.

Model results

Non-spatial model

The origin $E^0 = (0,0,0)$ is always a locally stable equilibrium of the model (3.45); if the male, female and pair densities are sufficiently close to zero, the population will inevitably go extinct. This is an obvious manifestation of the Allee effect due to lack of mating possibilities in a sexually reproducing population. Moreover, the model (3.45) has zero, one or two interior equilibria depending on parameter values. If two interior equilibria exist, the equilibrium E^u that is closer to the origin is unstable, while the more distant equilibrium E^s is locally stable; we already know that such a bistable regime is typical of strong Allee effects.

The locally stable equilibria E^0 and E^s are separated by a hypersurface corresponding to the Allee threshold (Fig. 3.17); populations starting below it go extinct, while those starting above it persist and equilibrate at E^s. If no pairs are initially present, sufficient numbers of single males and single females are required for the population to persist. On the other hand, if singles are absent a minimum number of breeding pairs is required to secure population persistence. Figure 3.17 shows that the minimum number of breeding pairs necessary for population persistence is lower than the minimum number of single males plus single females: paired individuals need not search for mates and may immediately begin to reproduce.
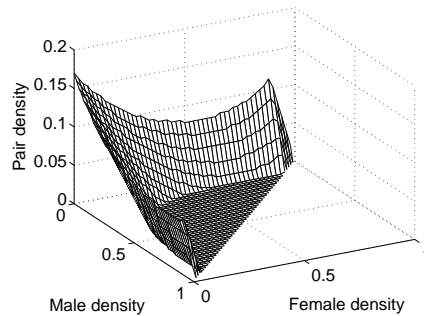

Fig. 3.17 The hypersurface characterizing the Allee threshold and separating the areas of attraction of the extinction and interior locally stable equilibria of the model (3.45). Parameters: $d_m = 0.01$, $d_f = 0.02$, $b = 0.2$, $\mu = 0.5$, $m_m = 0.2$, $m_f = 0.2$, $p_s = 0.6$, $m_p = 0.15$. We run the model for 10,000 time units and considered the population extinct if the total population density at the end of simulation decreased below $\varepsilon = 0.001$

The shape of the Allee threshold boundary leads to a somewhat counterintuitive result: for a specific range in the number of pairs (pair density around 0.1), and no or very few single males, a population goes extinct if there are either few (female density less than about 0.2) or many (female density around 0.85) single females (Fig. 3.17). In the former case, the population dies out due to low chances of singles to find mates. If the number of single females is sufficiently high, there are nearly no vacant sites to place newborns and male population thus cannot increase; minimum number of pairs needed for the population to persist thus has to be higher than for intermediate densities of single females (Fig. 3.17, female densities around 0.3-0.8). Analogous reasoning holds for males and females interchanged.

To assess population dynamical implications of the degree of mate choice and the degree of mate fidelity, we plot selected ecological characteristics of the model (3.45) as functions of the probability of successful pairing p_s and the divorce rate m_p (Fig. 3.18). While total population sizes in the interior model equilibria (Fig. 3.18a,b) give insight into the bistable Allee dynamics (small populations go extinct, large ones persist), time to extinction (Fig. 3.18c) sheds light on system dynamics under parameter combinations for which the Allee effect is too strong (i.e.

the origin is globally stable) and populations go extinct from any initial condition. Figure 3.18 shows that the degree of mate choice and the degree of mate fidelity are strongly correlated. For a population to persist, the room for mate choosiness decreases with increasing divorce rate, while the room for divorce rate increases with decreasing mate choosiness (i.e. increasing p_s). The boundary separating the parameter region with bistable regime from that with globally stable origin (we call it the bifurcation boundary further on) intersects the axes $m_p = 0$ and $p_s = 1$ in points $p_s = p_s^\star$ and $m_p = m_p^\star$, respectively. These points represent the minimum mate acceptance and the maximum divorce rate under which populations can persist. The initial condition used in Fig. 3.18c (lattice initially full of pairs) implies the slowest extinction rates. Other initial conditions generate similar results; in general, the farther we are from the bifurcation boundary and the smaller are the initial conditions, the faster is extinction.
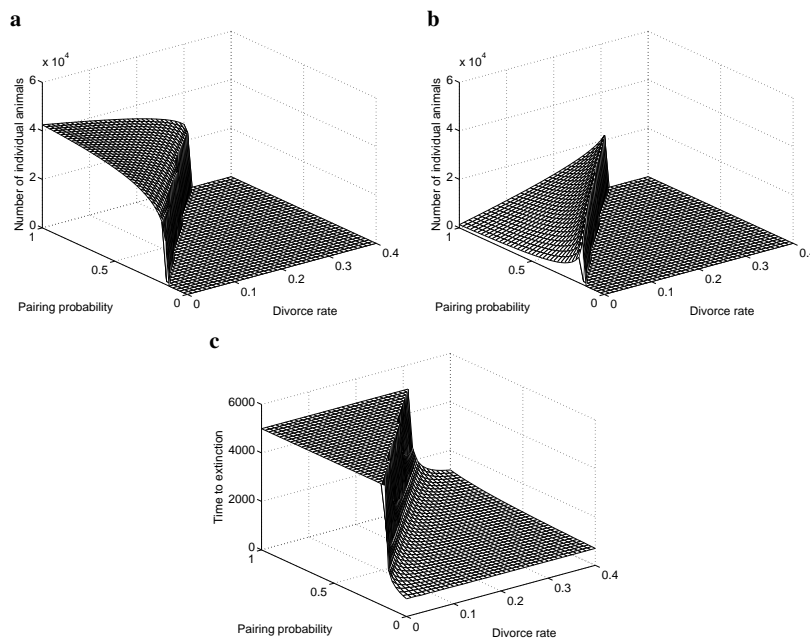
Fig. 3.18 Three currencies characterizing population dynamics of the model (3.45) as functions of the probability of successful pairing p_s and the divorce rate m_p. (a) Total population size in the interior locally stable equilibrium. (b) Total population size in the interior unstable equilibrium. (c) Time to extinction for a specific initial condition: lattice full of pairs. We run the model for 5,000 time units and considered the population extinct if the total population density at the end of simulation decreased below $\varepsilon = 0.001$. Other parameters as in Fig. 3.17

Local mate search strategies

Simulations show that on the population level, behavior of the spatially explicit, individual-based model does not differ qualitatively from that of the non-spatial model (3.45). Quantitative differences, however, do exist. Figure 3.19 compares results obtained with all three mate search strategies. In Fig. 3.19a, the divorce rate is set to $m_p = 0.05$, and the total population size in the interior locally stable (quasi)equilibrium (recall the intrinsic stochasticity of the spatially explicit, individual-based model) is calculated for various values of the successful pairing probability p_s. Relative to random searchers, we observe that the equilibrium population size increases and the bifurcation point (i.e. the point at which the global population extinction is replaced by the bistable Allee dynamics) shifts towards lower values of p_s if active mate searchers form the population. The active searchers thus persist at higher degrees of mate choice compared to the random searchers. An opposite result is observed for the passive mate search strategy: the room for mate choosiness shrinks for the passive searchers compared to the random ones. Results for the passive searchers approach those of the random searchers with increasing the maximal distance r of passive search (not shown). Figure 3.19b fixes the degree of mate choice to $p_s = 0.8$ and varies the divorce rate m_p. As a result, populations composed of the active searchers persist at much higher divorce rates than populations composed of individuals that use random or passive search to locate mates.
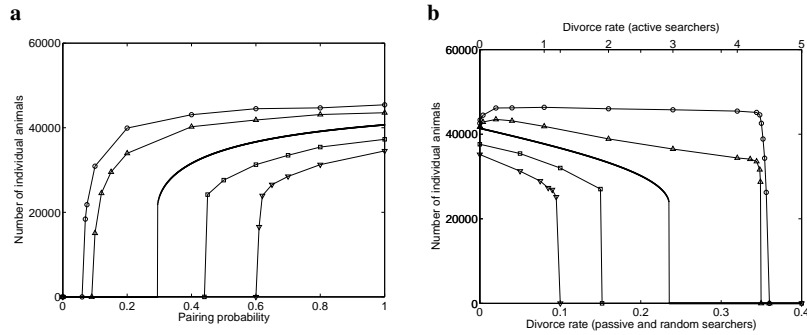
Fig. 3.19 Comparison of all three mate search strategies using total population size in the interior locally stable equilibrium as a currency. (a) $m_p = 0.05$, (b) $p_s = 0.8$. Symbols: bold line – random search, circles – active search ($s_m = s_f = 3$), upper triangles – active search ($s_m = s_f = 1$), squares – passive search ($r_m = r_f = 3$), lower triangles – passive search ($r_m = r_f = 1$). Other parameters as in Fig. 3.17

Longevity and mating strategies

Obviously, life history constraints are different in short-lived and long-lived animals. The role of longevity is summarized in Fig. 3.20 that shows the total population size in the interior locally stable equilibrium under the random search strategy. There is a limit on longevity such that populations composed of very short-lived individuals go extinct from any initial condition. Besides the birth rate b, this limit is affected by both the successful pairing probability p_s (Fig. 3.20a) and the divorce rate m_p (Fig. 3.20b). Figure 3.20a shows that all else being equal, a long-lived species persists (and reaches the same equilibrium population size) with more stringent mate choice than the short-lived one. In the same vein, Fig. 3.20b shows that all else being equal, a long-lived species survives (and reaches the same equilibrium population size) at higher divorce rates than the short-lived one. We observed the same trends for the two local mate search strategies (not shown).
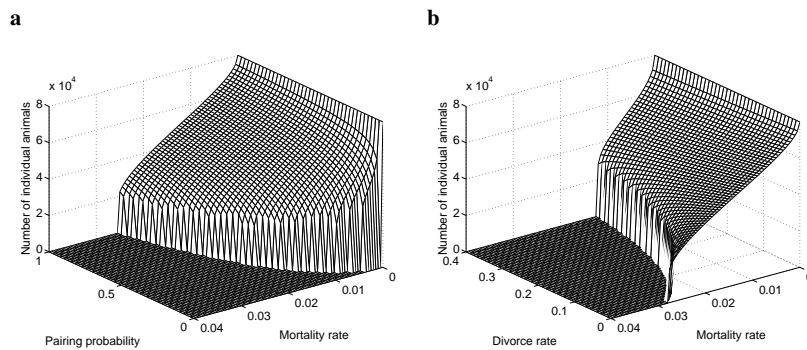
Fig. 3.20 Effects of longevity on population dynamics. Total population size in the interior locally stable equilibrium is plotted for the random search strategy. (a) $m_p = 0.05$, (b) $p_s = 0.8$. Other parameters: $d_m = d_f$ (varied), the remaining parameters as in Fig. 3.17

Summary

In this section, we examine how the process of mate search, degree of mate choice and degree of mate fidelity may interact to affect long-term population dynamics of sexually reproducing species. In particular, we address the following questions: Are degree of mate choice and degree of mate fidelity correlated? How does mate search shape this relationship? How does longevity affect mating behavior? To resolve these questions, we develop a spatially explicit, individual-based model of a sexually reproducing population with single (i.e. unpaired) males, single females, and pairs as focal units. Both this model and its mean-field approximation are shown

to give rise to a mate-finding Allee effect due to lack of mating possibilities – our models thus set ecological constraints for possible (co)evolution of mate choice and pair maintenance behavior. Our models also suggest that long-lived species persist at higher degrees of mate choice and lower degrees of mate fidelity relative to the short-lived ones.

Interplay between mate fidelity and mate choosiness

As the main result of this section, we demonstrate how population dynamics put (quantifiable) constraints on mate choice and mate fidelity. More precisely, we show that some trait combinations cannot exist because they would lead to population extinction. In addition, we show that the degree of mate choice and the degree of mate fidelity are strongly correlated. All else being equal, populations composed of individuals with longer pair-bonds (lower divorce rates) persist at higher degrees of mate choosiness compared to those that keep shorter pair-bonds; i.e. the room for mate choosiness decreases with increasing divorce rate for a population to persist under given life history. Put the other way round, individuals with higher acceptance of potential mates can still form a viable population, while maintaining shorter pair bonds.

In a monomorphic population described by our models, lifetime reproductive success of an individual is likely to be determined by the proportion of lifespan the individual spends paired. Thus, the link between the degree of mate choice and the degree of mate fidelity is mediated by a third factor: search costs. As an example, let females both initiate divorce and choose males. Increased divorce rate as well as increased female choosiness (i.e. decreased probability of successful pairing) increase the time female spends searching as a single and decrease its lifetime reproductive success. If, moreover, an increased mortality rate is associated with its single (i.e. searching) status, or a temporarily decreased reproductive output follows shortly after establishment of a new pair (Choudhury, 1995), the female's lifetime reproductive success decreases even more.

Effects of longevity

There is an ongoing debate in the literature about the relationship between longevity and mate fidelity (Saether, 1986; Choudhury, 1995; McNamara and Forslund, 1996). The evidence provided by theoretical models is ambivalent and competing hypotheses do exist. For example, it has been hypothesized that "in short-lived [migratory] species with high mortality rates, the probability that both pair members will survive to the following season will be low; selection may therefore not favor mate fidelity, since the costs of waiting for a mate that will not return are likely to be high" (Choudhury, 1995). On the other hand, "some authors have argued that divorce should be expected mainly in long-lived species, since they gain more in terms of improving lifetime reproductive success" (Choudhury, 1995). It seems that

longevity may shape the subtle relationship between mate choice and mate fidelity in various ways. Recently, Jeschke and Kokko (2008) have demonstrated that among birds, species with a high divorce rate tend to have a high mortality rate.

We add to this discussion by showing that all else being equal, long-lived species can persist with a more stringent mate choice and shorter pair bonds than short-lived ones. This result is, however, in contradiction with the findings of Saether (1986), who showed in a very simple model based on lifetime reproductive success that a promiscuous mating system (i.e. system with a high divorce rate) is more likely to evolve when the adult male mortality is high (i.e. in a short-lived species). McNamara and Forslund (1996) modeled divorce decisions of a single female over her lifetime and showed how different costs determine divorce rate in long-lived and short-lived species. Their arguments point to both directions: longevity and mate fidelity may be both positively and negatively correlated. Among other things, McNamara and Forslund (1996) showed that "a long-lived female can afford to be more discriminating in her choice of a lifetime mate because she will typically spend a long time with him once he has been chosen (female choosiness increases with longevity)". Our approach provides a mechanistic basis for this result.

Effects of mate search

All three mate search strategies we have studied preserve the qualitative results summarized in the previous paragraphs. However, they affect the exact location of both the Allee threshold in the state space and the bifurcation boundary in the parameter space. Active mate search by both sexes makes populations much less extinction-prone compared to passive search, and the random search strategy yields intermediate results. This 'ranking' follows from the complex interplay of mate search, pair maintenance, and offspring placement on the lattice. Spatial clumping, as a result of local mate search and local interactions, plays an important role in the spatio-temporal dynamics (Tilman et al, 1997; Berec et al, 2001) and hence in the strategy ranking. It increases chances of an individual to find a mate relative to random search, with the active mate searchers being most successful. On the other hand, due to local overcrowding, spatial clumping decreases chances of local searchers to place newborns into parents' neighbor sites. Relative to local passive search, local active search leads to faster pair formation and in turn to faster appearance of vacant sites.

Dubois et al (1998) hypothesized that opportunities for finding a better mate are likely to increase with the colony size and density because close proximity with conspecifics makes it easier for individuals to assess the quality of more potential partners, and showed that waterbird species forming large and dense colonies had on average higher divorce rates compared to species forming small or loose aggregations. Our results are consistent with these observations since colonial birds usually employ active mate search (visual contact, songs). For a fixed degree of mate choice, we showed that actively searching, clustered animals persist at higher divorce rates

than animals searching randomly for mates that are randomly distributed in the environment.

3.4 Multiple Allee effects and population management

Although not yet widely recognized, two or more Allee effects can occur simultaneously in the same population. Berec et al (2007) reviewed the evidence for multiple Allee effects, demonstrating their ubiquity, with examples from terrestrial and marine ecosystems, from plants, invertebrates and vertebrates, and from natural and exploited populations. Multiple Allee effects can be simultaneous, affecting the same life stage, or sequential, affecting different life stages within a generation or even affecting different generations. In addition, not all involved Allee effects need to be 'natural'. Instead, some might be created artificially, such as a mate-finding Allee effect imposed by a release of sterile males or a predation-driven Allee effect due to a release of generalist predators (Tobin et al, 2011). Mathematical modeling shows that Allee effects can also be created if species rarity enhances a price people are willing to pay for any remaining individual (Courchamp et al, 2006).

Implications of multiple Allee effects for population growth are also not yet understood. Given that the most distinctive feature of strong Allee effects is the occurrence of an Allee threshold, we focus on the magnitude of the Allee threshold that results from the interacting component Allee effects. For example, if each single Allee effect were to yield different extinction thresholds, what would be the value of the threshold resulting from the simultaneous presence of several Allee effects? Although there is currently no answer, an interaction is likely and potential consequences for the concerned populations are sufficient to warrant careful consideration by ecologists. Indirect evidence comes from the rare marsh gentian *Gentiana pneumonanthe* (Oostermeijer, 2000). In this species, lowered fecundity caused by a pollen-limitation Allee effect had little influence on the population viability, whereas increased inbreeding in small populations had a small yet significant effect; a strong reduction in population viability was found when the two acted simultaneously.

It is difficult to imagine cases in which the combined effect of multiple Allee effects is less than that of any single Allee effect. Therefore, we propose that the overall Allee threshold is equal or greater than the largest of the individual Allee thresholds. To be more specific, we develop and analyze a simple population model, so as to illustrate some of the possible outcomes of an interaction of two component Allee effects. The model population is subject to two component Allee effects, one linked to reproduction and the other to survival:

$$\frac{dN}{dt} = \sigma[1 - (1 - \theta)\exp(-\varepsilon N)]N - \delta\left(1 + \frac{N}{K}\right)N - \frac{\alpha N}{1 + \beta N} \qquad (3.49)$$

where N is population density. Divided by N, all terms are per capita, and the three terms on the right-hand side of the model (3.49) represent, in sequence, pos-

itively density-dependent birth rate (mate-finding Allee effect), negatively density-dependent intrinsic survival rate, and positively density-dependent survival rate owing to predation (predation-driven Allee effect). Positive constants $\theta < 1$ and ε define intensity of the mate-finding Allee effect, σ is the maximum birth rate, δ is the mortality rate at low densities and in the absence of predation, $K > 0$ scales the carrying capacity of the environment, and positive constants α and β scale the predation rate given by the type II functional response[1]. Because setting $\theta = 1$ and $\alpha = 0$ switches off the component Allee effect in reproduction and survival, respectively, we can assess the effects of both component Allee effects both in isolation and simultaneously.

A straightforward analysis of the model (3.49) shows that the extinction equilibrium $N^* = 0$ is unstable provided that $\delta + \alpha < \sigma\theta$, and locally stable if the opposite inequality holds. In the former case, there is one globally stable positive equilibrium corresponding to the environmental carrying capacity of the population. In addition, the population is subject to a weak Allee effect provided that $\sigma(1 - \theta)\varepsilon - \delta/K + \alpha\beta > 0$, and there is no demographic Allee effect if $\sigma(1-\theta)\varepsilon - \delta/K + \alpha\beta < 0$. If the origin $N^* = 0$ is locally stable, there can be either no or two positive equilibria depending on actual parameter values. In the former case, the origin is globally stable. In the latter, the lower positive equilibrium (Allee threshold) is unstable and the higher positive equilibrium (environmental carrying capacity) is locally stable. We failed to derive any analytical expression that would distinguish these two cases in the parameter space.

The ways in which the two component Allee effects interact are far from trivial. The outcomes of the model (3.49) vary depending on parameter values determining the strength of the individual component Allee effects (Fig. 3.21). To distinguish weak and strong interaction, the outcomes were classified according to whether the overall Allee threshold is higher or lower than the sum of the two individual Allee thresholds. We call these cases *superadditive and subadditive Allee effects*, respectively[2]. Of special interest are the cases in which none of the single Allee effects is strong, yet the double Allee effect is strong; we then speak of *dormant Allee effects*. A dormant Allee effect also occurs when only one of the single Allee effects is strong but the Allee threshold owing to the double Allee effect is higher than that of the single strong Allee effect. We use the word 'dormant' here to point out that although a weak Allee effect is rarely a reason for concern when alone, it may significantly increase the threat of population extinction when interacting with another demographic Allee effect, weak or strong. An implication of an occurrence of dormancy is that even a weak Allee effect represents a risk that should be accounted for: should another Allee effect occur, for example through human activities (Courchamp et al, 2006), it could cause the population to go extinct much faster than would be expected from the disturbance alone.

---

[1] Which implies positively density-dependent probability of an individual escaping predation.

[2] Note that superadditivity is in fact a synergistic interaction and that subadditivity represents a form of interference.
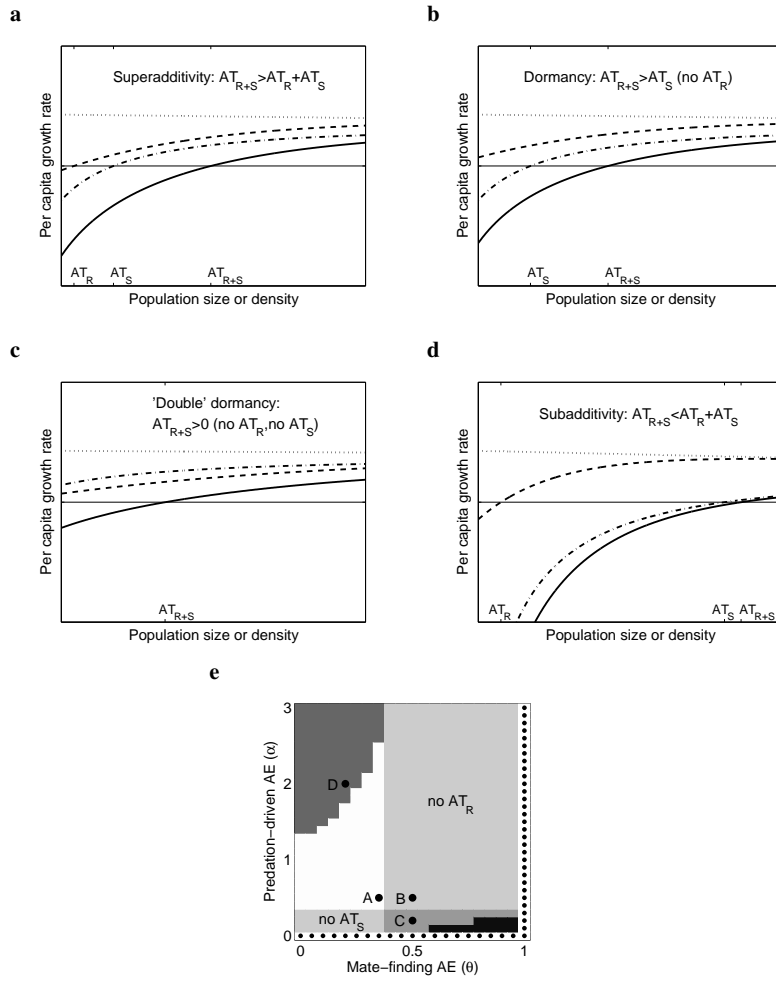
Fig. 3.21 Distribution of patterns in a section of the parameter space of how two component Allee effects interact in the model (3.49). The fixed parameters of $\sigma = 0.5$, $\varepsilon = 2$, $\delta = 0.2$, $K = 10$ and $\beta = 4$ were chosen to represent a wide spectrum of possible interaction outcomes. Panels (a) to (d) demonstrate how the per capita population growth rate depends on population size or density in the vicinity of Allee thresholds corresponding to single and double Allee effects, for specific parameter combinations shown in panel (e); dotted line, no Allee effect; dashed line, Allee effect in reproduction; dash-dot line, Allee effect in survival; solid line, double Allee effect. AT_R, AT_S and AT_{R+S} represent the Allee threshold owing to Allee effects in reproduction, survival and both components, respectively. In (e), small dots represent the combinations where there is only either a single or no component Allee effect. Six different patterns of how the two Allee effects (predation driven and mate finding) interact were observed for the parameter values examined, four of which are of particular importance here [corresponding to (a)–(d)]: superadditivity (white), $AT_{R+S} > AT_R + AT_S$; dormancy (light gray), either no AT_R or no AT_S, $AT_{R+S} > AT_S$ or $AT_{R+S} > AT_R$; double dormancy (mid gray), neither AT_R nor AT_S, $AT_{R+S} > 0$; subadditivity (dark gray), $AT_{R+S} < AT_R + AT_S$. The remaining two patterns correspond to the cases where two weak Allee effects combine to produce a joint weak Allee effect, and where a weak Allee effect and a strong Allee effect combine such that the overall Allee threshold equals that of the strong Allee effect (black)

As the model (3.49) does not allow for any detailed analysis of interaction between the mate-finding and predation-driven Allee effects, we are going to analyze its simpler version here:

$$\frac{dN}{dt} = bN\frac{N}{N+\theta} - dN - \frac{\alpha N}{1+\beta N} \tag{3.50}$$

In the absence of predation ($\alpha = 0$), the unique positive equilibrium (Allee threshold),

$$A_\theta = \frac{d\theta}{b-d} \tag{3.51}$$

exist if $b > d$ which we further assume to hold. In the absence of mate-finding Allee effect ($\theta = 0$), we have the Allee threshold

$$A_\alpha = \left(\frac{\alpha}{b-d} - 1\right)\bigg/ \beta \tag{3.52}$$

which is positive when $\alpha > b - d$, that is, when predation is strong enough. If both Allee effects co-occur, the Allee threshold is a solution of the quadratic equation

$$\beta(b-d)N^2 + (b-d-d\beta\theta-\alpha)N - \theta(d+\alpha) = 0 \tag{3.53}$$

Since the absolute term of this equation is negative and the quadratic term positive (recall we assume $b > d$), there will always be a solution to this equation, with one root negative and one root positive. The positive root,

$$A_{\theta\alpha} = \frac{-(b-d-d\beta\theta-\alpha) + \sqrt{(b-d-d\beta\theta-\alpha)^2 + 4\beta(b-d)\theta(d+\alpha)}}{2\beta(b-d)}$$
$$\tag{3.54}$$

is then the Allee threshold for the double Allee effect. This double Allee effect will be superadditive provided that

$$A_{\theta\alpha} > A_\theta + A_\alpha$$

which can be shown to always happen. Hence, for the model (3.50), the double Allee effect is always superadditive (Fig. 3.22).

Interactions of two or more component Allee effects cannot be disregarded in population management (Berec et al, 2007). Just on the contrary, management efforts can be optimized by considering multiple Allee effects, and can be negated by overlooking them. The consequences of failure to recognize all component Allee effects will largely be determined by the way in which these Allee effects interact. If only one component Allee effect is taken into account when two or more exist, the interaction of Allee effects can raise the overall Allee threshold to such an extent that conservation measures taken to cope with the recognized Allee effect will be inadequate. For example, introducing individuals so as to reach a given population size or density might prove insufficient if overlooked Allee effects raise the value of the extinction threshold. Mooring et al (2004) proposed the release of more than

a   **b**
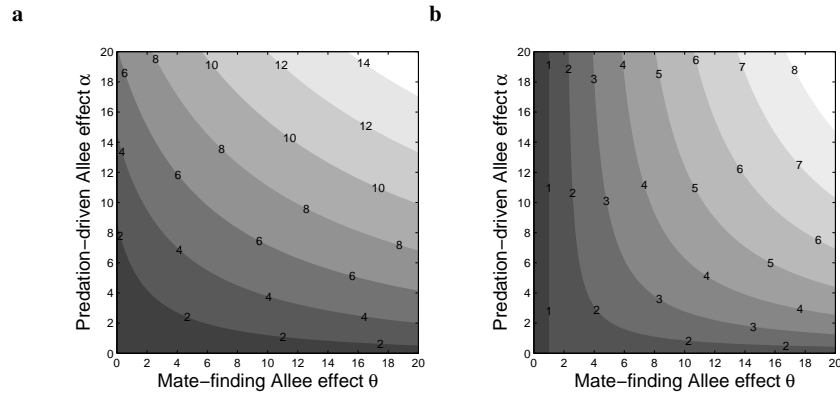
Fig. 3.22 Interaction of two component Allee effects in the model (3.50). (a) Allee threshold. (b) Degree of superadditivity: $A_{\theta\alpha} - (A_\theta + A_\alpha)$. Parameter values: $b = 3, d = 0.1, \beta = 1$

five individual desert bighorn sheep at any one time to overcome the Allee threshold owing to predation; however, managers might consider increasing this number to overcome safely its interaction with the anthropogenic Allee effect owing to trophy hunting (Courchamp et al, 2006).

To eradicate a pest population with a strong Allee effect, it is, in theory, sufficient to bring it below its Allee threshold (Liebhold and Bascompte, 2003). The higher this extinction threshold is, the less effort might be needed to achieve this goal. Several control tactics can artificially induce an Allee effect, by disrupting fertilization through the release of sterile males or sex pheromones (mate-finding Allee effect), by introducing a predator or parasitoid with a proper functional response (predation-driven Allee effect), or by removing individuals at a fixed rate (Allee effect owing to constant yield exploitation) (Dennis, 1989; Boukal and Berec, 2009; Tobin et al, 2011). If there were two or more Allee effects interacting in the pest population, the overall Allee threshold might disproportionately increase, and effort could be saved accordingly. Not all interactions can be superadditive, however. Imagine, for example, a release of sterile males together with a release of natural enemies. As the latter may also feed on the released sterile males, their interaction cannot be foreseen without careful modeling. As to our knowledge there is currently no documented example in the field, the plausibility of the idea of significant Allee threshold enhancement calls for both theoretical and empirical investigations of the conditions under which multiple Allee effects could help optimize pest control.

Some exploitation strategies can themselves be a source of a component Allee effect, as explained earlier. If a natural Allee effect acts in the same population, the overall Allee threshold might increase owing to an interaction of the two, and there is a significant risk of overexploitation if that interaction is not recognized or if the Allee threshold owing to the natural Allee effect is considered the safety limit for the stock size. Even if eventually halted, exploitation can bring the population close to or even below the Allee threshold corresponding to the natural Allee effect. Several

species of California abalones could be a typical example of stocks being unable to bounce back even after complete cessation of fishing, because of an unsuspected Allee effect acting in concert with overexploitation (Hobday et al, 2001). More than ten years after closing the fishery, it appears that an overlooked mating-related Allee effect – abalones as broadcast spawners need to exceed a critical density for an efficient fertilization (Babcock and Keesing, 1999; Gascoigne and Lipcius, 2004) – might have combined with an anthropogenic Allee effect (Courchamp et al, 2006) to drive the population below the levels that were then considered safe for exploitation.

In conclusion, interactions between component Allee effects can take several forms, many of which are far from inconsequential. As a consequence, more research is needed to assess the prevalence and interactions of multiple Allee effects, as failing to take them into account could have adverse consequences for the management of threatened, unwanted or exploited populations. On top of that, as it is impossible to estimate accurately the Allee threshold from a given component Allee effect, and to fine-tune management around this value, management of populations with Allee effects should be risk averse.

3.5 Conclusions and further research

In this chapter, we showed that the Allee threshold is generally not a single number, as frequently presented in the literature and various scientific discussions. Rather, its dimension and complexity is driven by an interaction between the examined component Allee effect and the adopted model structure. Thus, the Allee threshold due to a mate-finding Allee effects is a single number in unstructured population models, a compact curve in populations structured into juveniles and adults, a hyperbolic curve in populations structured into males and females, and a two-dimensional surface in population models comprising three model classes (juveniles, adult males, and adult females, or single males, single females, and male-female pairs). In addition, the exact location of such Allee threshold in the state space may delicately depend on details of any specific model, and help in decision making as regards optimal population management (our model with sterile males and culling and models of double Allee effects).

They are many more population models than presented here that are of an interest from the Allee threshold perspective. For example, unstructured, deterministic, discrete-time population models may demonstrate periodic solutions and even chaotic behavior (May, 1974; Case, 2000). Under (not too) strong Allee effects, an unstable equilibrium likewise appears and plays the role equivalent to the one in their continuous-time cousins. However, the high-density equilibrium, corresponding to the environmental carrying capacity in the unstructured, continuous-time models, need not be stable in their discrete-time counterparts. In the latter models, Allee effects may cause the so-called *essential extinction* where for almost every initial density population extinction occurs – the essential extinction happens once the amplitude of chaotic oscillations falls below the Allee threshold, even if it can

be preceded by long-term chaotic transients (Scheuring, 1999; Fowler and Ruxton, 2002; Schreiber, 2003). Interestingly, in such models, populations may avoid essential extinction when subject to relatively strong Allee effects (Fig. 3.23). Hence, contrary to the predominant view of Allee effects as a destabilizing force, in deterministic, discrete-time models Allee effects may sometimes stabilize population dynamics. The reason for this is that Allee effects reduce the maximum (per capita) population growth rate and hence the stronger they are the smaller are the amplitudes of population oscillations (Fig. 3.23).
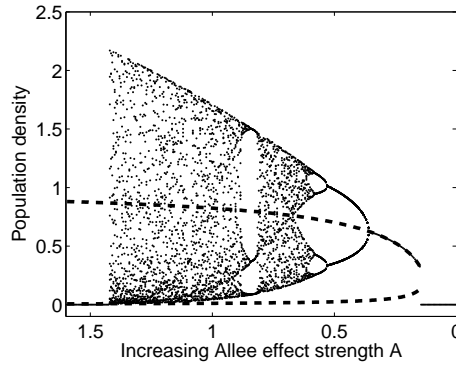
Fig. 3.23 In some deterministic, discrete-time population models with a strong Allee effect, chaotic behavior gets stabilized as the Allee effect strength increases. On the other hand, decreasing Allee effect strength can cause the population to go 'essentially' extinct (leftmost part of the figure). Model used to draw this figure: $N_{t+1} = N_t \exp[r(1 - N_t/K)]AN_t/(1 + AN_t)$, with $r = 4.5$ and $K = 1$

In deterministic population models, essential extinction notwithstanding, Allee thresholds divide the state space into two parts, one in which the population goes extinct and one in which it persists. We can express this also by saying that below the Allee threshold the probability or population extinction is one and above the Allee threshold it is zero. In stochastic population models, however, we need to interpret population fates entirely in terms of population (quasi)extinction probability. In the absence of (demographic) Allee effects, this extinction probability is an exponentially decreasing function of population size or density (Courchamp et al, 2008, and references therein). This is also the case for weak Allee effects although the exponential decrease is then much slower (Courchamp et al, 2008, and references therein). For strong Allee effects, the probability of population extinction becomes a sigmoidally decreasing function of increasing population size or density; populations are most likely to go extinct when rare, most likely to persist when abundant, but any outcome is similarly likely in a range of population sizes or densities (Courchamp et al, 2008, and references therein). In addition, the range of population sizes or densities for which the extinction probability is neither close to 1 nor 0 widens as the intensity of stochastic noise increases. As a consequence, in the stochastic world,

any population which drops below the Allee threshold may still grow and persist, while any population which starts above it may nonetheless eventually go extinct. Populations which escape extinction tend to fluctuate around the environmental carrying capacity given by the underlying deterministic model. More importantly from our perspective, Dennis (1989, 2002) showed that the Allee threshold in a deterministic population model corresponded to the inflection point of the sigmoidally decreasing extinction probability curve of an equivalent stochastic model.

These predictions are rather robust to the way deterministic models are transformed into stochastic ones (branching process or stochastic equation), type of stochasticity (demographic, environmental, or both), and life history details (continuous or pulsed reproduction, overlapping or non-overlapping generations, polygamous or monogamous mating system) (Dennis, 1989, 2002; Lamberson et al, 1992; Stephan and Wissel, 1994; Engen et al, 2003; Liebhold and Bascompte, 2003; Drake, 2004; Allen et al, 2005; Drake and Lodge, 2006). Many simulation models, including the individual-based models of Sections 3.2 and 3.3, are in fact complex branching processes whose predictions only corroborate conclusions drawn from their simpler cousins (Berec et al, 2001; Berec and Boukal, 2004).

Last but not least, virtually all of our models were non-spatial. Real populations are spatially extended and spatial population models have already become a common tool in population ecology. Recall that spatially explicit, individual-based models described in Sections 3.2 and 3.3 were developed to study the effects of spatial variation within (local) populations occupying a relatively homogeneous patch of habitat. Scaling one level up, there are models which describe the dynamics of spatially separated, local populations connected by dispersal. In this respect, an issue of immense practical importance is species invasion, a spatial phenomenon which usually consists of a localized appearance of a small number of plants or animals, establishment of an initial population, and spatial spread out of its initially small area of occurrence. Allee effects, together with demographic and environmental stochasticity, hamper successful establishment of invaders.

Models predominantly used to explore the implications of Allee effects for dynamics of invasive species treat space as a continuous entity, although discrete-space models also exist (e.g. Hadjiavgousti and Ichtiaroglou, 2004). The former include discrete-time, integro-difference equations (Kot et al, 1996; Veit and Lewis, 1996; Wang et al, 2002) and continuous-time, reaction-diffusion or reaction-diffusion-advection models (Lewis and Kareiva, 1993; Lewis and van den Driessche, 1993; Wang and Kot, 2001; Petrovskii and Li, 2003).

For passive dispersers, dispersal works to dilute the population at any given location, thereby requiring higher initial densities to overcome the Allee effect than in the counterpart non-spatial models (Taylor and Hastings, 2005). In other words, a founder population subject to a strong Allee effect may fail to establish, even when initially at levels which exceed the Allee threshold, because its growth may not be sufficient to offset the decline in local population density through dispersal. The success of a founder population in invasion will thus depend not only on the initial population density, but also on the shape and size of the area that the founder population initially occupies (Lewis and Kareiva, 1993; Kot et al, 1996). Generally, the

larger is the initially occupied area, the lower is the threshold density of local populations. The ability of a founder population to grow and spread will also depend on the habitat size (Shi and Shivaji, 2006; Courchamp et al, 2008) and the intensity of advection to which the population might be exposed (Petrovskii and Li, 2003; Almeida et al, 2006).

Currently unresolved questions surrounding Allee thresholds include interactions between structured population models and stochasticity or space. In fact, virtually all stochastic or spatial models with an Allee effect are unstructured, and those that consider a population structure do not study Allee thresholds in detail. So, how will the probability of population extinction look like in two-sex models? And how will Allee thresholds look like in spatial, age-structured models? Similarly, multiple Allee effects have so far been only studied in the deterministic, non-spatial framework. So, how will the probabilities of population extinction compose for a double Allee effect? And how will two critical spatial ranges corresponding to two Allee effects interact when these Allee effects co-occur? And how will speeds of the corresponding traveling waves combine? Also, one might be interested in the effects of stochasticity in discrete-time population models with Allee effect and prone to essential extinction. Last but not least, we have already mentioned above that it would be extremely useful to classify various interactions of specific Allee effects as regards their superadditivity or subadditivity, if such a classification is possible at all. These and other questions will inevitably throw more light onto dynamics of extinction, and can be addressed only through analyzing carefully developed mathematical models of population dynamics.

Finally, up to now, population models with Allee effects have assumed that the strength of these Allee effects does not vary with time, space, and/or individuals. This is unlikely to be the case in nature, as some studies start to demonstrate (Tobin et al, 2007). Therefore, a highly interesting avenue for further exploration of dynamics of populations subject to Allee effects considers exploration of the impacts of heterogeneity in the Allee effect strength across time, space, and/or individuals. We are currently working on some of these issues.

Chapter 4
Allee effects in predator-prey interactions

Most mathematical models used to study Allee effects are single-species population models. But even though these models have been very useful for understanding Allee effects, their failure to account for interspecific relationships is in many cases an oversimplification. The next step is to include the external ecological drivers of population dynamics of many species – predation, competition, parasitism, mutualism, or any combination of these. Any of these interactions can be affected by Allee effects and demonstrate dynamics which are different from those observed in the absence of Allee effects anywhere in the community.

In this chapter, we discuss some investigations on how Allee effects influence predator-prey interactions. In the first two sections, we consider predator populations that do not respond numerically to the target prey species; these are referred to as *generalist predators* further on, since this situation best fits a predator which is in a dynamic association with another, primary prey, and consumes the focal prey as a secondary resource. Then, in the other two sections, we consider *specialist predators*, i.e. interactions between a predator and its primary prey, assuming that either the prey or the predator are subject to an Allee effect.

Allee effects and generalist predators

Predators cause an extra mortality to their prey. A common framework to explore prey dynamics in the presence of generalist predators is

$$\frac{dN}{dt} = N g(N) - f(N, P) P \tag{4.1}$$

where N and P are prey and (constant) predator densities, respectively, $g(N)$ is the per capita growth rate of prey in the absence of predation, and $f(N, P)$ is a predator functional response. We already know from the previous chapter that if $g(N) = bN/(N + \theta) - (d + d_1 N)$, for example, the prey population in the absence of predation demonstrates an Allee effect. We also know from Section 3.4 on dou-

ble Allee effects that predation (and exploitation) can create component Allee effects in prey (Gascoigne and Lipcius, 2004; Berec et al, 2007). This requires that the ability of prey to escape predation increases as prey density increases. Denoting $p(N) = f(N,P)P$, the probability that a prey individual escapes predation in a (small) time interval Δt equals

$$F(N) = 1 - [p(N)/N]\Delta t \tag{4.2}$$

Hence, for a predation-driven component Allee effect to occur, we require $dF/dN > 0$ for all $N > 0$. This implies

$$\frac{\partial f(N,P)}{\partial N} < \frac{f(N,P)}{N} \quad \text{for all } N \geq 0 \text{ and any fixed } P \geq 0 \tag{4.3}$$

or that the per capita consumption rate of generalist predators (i.e. predator functional response) increases at a decelerating rate as a function of prey density. From the perspective of classical, predator-density-independent functional response types, this inequality holds true for type II and type IV functional responses, but not for type I and type III functional responses. For example, the type II functional response $f(N,P) = \alpha N/(\beta + N)$, which is the most frequently observed one (Hassell et al, 1976; Jeschke et al, 2002), is a hyperbolic curve that rises from zero to an asymptote (Fig. 4.1a). This means that although there is an increase in predator consumption rate with prey density, this increase is not enough to offset the rate of increase in prey density. As a consequence, as prey density increases, there are more prey individuals per predator attack, and thus a lower probability that any prey individual will be captured by a predator – a predation-driven Allee effect (Fig. 4.1b). Note that type III (sigmoid) functional responses can impose an equilibrium known as *predator pit* – rare prey populations do not go extinct but rather approach a locally stable, low-density equilibrium maintained by predation which is potentially far below the environmental carrying capacity of prey (Fig. 4.1b; May, 1977).

In some species, it is prey behavior rather than predator consumption of prey which is a mechanism for an Allee effect in prey. Consider a herding, flocking, or schooling prey species in which efficiency of anti-predator behavior decreases with declining prey abundance, and consider a predator with a linear functional response $f(N) = aN$, with a positive attack rate a. Since the efficiency of anti-predator behavior increases with increasing prey abundance N, the predator attack rate may be described, e.g. as $a = \alpha/(\beta + N)$. This implies $f(N) = \alpha N/(\beta + N)$, i.e. a type II functional response. Similarly, we can get a type IV functional responses when $a = \alpha/(\beta + N^2)$. Hence, models of predation-driven component Allee effects may, at least in some cases, be used to describe component Allee effects due to reduced efficiency of anti-predator behavior in low-density prey populations.
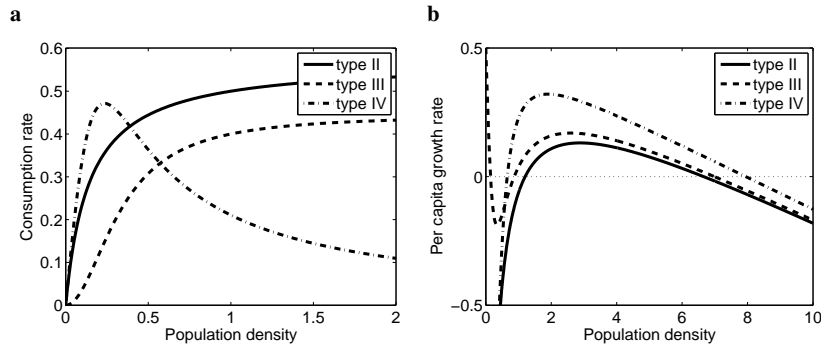
Fig. 4.1 Predator per capita consumption rates (a) and the corresponding per capita prey growth rates (b) for the model (4.1) with logistic prey growth and type II, type III, and type IV functional responses. Population densities for which the per capita growth rates equal zero in (b) define positive system equilibria

Allee effects and specialist predators

The standard framework mathematical modelers use to explore predator-prey dynamics involving specialist predators is the pair of ordinary differential equations, one for the prey population and the other for the predator population:

$$\frac{dN}{dt} = N g(N) - f(N,P) P$$

$$\frac{dP}{dt} = e f(N,P) P - m P$$

(4.4)

Here, in addition to the model (4.1), we have a dynamic equation for predators in which m is the predator per capita mortality rate and e is an efficiency with which energy obtained from consuming prey is transformed into predator offspring. Other frameworks for exploring predator-prey dynamics also exist (e.g. Murray, 1993).

Allee effects may occur both in prey (in term $g(N)$) and in predators (in term $f(N,P)$). In both cases, Allee effects generally destabilize predator-prey dynamics (Courchamp et al, 2008, and references therein). In particular, strong Allee effects may (i) cause a coexistence equilibrium to change from stable to unstable, (ii) extend the time needed to reach the stable coexistence equilibrium, (iii) reduce the equilibrium density of the affected species, and (iv) enlarge the range of parameter values for which prey and predators cannot coexist. In addition, weak Allee effects in prey cause the predator-prey systems to cycle for a wider range of parameter values than systems without Allee effects, provided that predators have a type II or weakly sigmoidal functional response (Boukal et al, 2007). In the latter two sections of this chapter, we present and analyze mathematical models of two specific predator-prey systems in which Allee effects occur respectively in prey and predator populations.

4.1 Caught between two Allee effects: trade-off between reproduction and predation risk

Reproductive activities are often associated with conspicuous morphology or behavior that could be exploited by predators. Individuals can therefore face a trade-off between reproduction and predation risk. Indeed, many species have evolved anti-predator behavior during which they stop mating and perform an escape manoeuvre (Svensson et al, 2004, 2007). Higher levels and/or prolonged periods of spatial movement (Anholt and Werner, 1995; Kotiaho et al, 1998) or sexual signalling (Zuk and Kolluru, 1998) during mate search help find a mate or choose a better one but can also attract predators. Predation risk may also be high during copulation, pregnancy, spawning and breeding period when the individuals are often less motile or easier to detect (Trochine et al, 2005; Svensson, 1997; Winfield and Townsend, 1983). Both reproductive success and probability of avoiding predation, involved in the reproduction-predation risk trade-off, may be positively related to population size or density and therefore subject to a component Allee effect (Courchamp et al, 1999, 2008; Stephens and Sutherland, 1999). In this section, we use simple models to explore population-dynamical consequences of such a trade-off for populations subject to a mate-finding Allee effect and an Allee effect due to predation. We distinguish several qualitative scenarios characterized by the shape and strength of the trade-off and, in particular, identify conditions for which the populations survive or go extinct. Although the literature offers no quantitative data on possible trade-off shapes in any taxa, indirect evidence suggests that the trade-off and both Allee effects can occur simultaneously, e.g. in the golden egg bug *Phyllomorpha laciniata*.

To quantify the extinction risk we use *population resilience*, defined as the maximum disturbance the population in a stable state may sustain to avoid extinction (Beisner et al, 2003), and *relative population resilience*, by which we mean a relative change in the resilience of the population after a predator removal/addition. When measuring relative resilience, we also distinguish prey with flexible and inflexible reproductive behavior. We assume that *flexible reproductive behavior* (determining strength of the mate-finding Allee effect) can be instantly changed after predator removal or addition, whereas *inflexible reproductive behavior* cannot respond to predator presence or absence. They represent extreme but useful approximations of real reproductive behavior, which can involve both morphological and behavioral traits. Most morphological traits such as bright coloration of males in many birds and many types of behavior such as lekking displays of various birds and flies (Andersson, 1994) are hardwired characteristics that individuals cannot change and therefore correspond to the inflexible behavior. On the other hand, quite a number of behavioral traits such as mating calls in some orthopteroid insects are plastic. They can be adjusted to the perceived predation risk (Zuk and Kolluru, 1998) and we represent them by the flexible behavior in our model. We ask the following questions: When do the two component Allee effects lead to extinction of the population? How are the results affected by the shape of the reproduction-predation risk

trade-off? And finally, do the results for prey with flexible and inflexible reproductive behavior differ?

Model development

We use several simplifying assumptions on the life histories and population densities of males and females: identical mortalities, balanced sex ratio at birth and equal initial densities. This allows us to follow changes of the total population density N in time without discerning between males and females (Box 4.2):

$$\frac{dN}{dt} = bN\frac{N}{N+\theta} - dN\left(1+\frac{N}{K}\right) - f(N)P \tag{4.5}$$

We thus use a variant of the generic model (4.1) for which we assume a mate-finding Allee effect (the first term on the right-hand side), negative density dependence in the prey mortality rate (the second term) and no predator interference in prey consumption (the third term); b is the per capita birth rate, d is the intrinsic mortality rate at low densities, K scales the environmental carrying capacity, θ represents strength of the mate-finding Allee effect, and P is a constant predator population density. In addition, we assume the predator functional response $f(N)$ to be of type II, and use two alternative descriptions for it, $f(N) = \alpha N/(1+N/\beta)$ and $f(N) = \lambda N/(1+\lambda hN)$. The latter form is the standard formulation due to Holling (1959), in which λ scales the predator-prey encounter rate and h is the handling time of one prey individual, and represents an Allee effect due to predator satiation (Gascoigne and Lipcius, 2004; Berec et al, 2007; Courchamp et al, 2008). The former expression can be interpreted as a predation-driven Allee effect invoked by a behavioral response of prey (e.g. herding or mobbing) to predators with an otherwise linear functional response: the behavioral response is more efficient at higher population densities and reduces the (linear) attack rate α by a factor of $1/(1+N/\beta)$. Note that β scales the maximum per capita attack rate ($= \alpha\beta$) but also defines the population density at which $f(N)$ declines to 50% of its maximum value, and we refer to β as *prey vulnerability* in this section.

We rescale models due to both versions of the type II functional response to reduce the number of parameters from seven to five. In the model with α and β, we rescale the state variable as $x = N/K$ and time as $\tau = td$ and define new parameters $\Theta = \theta/K$ (relative strength of the mate-finding Allee effect), $B = \beta/K$ (relative prey vulnerability), $g = b/d$ and $\delta = P/d$, to obtain

$$\frac{dx}{d\tau} = gx\frac{x}{x+\Theta} - x(1+x) - \frac{\alpha x\delta}{1+x/B} \tag{4.6}$$

Rescaling the model with λ analogously, we get

$$\frac{dx}{d\tau} = gx\frac{x}{x+\Theta} - x(1+x) - \frac{\lambda x \delta}{1+\lambda Hx} \tag{4.7}$$

where $H = hK$ (relative handling time) and the other parameters are as above. The parameters α, B and λ scale the strength of Allee effect due to predation: predation mortality in the models (4.6) and (4.7) increases with increasing α, B and λ. Only the parameter Θ scales the strength of mate-finding Allee effect in these models, and reproductive success declines with increasing Θ. We skip the adjective 'relative' when further referring to parameters Θ, B and H.

Reproduction-predation risk trade-off

Trade-off shapes can strongly influence evolutionary dynamics and endpoints (Bell, 1980; Rueffler et al, 2004; Hoyle et al, 2008). We thus consider a range of trade-off shapes that cover varying costs of reproduction in terms of predation risk, and investigate two trade-offs for the model (4.6),

$$\alpha = \alpha_{\max}\left(1 - \left(\frac{\Theta}{\Theta_{\max}}\right)^z\right)^{1/z} \tag{4.8}$$

and

$$B = B_{\max}\left(1 - \left(\frac{\Theta}{\Theta_{\max}}\right)^z\right)^{1/z} \tag{4.9}$$

and one trade-off for the model (4.7),

$$\lambda = \lambda_{\max}\left(1 - \left(\frac{\Theta}{\Theta_{\max}}\right)^z\right)^{1/z} \tag{4.10}$$

These three trade-offs can describe a range of situations in which increasing reproductive success of the population (i.e. decreasing Θ) leads to increasing attack rate (α increases, e.g. since individuals become less vigilant or unable to escape), increasing prey vulnerability (B increases, e.g. since individuals devote less time to herding or chasing away predators), or increasing encounter rate (λ increases, e.g. since individuals become more conspicuous). Further on, we refer to the model (4.6) with the trade-off (4.8) as the *attack rate model*, abbreviated as AR, to the model (4.6) with the trade-off (4.9) as the *prey vulnerability model*, abbreviated as PV, and to the model (4.7) with the trade-off (4.10) as the *encounter rate model*, abbreviated as ER.

   Maximum predation pressure ($\alpha = \alpha_{\max}$, $B = B_{\max}$ and $\lambda = \lambda_{\max}$) occurs for $\Theta = 0$ when there is no mate-finding Allee effect, and predation ceases ($\alpha = 0$, $B = 0$, and $\lambda = 0$) for $\Theta \geq \Theta_{\max}$ when reproductive activities become so suppressed that predators can no longer exploit the prey. The parameter z quantifies the overall predation risk associated with reproduction. Values of $z < 1$ (convex trade-offs) correspond to 'cheap' reproductive activities, for which the predation risk remains low

until Θ is relatively small, i.e. until the mate-finding Allee effect is relatively weak due to efficient prey reproductive activities. On the other hand, values of $z > 1$ (concave trade-offs) correspond to 'costly' reproduction, for which the predation risk remains elevated for a wide range of effort associated with reproductive activities, e.g. because courting or gravid individuals are more conspicuous (Fig. 4.2).
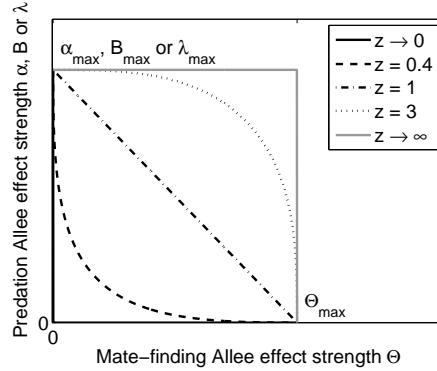

Fig. 4.2 Trade-offs (4.8) to (4.10) as they vary with the shape parameter z

Analysis

The models (4.6) and (4.7) can have, in addition to the extinction equilibrium $x_0 = 0$, either no positive equilibrium or a unique positive equilibrium that is stable or two positive equilibria, of which the higher (labelled S) is stable and the lower (U) unstable (see below for the exact results). We focus here only on the difference $R = S - U$ and call it population resilience. It can be interpreted as the maximum disturbance after which the population can still return back to the stable equilibrium without going extinct. If there is only a unique positive equilibrium that is stable, we set $U = 0$.

We start with standard viability analysis of the models (4.6) and (4.7) and search for the stable and unstable equilibria and conditions for their existence. In the simplest cases when Θ and/or α or λ are zero or B infinitely small (that is, one or both component Allee effects are absent), the equilibria can be calculated analytically. We use Matlab 7 (The MathWorks, Inc.) to find the equilibria numerically when both Allee effects are present.

To investigate the role of reproduction-predation risk trade-off, we examine the impact of changes in the strength of mate-finding Allee effect Θ on the population resilience R along the trade-off in the AR, PV and ER models. In addition, we explore relative population resilience along the trade-off for prey with flexible and inflexible reproductive behavior. In line with the general considerations above, by

'flexible' we mean that prey reproductive behavior can be changed instantly such that there is no mate-finding Allee effect ($\Theta = 0$) in the absence of predators and there is some ($\Theta > 0$) in their presence, while prey with inflexible reproductive behavior are assumed to keep the same $\Theta > 0$ regardless of predators. For prey with flexible behavior, we therefore measure the relative population resilience as $\rho_f = (S - U)/(S_0 - U_0)$, where S_0 and U_0 correspond to no predation ($P = 0$) and no mate-finding Allee effect ($\Theta = 0$), i.e. $U_0 = 0$; in fact ρ_f is just a multiple of the population resilience R. For prey with inflexible behavior, we measure the relative population resilience as $\rho_i = (S - U)/(S_1 - U_1)$, where S_1 and U_1 correspond to no predation and the mate-finding Allee effect remaining at the unchanged strength $\Theta > 0$; ρ_i always equals 1 if there is no predation.

Model results

Model equilibria and their stability

The extinction equilibrium $x_0 = 0$ of the model (4.6) is locally stable for any mate-finding Allee effect ($\Theta > 0$). It is globally stable, i.e. the population goes extinct regardless of its density, and no other equilibria exist if the mate-finding Allee effect and/or the predation-driven Allee effect are sufficiently strong (i.e. if Θ and/or α are sufficiently large). For no mate-finding Allee effect ($\Theta = 0$), x_0 is locally or globally stable if $\alpha > (g-1)/\delta$ and unstable if $\alpha < (g-1)/\delta$. In the latter case, the population always reaches a unique positive equilibrium (environmental carrying capacity) regardless of its (positive) initial density. A complete analysis of the case with no mate-finding Allee effect is given in Box 4.1.

If the extinction equilibrium $x_0 = 0$ is only locally stable, two positive equilibria exist of which the lower is unstable (Allee threshold) and the upper is locally stable (environmental carrying capacity). All else being equal, the two positive equilibria approach one another with increasing Θ and/or α until both merge and cease to exist in a saddle-node bifurcation; the extinction equilibrium then becomes globally stable (Fig. 4.4a). The population resilience R is maximized for no mate-finding Allee effect and no predation ($\Theta = 0$ and $\alpha = 0$; $R = g - 1$) and declines as the strength of mate-finding Allee effect Θ and/or the attack rate α increase (Fig. 4.5a; the thin lines depict isolines along which the resilience is constant). The lower limit of the isolines is the viability limit at which the positive equilibria merge and $R = 0$. For Θ and/or α to the right and above the viability limit, the population cannot persist as deaths exceed births for any population density. We denote the mate-finding Allee effect strength and the attack rate at which the viability limit intersects the respective axes as Θ_{lim} and α_{lim} ($\Theta_{\text{lim}} = 0.172$ and $\alpha_{\text{lim}} = 2.55$ in Fig. 4.5a). The relative population resilience ρ_i of prey with inflexible reproductive behavior is maximized in the absence of predation ($\alpha = 0$) and declines with increasing α for any $0 < \Theta < \Theta_{\text{lim}}$ (Fig. 4.5b).

Box 4.1 Analysis of the models (4.6) **and** (4.7)

Setting the right-hand side of the equation (4.6) to zero always has the trivial solution $x_0 = 0$, corresponding to population extinction. The extinction equilibrium x_0 is locally stable for $\Theta > 0$ as the derivative of the right-hand side of the equation (4.6) with respect to x, evaluated at x_0, is $-1 - \alpha\delta < 0$ (all model parameters are positive).

To find positive model equilibria for $\Theta > 0$, we solve the equation

$$G(x) = g\frac{x}{x+\Theta} - (1+x) - \frac{\alpha\delta}{1+x/B} = 0 \qquad (4.11)$$

Since G is always concave ($G''(x) < 0$), model (4.6) can have at most two different positive equilibria. We used Matlab to find out numerically that there is either no positive equilibrium or that they are just two of which the lower is unstable (Allee threshold) and the upper is locally stable (environmental carrying capacity).

The case $\Theta = 0$ (no mate-finding Allee effect, only the Allee effect due to predation) allows for more detailed analysis. Straightforward yet tedious algebra gives the results summarized in Table 4.1; the areas I-IV are shown in Fig. 4.3a.

For the model (4.7) and $\Theta > 0$, the analysis follows the same lines as above with analogous results. The results for $\Theta = 0$ are summarized in Table 4.2; the areas I-V are shown in Fig. 4.3b.

For both models (4.6) and (4.7) and $\Theta > 0$, the extinction equilibrium x_0 can also be unique and globally stable if the mate-finding Allee effect and/or the Allee effect due to predation are sufficiently strong; for $\alpha = 0$ or $B \to 0$ or $\lambda = 0$, this happens when $\Theta > \Theta_{\lim} = (1 - \sqrt{g})^2$.
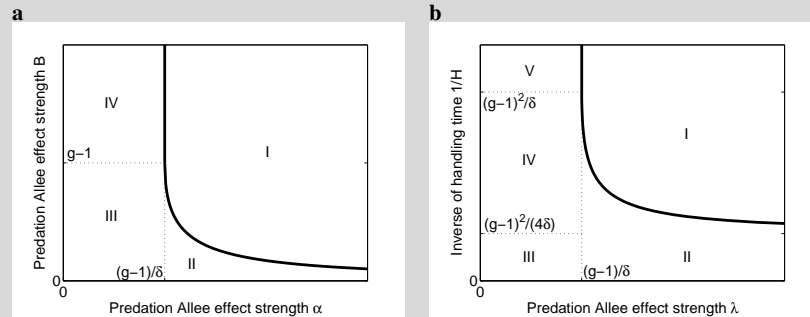
Fig. 4.3 Model analysis for no mate-finding Allee effect ($\Theta = 0$). (a) Numbers and stability of equilibria of the model (4.6) in the $\alpha - B$ parameter space. Areas I-IV explained in Table 4.1. (b) Numbers and stability of equilibria of the model (4.7) in the $\lambda - H$ parameter space. Areas I-V explained in Table 4.2

Area	Conditions	Extinction equilibrium $x_0 = 0$	Positive equilibria
I	$\alpha > (g-1)/\delta$ and $\alpha > \alpha_{\lim}(B)$ (alternatively $B > B_{\lim}(\alpha)$)	globally stable	no positive equilibrium
II	$\alpha > (g-1)/\delta$ and $\alpha < \alpha_{\lim}(B)$	locally stable	two equilibria: lower unstable (Allee threshold), upper locally stable (carrying capacity)
III	$\alpha < (g-1)/\delta$ and $B < g-1$	unstable	unique, globally stable equilibrium (carrying capacity)
IV	$\alpha < (g-1)/\delta$ and $B > g-1$	unstable	unique, globally stable equilibrium (carrying capacity) that vanishes at $\alpha = (g-1)/\delta$

Table 4.1 Analysis of the model (4.6) for no mate-finding Allee effect ($\Theta = 0$). Parameters α, g, δ and B are explained in the main text; $\alpha_{\lim}(B) = [B(1+1/B-g/B)^2/4 + g - 1]/\delta$ and $B_{\lim}(\alpha) = (g-1)^2/[2\alpha\delta - g + 1 + \sqrt{(2\alpha\delta - g + 1)^2 - (g-1)^2}]$

Area	Conditions	Extinction equilibrium $x_0 = 0$	Positive equilibria
I	$\lambda > (g-1)/\delta$ and $\lambda > \lambda_{\lim}(H)$	globally stable	no positive equilibrium
II	$\lambda > (g-1)/\delta$ and $\lambda < \lambda_{\lim}(H)$	locally stable	two equilibria: lower unstable (Allee threshold), upper locally stable (carrying capacity)
III	$\lambda < (g-1)/\delta$ and $1/H < (g-1)^2/(4\delta)$	unstable	unique, globally stable equilibrium (carrying capacity)
IV	$\lambda < (g-1)/\delta$ and $(g-1)^2/(4\delta) < 1/H < (g-1)^2/\delta$	unstable	unique, globally stable equilibrium (carrying capacity)
V	$\lambda < (g-1)/\delta$ and $1/H > (g-1)^2/\delta$	unstable	unique, globally stable equilibrium (carrying capacity) that vanishes at $\lambda = (g-1)/\delta$

Table 4.2 Analysis of the model (4.7) for no mate-finding Allee effect ($\Theta = 0$). Parameters λ, g, δ and H are explained in the main text; $\lambda_{\lim}(H) = 1/(H(1-g) + 2\sqrt{H\delta})$

For high attack rates, $\alpha > (g-1)/\delta$, the dependence of equilibria of the model (4.6) on the mate-finding Allee effect strength Θ and the prey vulnerability B is qualitatively the same as in Fig. 4.4a and the corresponding (relative) population resilience plots are analogous to Fig. 4.5a-b. For low attack rates, $\alpha < (g-1)/\delta$, the results differ qualitatively and high values of B do not affect the equilibria (Fig. 4.4b). This is because for highly vulnerable prey ($1/B$ close to 0) the predation term in the model (4.6) reduces to $\alpha\delta x < (g-1)x$, and hence for $\Theta = 0$ the population always attains a unique positive equilibrium (carrying capacity) that is globally stable. In biological terms, the prey cannot go extinct if the mate-finding
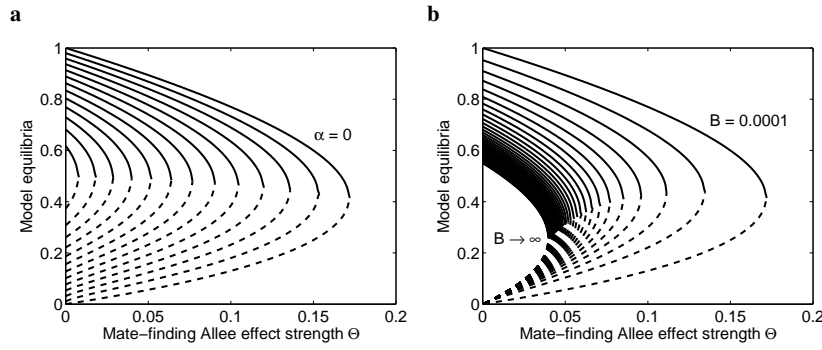
Fig. 4.4 Equilibria of the model (4.6). Stable (solid lines) and unstable (dashed lines) equilibria of the model (4.6) as they depend on (a) the mate-finding Allee effect strength Θ and the predator attack rate α for $g = 2$, $B = 0.01$ and $\delta = 10$ and on (b) the mate-finding Allee effect strength Θ and the prey vulnerability B for $g = 2$, $\alpha = 0.05$, $\delta = 10$. Lines of equilibria in panel (a) range from $\alpha = 0$ until 2.4 (step size 0.2; no equilibria beyond $\alpha = 2.55$), and lines of equilibria in panel (b) start with $B = 0.0001$ and have step size 0.1 (lines for large B approach the leftmost line corresponding to $B \rightarrow \infty$)

Allee effect is absent and the attack rate is low enough. Consequently, the viability limit and isolines of the (relative) population resilience in the $\Theta - B$ parameter space are much more convex (Fig. 4.5c-d).

Similar conclusions hold for the existence and stability of equilibria of the model (4.7). The extinction equilibrium $x_0 = 0$ is locally or globally stable for any mate-finding Allee effect ($\Theta > 0$). For no mate-finding Allee effect ($\Theta = 0$), $x_0 = 0$ is locally or globally stable for high prey encounter rates $\lambda > (g-1)/\delta$ and unstable for $\lambda < (g-1)/\delta$. A complete analysis for $\Theta = 0$ (see Box 4.1) implies that if the handling time is sufficiently short, $H < 4\delta/(g-1)^2$, the positive equilibria of the model (4.7), population resilience and relative population resilience behave similarly as shown in Figs. 4.4a, 4.5a and 4.5b, respectively. On the other hand, long handling times, $H > 4\delta/(g-1)^2$, yield results that are qualitatively analogous to Figs. 4.4b, 4.5c and 4.5d and the encounter rate λ affects the location of equilibria only when relatively small. This is because the predation-driven Allee effect is not strong enough to drive the population to inevitable extinction even for virtually infinite encounter rates λ, for which the predation term in the model (4.7) reduces to a constant δ/H.

The isoline plots of (relative) population resilience in Fig. 4.5 also reveal that the prey population can or cannot always be eliminated by strong predation. Populations that can always be eliminated by strong predation are characterized by plots in which the viability limit intersects the y-axis at some $\alpha_{\text{lim}} < \infty$ (Fig. 4.5a-b). These populations will be wiped out by predation with $\alpha > \alpha_{\text{lim}}$ irrespective of the strength of mate-finding Allee effect Θ; we call them *populations with predation limit*. On the other hand, the viability limit of some populations may not intersect the y-axis (Fig. 4.5c-d). These populations cannot be wiped out by predation of any strength
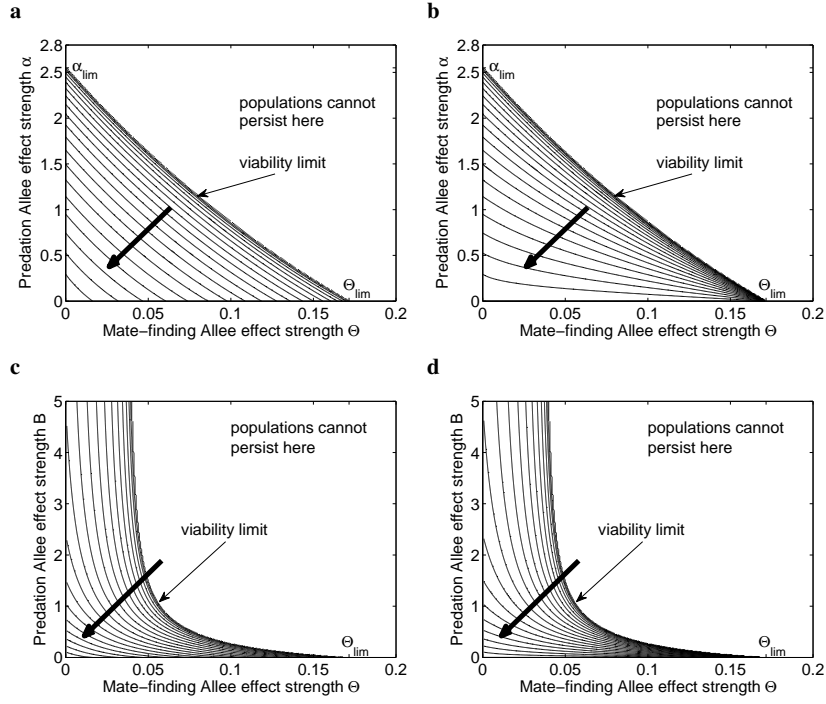
Fig. 4.5 Population resilience (panels (a) and (c)) and relative population resilience for prey with inflexible reproductive behavior (panels (b) and (d)) for the model (4.6), plotted as a function of the mate-finding Allee effect strength Θ and the predator attack rate α (panels (a) and (b)) and the mate-finding Allee effect strength Θ and the prey vulnerability B (panels (c) and (d)). Parameter values: (a-b) $g = 2$, $B = 0.01$ and $\delta = 10$, so that $\Theta_{lim} = 0.17$ and $\alpha_{lim} = 2.55$. (c-d) $g = 2$, $\alpha = 0.05$ and $\delta = 10$, so that $\Theta_{lim} = 0.17$ and there is no B_{lim}. The thin lines are isolines of the (relative) population resilience, increasing from 0 to $g - 1$ with stepsize 0.05 (indicated by thick arrow). These two pairs of panels ((a) with (b) and (c) with (d)) represent two generic outcomes that all models analyzed in this section produce

when the mate-finding Allee effect strength Θ is sufficiently low and we call them *populations without predation limit*. Populations without predation limit appear in the PV model with low attack rates α and in the ER model with long handling times H (Table 4.3).

Population resilience under reproduction-predation risk trade-off

How do population resilience and relative population resilience change along the reproduction-predation risk trade-off? And how is the population affected by the shape of the trade-off? We first explain several examples, based on the AR model, in detail before giving the complete results. We have already shown how the pop-

Model	Populations with predation limit (Fig. 4.5a-b)	Populations without predation limit (Fig. 4.5c-d)
AR	Always	Never
PV	$\alpha > (g-1)/\delta$	$\alpha < (g-1)/\delta$
ER	$H < 4\delta/(g-1)^2$	$H > 4\delta/(g-1)^2$

Table 4.3 Two generic cases distinguishing the qualitative shape of the (relative) population resilience surface plots in Fig. 4.5

ulation resilience changes with the strength of mate-finding Allee effect and the predation pressure (Fig. 4.5a). We now overlay different trade-off shapes over the isoline landscape. The curves A, B and C in Fig. 4.6a are three trade-off curves (4.8) that exemplify the main differences in the qualitative outcomes reported here.

First, there is a difference between cheap and costly reproduction. For sufficiently 'cheap' reproductive activities characterized by a convex trade-off curve ($z < 1$, curve A in Fig. 4.6a), the resilience R can be maximized at intermediate values of the mate-finding Allee effect strength (curve A in Fig. 4.6b). Populations with more costly reproductive activities characterized by linear and concave trade-offs ($z \geq 1$, curve B in Fig. 4.6a) have the resilience always maximized either in the absence of predation ($\Theta = \Theta_{\max}$ and $\alpha = 0$) or in the absence of the mate-finding Allee effect ($\Theta = 0$ and $\alpha = \alpha_{\max}$; as for curve B in Fig. 4.6b). The exact value of z above which the maximum resilience can no longer occur at an intermediate Θ depends on the curvature of the trade-off relative to the curvature of the isolines; the value will be $z < 1$ because the isolines are always convex.

Second, populations might be always safe or liable to extinction as the strength of mate-finding Allee effect and the predation pressure vary along the trade-off. This is determined by the location of the trade-off relative to the viability limit: populations characterized by trade-off curves A and B persist for any Θ between 0 and $\Theta_{\max}$ and only go extinct if $\Theta > \Theta_{\lim}$, while populations characterized by trade-off curve C go extinct for intermediate values of Θ between 0 and $\Theta_{\max}$ (curve C in Fig. 4.6b; the maximum strengths of the two Allee effects due to mate-finding and predation are larger for curve C than for curve B). In extreme cases, the trade-off can be so severe that the population always goes extinct (see below).

Finally, we note that predation ceases and only the mate-finding Allee effect operates for $\Theta > \Theta_{\max}$. Any two trade-offs thus give the same results for Θ above the larger of their $\Theta_{\max}$ values. In addition, if $\Theta_{\max} < \Theta_{\lim}$, the population resilience declines with increasing Θ for $\Theta > \Theta_{\max}$ until it reaches zero at $\Theta = \Theta_{\lim}$ (all curves in Fig. 4.6b).

Now we give the complete results. Results for populations with predation limit can be classified into five qualitatively different scenarios, characterized by the location of the point corresponding to the maximum double Allee effect without any trade-off, i.e. point $[\Theta_{\max}, \alpha_{\max}]$ or $[\Theta_{\max}, B_{\max}]$ for model (4.6) and point $[\Theta_{\max}, \lambda_{\max}]$ for the model (4.7), relative to the viability limit. The five scenarios correspond to the five areas marked as A to E in Fig. 4.7a. Results for populations
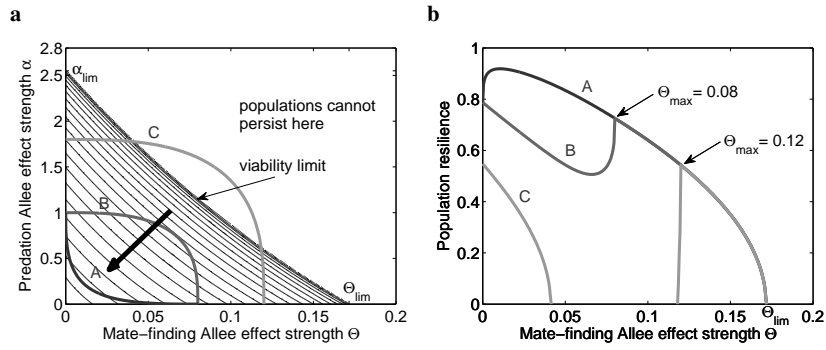
Fig. 4.6 Population resilience under reproduction-predation risk trade-off. (a) The population resilience R as a function of Θ and α with examples of three trade-off curves marked A, B and C. Thin black lines = isolines of population resilience, increasing from 0 to $g-1$ with stepsize 0.05 (indicated by thick arrow). Populations cannot persist above the viability limit = the isoline connecting the points $[\Theta_{\lim}, 0]$ and $[0, \alpha_{\lim}]$ at which $R = 0$; R is maximized for $\Theta = 0$ and $\alpha = 0$ where $R = g - 1$. (b) The population resilience R as a function of Θ along the three trade-off curves shown in panel (a). Trade-offs A and B yield the same resilience for $\Theta > \Theta_{\max} = 0.08$ and trade-offs A, B and C for $\Theta > \Theta_{\max} = 0.12$. See the main text for details. Parameter values: $g = 2$, $B = 0.01$, $\delta = 10$; trade-off curves: $\Theta_{\max} = 0.08$, $\alpha_{\max} = 1$, $z = 0.4$ (A), $\Theta_{\max} = 0.08$, $\alpha_{\max} = 1$, $z = 3$ (B), and $\Theta_{\max} = 0.12$, $\alpha_{\max} = 1.8$, $z = 3$ (C)

without predation limit can be described by only three scenarios (areas A to C in Fig. 4.7b), which are covered by the former five: parameter combinations from areas A to C in Fig. 4.7a and Fig. 4.7b give qualitatively analogous results. We thus present and discuss only the results for populations with predation limit.
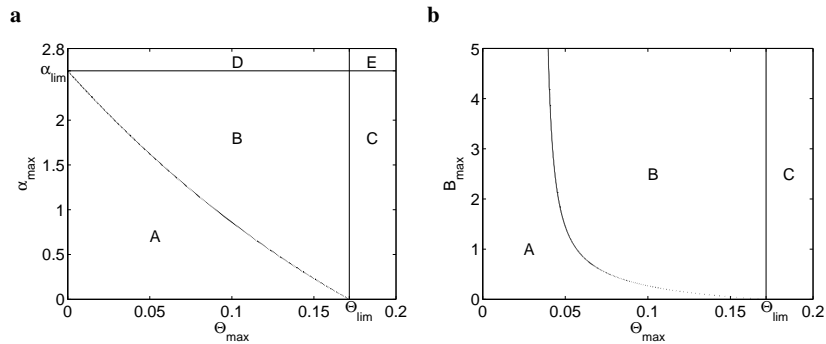
Fig. 4.7 Parameter regions yielding the five different scenarios for populations with predation limit (a) and the three scenarios for populations without predation limit (b). See also Table 4.3 and the main text for details
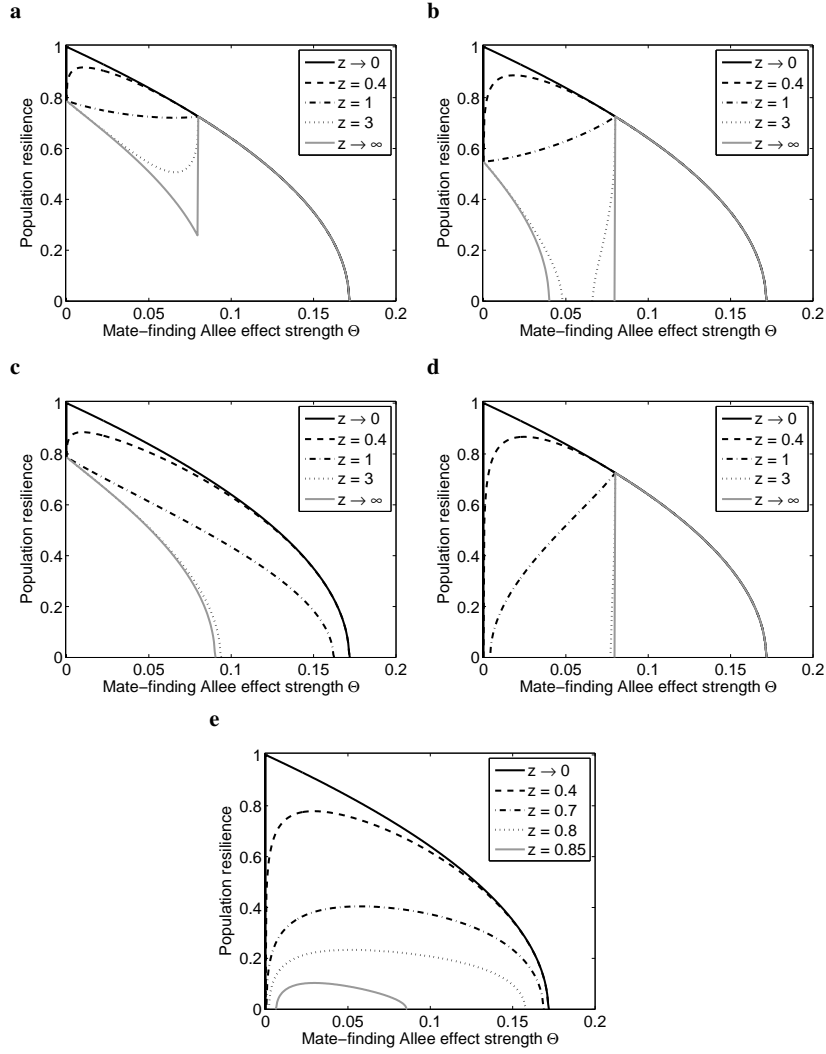
In all five scenarios, the population resilience declines with increasing cost of reproduction (i.e. increasing z) for the mate-finding Allee effects satisfying $\Theta < \Theta_{lim}$ (Fig. 4.8). The main distinguishing feature of each scenario is whether and for what values of Θ the population cannot persist. The population will survive predation irrespective of the strength of mate-finding Allee effect and the shape of the trade-off only in scenario A (Fig. 4.8a). In biological terms, this scenario corresponds to prey that can survive predation even when both Allee effects are at maximum strength. In all other scenarios, the population may go extinct; the range of Θ that lead to extinction increases with z. In scenario B, the population will not survive predation for intermediate Θ and sufficiently costly reproduction (i.e. concave trade-offs with high values of z; Fig. 4.8b). This contrasts with the remaining three scenarios in which intermediate values of Θ are typically 'the safest' and the population goes extinct for high, low, and both high and low levels of reproductive activity in scenarios C, D and E, respectively (Fig. 4.8c-e). In other words, extinction occurs for strong mate-finding Allee effects (high Θ) if their maximum strength is very high (cases C and E) and for weak mate-finding Allee effects (low but positive Θ) if the maximum strength of Allee effect due to predation is very high (cases D and E). In the latter case, the trade-off results in strong Allee effects due to predation. Finally, the population is never viable for sufficiently costly reproduction in scenario E (Fig. 4.8e).

The relative population resilience ρ_f of prey with flexible reproductive behavior is a multiple of the population resilience R and can thus be taken from Fig. 4.8. We observe the same five qualitatively different scenarios for the relative population resilience ρ_i of prey with inflexible reproductive behavior (Fig. 4.9), although the value of Θ at which the relative population resilience ρ_i is maximized (or minimized) can be different from that for the (relative) population resilience R (ρ_f) (compare the corresponding panels in Figs. 4.8 and 4.9).

Summary

A trade-off between reproduction and predation risk occurs in many animals but its impact on population viability has been little studied. We have focused in this section on the viability of a population that faces, along with this trade-off, two different Allee effects due to reproduction and predation, and examined how various characteristics of the population and shapes of the trade-off affect its resilience to disturbances. We have also compared the results for prey that can or cannot adjust their reproductive activity to the predation level.

We have found that the fate of a population, given its demographic rates g and δ, depends on three main factors: the cost of reproduction (that is, the trade-off shape characterized by the parameter z), the maximum strength of mate-finding Allee effect at which predation ceases, and the maximum strength of Allee effect due to predation in the absence of the mate-finding Allee effect (that is, the trade-off location characterized by the parameters α_{max}, B_{max} or λ_{max}, respectively). While the

Fig. 4.8 Examples of the five scenarios of the impact of reproduction-predation risk trade-off between the mate-finding Allee effect strength Θ and the attack rate α on the population resilience R for the AR model. Panels (a-e) represent examples from the equally marked areas in Fig. 4.7a. Parameter values: $g = 2$, $B = 0.01$ and $\delta = 10$, so that $\Theta_{\lim} = 0.17$ and $\alpha_{\lim} = 2.55$; (a) $\Theta_{\max} = 0.08 < \Theta_{\lim}$ and $\alpha_{\max} = 1 < \alpha_{\lim}$; (b) $\Theta_{\max} = 0.08 < \Theta_{\lim}$ and $\alpha_{\max} = 1.8 < \alpha_{\lim}$; (c) $\Theta_{\max} = 0.18 > \Theta_{\lim}$ and $\alpha_{\max} = 1 < \alpha_{\lim}$; (d) $\Theta_{\max} = 0.08 < \Theta_{\lim}$ and $\alpha_{\max} = 2.6 > \alpha_{\lim}$; (e) $\Theta_{\max} = 0.18 > \Theta_{\lim}$ and $\alpha_{\max} = 2.6 > \alpha_{\lim}$

results depend strongly on the reproduction-predation risk trade-off, the flexibility or inflexibility of prey reproductive behavior as well as the type of Allee effect due
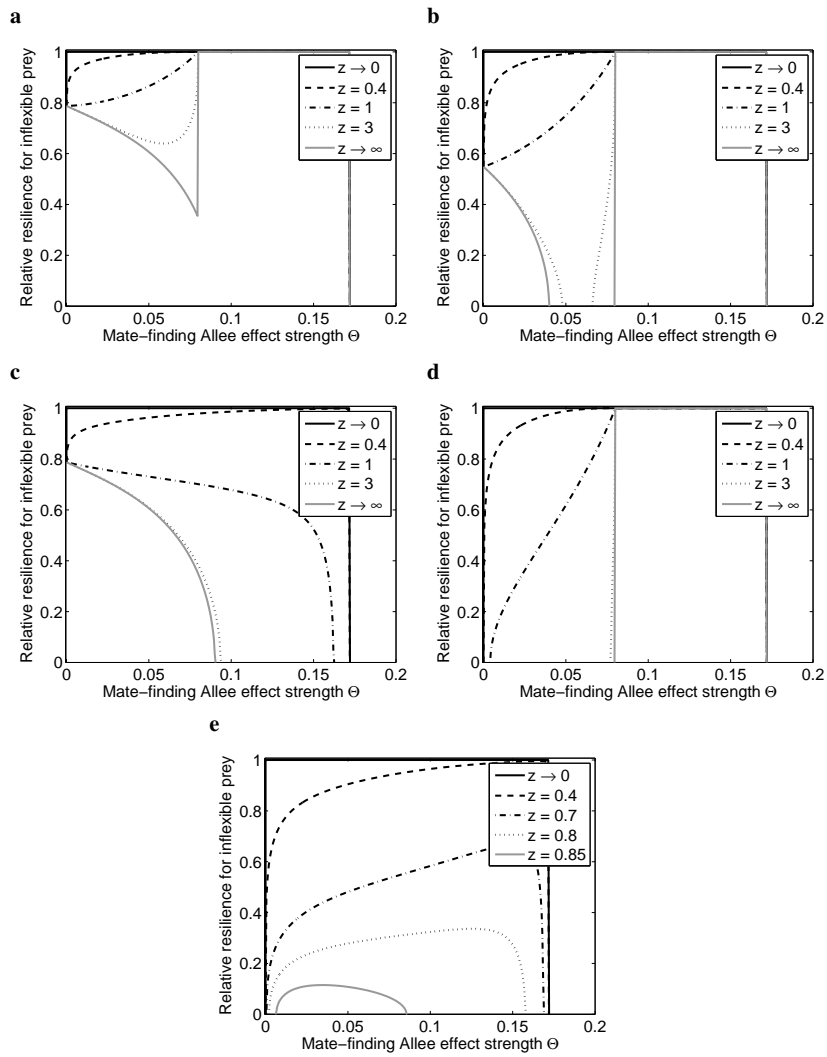
Fig. 4.9 Examples of the five scenarios of the impact of reproduction-predation risk trade-off between the mate-finding Allee effect strength Θ and the attack rate α on the relative population resilience ρ_i for prey with inflexible reproductive behavior for the AR model. Legend as in Fig. 4.8

to predation (that is, models AR, PV and ER) do not produce qualitatively different outcomes. We summarize all results jointly in what follows.

Overall, the (relative) population resilience declines with increasing cost of reproduction embodied in the parameter z that represents the strength of reproduction-predation risk trade-off. In some cases, reproduction can be so costly in terms of predation that the population always goes extinct. In other cases, the population

goes extinct only over a certain range of mate-finding Allee effects, which may correspond to high, low or intermediate levels of reproductive activity. For example, intermediate levels of reproductive activity might be the only ones that guarantee population survival (e.g. sufficiently convex trade-offs in scenario E in Fig. 4.8e) or that, on the contrary, lead to population extinction (e.g. sufficiently concave trade-offs in scenario B in Fig. 4.8b).

Our results on the relative population resilience imply that the impact of predator manipulation (i.e. removal or addition) differs quantitatively but not qualitatively for prey with flexible and inflexible reproductive behavior. That is, our main results are equally valid if predators exploit hardwired traits associated with reproduction (such as coloration) or if they exploit adjustable prey behavior such as the intensity and duration of mating calls. All else being equal, predator manipulation has the largest effect on populations with high cost of reproduction in terms of predation. This can have either positive or negative consequences depending on the application: conservation biologists have obviously opposing goals to pest managers.

Predator removal is often considered among conservation management strategies because it can increase survivorship in endangered populations (Sinclair et al, 1998). Our modeling results show that removal of predators can be particularly worthwhile for populations with predation limit that can be heavily predated and must suppress their reproductive behavior considerably in order to avoid predation (i.e. have relatively high α_{max} and Θ_{max}; area E in Fig. 4.7a). On the contrary, pest management might attempt to remove a pest by augmenting existing or introducing entirely new predators (Solomon et al, 2000). Here we demonstrate that, within the types of life histories and ecological interactions considered in our models, the most difficult pests fall into the category of populations that are without predation limit and face relatively few difficulties in finding mates when they manage to avoid predation (i.e. have relatively small Θ_{max}; area A in Fig. 4.7b).

Given the disparate results on population viability that depend on quantitative details of the reproduction-predation risk trade-off, it is clear that no general rule of thumb can be put forward and the fate of a population subject to antagonistic mate-finding and predation-driven Allee effects should be evaluated on a case-by-case basis. In every case, as our results suggest, searching for multiple Allee effects and their relationship in plant and animal populations could reveal new and interesting insights and is worth further research both by theoreticians and field workers.

Last but not least, we have also highlighted how surprisingly little is known on the processes that, according to our results, drive population dynamics under the reproduction-predation risk trade-off. More data are needed to assess which shapes of the trade-off are most common in nature and how often species are actually caught between two Allee effects caused by reproduction and predation.

4.2 Impacts of predation on dynamics of age-structured prey: Allee effects and multi-stability

Understanding the mechanisms that allow predators to regulate density of their prey may help in efficient population management, be it pest biocontrol, harvesting of economically important species, or endangered species protection (Hajek, 2004; Berec et al, 2007; Hunter and Gibbs, 2007). Examples abound of different predator species feeding on juveniles and adults of a prey species. For example, juveniles of the Utah prairie dog *Cynomys parvidens* are more prone to predation by northern goshawks, whereas adults, especially pregnant females, are more often killed by foxes (Hoogland et al, 2006). As the different predator species feeding on different age classes of prey may often be representatives of different genera or even classes, they may be expected to possess different foraging habits and hence different functional responses, quantitatively or even qualitatively. We are also interested in prey dynamics where only juveniles or adults are consumed by a generalist predator. Predation of or escape from predation in one of the age classes of prey may have important consequences for dynamics of the prey population as a whole. For example, the lack of predation on pupae was suspected to cause outbreaks of such prey species as the winter moth *Operophtera brumata* (Raymond et al, 2002).

Importance of predator-prey models that incorporate an age structure in prey for getting more realistic predictions of dynamics of the involved populations has already been acknowledged (Wikan, 2001; de Roos et al, 2003; Jang, 2007, 2010). Specifically, in a series of papers, Hastings demonstrated that age-dependent predation can have a stabilizing effect on predator-prey dynamics (Hastings, 1983, 1984a,b,c). However, all models developed and analyzed in these studies assumed specialist predators[1], which attacked one or more prey age classes. To our best knowledge, there has been no study so far that would explore dynamics of an age-structured population of prey consumed by generalist, age-specific predators[2].

Therefore, in this section, we develop and analyze a simple predator-prey model (albeit with relatively complex behavior) in which juvenile and adult prey are exploited each by a different generalist predator (or no predator). We use this model to explore impacts of various combinations of predator functional responses (or no functional response) on prey population dynamics, assuming that at least one of the functional responses is of type II, the most frequently observed type of functional response (Hassell et al, 1976; Jeschke et al, 2002). In particular, we focus on the potential of predators to generate strong Allee effects or more generally multiple stable equilibria in prey. In practical terms, we ask about the possibility of prey population suppression or even complete eradication. From here on, we will briefly speak of Allee effects to mean strong Allee effects with an Allee threshold.

---

[1] Predators that numerically responded to prey densities.

[2] Generalist predators are predators that do not numerically respond to changes in prey abundance.

Model development

We structure the prey population into two age classes – juveniles and adults – and assume its growth to be resource-limited, with juveniles and adults feeding on different resources:

$$\frac{dJ}{dt} = bA - mJ - d_j J \left(1 + \frac{J}{K_j}\right) - P_j$$

$$\frac{dA}{dt} = mJ - d_a A \left(1 + \frac{A}{K_a}\right) - P_a$$

(4.12)

Here J and A represent juvenile and adult density, respectively, b is the per adult birth rate, m is the maturation rate, d_j (d_a) is the intrinsic mortality rate of juveniles (adults) due to factors other than consumption by focal predators, and K_j (K_a) scales the environmental carrying capacity of juveniles (adults). As we assume generalist predators with constant densities, there are no dynamic equations for predators. For the predation terms P_j and P_a, we use five different combinations (Table 4.4) of no predation, $P_j = 0$ or $P_a = 0$, a type II functional response,

$$P_j = \frac{L_j J}{1 + B_j J} \quad \text{or} \quad P_a = \frac{L_a A}{1 + B_a A}$$

(4.13)

and a type III functional response

$$P_j = \frac{L_j J^2}{1 + B_j J^2} \quad \text{or} \quad P_a = \frac{L_a A^2}{1 + B_a A^2}$$

(4.14)

In these expressions, L_j/B_j is the maximum attack rate of predators at high juvenile densities and B_j is the inverse of juvenile density (type II) or of square of juvenile density (type III) at which the attack rate reaches 50% of its maximum value. The parameters L_a and B_a have an analogous interpretation for adults.

Case	Juveniles – P_j	Adults – P_a
A	Type II	no predation
B	no predation	Type II
C1	Type II	Type II
C2	Type II	Type III
C3	Type III	Type II

Table 4.4 Examined combinations of predator functional responses on juveniles and adults

We analyze dynamics of the prey population with respect to parameters m, L_j and L_a, as representatives of the age structure of the prey population and of the predation pressure. The other parameters were set to somewhat arbitrary values which nonetheless follow some reasonable assumptions about the age classes, such

as lower mortality rate of adults relative to juveniles (Table 4.5). Simulations with other parameter values than those in Table 4.5 produced qualitatively similar results.

Parameter	Meaning	Baseline value
b	Per adult birth rate	1
d_j	Intrinsic mortality rate of juveniles	0.02
d_a	Intrinsic mortality rate of adults	0.01
K_j	Parameter scaling carrying capacity for juveniles	5
K_a	Parameter scaling carrying capacity for adults	3
B_j	Parameter scaling functional response for juveniles	0.8
B_a	Parameter scaling functional response for adults	0.5

Table 4.5 Baseline parameter values

Model results

The point $E_0 = (J_0, A_0) = (0, 0)$ is a steady state of the model (4.12) for any of the examined cases and will be referred to as the extinction equilibrium further on. When there is no predation ($P_j = P_a = 0$), E_0 is unique and globally stable if $m(b - d_a) - d_j d_a < 0$ or equivalently $b < d_a(1 + d_j/m)$ (Box 4.2). Local stability results for E_0 when there is predation are summarized in Table 4.6. In general, E_0 is locally stable if the death rate exceeds the birth rate for either only low or any prey population densities. In the former case, the prey population is subject to an Allee effect and an interior steady state exists. In the latter case, E_0 is unique and globally stable.

Box 4.2 Interior equilibria of the model (4.12) **in case of no predation**

Interior equilibria of the model (4.12) do exist if the model isoclines,

$$f_1(J) = A = \frac{m}{b}J + \frac{d_j}{b}J\left(1 + \frac{J}{K_j}\right) + \frac{P_j}{b}$$

$$f_2(A) = J = \frac{d_a}{m}A\left(1 + \frac{A}{K_a}\right) + \frac{P_a}{m}$$

(4.15)

intersect in the first quadrant ($J > 0$ and $A > 0$) of the state space. For no predation ($P_j = P_a = 0$), the isoclines represent two parabolic functions that intersect at $J = A = 0$ and that have their vertices in the fourth quadrant ($J < 0$ and $A < 0$) of the state space – so their parts in the first quadrant are increasing functions. Whether they also intersect in the first quadrant depends on the

tangent lines of the parabolic functions at the origin. Imagining J as the x-axis and A as the y-axis, the tangent line corresponding to the f_1 isocline with $P_j = 0$ is

$$S_1 = \left.\frac{\partial f_1}{\partial J}\right|_{J=0} = \frac{m+d_j}{b} \tag{4.16}$$

Similarly, the tangent line corresponding to the f_2 isocline with $P_a = 0$ is (note that $A = f_2^{-1}(J)$ in the first quadrant)

$$S_2 = 1 \left/ \left[\left.\frac{\partial f_2}{\partial A}\right|_{A=0}\right]\right. = \frac{m}{d_a} \tag{4.17}$$

The two isoclines intersect in the first quadrant provided that $S_1 < S_2$ which happens if

$$m(b - d_a) - d_j d_a > 0 \tag{4.18}$$

Also, due to the form of the two isoclines in the first quadrant, the respective interior equilibrium denoted here as E_1 is unique.

Now, let $f(J,A)$ and $g(J,A)$ denote the right-hand sides of equations for J and A of the model (4.12), respectively. For no predation ($P_j = P_a = 0$), $f(K,K) < 0$ if and only if $K > K_j(b - m - d_j)/d_j$. Similarly, $g(K,K) < 0$ if and only if $K > K_a(m - d_a)/d_a$. Hence, for any fixed

$$K > \max\left\{K_j \frac{b - m - d_j}{d_j}, K_a \frac{m - d_a}{d_a}\right\}$$

$dJ/dt < 0$ for $J = K$ and $A \in [0,K]$ and $dA/dt < 0$ for $A = K$ and $J \in [0,K]$. This all implies that the area $[0,K] \times [0,K]$ is attracting for any trajectory of the system (4.12). In addition, since

$$\frac{\partial f}{\partial J} + \frac{\partial g}{\partial A} = -m - d_j - \frac{2d_j}{K_j}J - d_a - \frac{2d_a}{K_a}A < 0$$

for $J \geq 0$ and $A \geq 0$, then according to the Bendixson's criterion there are no periodic orbits of the system (4.12) in $[0,K] \times [0,K]$.

If $m(b - d_a) - d_j d_a < 0$ we already know that E_0 is the only equilibrium of the model (4.12). The Jacobian evaluated in this equilibrium is

$$\mathbf{J} = \begin{pmatrix} -m - d_j & b \\ m & -d_a \end{pmatrix} \tag{4.19}$$

This implies $Tr(J) < 0$. In addition, $Det(J) > 0$ if and only if $m(b - d_a) - d_j d_a < 0$. Hence, once $m(b - d_a) - d_j d_a < 0$, the unique equilibrium E_0 is locally stable. Given the above derivations, the Poincaré-Bendixson theory implies that E_0 is also globally stable.

If $m(b - d_a) - d_j d_a > 0$, E_0 is unstable and we already know that there is an interior equilibrium E_1. In addition, it can be shown that the tangent line to the stable manifold of E_0 evaluated at E_0 crosses the second and fourth quadrants of the state space and the tangent line of its unstable manifold crosses the first and third quadrants. We thus exclude the possibility that trajectories of the system (4.12) approach a cycle graph. As a consequence, the Poincaré-Bendixson trichotomy implies that all system trajectories must approach an equilibrium. Since trajectories starting in the interior of $[0, K] \times [0, K]$ cannot approach E_0 they much approach the interior equilibrium E_1. Thus, we conclude that E_1 is globally stable (and hence also locally stable) whenever it exists.

Case	Determinant and trace of Jacobian at E_0	Conditions on local stability of E_0
A and C2	$Det(J) = -[m(b - d_a) - d_j d_a] + L_j d_a$, $Tr(J) = -(m + d_j + d_a + L_j)$	$L_j > \frac{m(b-d_a)-d_j d_a}{d_a}$ or equivalently $m < \frac{(L_j+d_j)d_a}{b-d_a}$ for $b > d_a$; $m > 0$ (i.e. always) for $b < d_a$
B and C3	$Det(J) = -[m(b-d_a)-d_j d_a] + L_a(d_j+m)$, $Tr(J) = -(m + d_j + d_a + L_a)$	$L_a > \frac{m(b-d_a)-d_j d_a}{d_j+m}$ or equivalently $m < \frac{(L_a+d_a)d_j}{b-d_a-L_a}$ for $b > d_a + L_a$; $m > 0$ (i.e. always) for $b < d_a + L_a$
C1	$Det(J) = -[m(b - d_a) - d_j d_a] + L_j d_a + L_a(d_j + m) + L_j L_a$, $Tr(J) = -(m + d_j + L_j + d_a + L_a)$	$L_a > \frac{m(b-d_a)-d_j d_a - L_j d_a}{d_j+m+L_j}$ or equivalently $m < \frac{(L_a+d_a)(L_j+d_j)}{b-d_a-L_a}$ for $b > d_a + L_a$; $m > 0$ (i.e. always) for $b < d_a + L_a$

Table 4.6 Conditions on local stability of the extinction equilibrium $E_0 = (0, 0)$. Since the trace $Tr(J)$ of the Jacobian of the model (4.12) stays always negative for any of the examined cases, whether E_0 is locally stable or not depends on the sign of its determinant $Det(J)$; E_0 is locally stable if $Det(J) > 0$ and unstable if $Det(J) < 0$

Due to negative density dependence in prey growth, the model (4.12) possesses an interior equilibrium once the extinction equilibrium ceases to be stable. Indeed, when there is no predation ($P_j = P_a = 0$), this equilibrium exists if $m(b - d_a) - d_j d_a > 0$ or equivalently $b > d_a(1 + d_j/m)$, and is unique and globally stable (E_0 is unstable; Box 4.2). On the contrary, two or even more interior equilibria may exist once predation acts ($P_j > 0$ and/or $P_a > 0$; see below). Although the graphical analysis of isoclines can tell us how many positive equilibria the model (4.12) may have in any of the examined cases A to C3, these equilibria are not analytically tractable (they are roots of higher-order polynomials that cannot be factorized). We thus perform their stability and bifurcation analyses using Matlab 7 (The MathWorks, Inc.), including the third-party Matlab package Matcont that al-

lows for numerical bifurcation analysis of dynamical systems defined by ordinary differential equations (Dhooge et al, 2003).

We observe several types of prey dynamics due to different prey maturation rates (parameter m), different predator functional responses (no, type II, or type III), and different predation pressure (parameters L_j and/or L_a). Most frequently, we observe (i) a unique interior equilibrium which is globally stable (the extinction equilibrium is here unstable), (ii) an additional, unstable interior equilibrium, defining an Allee threshold, as a result of an emerging, predation-driven Allee effect (the extinction equilibrium is here locally stable), and (iii) still another, locally stable, low-density equilibrium corresponding to a predator pit whereby the prey population is able to persist at two alternative stable densities, low and high (the extinction equilibrium is here unstable). In addition to these major and fairly expected patterns (although not always expected where they actually occur; see below), there are situations in which even three (locally) stable interior equilibria coexist or where two (locally) stable interior equilibria co-occur with the (locally) stable extinction equilibrium. We now go through the examined cases A to C3 one by one.

Case A. Once there is predation only on juveniles and the predator exhibits a type II functional response, the model (4.12) may possess up to three interior equilibria (Box 4.3; examples given in Fig. 4.10). Slow maturation (low m) and sufficiently strong predation (high L_j) make prey extinction the globally stable event, for obvious reasons of the prey population not being able to replicate itself. The higher is the maturation rate, the wider is the range of predation pressure under which the prey population is able to persist (Fig. 4.10). When maturation is fast enough (high enough m), there is a unique interior equilibrium which is globally stable (Fig. 4.10; Box 4.3). This is because fast maturation allows juveniles to swiftly escape the danger of predation and enjoy safe life as adults. At intermediate maturation rates there is a range of L_j values for which an Allee effect develops (two interior equilibria) and even a range of L_j values for which a predator pit occurs (three interior equilibria) (Fig. 4.10). Where both an Allee effect and a predator pit occur for the same m, the Allee effect occurs for higher predation pressures L_j (Fig. 4.10).

Box 4.3 Up to three interior equilibria in case A

For $P_a = 0$ and $P_j = L_j J/(1 + B_j J)$, the juvenile isocline $f_1(J)$ becomes

$$f_1(J) = A = \left(\frac{m}{b} + \frac{d_j}{b}\right)J + \frac{d_j}{bK_j}J^2 + \frac{(L_j/b)J}{1 + B_j J} \qquad (4.20)$$

while the adult one is given by (4.15). Thus, $f(J)$ is increasing ($f'(J) > 0$) for all $J > 0$, concave ($f''(J) < 0$) for $0 < J < (\sqrt[3]{B_j L_j K_j/d_j} - 1)/B_j$ and convex ($f''(J) > 0$) for $J > (\sqrt[3]{B_j L_j K_j/d_j} - 1)/B_j$. Hence, for $B_j L_j K_j < d_j$, the model (4.12) can have at most one interior equilibrium, for the same reasons as in Box 4.2, while for $B_j L_j K_j > d_j$, due to concave-convex form of one isocline and concave form of the other, the model (4.12) can have up to three
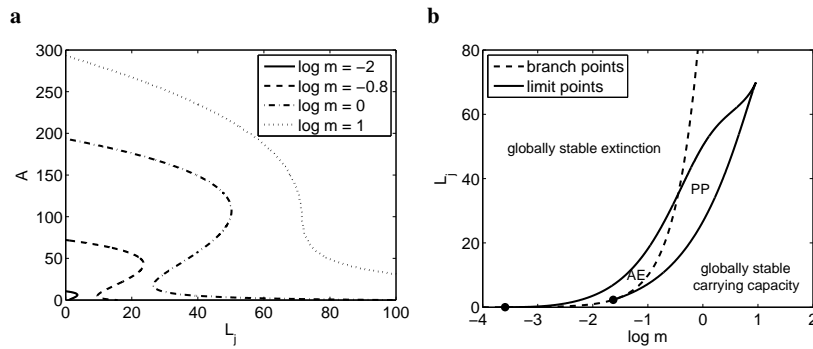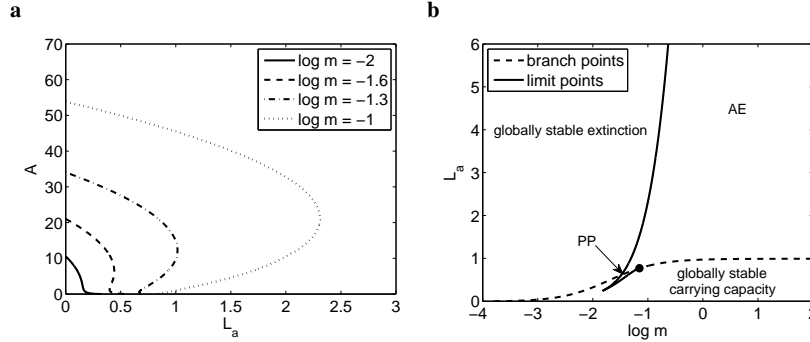
Fig. 4.10 Type II predation on juveniles. (a) Stable (decreasing parts with increasing L_j of equilibrium curves) and unstable (increasing parts with increasing L_j of equilibrium curves) equilibria of the model (4.12) in the case A. (b) Areas in the $m - L_j$ parameter space in which different numbers of stable and unstable equilibria exist. Solid lines mark the limit points at which the equilibria merge and cease to exist in a saddle-node bifurcation, and the dashed line denotes the branch points at which the equilibria start to become negative and biologically not feasible. Solid points show where the solid lines touch the dashed line and cease to exist. AE = Allee effect, PP = predator pit. See Table 4.5 for the other parameter values

interior equilibria. For specific examples, see Fig. 4.10. For analogous reasons as given in Box 4.2, if the interior equilibrium is unique, it is globally stable.

The observation of a predator pit in this case is amazing, as this phenomenon has generally been associated with the predator-prey system in which a generalist predator with a type III functional response consumes an unstructured, logistically growing population of prey (May, 1977). We claim here that a predator pit can also be a consequence of type II functional responses of generalist predators attacking only prey juveniles. More generally, this implies that accounting for an age-structure in prey can qualitatively change operation of functional responses.

Case B. If only adults suffer from predation via a type II functional response, the situation becomes sort of symmetric. Although the model (4.12) can also possess up to three interior equilibria in this case (Box 4.4; examples given in Fig. 4.11), contrary to the case A, there is neither an Allee effect nor a predator pit observed for low maturation rates (Fig. 4.11). With faster maturation, a predator pit arises first, followed by an Allee effect (Fig. 4.11). If maturation is very fast, the juveniles tend to quickly leave their class and the system virtually behaves as the one-dimensional system with an unstructured prey and a type II functional response – Allee effect thus occurs for high enough predation pressure L_a (Fig. 4.11). Similarly to the case A, at higher maturation rates prey can persist at higher predation pressures (Fig. 4.11). What was concluded above for the case A thus equally holds for the case B.

Allee effects are thus more prevalent here relative to the case A. On the other hand, the range $-2 < \log m < -1$ of maturation rates within which a predator pit occurs here is much smaller than the corresponding range in the case A ($-2 < \log m < 1$). The area in parameter space in which three interior steady states exist can be made larger, and the predator pit thus more widespread, by decreasing the mortality rates of both age classes, increasing the birth rate, or increasing the parameter B_j, but it nonetheless cannot be made as large as in the case A for a comparable parameter set.

Fig. 4.11 Type II predation on adults. (a) Stable (decreasing parts with increasing L_a of equilibrium curves) and unstable (increasing parts with increasing L_a of equilibrium curves) equilibria of the model (4.12) in the case B. (b) Areas in the $m - L_a$ parameter space in which different numbers of stable and unstable equilibria exist. Legend as in Fig. 4.10. See Table 4.5 for the other parameter values

Box 4.4 Up to three interior equilibria in case B

For $P_j = 0$ and $P_a = L_a A / (1 + B_a A)$, the adult isocline $f_2(A)$ becomes

$$f_2(A) = J = \frac{d_a}{m}A + \frac{d_a}{mK_a}A^2 + \frac{(L_a/m)A}{1 + B_a A} \qquad (4.21)$$

while the juvenile one stays as in (4.15). Analogous reasoning can be made here as in Box 4.3; see also Fig. 4.11 for specific examples.

Case C1. In this case, both juveniles and adults are decimated by predation through a type II functional response. Graphical analysis of isoclines reveals a possibility of up to four interior equilibria (Box 4.5). Figure 4.12a exemplifies the situation with four interior equilibria, showing how with increasing L_a, initially one interior equilibrium first bifurcates to two, with a relatively low Allee threshold, then to four and eventually to two again, now with a relatively high Allee threshold, before a too high predation pressure prevents persistence of any prey population. Of

particular importance here is that there is a critical predation pressure L_a^* at which the Allee threshold undergoes an instant and dramatic increase. As a consequence, if a population resides at the stable, low-density equilibrium below L_a^* it finds itself far below the Allee threshold when the predation pressure rises above it (Fig. 4.12a).

Still, an Allee effect with two interior equilibria is the most common pattern we observed in this case. The combinations of L_j and L_a at which the system undergoes a saddle-node bifurcation and the extinction equilibrium becomes globally stable are negatively correlated (Fig. 4.12b). In addition, the higher is the maturation rate m, the larger is the area in the $L_a - L_j$ parameter space for which the prey population can persist (not shown). So, whereas for prey with fast maturation predation on juveniles or adults can be extensive, slowly maturing prey can stand only relatively weak predation on both classes. In general, figures like Fig. 4.12b can be used to assess what combinations of L_a and L_j are the most cost-effective for prey eradication, once cost isolines are overlaid.
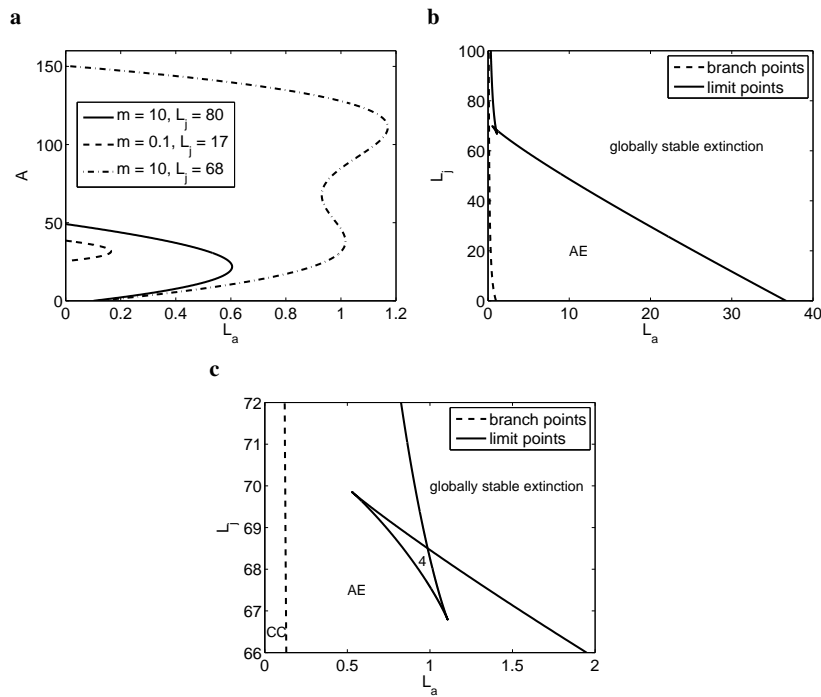
Fig. 4.12 Type II predation on both juveniles and adults. (a) Stable (decreasing parts with increasing L_a of equilibrium curves) and unstable (increasing parts with increasing L_a of equilibrium curves) equilibria of the model (4.12) in the case C1. (b) Areas in the $L_a - L_j$ parameter space in which different numbers of stable and unstable equilibria exist; $\log m = 1$ (plots for other values of m are qualitatively similar). (c) A zoomed portion of panel (b). Legend as in Fig. 4.10; CC = only a unique interior equilibrium exists (stable carrying capacity), 4 = four interior equilibria. See Table 4.5 for the other parameter values

Box 4.5 Up to three interior equilibria in case C1

For $P_j = L_j J/(1+B_j J)$ and $P_a = L_a A/(1+B_a A)$, the system of isoclines becomes

$$f_1(j) = A = \frac{m+d_j}{b} J + \frac{d_j}{bK_j} J^2 + \frac{(L_j/b)J}{1+B_j J}$$

$$J = \frac{d_a}{m} A + \frac{d_a}{mK_a} A^2 + \frac{(L_a/m)A}{1+B_a A}$$

(4.22)

Now, isoclines in their most complex form are of the concave-convex and convex-concave shape, respectively. Because of this, the model (4.12) can have up to four interior equilibria. For specific examples, see Fig. 4.12.

Type III functional response. When only a type III functional response operates on juveniles or adults, graphical analysis of isoclines shows that the system may have one or three interior equilibria, if any (Box 4.6; examples given in panels A and B of Fig. 4.13). We now very shortly present results for the two remaining cases C2 and C3 in which both age classes of prey are being consumed, one via a type II functional response and the other via a type III functional response.

Box 4.6 A type III functional response on juveniles or adults

For $P_j = L_j J^2/(1+B_j J^2)$ and $P_a = 0$, or $P_j = 0$ and $P_a = L_a A^2/(1+B_a A^2)$, the model (4.12) can have one or three interior equilibria, if any. This is because, in the former case, the f_2 isocline is a parabolic function rooted in the origin $J = A = 0$ and increasing at a decelerating rate, while the f_1 isocline is of the convex-concave-convex shape. Thus, if $S_1 < S_2$ (these quantities are defined in Box 4.2), the isoclines intersect in one or three interior equilibria. If $S_1 > S_2$, on the other hand, they do not intersect at all, since in this case they do not intersect in the absence of predation, and predation causes a 'distance' between the isoclines yet to increase. Hence, we cannot have an Allee effect in this case.

Case C2. This case covers predators that exploit juveniles via a type II functional response and adults via a type III functional response. Although up to five interior equilibria are possible in this case (Box 4.7), for the examined set of parameter values a predator pit is the most frequent multi-stability pattern, but the scenario with five interior equilibria is not uncommon (Fig. 4.13). For negligible values of the predation pressure on adults L_a, the number of interior equilibria obviously corresponds to that of the case A, but this may soon change as L_a increases. For example, the system with only a unique interior equilibrium at $L_a = 0$ may soon possess three interior equilibria, then five, then again three, and finally just one again, this time with an extremely low prey density (Fig. 4.13a). Allee effects arise when the juveniles mature slowly and are under heavy predation, in which case the type II functional

response has a stronger influence on prey population dynamics than the type III one (Fig. 4.13d). The faster the juveniles mature, the more the system behaves as an unstructured one and the more the type III functional response dominates. For the examined parameter set we did not find any situation with four interior equilibria but this situation may occur for other parameter sets.
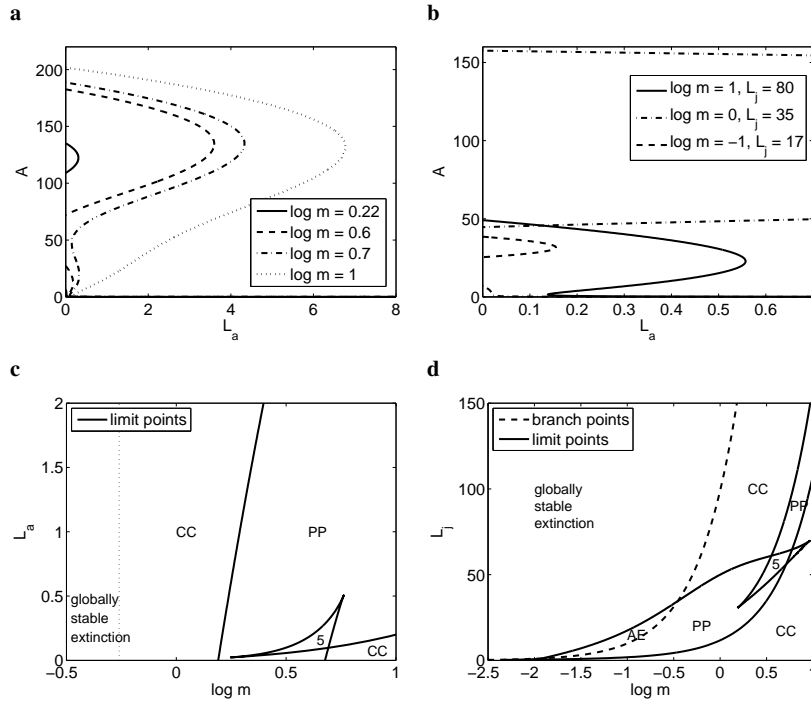
Fig. 4.13 Type II predation on juveniles and type III predation on adults. (a) and (b) Stable (decreasing parts with increasing L_a of equilibrium curves) and unstable (increasing parts with increasing L_a of equilibrium curves) equilibria of the model (4.12) in the case C2; $L_j = 55$ in (a). (c) Areas in the $m - L_a$ parameter space for which different numbers of stable and unstable equilibria exist; $L_j = 55$. (d) Areas in the $m - L_j$ parameter space for which different numbers of stable and unstable equilibria exist; $L_a = 0.1$. Legend as in Fig. 4.10; 5 = five interior equilibria. See Table 4.5 for the other parameter values

Box 4.7 Up to five interior equilibria in case C2

For $P_j = L_j J^2/(1 + B_j J^2)$ and $P_a = L_a A/(1 + B_a A)$, the juvenile isocline $f_1(J)$ becomes

$$f_1(J) = A = \frac{m + d_j}{b} J + \frac{d_j}{b K_j} J^2 + \frac{(L_j/b) J^2}{1 + B_j J^2} \qquad (4.23)$$

while the adult one is given by the equation (4.21). Thus, both $f_1(J)$ and $f_2(A)$ are increasing functions of J and A, respectively. In addition, the $f_1(J)$ isocline has in its most complex form a convex-concave-convex shape with increasing J, while the $f_2(A)$ isocline has in its most complex form a convex-concave shape with increasing A. Hence, the model (4.12) can have up to five interior equilibria.

Case C3. Here predators exhibit a type III functional response with respect to prey juveniles and a type II functional response with respect to prey adults. And here as well, up to five positive equilibria are possible (Box 4.8; examples given in panels A and B of Fig. 4.14). While Allee effects are not surprisingly the most frequent pattern observed at high maturation rates, scenarios with three and four interior equilibria are quite common at intermediate maturation rates; low maturation rates give rise to a unique interior equilibrium (Fig. 4.14c). On the contrary, the scenario with five interior equilibria is relatively rare for the examined set of parameter values (Fig. 4.14c). For negligible values of the predation pressure on juveniles L_j, the system is obviously close to that of the case B – also here, the number of equilibria may quickly change as L_j increases. As already emphasized for the case C1, the scenario with four interior equilibria might have far-reaching consequences for population management (Fig. 4.14a, dashed line). Although this scenario was relatively rare in the case C1, it is quite common here.

Box 4.8 Up to five interior equilibria in case C3

The situation here is essentially symmetric to the predation scenario C2. For $P_j = L_j J/(1+B_j J)$ and $P_a = L_a A^2/(1+B_a A^2)$, the juvenile isocline $f_1(J)$ is given by the equation (4.20), while the adult one becomes

$$f_2(A) = J = \frac{d_a}{m}A + \frac{d_a}{mK_a}A^2 + \frac{(L_a/m)A^2}{1+B_a A^2} \tag{4.24}$$

Thus, both $f_1(J)$ and $f_2(A)$ are increasing functions of J and A, respectively. In addition, the $f_1(J)$ isocline has in its most complex form a concave-convex shape with increasing J, while the $f_2(A)$ isocline has in its most complex form a concave-convex-concave shape with increasing A. Hence, also here, the model (4.12) can have up to five interior equilibria.

Summary

In this section, we developed a mathematical model to study dynamics of an age-structured population preyed upon by age-specific, generalist predators. The age-
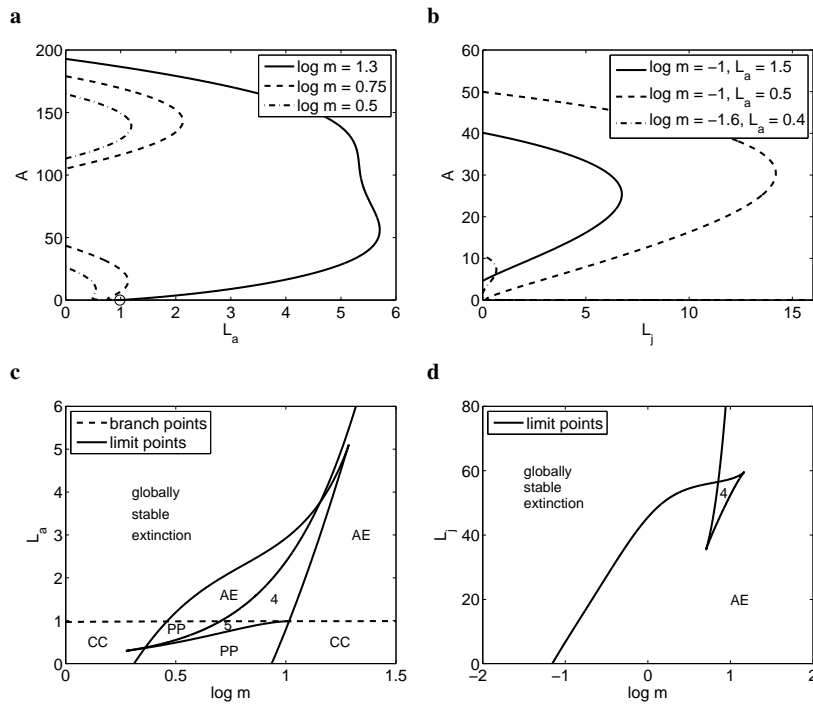
Fig. 4.14 Type III predation on juveniles and type II predation on adults. (a) and (b) Stable (decreasing parts with increasing L_a of equilibrium curves) and unstable (increasing parts with increasing L_a of equilibrium curves) equilibria of the model (4.12) in the case C3; $L_j = 55$ in (a) and the empty circle marks the location of a branch point, common to all three curves. (c) Areas in the $m - L_a$ parameter space in which different numbers of stable and unstable equilibria exist; $L_j = 55$. (d) Areas in the $m - L_j$ parameter space in which different numbers of stable and unstable equilibria exist; $L_a = 1.5$. Legend as in Fig. 4.10. See Table 4.5 for the other parameter values

specific predation on an otherwise logistically growing prey population offered three frequent types of dynamics: a unique stable interior equilibrium, a strong Allee effect, and a predator pit. This is partly consistent with what was observed for a logistically growing, unstructured prey consumed by generalist predators – the strong Allee effect for type II functional responses (Berec et al, 2007) and the predator pit for type III functional responses (May, 1977). Indeed, fast maturation causes the age-structured system to behave nearly as an unstructured one composed only of adults and predation on adults (if present) thus dominates system dynamics. It is low or intermediate maturation rates for which novel dynamics emerge. First, when only one of the prey age classes is consumed, predator pits can occur even for type II functional responses; we found this outcome more prevalent for predation on juveniles. Second, in some situations, the strong Allee effects and predator pits combined to give rise to four or five interior steady states of which two and three, respectively, were (locally) stable.

From the pest control perspective, age-specificity of a biocontrol agent and hence replacement of a strong Allee effect (unstructured model) by a predator pit (age-structured model) might prevent efficient eradication of invasive pest species (Liebhold and Bascompte, 2003; Liebhold and Tobin, 2008; Boukal and Berec, 2009; Tobin et al, 2011). For native pests, however, the goal is rather to reduce their levels below an economic threshold, and this can be equally achieved with the predator pit if the corresponding low-density equilibrium lies below that threshold. From the population management perspective in general, the scenario with two interior stable equilibria, two interior unstable equilibria, and the stable extinction equilibrium may have far-reaching consequences for the population persistence or extinction. When the prey population is at the lower interior stable equilibrium and, as predation pressure increases, this equilibrium vanishes before the upper interior stable equilibrium does, then the Allee threshold undergoes an instant dramatic increase if the predation pressure is sufficiently enhanced (Fig. 4.12). The change in the predation pressure itself can however be relatively small. The prey population formerly in a stable (interior) equilibrium suddenly occurs far below the Allee threshold and is doomed to extinction. Hence, further release or immigration of a relatively small amount of predators may cause the system to collapse.

Since Allee effects in prey may result from a type II functional response of generalist predators in an unstructured prey population (Gascoigne and Lipcius, 2004; Berec et al, 2007), one of our main goals in this section was to explore how prevalent is this phenomenon in a more realistic, age-structured prey population consumed by age-specific predators. Strong Allee effects occurred for all combinations of functional responses that we considered. Not surprisingly, strong Allee effects have been predominantly observed where adults were consumed via a type II functional response (cases B, C1 and C3), especially at high maturation rates at which the age-structured system is close to an unstructured one (see above), but they were observed also in cases A and C2 if maturation rates were low and the effect of predation on adults relatively weak. The possibility of total eradication of a pest species by suppressing its density below a certain extinction threshold thus remains viable (Liebhold and Bascompte, 2003).

Choice of an optimal biocontrol agent is crucial if a biocontrol action is to be successful. Our models are simple and therefore the information obtained through them cannot be used directly for making any predictions or decisions in any particular system. In particular, an optimal biocontrol agent has to be suitable in a range of other features (taxonomic compatibility, climatic matching, risk to the environment, etc.; Hoelmer and Kirk, 2005) and its efficiency must be assessed with respect to these. Nevertheless, in this section we presented and analyzed some predator-prey interactions (age-specific generalist predators) that can work well towards the best biocontrol agent selection if reflected or reduce the success of the biocontrol action if neglected and that certainly occur in natural ecosystems. In addition, our results also contribute to general ecological theory, thanks to our novel findings on Allee effects, predator pits, and their combinations.

4.3 Does sex-selective predation stabilize or destabilize predator-prey dynamics?

Since many prey species exhibit sexual dimorphism in appearance, physiology and behavior, while predators often prefer prey with certain size, conspicuousness, morphology or habits (for a review, see Boukal et al, 2008), sex-selective predation should be widespread. As a consequence, male- and female-biased predation can impact population dynamics differently; the net result will be a combination of direct effects due to reduced male and female densities in the prey and indirect effects due to apparent competition between both sexes of the prey mediated by the shared predator. Since previous studies showed that population dynamics of sexually reproducing species are shaped by the mating system and, consequently, by the reproductive success of individual females (Caswell and Weeks, 1986), and that more and more species are observed to demonstrate mate-finding Allee effects (Stephens et al, 1999; Gascoigne et al, 2009; Kramer et al, 2009), we for the first time develop and analyze mathematical models of predator-prey dynamics that incorporate sex structure in prey, and the implied sex selectivity of predators and mate-finding Allee effect in prey. Our models can also describe dynamics of an exploited species in which the sexes are harvested at different rates, extending the model studied in Courchamp et al (2006). Using these simple models, we aim at answering the following questions: Can sex-selective predation alone stabilize predator-prey dynamics? How are the (de)stabilizing properties of male- or female-biased predation linked to the prey mating system? How do the mate-finding Allee effect and other (de)stabilizing mechanisms influence the results? Finally, we discuss how the observed prevalence of male-biased predation can relate to our modeling results and what implications our results can have for exploited species. Throughout this section, all issues related to males, females and sex-specificity in general always pertain to the prey.

Model development

To expose the consequences of sex-selective predation for predator-prey dynamics, we first examine a simple extension of the classical Lotka-Volterra predator-prey model. The model distinguishes between male (m) and female (f) prey and unstructured predator (x) populations. It accounts for a range of prey mating systems and can include a mate-finding Allee effect in the prey:

$$\frac{dm}{dt} = \frac{b}{2}p(m,f,\theta)f - dm - \lambda_1 mx$$
$$\frac{df}{dt} = \frac{b}{2}p(m,f,\theta)f - df - \lambda_2 fx \qquad (4.25)$$
$$\frac{dx}{dt} = -Mx + e_1\lambda_1 mx + e_2\lambda_2 fx$$

We assume that the prey sex ratio at birth is unbiased, the intrinsic mortality rate d is equal in male and female prey, and the birth rate b per female prey in the absence of mating constraints is sufficiently high ($b/2 > d$) such that the prey population has positive growth rate in the absence of predation and Allee effects. Parameters λ_i scale the linear sex-specific functional responses of the predator to male and female prey, e_i denote the efficiencies with which consumed male and female prey are converted into new predators, and M is the predator per capita mortality rate. The maximum prey birth rate is scaled by $p(m, f, \theta)$, which is the female mating rate or the probability that a female becomes fertilized per unit time (McCarthy, 1997; Boukal and Berec, 2002; Courchamp et al, 2008).

Function p incorporates both the mate-finding Allee effect in the prey (through parameter θ) and the prey mating system. If mating opportunities are unlimited, $p = 1$. For the mate-finding Allee effect and unlimited male mating potential, the female mating rate can be described by the negative exponential function of male density (Dennis, 1989; McCarthy, 1997)

$$p(m, f, \theta) = 1 - \exp(-m/\theta) \tag{4.26}$$

We refer to this mating function as unlimited polygyny (Table 4.7). Constraints on male mating potential or social system that lead to 'limited' polygyny, monogamy or polyandry can be described as

$$p(m, f, \theta) = \frac{hm \exp((hm - f)/(h\theta)) - hm}{hm \exp((hm - f)/(h\theta)) - f} \tag{4.27}$$

in which h represents, depending on the mating system, the number of matings a male can achieve with different females per unit time or a male's harem size (Fig. 4.15). Values of $h > 1$ correspond to limited polygyny, $h = 1$ to monogamy, and $h < 1$ to polyandry. Formula (4.27) reduces to the frequently used minimum function $p(m, f) = \min(hm/f, 1)$ in the absence of the mate-finding Allee effect ($\theta \to 0$) and to (4.26) if the constraints on male mating potential are removed ($h \to \infty$); see McCarthy (1997) and Bessa-Gomes et al (2004) for details.

To reduce the number of parameters, we scale all population densities in the model (4.25) by a multiplicative factor $\lambda_2 > 0$ and introduce the predation bias $\Lambda = \lambda_1/\lambda_2$ (male bias: $\Lambda > 1$, female bias: $\Lambda < 1$) and the new Allee effect parameter $\Theta = \lambda_2 \theta$:

$$\frac{dm}{dt} = \frac{b}{2} p(m, f, \Theta) f - dm - \Lambda mx$$
$$\frac{df}{dt} = \frac{b}{2} p(m, f, \Theta) f - df - fx \tag{4.28}$$
$$\frac{dx}{dt} = -Mx + e_1 \Lambda mx + e_2 fx$$

For simplicity, we keep the same notation m, f, and x for the rescaled state variables as in the model (4.25): whether we use the model (4.25) or (4.28) is always clear
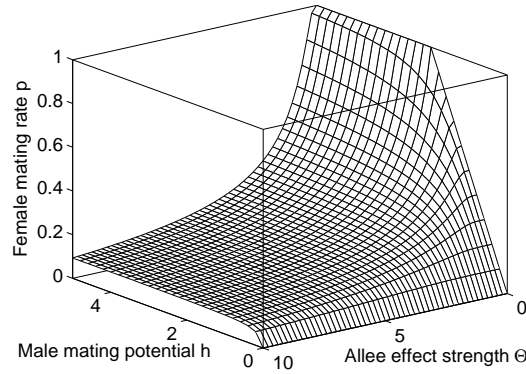
Fig. 4.15 Shape of the mating function (4.27). The mating function increases in h, decreases in θ, and reduces to $p(m, f) = \min(hm/f, 1)$ in the absence of the mate-finding Allee effect ($\theta = 0$). Male and female population densities in the figure: $m = 1$, $f = 2$

from the context and the only difference in the rescaled mating functions (4.26) and (4.27) is that Θ replaces θ.

Inevitably, the dynamics and long-term stability of any predator-prey system will be affected by a multitude of various mechanisms, often with opposite impacts, and additional mechanisms may overshadow the effect of sex-selective predation. For example, negative density dependence in prey growth is known to have a strong stabilizing effect in predator-prey interactions (Murdoch et al, 1998). Therefore, we also account for negative density dependence in prey growth and different types of predator-prey interactions (different forms of the functional response). To demonstrate their additional impact on stability of the predator-prey coexistence equilibrium, we will introduce them one by one in the basic model (4.28) with unlimited polygyny and no Allee effect.

The model (4.28) admits at most three steady states: the extinction equilibrium $E^0 = (0, 0, 0)$, a prey-only equilibrium E^1, and a predator-prey coexistence equilibrium E^2 (Box 4.9). E^1 is unstable and E^0 locally stable if $\Theta > 0$. E^1 arises as a direct consequence of the mate-finding Allee effect in prey and defines the Allee threshold[3]. E^0 is unstable, i.e. both populations can recover from near-extinction, if there is no Allee effect ($\Theta = 0$). We analyze the model (4.28) numerically using Matlab 7 (The MathWorks, Inc.) package Matcont (Dhooge et al, 2003), focusing primarily on stability of the coexistence equilibrium E^2. In the following, stability of the system (4.28) is used synonymously with stability of E^2.

---

[3] See Section 3.1: a prey population above the Allee threshold will grow, but a decline to extinction occurs if the prey falls below.

Box 4.9 Steady states of the rescaled model (4.28) **and their stability**

The rescaled model (4.28) admits at most three equilibria. Introducing functions

$$\Phi_\Theta(m) = p(m,m,\Theta)$$

$$\Psi_{\Theta,\Lambda}(m) = p\left(m, \frac{1}{e_2}(M - e_1\Lambda m), \Theta\right)$$

(both of them increase from 0 to 1 as m grows from 0 to ∞) and assuming positivity of the second argument in $\Psi_{\Theta,\Lambda}(m)$, the equilibria can be written as

$$E^0 = \{0,0,0\}$$

$$E^1 = \{\overline{m},\overline{m},0\} = \left\{\Phi_\Theta^{-1}\left(\frac{2d}{b}\right), \Phi_\Theta^{-1}\left(\frac{2d}{b}\right), 0\right\}$$

and

$$E^2 = \{m^\star, f^\star, x^\star\} = \left\{m^\star, \frac{1}{e_2}(M - e_1\Lambda m^\star), \frac{b}{2}\Psi_{\Theta,\Lambda}(m^\star) - d\right\}$$

in which $m^\star$ is the (single) root of the equation

$$\frac{b}{2e_2}(M - \Lambda m(e_1 + e_2))\Psi_{\Theta,\Lambda}(m) - dm(1 - \Lambda) = 0$$

The extinction equilibrium E^0 is always unstable in the absence of the Allee effect (when $\theta = 0$ and hence $\Theta = 0$) since we assume $b/2 > d$. In that case the prey-only equilibrium E^1 disappears and the prey grows exponentially in the absence of predators. For the female mating rate functions p considered in this section, E^0 is locally stable and E^1 unstable if the Allee effect is present ($\Theta > 0$).

E^2 is meaningful only if $m^\star$, $f^\star$ and $x^\star$ are all positive, and ceases to exist when it collides with E^1 for a $\Theta > 0$ (saddle-node bifurcation).

We note that the structure of the model (4.28) becomes particularly simple when mating opportunities are unlimited ($p = 1$): the male prey influence the female prey only indirectly through the shared predator. For unlimited mating opportunities, unbiased predation ($\Lambda = 1$), and equal initial densities of the male and female prey, the model (4.28) is identical to the classic Lotka-Volterra predator-prey model introduced in Chapter 1.

Model results

Stability of the predator-prey system (4.28) depends primarily on two factors: the prey mating system and predation bias for one sex of the prey. Male- and female-biased predation generally have opposite consequences for the stability (Table 4.7). The results are particularly simple for unlimited polygyny and no Allee effect (i.e. $p = 1$): male-biased predation ($\Lambda > 1$) leads to stable coexistence, while female-biased predation ($\Lambda < 1$) gives rise to increasing oscillations (Fig. 4.16a).

| Mating system	Mating function	Female-biased predation	Male-biased predation
Unlimited polygyny	(4.26)	I: Extinction	II: Coexistence possible (stable equilibrium)
Limited polygyny	(4.27) with $1 < h < \infty$	I: Cycles or extinction	II: Coexistence possible (stable equilibrium or cycles)
Polyandry	(4.27) with $h < 1$	III: Coexistence possible (stable equilibrium)	IV: Coexistence possible but very unlikely (stable equilibrium or cycles)

Table 4.7 Summary of dynamics of the predator-prey system (4.28) with different types of sex-selective predation and prey mating systems. Roman numerals correspond to the areas in Fig. 4.17b. Extinction includes increasing oscillations that drop very close to zero

The outcome for limited polygyny, i.e. finite $h > 1$ in (4.27), is similar: only male-biased predation can lead to stable predator-prey equilibrium (area II in Fig. 4.17b and Table 4.7). In polyandrous prey ($h < 1$), the roles of both sexes in prey dynamics are reversed, which is also reflected in the stabilizing role of sex-selective predation. Only female-biased predation, together with strongly male-biased predation, can stabilize the predator-prey dynamics (areas III and IV in Fig. 4.17b and Table 4.7). Otherwise, sex-biased predation leads to stable predator-prey cycles (area I and parts of areas II, III and IV); often, the troughs of these cycles are very low and the system thus prone to collapse, e.g. due to the Allee effect in the prey (see below) or stochasticity.

To illustrate the mechanism causing the observed differences between male- and female-biased predation, we plot the per capita growth rate of the entire prey population,

$$\frac{1}{m+f} \frac{\mathrm{d}(m+f)}{\mathrm{d}t}$$

as a function of the total prey population density $m + f$ (Fig. 4.16b-c). This illustration is not relevant for specialized predators that feed only on male or female prey, which we discuss in Box 4.10. Male-biased predation of polygynous prey gives rise to an emergent negative density-dependence in prey growth (Fig. 4.16b). Populations perturbed away from the coexistence equilibrium thus return to it (Fig. 4.16a).
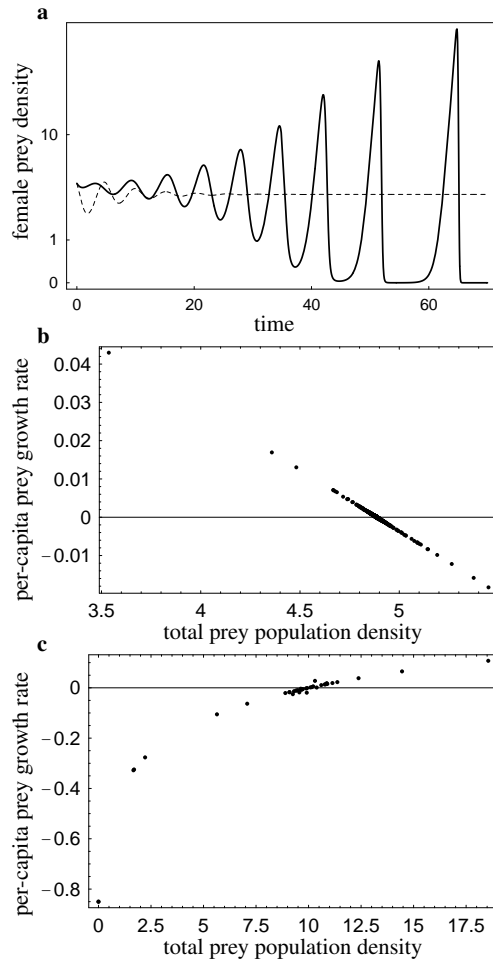
Fig. 4.16 Illustration of population dynamics and the stabilizing and destabilizing effect of sex-selective predation in the model (4.28). (a) Two types of dynamics for unlimited polygyny and no Allee effect. Male-biased predation leads to a stable coexistence equilibrium E_2 (thin dashed curve; $\Lambda = 2$); female-biased predation leads to increasing oscillations prone to collapse (thick curve; $\Lambda = 0.5$). Other parameters: $b = 3$, $d = 0.2$, $e_1 = 0.2$, $e_2 = 0.1$, $M = 1$, $\Theta = 0$. Initial conditions: $m = f = 4$, $x = 1.5$. (b) Stabilizing effect of the male-biased predation, shown in the per capita population growth rate of the total prey population as a function of the total prey density, $m + f$; data were generated by computing trajectories for ten random initial conditions and selecting points with predator density close to equilibrium, $x \sim x^*$ (results for other fixed predator densities were similar). $\Lambda = 2$, other parameters as in (a). (c) Destabilizing effect of the female-biased predation, shown as in (b). $\Lambda = 0.5$, other parameters as in (a)

On the other hand, female-biased predation of polygynous prey leads to an emergent positive density dependence (i.e. not linked to the Allee effect if the latter is also present; see below) and thus has a destabilizing effect (Fig. 4.16c). Predators feed-
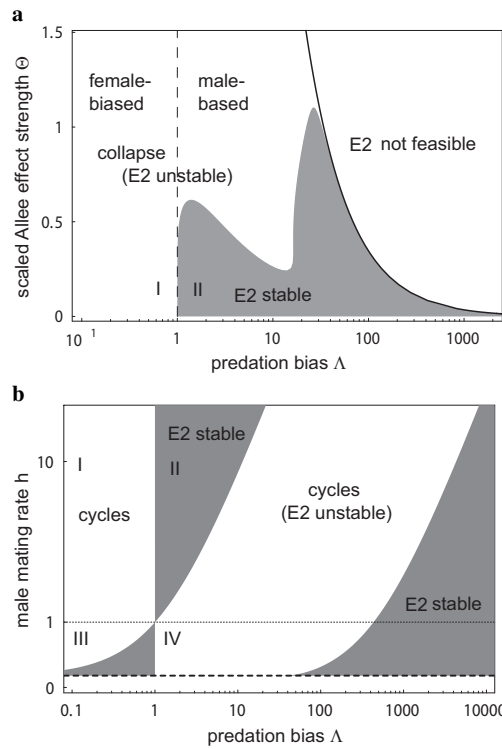
Fig. 4.17 Stability of the coexistence equilibrium E^2 in the model (4.28). Common parameters: $b = 3$, $d = 0.2$, $e_1 = 0.2$, $e_2 = 0.1$, and $M = 1$. (a) Combined effect of predation bias and the Allee effect under unlimited polygyny. E^2 is feasible to the left of the solid black curve and locally stable within the grey area. (b) Combined effect of predation bias and prey mating system with no Allee effect ($\Theta = 0$). The equilibrium is feasible above $h \sim 0.133$ (dashed line) and locally stable within each grey area. Areas I-IV delimited by lines $h = 1$ and $\Lambda = 1$ correspond to Table 4.7

ing on female prey close to the equilibrium density first increase in numbers, while the female prey density decreases, leading to poor prey growth and subsequent die-off of the predators; as predators become scarce, the prey is released from predation and its density increases above the equilibrium level, followed by predators. These cycles spiral away from the equilibrium (Fig. 4.16a). The (de)stabilizing effect of sex-biased predation is caused by the concomitant changes in male prey density: the model (4.28) with male prey density kept fixed at an arbitrary value, no Allee effect and unlimited polygyny is a neutrally stable, Lotka-Volterra predator-prey system.

Box 4.10 Predators feeding only on male or female prey

The rescaled model (4.28) does not cover specialized predators that feed on only one prey sex, and we return to the original unscaled model (4.25) with

unlimited polygyny to explain the population consequences. First, male prey
will remain constant while female prey and predators will grow indefinitely if
predators feed only on male prey and the mate-finding Allee effect is absent
or limited in magnitude; strong Allee effects always lead to collapse. Sec-
ond, the dynamics of female prey and predator in the model (4.25) reduce
to the classical Lotka-Volterra predator-prey system with neutrally stable cy-
cles surrounding the coexistence equilibrium when predators feed only on
female prey and there is no Allee effect. Any mate-finding Allee effect makes
the equilibrium unstable and leads to collapse. This can be seen as follows.
For predators feeding only on females ($\lambda_1 = 0$), the characteristic equation
resulting from the Jacobian evaluated at the predator-prey equilibrium E^2 is
$s^3 + a_1 s^2 + a_2 s + a_3 = 0$ where

$$a_1 = d - \frac{d^2 e_2 \theta \lambda_2}{bM\mu}$$

$$a_2 = \frac{1}{\mu^2} \left(\frac{d^2 e_2 \theta \lambda_2 (1-\mu)(d e_2 \theta \lambda_2 - bM\mu)}{bM^2} \right.$$
$$\left. + \mu [bM(1-\mu)\mu - d(e_2 \theta \lambda_2 (1-\mu) + M\mu)] \right)$$

$$a_3 = \frac{d(d e_2 \theta \lambda_2 - bM\mu)[d(e_2 \theta \lambda_2 (1-\mu) + M\mu) - bM(1-\mu)\mu]}{bM\mu^2}$$

Hence,

$$a_1 a_2 - a_3 = -\frac{d^3 e_2 \theta \lambda_2 (1-\mu)(d e_2 \theta \lambda_2 - bM\mu)^2}{b^2 M^3 \mu^3}$$

That is, $a_1 a_2 - a_3 < 0$ except a biologically irrelevant set of parameters with
$d e_2 \theta \lambda_2 = bM\mu$. Application of the Routh-Hurwitz criterion yields that the
coexistence equilibrium E^2 of the model (4.25) is always unstable if preda-
tors feed only on females. The persistence of predator-prey systems with
both types of specialized predation thus requires additional stabilizing mech-
anisms.

These conclusions do not change substantially in the presence of the mate-finding
Allee effect ($\Theta > 0$). All additional differences in the results can be attributed to
the presence of the Allee threshold. The prey population will fall below it and the
predator-prey system can also collapse for male-biased predation ($\Lambda \gg 1$). In terms
of the unscaled model (4.25), the maximum strength θ of the mate-finding Allee ef-
fect allowing for stable predator-prey coexistence levels off asymptotically at highly
male-biased predation for unlimited polygyny (Fig. 4.18). Such prey populations
with a pronounced mate-finding Allee effect (high θ) can be stabilized only by
predators that feed very little on females (low λ_2) and moderately on males (inter-

mediate λ_1). The stability for limited polygyny and polyandry is limited in a similar way (Box 4.11). For all mating systems with the Allee effect, coexistence also becomes more difficult to achieve as predation strength relative to the intrinsic per capita growth rate of the prey increases, e.g. through increased prey conversion efficiency e_i which leads to higher predator and lower prey density at the equilibrium (results not shown).
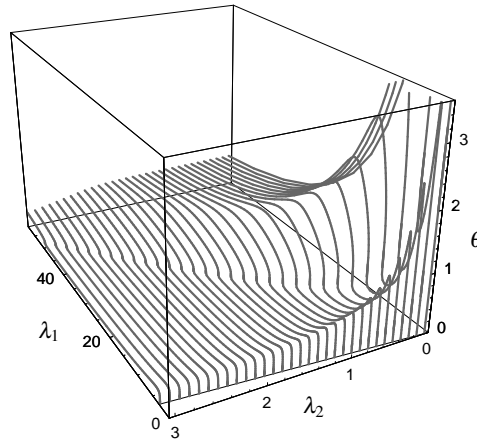
Fig. 4.18 Combined effect of predation rates and the Allee effect in the prey in the unscaled model (4.25). The curves trace a surface separating stable (below) and unstable (above) dynamics; points with $\lambda_1 = \lambda_2$ (shown for $\theta = 0$, thin line bottom front) separate male- and female-biased predation. Other parameters as in Fig. 4.17a

In the final set of results, we summarize the impact of various additional mechanisms on the dynamics. A finite prey carrying capacity stabilizes the dynamics, and stable coexistence becomes possible also for female-biased predation. The range of carrying capacities leading to stabilization can change with sex bias in predation (Box 4.11). A similar effect is observed when the predators are allowed to switch between the male and female prey to maximize their food intake rate (Box 4.11). On the contrary, a Holling type II functional response destabilizes the dynamics: as the handling time of the captured prey increases, the coexistence equilibrium becomes unstable also for male-biased predation, which is stabilizing for the linear functional response, and the predation always leads to unstable dynamics above a certain critical handling time (Box 4.11).

Box 4.11 Impact of some other mechanisms on predator-prey dynamics

The mate-finding Allee effect
In the main text we show that the mate-finding Allee effect limits the

range of predation bias for which the coexistence equilibrium can be stable under unlimited polygyny. Figure 4.19 illustrates the same effect for limited polygyny and polyandry. The Allee effect will take away cyclic predator-prey dynamics in which the prey densities fall too low, and stable predator-prey cycles which emerge for some parameter combinations (Fig. 4.19) thus have the prey density always bounded away from zero by the Allee threshold. Decreasing male mating potential in limited polygyny also has a destabilizing impact on the dynamics; for example, the range of the Allee effect and predation bias combinations leading to stable predator-prey coexistence is larger for unlimited than for limited polygyny (Fig. 4.19b; area below the dotted curve and grey areas, respectively).

Logistic prey growth

We capture the logistic prey growth in the model (4.28) by considering negative density dependence in prey mortality rate:

$$
\begin{aligned}
\frac{dm}{dt} &= \frac{b}{2} p(m, f, \Theta) f - d\left(1 + \frac{m+f}{K}\right) m - \Lambda m x \\
\frac{df}{dt} &= \frac{b}{2} p(m, f, \Theta) f - d\left(1 + \frac{m+f}{K}\right) f - f x \qquad (4.29) \\
\frac{dx}{dt} &= -Mx + e_1 \Lambda m x + e_2 f x
\end{aligned}
$$

Modeled this way, prey survival rate decreases with total prey density. Carrying capacity of the prey in the absence of predation increases with K irrespective of the mating system. The stabilizing property of the logistic prey growth is shown in Fig. 4.20.

The model (4.29) is based on rescaled variables and parameters, which also pertains to the carrying capacity of the prey: $K = \lambda_2 k$, where k is the unscaled carrying capacity parameter in the model (4.25). All else being equal, decreasing the predation bias $\Lambda = \lambda_1 / \lambda_2$ either corresponds to decreasing predation on male prey or increasing predation on female prey. As Λ decreases from 1 to 0 by lowering the predation on male prey (λ_1), the destabilizing effect of female-biased predation, mediated indirectly by predation on male prey, weakens and allows for a wider range of carrying capacities to stabilize the dynamics. In the complete absence of predation on males ($\lambda_1 = 0$), the model (4.29) turns into a Lotka-Volterra system with a carrying capacity in the prey, for which any finite carrying capacity stabilizes the dynamics. On the other hand, if the predation bias decreases from 1 to 0 through increased predation on female prey (λ_2), the destabilizing effect of female-biased predation remains the same and the unscaled carrying capacity parameter k yielding a stable coexistence equilibrium remains approximately constant (Fig. 4.20).
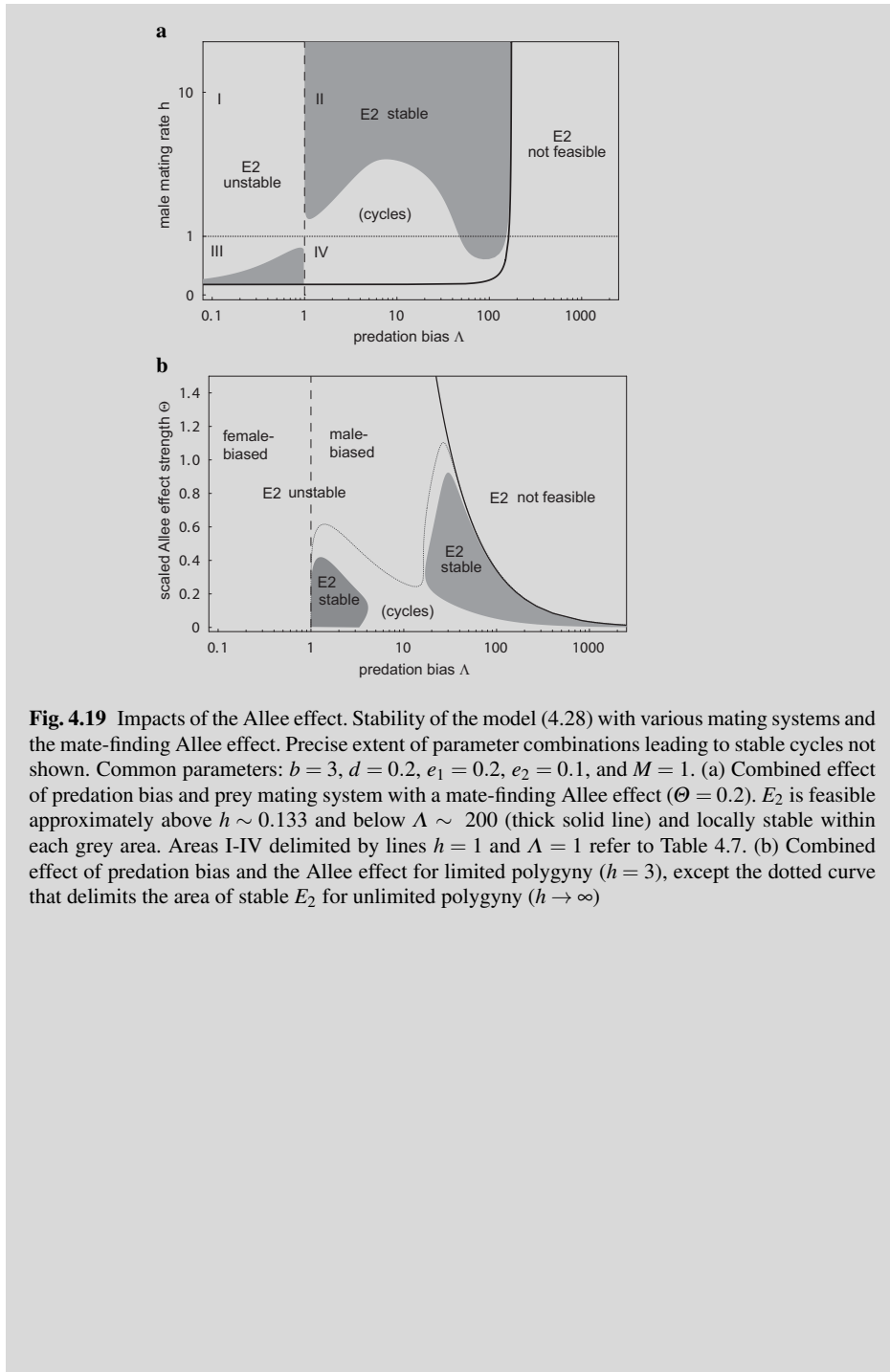
Fig. 4.19 Impacts of the Allee effect. Stability of the model (4.28) with various mating systems and the mate-finding Allee effect. Precise extent of parameter combinations leading to stable cycles not shown. Common parameters: $b = 3$, $d = 0.2$, $e_1 = 0.2$, $e_2 = 0.1$, and $M = 1$. (a) Combined effect of predation bias and prey mating system with a mate-finding Allee effect ($\Theta = 0.2$). E_2 is feasible approximately above $h \sim 0.133$ and below $\Lambda \sim 200$ (thick solid line) and locally stable within each grey area. Areas I-IV delimited by lines $h = 1$ and $\Lambda = 1$ refer to Table 4.7. (b) Combined effect of predation bias and the Allee effect for limited polygyny ($h = 3$), except the dotted curve that delimits the area of stable E_2 for unlimited polygyny ($h \to \infty$)
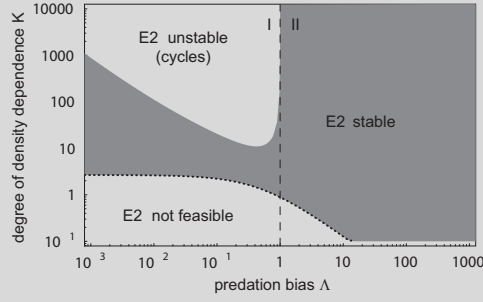
Fig. 4.20 Impacts of the upper bound on prey population growth. Stability of the model (4.29) with unlimited polygyny and no mate-finding Allee effect. Combined effect of predation bias and parameter K scaling the prey carrying capacity. Other parameters: $b = 3$, $d = 0.2$, $\Theta = 0$, $e_1 = 0.2$, $e_2 = 0.1$, and $M = 1$. E_2 is locally stable within the grey area. Areas I and II delimited by line $\Lambda = 1$ refer to Table 4.7

### Behavioral response of the predator (predator switching)

The predation bias for prey sex will no longer be constant if predators can adjust their foraging mode in response to changing male and female prey densities. One plausible mechanism involves optimal foraging, in which predators adjust their feeding to maximize their food intake rate (Stephens and Krebs, 1986). In this modification of the model (4.28), we assume that predators use search images to locate the currently more profitable sex of the prey, i.e. they aim at maximizing their instantaneous food intake rate $e_1 \Lambda m + e_2 f$, and that the male and female prey search images are traded off against each other. We denote by u the probability that the predator will use a search image to capture only males. Optimal foraging theory predicts that predators with perfect information about their environment will eat only males ($u = 1$) when $e_1 \Lambda m > e_2 f$ and only females ($u = 0$) when $e_1 \Lambda m < e_2 f$. We embed this optimal foraging mode into a more general family of predator switching rules described by the function

$$u(m, f, a) = \frac{1}{1 + \exp(-a(e_1 \Lambda m - e_2 f))} \qquad (4.30)$$

In this formula, parameter a gives the slope of the switching: $a \to \infty$ corresponds to the optimal foraging mode described above, while $a = 0$ gives $u = 0.5$ irrespective of the male and female prey population densities. We include this family of predator switching rules in the rescaled model (4.28) as:

$$\frac{dm}{dt} = \frac{b}{2} p(m, f, \Theta) f - dm - 2u(m, f, a) \Lambda m x$$

$$\frac{df}{dt} = \frac{b}{2} p(m, f, \Theta) f - df - 2(1 - u(m, f, a)) f x \qquad (4.31)$$

$$\frac{dx}{dt} = -Mx + 2u(m, f, a) e_1 \Lambda m x + 2(1 - u(m, f, a)) e_2 f x$$

In this setting, $a = 0$ represents the model (4.28). The stabilizing property of the switching for unlimited polygyny and no mate-finding Allee effect ($\Theta = 0$) is illustrated in Fig. 4.21. The switching greatly enhances the stability of the coexistence equilibrium E_2 when predation is female-biased. Some combinations of male-biased predation and nearly optimal foraging give rise to a stable predator-prey limit cycle and hence destabilize E_2. This predator-prey cycle with a limited amplitude, characteristic of optimal foraging (Křivan, 1997), can also arise for female-biased predation when the switching is sufficiently steep (high a).
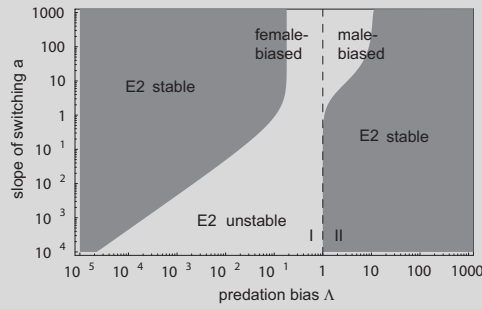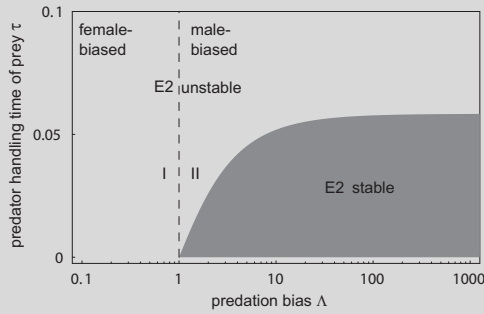

Fig. 4.21 Impacts of adaptivity in predator feeding decisions. Stability of the model (4.31) with unlimited polygyny and no mate-finding Allee effect. Combined effect of predation bias and steepness in predator switching on the stability of the coexistence equilibrium E^2. Parameters: $b = 3$, $d = 0.2$, $\Theta = 0$, $e_1 = 0.2$, $e_2 = 0.1$, and $M = 1$. E_2 is locally stable within the grey area. Areas I and II delimited by line $\Lambda = 1$ refer to Table 4.7

Holling type II functional response

Holling type II predator functional response is known to destabilize predator-prey dynamics (Murdoch and Oaten, 1975). We include type II functional response in the model (4.28), assuming the same handling time τ for male and female prey:

$$
\begin{aligned}
\frac{dm}{dt} &= \frac{b}{2}p(m, f, \Theta)f - dm - \frac{\Lambda mx}{1 + \tau\Lambda m + \tau f} \\
\frac{df}{dt} &= \frac{b}{2}p(m, f, \Theta)f - df - \frac{fx}{1 + \tau\Lambda m + \tau f} \\
\frac{dx}{dt} &= -Mx + \frac{e_1\Lambda mx + e_2 fx}{1 + \tau\Lambda m + \tau f}
\end{aligned}
\tag{4.32}
$$

In this setting, $\tau = 0$ gives the model (4.28). The increasingly destabilizing impact of the handling time is shown in Fig. 4.22.

Fig. 4.22 Impacts of the type II predator functional response. Stability of the model (4.32) with un-limited polygyny and no mate-finding Allee effect. Combined effect of predation bias and handling time of the predator with Holling type II functional response. Other parameters: $b = 3$, $d = 0.2$, $\Theta = 0$, $e_1 = 0.2$, $e_2 = 0.1$, and $M = 1$. E_2 is locally stable within the grey area. Areas I and II delimited by line $\Lambda = 1$ refer to Table 4.7

Summary

Using a simple model of a predator feeding on sexually reproducing prey, we show in this section that sex-selective predation can substantially affect predator-prey dynamics. Thus, sex-selective predation should be taken into account along with other, well-established factors influencing the stability of predator-prey interactions. In the simplest setting, males affect females only indirectly through apparent competition via the shared predator. Males can also affect females directly via the mate-finding Allee effect. We demonstrated that the impact of sex-selective predation depends on the interplay of the predation bias and the prey mating system. Only predation on the less limiting prey sex usually yields stable equilibria. This contrasts with pre-dation on the more limiting prey sex, which usually promotes unstable dynamics and thus makes the predator-prey system prone to collapse. Male-biased predation is therefore stabilizing in polygynous prey, while female-biased predation can only stabilize the dynamics if the prey mating system is polyandrous (Table 4.7). The presence of the Allee effect in the prey, apart from the collapse of the predator-prey system if the Allee effect is too strong, does not substantially alter these differences.

These results have general repercussions for predator-prey dynamics: many of the prey with quantified male-biased predation are likely to be polygynous (Boukal et al, 2008). For this class of prey, male-biased predation can stabilize the dynamics even if no other stabilizing mechanisms were present. The results are also puzzling: none of the prey with quantified female-biased predation is known to be polyandrous (Boukal et al, 2008). In general, polyandry is uncommon. How can female-biased predation exist? A value of our model lies in showing, among other things, that other

stabilizing mechanisms, such as a finite carrying capacity of the prey or predator switching, can be essential for long-term coexistence of these predator-prey systems. In intuitive terms, the negative density dependence in per capita prey growth rate arising from such mechanisms must override the emergent positive density dependence brought by the female-biased predation. On the other hand, we demonstrate that the destabilization of the predator-prey dynamics by sex-selective predation can be further exacerbated, and stabilization overshadowed, by other mechanisms such as type II predator functional responses.

Bias towards one sex is also common to harvesting of commercially important species and trophy hunting. Our model can, along with predator-prey dynamics, describe the temporal dynamics in harvesting/hunting effort and the density of a harvested/hunted population subject to open-access exploitation (Clark, 1990). Harvesting is usually male-biased in ungulates (Milner et al, 2006) and their mating systems are more or less polygynous; our model therefore predicts that moderate open-access exploitation tends to have a stabilizing effect. On the other hand, exploitation of many fish stocks is biased towards larger or more active individuals and may be therefore female- or male-biased depending on the species and type of gear (Rowe and Hutchings, 2003; Olsen et al, 2006). Over longer timescales, bias towards either sex might therefore contribute to stability or large fluctuations and collapses in open-access fisheries. We emphasize that our conclusions are only relative and focus only on the differences between male- and female-biased exploitation. Sustainability of any exploitation scheme and its impact on the target population should be assessed on a case-by-case basis, as it will be influenced by a number of other factors, among them the exploitation intensity, mating system and any Allee effects in the exploited population.

Finally, we combine an evolutionary and population-dynamical argument to provide one more possible explanation of the observed skew towards male-biased predation. Given our theoretical results, it seems plausible that the skew reflects the evolutionary history of sex-selective predator-prey interactions. The inherent instability of female-biased predation might have prevented the persistence of such systems on longer timescales if other counter-acting stabilizing mechanisms have been absent or weak, leading to population-level selection. Current evidence for this hypothesis is weak due to lack of direct evidence, which should simultaneously include time series of predator and prey densities, information on the sex bias in predation, the mating system, and the presence and strength of other mechanisms influencing prey stability. Data analyzed by Boukal et al (2008) provide only circumstantial evidence: with one exception, none of the reviewed predator-prey systems appears to involve a single predator specialized on a particular prey and feeding predominately on females.

4.4 Impacts of foraging facilitation among predators on predator-prey dynamics

Predator-prey theory has largely dangled round the concept of predator functional response, that is, the per capita feeding rate of predators upon their prey (Solomon, 1949; Murdoch and Oaten, 1975; Begon et al, 1990; Berryman, 1992; Gascoigne and Lipcius, 2004). Despite a great variety of functional response types proposed in the literature (Jost, 1998; Jeschke et al, 2002), the theory has been dominated by the Holling type II and linear Lotka-Volterra functional responses (Skalski and Gilliam, 2001). Whereas the type II functional responses have been most frequently observed (Hassell et al, 1976; Begon et al, 1990), the linear functional response is sufficiently simple to deal with mathematically (e.g. Křivan, 2007). In addition, virtually any textbook on population ecology adheres to the traditional classification of functional responses into three, predator-density-independent, "Holling" types: type I (initially linear, then constant), type II (decelerating, approaching an asymptote) and type III (sigmoid, also approaching an asymptote) (Begon et al, 1990; Krebs, 2001; Gascoigne and Lipcius, 2004).

Independence of a predator functional response of predator density actually means that any single predator affects the prey population growth rate independently of its conspecifics, that effects of two or more predators sum up, and that competition among predators for food occurs only through prey depletion. This is hardly always true, and even when prey density does not limit predator consumption, the feeding rate is often likely to decrease as the predator density increases; one then speaks of *predator interference*. Predator interference or simply interference is a collective term that embraces a number of specific mechanisms such as behavior typical of territorial animals where individuals 'waste time' in direct contests thereby decreasing time each could otherwise devote to foraging (searching for or handling prey) or predators that steal already subdued prey from one another (Berec, 2010, and references therein). Despite this variety, a common pattern that appears to emerge from modeling interference is its stabilizing effect on predator-prey dynamics (Rogers and Hassell, 1974; Ruxton et al, 1992; Ruxton, 1995; Huisman and DeBoer, 1997).

An alternative possibility for the predator functional response to depend on predator density, largely neglected in current predator-prey theory, is the process 'inverse' to predator interference, that is, *foraging facilitation*. In such a case, higher predator densities give rise to an increased foraging efficiency and hence feeding rate for any member of the foraging party, at least at lower predator densities. Mechanisms of foraging facilitation also vary. They include an increased ability of larger groups to locate food or prevent kleptoparasites from stealing already subdued prey (Berec, 2010, and references therein). Any of these mechanisms can, in turn, enhance individual reproduction and/or survival of predators, and even enhance survival of their offspring by teaching them to hunt collectively (Dawson and Mannan, 1991). Surprisingly, however, the question of how foraging facilitation affects predator-prey dynamics has not been addressed yet.

This section addresses the question of how foraging facilitation modifies predator-prey dynamics set by a type II functional response. It does so via developing a novel set of reasonably realistic, predator-density-dependent functional responses of which the type II functional response as well as common types of predator functional responses with interference are special cases. Although we primarily focus on foraging facilitation, we explore also the effects of predator interference of various strength on predator-prey dynamics, as this requires no extra computational time and makes the picture "symmetric" and complete. In addition, since foraging facilitation is a component Allee effect (that is, a mechanism invoking an Allee effect) on the side of predators (an increase in their population or group size leads to an increase in a fitness component of each of its individual members; Courchamp et al, 2008), we ask a couple of related questions. Does this component Allee effect generate a strong Allee effect, that is, an Allee threshold in predators in need to be crossed for predators to persist? And does it affect overall predator-prey dynamics?

Model development

Setting the stage: guessing effects of foraging facilitation

We start by considering the Rosenzweig-MacArthur predator-prey model

$$
\begin{aligned}
\frac{dN}{dt} &= rN\left(1 - \frac{N}{K}\right) - f(N,P)P \\
\frac{dP}{dt} &= ef(N,P)P - mP
\end{aligned}
\tag{4.33}
$$

where the functional response $f(N,P)$ is of (Holling) type II:

$$
f(N,P) = \frac{\lambda N}{1 + h\lambda N}
\tag{4.34}
$$

The prey population thus grows logistically in the absence of predators and the predator population dies out exponentially in the absence of prey. In this model, N and P are prey and predator density, respectively, r is the intrinsic per capita growth rate of prey, K is the environmental carrying capacity of prey, m is the per capita predator mortality rate, and e determines the efficiency with which consumed prey are transformed into new predators.

Two quantities that characterize consumption of prey by predators are λ, a positive constant scaling encounter rate of predators with their prey, and h, the predator handling time of a prey individual. How could these quantities depend on predator density P if foraging facilitation or predator interference are assumed to act? When any of these mechanisms operates, then λ might no longer be a constant, but rather an increasing (facilitation) or decreasing (interference) function of predator

density P. Similarly, h need not be a constant, but rather a decreasing (facilitation) or increasing (interference) function of predator density P.

To guess a priori how dependence of parameters λ and h on predator density might affect predator-prey dynamics, it is illuminating to consider the effects of leaving h, λ, and K as parameters and see what happens when these parameters are simply increased or decreased. In model (4.33) with the type II functional response (4.34), destabilization occurs if the vertical predator isocline $N = m/[\lambda(e - hm)]$ moves from the right side of the peak $N = (K - 1/(h\lambda))/2$ in the prey isocline to the left side. Increasing K moves the peak of the prey isocline to the right and leaves the predator isocline fixed, which eventually causes them to cross and leads to destabilization – this is the so-called paradox of enrichment (Rosenzweig, 1971). Increasing λ moves the peak of the prey isocline to the right and the predator isocline to the left, in a way that causes them to cross eventually, so that is also destabilizing. On the other hand, decreasing h moves both the peak of the prey isocline and the predator isocline to the left, so it is unclear in general whether it will cause them to cross. Actually, they may or may not cross depending on the other parameters; in the former case, the peak of the prey isocline may cross the predator isocline both from the left and from the right (just plot the above two expressions for h in the interval $(0,1)$ and $e = 1$, $m = 1$, $K = 8$ and $\lambda = 5$). This simple algebraic analysis suggests that facilitation increasing encounter rate might be destabilizing to predator-prey dynamics, while facilitation decreasing handling time might not be.

Alternatively, given the proclaimed stabilizing effect of predator interference and the destabilizing effect of Allee effects, we may hypothesize that foraging facilitation will generally destabilize predator-prey dynamics. With regard to the notion that predator interference is stabilizing, the most widely studied models for interference (Beddington-DeAngelis, Hassell-Varley, and ratio-dependent functional responses) can all be interpreted as arising from encounter rates that decrease with predator density (see below). Perhaps the conventional wisdom that interference is stabilizing is due to the fact that there has been little study of models for interference that cannot be interpreted as arising from reduced encounter rates. Therefore, we also account for a novel possibility that handling time h might alternatively be affected by foraging facilitation or predator interference.

Foraging facilitation, predator interference and functional response

A variety of predator-density-dependent functional responses have already been proposed in the literature (Jost, 1998; Skalski and Gilliam, 2001; Jeschke et al, 2002). Some have been designed as phenomenological extensions of functional responses dependent only on prey density, some have involved a mechanistic argument, but virtually all have been developed to model predator interference. The only exception we are aware of was provided by Cosner et al (1999), who suggested to model the per capita feeding rate of predators as

$$f(N,P) = \frac{\lambda_0 NP}{1 + h\lambda_0 NP} \tag{4.35}$$

for predators that forage in a linear school and aggregate when a school of prey is encountered. Here h is the time a predator spends handling one prey item and λ_0 is a positive constant.

To assess impacts of foraging facilitation on predator-prey dynamics and make the presentation as simple as possible at the same time, we would like to come up with a functional response that is based on some mechanistic arguments, covers foraging facilitation and predator interference in a unified way, and recovers the type II functional response (4.34) as well as (some) common functional responses used to model predator interference as special cases. A starting choice could be functional responses of the Hassell-Varley type:

$$f(N,P) = \frac{\lambda_0(N/P^w)}{1 + h\lambda_0(N/P^w)} \tag{4.36}$$

where $w > 0$ corresponds to interference, $w = 0$ recovers the type II functional response (4.34) and $w < 0$ can describe facilitation; note that $w = -1$ corresponds to the functional response (4.35). Note also that this form can be understood as a generalization of (4.34) with $\lambda = \lambda_0/P^w$. The disadvantage of this form is, however, that for negative w the per capita feeding rate of predators goes to zero as predator density P goes to zero, and that for positive w this form is close to ratio-dependent functional responses which are considered by many rather controversial (Abrams and Ginzburg, 2000, and references therein). Therefore, we generalize this form to overcome these disadvantages, by considering

$$\lambda(P) = \frac{\lambda_0}{(b+P)^w} \tag{4.37}$$

for some $b \geq 0$, where $w > 0$ corresponds to interference, $w = 0$ recovers the type II functional response (4.34), and $w < 0$ models facilitation. By incorporating (4.37) into (4.34), the resulting functional response covers the Hassell-Varley functional response (4.36) for $b = 0$, including (4.35) if $w = -1$ and ratio-dependent functional responses if $w = 1$. In addition, it covers the Beddington-DeAngelis functional response if $b > 0$ and $w = 1$ (Beddington, 1975; DeAngelis et al, 1975). Hence, all the common functional responses that model predator interference can be viewed as arising from encounter rates that decrease with increasing predator density. We refer to the functional response (4.34) with λ defined by the formula (4.37) as the *encounter-driven functional response*.

Regarding the handling time h, we analogously define

$$h(P) = h_0(b+P)^w \tag{4.38}$$

for some $b \geq 0$. Again, we have facilitation for $w < 0$, type II functional response for $w = 0$, and interference for $w > 0$. We refer to the functional response (4.34) with h defined by the formula (4.38) as the *handling-driven functional response*.

Apparently, predators cannot profit from facilitation indefinitely, that is, even if their density gets very high. In such a case, interference is likely to overpower facilitation. Therefore, the formulas (4.37) and (4.38) with $w < 0$ can best be applied once predator density at the coexistence equilibrium or maximum predator density in case of oscillatory behavior does not grow too high. Otherwise, one should adopt a more realistic scenario where the effects of predator density on foraging efficiency are positive up to a critical predator density and negative beyond that value. For the parameter λ we somewhat arbitrarily define:

$$\lambda(P) = A + \frac{B - A}{(P/P_c - 1)^2 + 1} \qquad (4.39)$$

where A and B are non-negative constants, with $B > A$. In this way, λ initially increases with predator density (facilitation) and later starts to decline after the critical predator density P_c is exceeded (interference). Here, $(A + B)/2$ is the limit of $\lambda(P)$ as P tends to zero, B is the maximum value of $\lambda(P)$ achieved at $P = P_c$, and $\lambda(P)$ approaches A as P grows large. We refer to the functional response (4.34) with λ defined by the formula (4.39) as the *functional response with humped λ*. Similarly, for the parameter h we define:

$$h(P) = B - \frac{B - A}{(P/P_c - 1)^2 + 1} \qquad (4.40)$$

Again, we assume $B > A$. In this way, h initially decreases with predator density (facilitation) and later starts to increase after the critical predator density P_c is exceeded (interference). Here, $(A + B)/2$ is the limit of $h(P)$ as P tends to zero, A is the minimum value of $h(P)$ achieved at $P = P_c$, and $h(P)$ approaches B as P grows large. We refer to the functional response (4.34) with h defined by the formula (4.40) as the *functional response with humped h*.

In what follows, we study dynamics of the predator-prey model (4.33) in which parameters λ and h of the functional response (4.34) are given in turn by expressions (4.37) to (4.40). For each of these adopted functional responses, we start by exploring the number of coexistence equilibrium points and how this number varies with changing model parameters, and then go on to analyze local stability of these points. For the latter, we use the Matlab 7 (The MathWorks, Inc.) package Matcont that allows for numerical bifurcation analysis of dynamical systems defined via ordinary differential equations (Dhooge et al, 2003). To set up terminology we use below, we will speak on unstable nodes and unstable foci jointly as unstable equilibria and refer to saddle points just as saddle points (so that 'unstable equilibrium' never means saddle point throughout the following text).

As we will see below, except for the extinction equilibrium $N = 0$ and $P = 0$ and the prey-only equilibrium $N = K$ and $P = 0$ that both always exist, for many parameters the predator-prey system (4.33) has either no coexistence equilibrium, a unique stable coexistence equilibrium or a unique unstable coexistence equilibrium. However, we also observe a number of multi-equilibrial regimes. One of these regimes occurs in the domain of predator interference ($w > 0$) and represents a previously

unreported phenomenon: predator interference is able to generate multiple stable co-existence attractors. Another such regime lies in the domain of foraging facilitation ($w < 0$) and corresponds to bistability due to a strong Allee effect among predators.

Model results

Dynamical behavior of the model (4.33) with the type II functional response (4.34) is well known. This model is a prototype for the paradox of enrichment (Rosenzweig, 1971): increasing prey carrying capacity K (enrichment) causes the system to change from the state with a stable coexistence equilibrium to the state with a stable limit cycle around an unstable coexistence equilibrium.

We now analyze the model (4.33) with the functional response (4.34) and first the functions (4.37) and (4.38), and then (4.39) and (4.40). Stability analysis of the extinction equilibrium $E_0 = (0,0)$ and the prey-only equilibrium $E_K = (K,0)$ is carried out in Box 4.12. Apart from the functional responses that arise by setting $b = 0$ in the formulas (4.37) and (4.38), the analysis gives results analogous to all model variants that we examine: the extinction equilibrium E_0 is a saddle point so that prey and predators cannot go simultaneously extinct, and the prey-only equilibrium E_K is locally stable for sufficiently small K provided that $e > mh(P = 0)$, where $h(P = 0)$ denotes the handling time when predator density gets very low so that there are no effects of facilitation or interference, and for any K if $e < mh(P = 0)$. For $b = 0$ and some values of w, some system trajectories might be attracted by the extinction equilibrium E_0, implying that sometimes it is possible to have simultaneous extinction of predators and prey even if both are initially present at positive densities; see Box 4.12 and references therein. Conditions on local stability of the prey-only equilibrium E_K in the case $b = 0$ are also given in Box 4.12.

Box 4.12 Stability of extinction and prey-only equilibria

The Jacobian corresponding to the model (4.33) with a general functional response $f(N,P)$ is

$$J = \begin{pmatrix} r - 2rN/K - P\dfrac{\partial f}{\partial N} & -P\dfrac{\partial f}{\partial P} - f \\ eP\dfrac{\partial f}{\partial N} & -m + e\left(P\dfrac{\partial f}{\partial P} + f\right) \end{pmatrix} \tag{4.41}$$

For any of the adopted functional response forms, except for $b = 0$ and $w > 0$ in the formula (4.37) and $b = 0$ and $w < 0$ in the formula (4.38), this Jacobian evaluated at the extinction equilibrium $E_0 = (0,0)$ is

$$J = \begin{pmatrix} r & 0 \\ 0 & -m \end{pmatrix} \tag{4.42}$$

Hence, in all these cases E_0 is a saddle point – no trajectory can end up in it unless the system starts with no prey.

For $b = 0$ and $w > 0$ in (4.37) and $b = 0$ and $w < 0$ in (4.38), the predator-prey system (4.33) has a singularity at E_0. Several authors studied the predator-prey system (4.33) with the ratio-dependent functional response, corresponding to $b = 0$ and $w = 1$ in (4.37), proving that E_0 can be either a saddle point or an attractor for certain or even for all system trajectories (Kuang and Beretta, 1998; Jost et al, 1999; Xiao and Ruan, 2001). Whether this is true also for $b = 0$ and other positive w in (4.37) and for $b = 0$ and $w < 0$ in (4.38) is so far unknown.

The Jacobian (4.41) evaluated at the prey-only equilibrium $E_K = (K,0)$ is

$$J = \begin{pmatrix} -r & -f(K,0) \\ 0 & -m + ef(K,0) \end{pmatrix} \tag{4.43}$$

E_K is therefore locally stable (node) if $f(K,0) < m/e$ and a saddle point if $f(K,0) > m/e$. From the general functional response,

$$f(N,P) = \frac{\lambda(P)N}{1 + h(P)\lambda(P)N}$$

we have

$$f(K,0) = \left. \frac{\lambda(P)K}{1 + \lambda(P)h(P)K} \right|_{P=0}$$

This implies that except for $b = 0$ in the formulas (4.37) and (4.38), E_K is locally stable (i) if $K < m/[\lambda(0)(e - mh(0))]$ when $e > mh(0)$, and (ii) for any positive K provided that $e < mh(0)$. If $K > m/[\lambda(0)(e - mh(0))]$ in the case (i) then E_K is a saddle point. In these conditions, $\lambda(0) = \lambda_0/b^w$ and $h(0) = h$ for the encounter-driven functional response (4.37), $\lambda(0) = \lambda$ and $h(0) = h_0 b^w$ for the handling-driven functional response (4.38), $\lambda(0) = (A + B)/2$ and $h(0) = h$ for the functional response with humped λ (4.39), and $\lambda(0) = \lambda$ and $h(0) = (A + B)/2$ for the functional response with humped h (4.40). For $b = 0$ in the formulas (4.37) and (4.38), results are summarized in Table 4.8.

Expr.	w	$f(K,0)$	Stability of E_K
(4.37)	> 0	$1/h$	stable if $mh > e$, saddle point if $mh < e$
(4.37)	< 0	0	always stable
(4.38)	> 0	λK	stable if $K < m/(\lambda e)$, saddle point if $K > m/(\lambda e)$
(4.38)	< 0	0	always stable

Table 4.8 Local stability of the prey-only equilibrium E_K when $b = 0$ in the formulas (4.37) and (4.38)

To calculate the number of coexistence equilibria, we set the right-hand sides of the system (4.33) to zero and solve the resulting system of equations. Solving the second equation for the functional response and inserting the result to the first equation relates P to N as

$$P = \frac{e}{m} rN \left(1 - \frac{N}{K} \right) \tag{4.44}$$

This expression defines a concave parabolic curve crossing the prey density axis at $N = 0$ and $N = K$ and attaining the maximum $(erK)/(4m)$ at $N = K/2$. Inserting the general form of our functional response

$$f(N, P) = \frac{\lambda(P)N}{1 + h(P)\lambda(P)N} \tag{4.45}$$

to the second equation then relates N to P as

$$N = \frac{m}{\lambda(P)[e - mh(P)]} \tag{4.46}$$

Analyzing properties of the function (4.46) for each of the functional responses we consider allows us to find the number of coexistence equilibria and how this number varies with model parameters.

Encounter-driven functional response

For the encounter-driven functional response, we have $\lambda(P) = \lambda_0(b + P)^{-w}$ and $h(P) = h$. Equation (4.46) thus becomes

$$N = \frac{m(b + P)^w}{\lambda_0(e - mh)} \tag{4.47}$$

Obviously, $e < mh$ results in no coexistence equilibrium and we thus assume $e > mh$. For $w = 0$, this formula reduces to $N = m/(\lambda_0(e - mh))$ which is a vertical line that intersects the function (4.44) just once provided that $m/(\lambda_0(e - mh)) < K$ and does not intersect it otherwise. Not surprisingly, we thus have one or no coexistence equilibrium, respectively, for the type II functional response (4.34). For $w \neq 0$, we rewrite (4.47) as

$$P = \left[\frac{\lambda_0(e - mh)}{m} \right]^{1/w} N^{1/w} - b \tag{4.48}$$

Specifically, for $w = 1$ and $b > 0$ (the Beddington-DeAngelis functional response), (4.48) becomes an increasing linear function of N, starting at $P = -b$ for $N = 0$ and thus crossing (4.44) at no or just one point; the latter occurs if $P(N = K) = \lambda_0(e - mh)K/m - b > 0$. The Beddington-DeAngelis functional response thus gives rise to either no coexistence equilibrium or a unique coexistence equilibrium; multiple coexistence equilibria cannot occur.

For $0 < w < 1$ or $1/w > 1$, the function (4.48) is convex and starting at $P = -b$ for $N = 0$. Thus, the system (4.33) can have at most one coexistence equilibrium, as at most one intersection of (4.48) with (4.44) is possible in this case. For $w > 1$ or $(0 < 1/w < 1$, (4.48) defines a concave function that starts at $P = -b$ for $N = 0$. Depending on its exact shape, it may intersect the function (4.44) at no, one or three points with positive N and P and we thus expect no, one or three coexistence equilibria in this case, depending on exact parameter values. Sufficient conditions on model parameters for the most interesting case, three co-occurring coexistence equilibrium points, are given in Box 4.13.

Box 4.13 Sufficient conditions for multiple coexistence equilibria
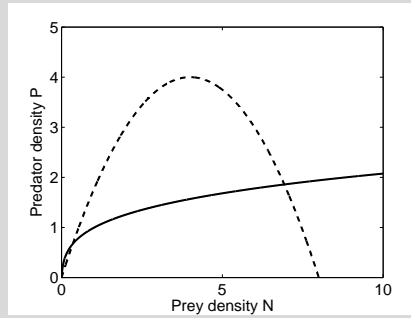
Three coexistence equilibria in case $w > 1$

Irrespectively of the value of $w > 1$, all curves defined by the equation (4.48) cross the point $\hat{P} = 1 - b$ at $\hat{N} = m/[\lambda_0(e - mh)]$. As (4.48) is an increasing function of N, starting at $P = -b$ for $N = 0$, then to get three intersections with function (4.44), it is sufficient to require that $\hat{P}$ lies above the increasing part of (4.44) and the value of P at $N = K/2$, where (4.44) attains its maximum $(erK)/(4m)$, is lower than this maximum. These requirements result in the following two respective conditions on model parameters:

$$\frac{er}{m}\hat{N}\left(1 - \frac{\hat{N}}{K}\right) < \hat{P} = 1 - b$$

$$\left[\frac{\lambda_0(e - mh)}{m}\frac{K}{2}\right]^{1/w} - b < \frac{erK}{4m}$$

An example of this situation is plotted in Fig. 4.23.

Fig. 4.23 An example of three co-occurring coexistence equilibria for the encounter-driven functional response and predator interference. Solid line = eq. (4.48), dashed line = eq. (4.44). Parameters: $w = 4$, $r = 2$, $K = 8$, $e = 1$, $m = 1$, $h = 0.25$, $\lambda_0 = 5$, $b = 0.4$
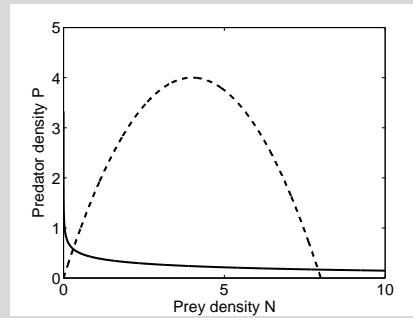
Two coexistence equilibria in case $w < 0$

For $w < 0$, the equation (4.49) is a decreasing, convex function. To get two intersections with the function (4.44), it is thus sufficient to require that the value of (4.49) at $N = K$ is positive and the value of P at $N = K/2$ is lower than $(erK)/(4m)$. That is:

$$\left[\frac{m}{\lambda_0(e - mh)K}\right]^{-1/w} - b > 0$$

$$\left[\frac{m}{\lambda_0(e - mh)K/2}\right]^{-1/w} - b < \frac{erK}{4m}$$

An example of this situation is plotted in Fig. 4.24.

Fig. 4.24 An example of two co-occurring coexistence equilibria for the encounter-driven functional response and foraging facilitation. Solid line = eq. (4.49), dashed line = eq. (4.44). Parameters: $w = -6$, $r = 2$, $K = 8$, $e = 1$, $m = 1$, $h = 0.25$, $\lambda_0 = 5$, $b = 0.4$

Finally, for $w < 0$, that is, foraging facilitation, we may rewrite (4.47) as

$$P = \left[\frac{m}{\lambda_0(e - mh)}\right]^{-1/w} \frac{1}{N^{-1/w}} - b \qquad (4.49)$$

where $-1/w > 0$. For positive N, (4.49) is thus a decreasing, convex function for which $P \to \infty$ as $N \to 0$ from the right and $P \to -b$ as $N \to \infty$. Such a function may cross (4.44) at most twice; we thus expect no, one or two coexistence equilibria in this case. Sufficient conditions on model parameters that give rise to two coexistence equilibrium points are given in Box 4.13.

Figure 4.25a-b shows an example of how the number and character of coexistence equilibria change with w. For sufficiently low negative w, we observe a strong Allee effect among predators – a coexistence equilibrium corresponding to a saddle point separates the stable prey-only equilibrium from another coexistence equi-

librium; this latter coexistence equilibrium is in this particular case unstable and surrounded by a stable limit cycle. This bistability regime including both predator extinction and predator persistence is a direct consequence of the component Allee effect among predators due to foraging facilitation.

For high enough positive w, there is another multi-equilibrial regime where a saddle point separates either two stable coexistence equilibria or one stable coexistence equilibrium and one unstable coexistence equilibrium (Fig. 4.25a-b). The observation of multiple coexistence equilibria as a consequence of predator interference has not been reported in the literature yet. This 'omission' most likely stems from the fact that the flagship model of predator interference has been the Beddington-DeAngelis functional response (for which we show above that it gives rise to at most one coexistence equilibrium). In between the areas with multiple equilibria the predator-prey system (4.33) possesses either a unique stable coexistence equilibrium or a unique unstable coexistence equilibrium (Fig. 4.25).

Exploration of predator-prey dynamics with respect to some parameter pairs is summarized in Fig. 4.25c-d. Most importantly, we observe that the multi-equilibrial regimes are by no means marginal to the explored system but rather cover significant portions of the parameter space. This figure can also help us address the question whether foraging facilitation stabilizes or destabilizes predator-prey dynamics. Let us assess the (de)stabilizing effect of foraging facilitation according to how the value of prey carrying capacity K at which the paradox of enrichment originates changes with the degree of facilitation w. Figure 4.25c shows that in this particular case of encounter-driven functional response, increasing the degree of foraging facilitation (i.e. decreasing w) destabilizes predator-prey dynamics, in agreement with our expectation. In addition, there is a wide range of parameters in the negative w domain for which predators suffer a strong Allee effect and hence predator extinction is a locally stable event; this can also be viewed as destabilizing to predator-prey dynamics. Looking at positive w, we observe that increasing the degree of predator interference stabilizes population dynamics until multiple equilibria arise (Fig. 4.25c).

Handling-driven functional response

For the handling-driven functional response, we have $\lambda(P) = \lambda$ and $h(P) = h_0(b + P)^w$. Equation (4.46) now becomes

$$N = \frac{m}{\lambda\left(e - mh_0(b + P)^w\right)} \tag{4.50}$$

Let us start with $w > 0$, that is, predator interference. It can be shown by standard tools of mathematical analysis that N as a function of P is increasing for all $P > -b$ for which it is formally defined, and that it has a point of discontinuity at P for which $e - mh_0(b + P)^w$ vanishes, i.e. at $P^* = (e/mh_0)^{1/w} - b$. In addition, $N \to N^* = m/[\lambda(e - mh_0 b^w)]$ as $P \to 0$, $N \to 0$ from the left as $P \to \infty$, $N \to \infty$ as $P \to P^*$ from the left and $N \to -\infty$ as $P \to P^*$ from the right. The function (4.50) is thus composed of two hyperbolic branches, one of which ($P > P^*$) lies outside the first

a

b

c

d
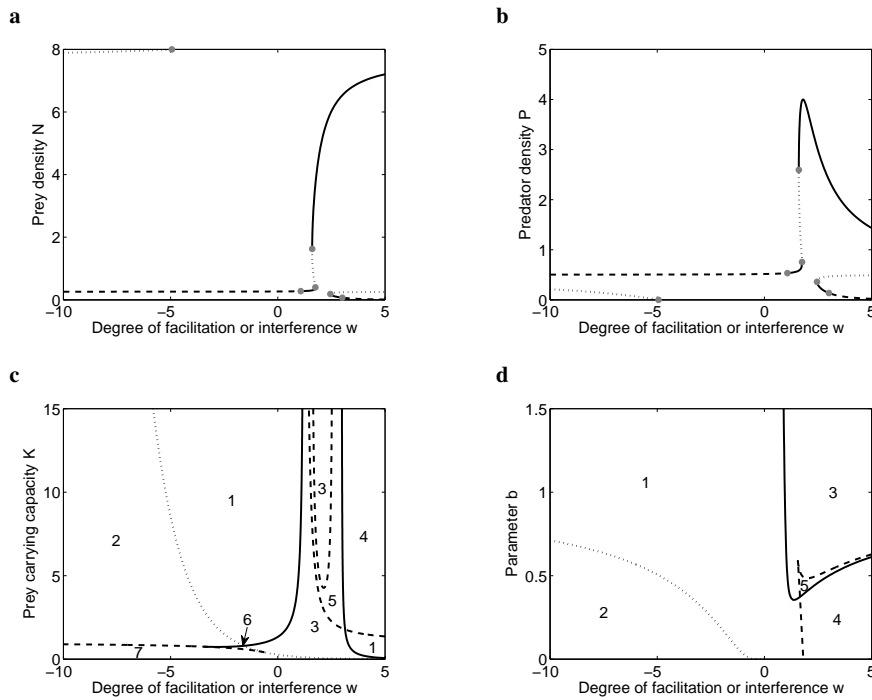
Fig. 4.25 Effects of the encounter-driven functional response (4.37) on predator-prey dynamics. (a) and (b) Prey and predator equilibrium densities as functions of the degree of foraging facilitation or predator interference. Solid line = locally stable equilibrium, dashed line = unstable equilibrium, dotted line = saddle point. Grey dots indicate transition points between the equilibrium stability types. Parameters: $r = 2$, $K = 8$, $e = 1$, $m = 1$, $h = 0.25$, $\lambda_0 = 5$, $b = 0.5$. (c) and (d) Bifurcation diagrams for selected pairs of model parameters. Legend: 1 = a unique unstable coexistence equilibrium, 2 = strong Allee effect: predator extinction equilibrium co-occurs with a stable limit cycle surrounding an unstable coexistence equilibrium, 3 = a unique stable coexistence equilibrium, 4 = a stable coexistence equilibrium co-occurs with an unstable one with the two separated by a saddle point, 5 = two stable coexistence equilibria co-occur and are separated by a saddle point, 6 = strong Allee effect: predator extinction equilibrium coexists with a stable coexistence equilibrium, 7 = predator extinction is globally stable. Solid curves represent the curves of Hopf bifurcation points, dashed curves are the curves of limit points, and dotted curves represent the curves of branch points. Parameters: $r = 2$, $K = 8$ (d), $e = 1$, $m = 1$, $h = 0.25$, $\lambda_0 = 5$, $b = 0.5$ (c)

quadrant with positive N and P (see Box 4.14 for an example). This implies that P as a function of positive N for the other branch (inverse function to (4.50)) is an increasing, concave function that is rooted at N^* (where $P = 0$) and approaches P^* as N grows large. Since $N^* > 0$ if and only if $P^* > 0$, (4.50) can intersect the function (4.44) at no, one or three points with positive N and P. Sufficient conditions on model parameters for three co-occurring coexistence equilibrium points are given in Box 4.14.

**Box 4.14 Sufficient conditions for multiple coexistence equilibria**

Three coexistence equilibria in case $w > 0$

Irrespectively of the value of $w > 0$, all curves defined by the equation (4.50) cross the point $\hat{N} = m/[\lambda(e - mh_0)]$ at $\hat{P} = 1 - b$. As we showed that (4.50), viewed as a function P of positive N, is an increasing, concave function rooted at $N^* = m/[\lambda(e - mh_0 b^w)]$ (where $P = 0$) and approaching $P^* = (e/mh_0)^{1/w} - b$ as N grows large, then to get three intersections with the function (4.44), it is sufficient to require that $\hat{P}$ lies above the increasing part of (4.44) and at the same time the value of P^* is lower than the value of (4.44) evaluated at $N = K/2$, where (4.44) attains its maximum $(erK)/(4m)$. These requirements result in the following two respective conditions on model parameters:

$$\frac{er}{m}\hat{N}\left(1 - \frac{\hat{N}}{K}\right) < \hat{P} = 1 - b$$

$$P^* = (e/mh_0)^{1/w} - b < \frac{erK}{4m}$$

An example of this situation is plotted in Fig. 4.26.
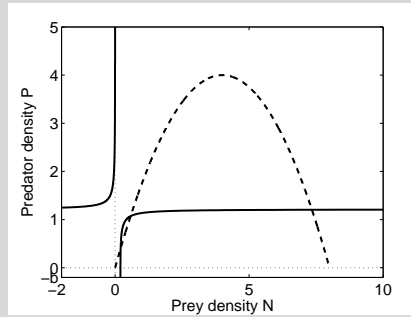
Fig. 4.26 An example of three co-occurring coexistence equilibria for the handling-driven functional response and predator interference. Solid line = eq. (4.50), dashed line = eq. (4.44). Parameters: $w = 4$, $r = 2$, $K = 8$, $e = 1$, $m = 1$, $h_0 = 0.25$, $\lambda = 5$, $b = 0.2$

Two coexistence equilibria in case $w < 0$

For $w < 0$, the equation (4.52), viewed as a function P of positive N, is a decreasing, convex function. We also know that $N \rightarrow N^* = m/(\lambda e)$ from above as $P \rightarrow \infty$ and that $N \rightarrow \infty$ as $P \rightarrow P^* = (e/mh_0)^{-1/w} - b$ from the right. We may therefore consider only the case $N > m/(\lambda e)$, which allows us to rewrite (4.52) as
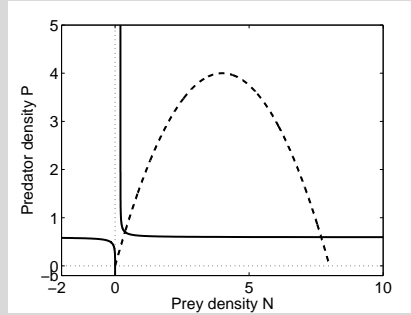
$$P = \left(\frac{mh_0}{e - m/(\lambda N)}\right)^{-1/w} - b \qquad (4.51)$$

Then, to get two intersections with the function (4.44), it is sufficient to require that the value of (4.51) at $N = K$ is positive and the value of (4.51) at $N = K/2$, where (4.44) attains its maximum $(erK)/(4m)$, is lower than this maximum. That is:

$$\left(\frac{mh_0}{e - m/(\lambda K)}\right)^{-1/w} - b > 0$$

$$\left(\frac{mh_0}{e - m/(\lambda K/2)}\right)^{-1/w} - b < \frac{erK}{4m}$$

An example of this situation is plotted in Fig. 4.27.

Fig. 4.27 An example of two co-occurring coexistence equilibria for the handling-driven functional response and foraging facilitation. Solid line = eq. (4.51), dashed line = eq. (4.44). Parameters: $w = -6$, $r = 2$, $K = 8$, $e = 1$, $m = 1$, $h_0 = 0.25$, $\lambda = 5$, $b = 0.2$

For $w < 0$, that is, foraging facilitation, we may rewrite (4.50) as

$$N = \frac{m}{\lambda\left(e - mh_0/(b+P)^{-w}\right)} \tag{4.52}$$

with $-w > 0$. One can easily show that $N \to N^* = m/(\lambda e)$ as $P \to \infty$, $N \to 0$ as $P \to -b$ from the right, $N \to -\infty$ as $P \to P^*$ from the left, where now $P^* = (e/mh_0)^{-1/w} - b$, and $N \to \infty$ as $P \to P^*$ from the right. In addition, N as a function of P is a decreasing function for all admissible $P > -b$. This implies that the function (4.52) is formed by two hyperbolic branches, one of which ($P < P^*$) lies outside the first quadrant (see Box 4.14 for an example). Therefore, P as a function of positive N for the other branch (inverse function to (4.52)) is a decreasing, convex function, and can thus intersect function (4.44) at most twice – we thus have up to two coexistence equilibria. Sufficient conditions on model parameters that give rise to two coexistence equilibrium points are given in Box 4.14.

Figure 4.28a-b shows an example of how the number and character of coexistence equilibria change with w. As in the previous case, also here we observe a

strong Allee effect for sufficiently low negative w. Similarly to the previous case, we also observe a parameter range for which there are three coexistence equilibria in the interference domain ($w > 0$). The existence of these multi-equilibrial regimes is thus independent of what parameter in the functional response is actually affected by predator density, and makes our conclusions more robust and appealing. In between the areas with multiple equilibria and in this case also for some model parameters and strong enough predator interference (high $w > 0$) the predator-prey system (4.33) possesses either a unique stable coexistence equilibrium or a unique unstable coexistence equilibrium (Fig. 4.28).

Exploration of predator-prey dynamics with respect to some parameter pairs is summarized in Fig. 4.28c-d. Also in this case, the multi-equilibrial regimes are by no means marginal to the explored system but rather cover a significant portion of the parameter space. Likewise, Fig. 4.28c shows that as w decreases, the paradox of enrichment occurs at still lower values of K, and there is a wide range of parameters for which predators suffer a strong Allee effect. Therefore, also here, increasing the degree of foraging facilitation (decreasing w) destabilizes predator-prey dynamics, and increasing the degree of predator interference (increasing w) stabilizes predator-prey dynamics until multiple equilibria arise.

Functional response with humped λ

For the functional response with humped λ, we have

$$\lambda(P) = A + \frac{B-A}{(P/P_c - 1)^2 + 1} \tag{4.53}$$

with $B > A$, and $h(P) = h$. Equation (4.46) now becomes

$$N = \frac{m}{e - mh} \left/ \left[A + \frac{B-A}{(P/P_c - 1)^2 + 1} \right] \right. \tag{4.54}$$

We assume that $e > mh$; otherwise, $N < 0$ and there is no coexistence equilibrium. This implies $N = \frac{m}{e-mh} \left/ \left(\frac{A+B}{2} \right) \right.$ at $P = 0$ and $N \to \frac{m}{(e-mh)A}$ as $P \to \infty$. Moreover, by calculating dN/dP one can show that the function (4.54) decreases for $P < P_c$ and increases for $P > P_c$; at $P = P_c$, it attains the minimum value $N(P_c) = m/[(e-mh)B]$. As a result, (4.54) can cross the function (4.44) at no, one, two or three points with positive N and P. Sufficient conditions on model parameters that give rise to two or three coexistence equilibrium points are given in Box 4.15.

Box 4.15 Sufficient conditions for multiple coexistence equilibria

Three coexistence equilibria
We already know that the function (4.54) attains its minimum value $N(P_c) = m/[(e-mh)B]$ at $P = P_c$. To get three intersections with the function (4.44),
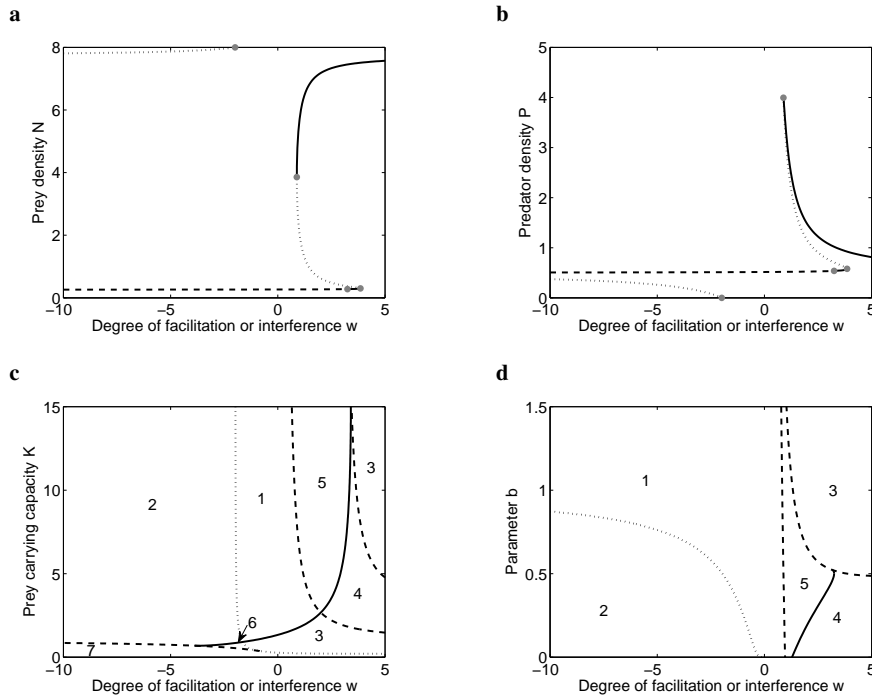
Fig. 4.28 Effects of the handling-driven functional response (4.38) on predator-prey dynamics. (a) and (b) Prey and predator equilibrium densities as functions of the degree of foraging facilitation or predator interference. Legend as in Fig. 4.25. Parameters: $r = 2$, $K = 8$, $e = 1$, $m = 1$, $h_0 = 0.25$, $\lambda = 5$, $b = 0.5$. (c) and (d) Bifurcation diagrams for selected pairs of model parameters. Legend as in Fig. 4.25. Parameters: $r = 2$, $K = 8$ (d), $e = 1$, $m = 1$, $h_0 = 0.25$, $\lambda = 5$, $b = 0.5$ (c)

it thus suffices to require that P_c lies above the increasing part of (4.44) and at the same time the value of (4.54) evaluated at $N = K/2$, where (4.44) attains its maximum $(erK)/(4m)$, is lower than this maximum. These requirements result in the following two respective conditions on model parameters:

$$P_c > \frac{er}{m} N(P_c) \left(1 - \frac{N(P_c)}{K} \right)$$

$$\max \left[\text{solution} \left(\frac{m}{e - mh} \middle/ \left[A + \frac{B - A}{(P/P_c - 1)^2 + 1} \right] = \frac{K}{2}, P \right) \right] < \frac{erK}{4m}$$

where the symbol solution$(f(x, y, \ldots) = c, x)$ denotes the set of solutions of an equation $f(x, y, \ldots) = c$ with respect to variable x; c is a constant. An example of this situation is plotted in Fig. 4.29.
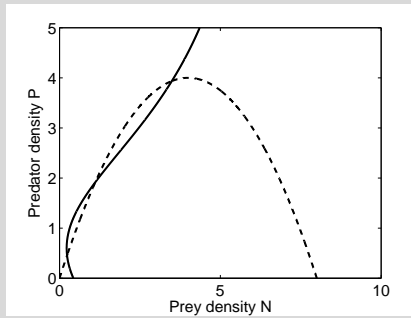
Fig. 4.29 An example of three co-occurring coexistence equilibria for the functional response with humped λ. Solid line = eq. (4.54), dashed line = eq. (4.44). Parameters: $r = 2$, $K = 8$, $e = 1$, $m = 1$, $h = 0.25$, $A = 0.2$, $B = 6$, $P_c = 0.6$
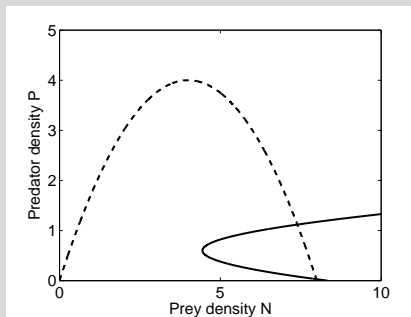
Two coexistence equilibria

To get two intersections with the function (4.44), it is sufficient to require that the value of (4.54) at $P = 0$ is higher than K and that P_c lies below (4.44). This gives:

$$K < N(P = 0) = \frac{m}{e - mh} \bigg/ \left(\frac{A + B}{2} \right)$$

$$P_c < \frac{er}{m} N(P_c) \left(1 - \frac{N(P_c)}{K} \right)$$

An example of this situation is plotted in Fig. 4.30.

Fig. 4.30 An example of two co-occurring coexistence equilibria for the functional response with humped λ. Solid line = eq. (4.54), dashed line = eq. (4.44). Parameters: $r = 2$, $K = 8$, $e = 1$, $m = 1$, $h = 0.25$, $A = 0.02$, $B = 0.3$, $P_c = 0.6$

Figure 4.31 exemplifies behavior of the predator-prey system (4.33) and the functional response with humped λ, with respect to the peak height B. Parameter B can here be viewed as a degree of foraging facilitation or predator interference – increasing (decreasing) B means that prey encounter rate by predators increases (decreases) for all predator densities P. The system is stable for low B and any K and for higher B as soon as K is low (Fig. 4.28c). In addition, multiple equilibria may occur with either two stable equilibria or one stable and one unstable equilibrium when K gets sufficiently high and B attains some intermediate values (Fig. 4.31c). Although we do not observe the bistability regime corresponding to a strong Allee effect among predators for the particular choice of model parameters used in Fig. 4.31, we know from Box 4.15 that such a regime exists: when there are just two coexistence equilibria, the one with lower predator density is always a saddle point while the one with higher predator density is either a stable equilibrium or an unstable equilibrium surrounded by a stable limit cycle; moreover, the prey-only equilibrium is in this case stable (numerical results not shown). Altogether, in the case of the functional response with humped λ, the paradox-of-enrichment curve in Fig. 4.31c suggests that increasing foraging facilitation (predator interference) reduces (enhances) stability of the predator-prey system (4.33).

Functional response with humped h

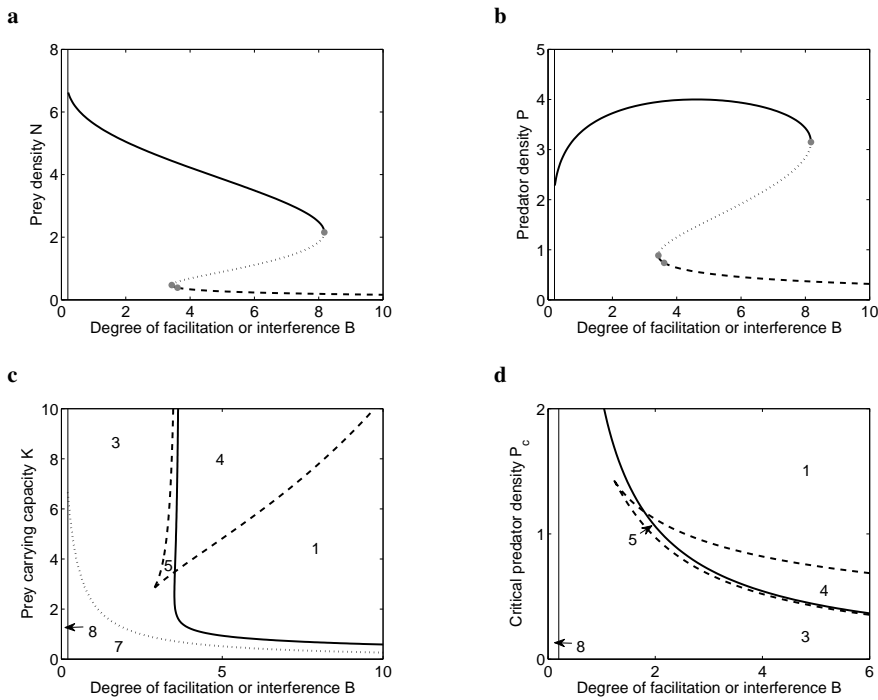For the functional response with humped h, we have $\lambda(P) = \lambda$ and

$$h(P) = B - \frac{B-A}{(P/P_c - 1)^2 + 1} \tag{4.55}$$

with $B > A$. Equation (4.46) thus becomes

$$N = \frac{m}{\lambda} \left/ \left(e - m \left[B - \frac{B-A}{(P/P_c - 1)^2 + 1} \right] \right) \right. \tag{4.56}$$

This implies $N = m/[\lambda(e - m[(A + B)/2])]$ at $P = 0$ and $N \to m/[\lambda(e - mB)]$ as $P \to \infty$. Moreover, by calculating dN/dP one can show that the function (4.56) decreases when $P < P_c$ and increases when $P > P_c$; at $P = P_c$, it attains the minimum value $N(P_c) = \frac{m}{\lambda(e-mA)}$. In addition, the function (4.56) has two discontinuity points at $P = P_c(1 \pm \sqrt{(e/m - A)/(B - e/m)})$ provided that $A < e/m$ and $B > e/m$, and no discontinuity points otherwise ($B < e/m$ or $A > e/m$). If there are no discontinuity points, (4.56) has the same qualitative form as in the previous case of humped λ, and the predator-prey system (4.33) can thus have up to three coexistence equilibria. Note, however, that for $A > e/m$ and hence $B > e/m$ the above limits imply that N in (4.56) is always negative, so that there are no coexistence equilibria in this particular case.

If there are two discontinuity points ($A < e/m$ and $B > e/m$), the function (4.56) is composed of two hyperbolic branches that surround a parabolic curve (see Box

Fig. 4.31 Effects of the functional response with humped λ on predator-prey dynamics. (a) and (b) Prey and predator equilibrium densities as functions of the degree of foraging facilitation or predator interference; there is an inaccessible domain to the left of the vertical solid line as $B < A$ there. Legend as in Fig. 4.25. Parameters: $r = 2$, $K = 8$, $e = 1$, $m = 1$, $h = 0.25$, $A = 0.2$, $P_c = 0.6$. (c) and (d) Bifurcation diagrams for selected pairs of model parameters. Legend as in Fig. 4.25, 8 = inaccessible domain as $B < A$ there. Parameters: $r = 2$, $K = 8$ (d), $e = 1$, $m = 1$, $h = 0.25$, $A = 0.2$, $P_c = 0.6$ (c)

4.16 for an example). It can be shown analytically that none of the hyperbolic branches can cross the function (4.44). Therefore, the system can have up to four coexistence equilibrium points that are intersections of the parabolic curve and the function (4.44), depending on exact parameter values. Sufficient conditions on model parameters that give rise to two, three or even four coexistence equilibria are given in Box 4.16.

Box 4.16 Sufficient conditions for multiple coexistence equilibria

If $B < e/m$ and hence $A < e/m$ then we showed in the main text that the function (4.56) has qualitatively the same shape as the function (4.54). Hence, sufficient conditions for the co-occurrence of three or two coexistence equilibria can be derived along the same lines as in Box 4.14. In what follows, we

assume that $B > e/m$ and $A < e/m$, and give sufficient conditions for the simultaneous existence of four, three or two coexistence equilibria. For the case $B > e/m$ and $A < e/m$, we present a figure first and only then derive the conditions. The function is composed of two hyperbolic branches in between which there is a parabolic-like form (Figs. 4.32-4.34); the points of discontinuity at which hyperbolic branches 'pass' to a parabolic form are

$$P_1 = P_c(1 + \sqrt{(e/m - A)/(B - e/m)})$$

and

$$P_2 = P_c(1 - \sqrt{(e/m - A)/(B - e/m)})$$
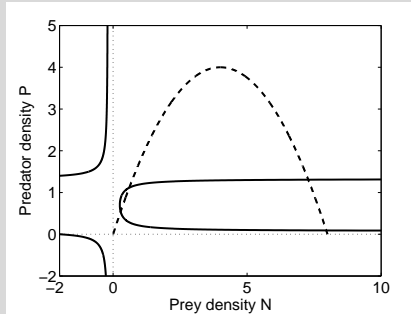
Four coexistence equilibria

We already know that the function (4.56) attains its minimum value $N(P_c) = m/[\lambda(e - mA)]$ at $P = P_c$. To get four intersections with the function (4.44), it thus suffices to require that P_c lies above the increasing part of (4.44) and at the same time $P_2 > 0$ and P_1 is lower than $(erK)/(4m)$, the maximum value attained by (4.44). These requirements result in the following three respective conditions on model parameters:

$$P_c > \frac{er}{m} N(P_c) \left(1 - \frac{N(P_c)}{K}\right)$$

$$P_1 = P_c(1 - \sqrt{(e/m - A)/(B - e/m)}) < \frac{erK}{4m}$$

$$P_2 = P_c(1 - \sqrt{(e/m - A)/(B - e/m)}) > 0$$

An example of this situation is plotted in Fig. 4.32.

Fig. 4.32 An example of four co-occurring coexistence equilibria for the functional response with humped h. Solid line = eq. (4.56), dashed line = eq. (4.44). Parameters: $r = 2$, $K = 8$, $e = 1$, $m = 1$, $\lambda = 5$, $A = 0.2$, $B = 2$, $P_c = 0.7$. Note that (4.56) defines function N as it depends on P
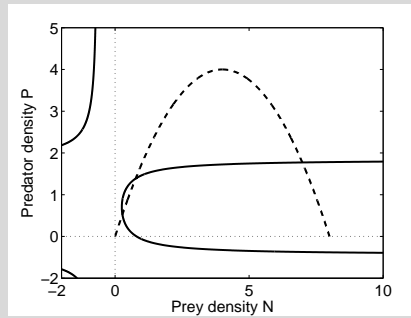
Three coexistence equilibria

To get three intersections with the function (4.44), it suffices to require that P_c lies above the increasing part of (4.44), that P_1 is lower than $(erK)/(4m)$, the maximum value attained by (4.44), and that the lower P at which (4.56) equals K is lower than 0. These requirements result in the following three respective conditions on model parameters:

$$P_c > \frac{er}{m} N(P_c) \left(1 - \frac{N(P_c)}{K}\right)$$

$$P_1 = P_c(1 - \sqrt{(e/m - A)/(B - e/m)}) < \frac{erK}{4m}$$

$$\min\left[\text{solution}\left(\frac{m}{\lambda} \bigg/ \left(e - m\left[B - \frac{B - A}{(P/P_c - 1)^2 + 1}\right]\right) = K, P\right)\right] < 0$$

An example of this situation is plotted in Fig. 4.33.

Fig. 4.33 An example of three co-occurring coexistence equilibria for the functional response with humped h. Solid line = eq. (4.56), dashed line = eq. (4.44). Parameters: $r = 2$, $K = 8$, $e = 1$, $m = 1$, $\lambda = 5$, $A = 0.2$, $B = 1.3$, $P_c = 0.7$

Two coexistence equilibria

There are actually two qualitatively different possibilities of how to get two coexistence equilibria. Firstly, we may modify the case with four equilibria and require that P_c lies below (4.44) and at the same time $P_2 > 0$ and P_1 is lower than $(erK)/(4m)$, the maximum value attained by (4.44). These requirements result in the following three respective conditions on model parameters:

$$P_c < \frac{er}{m} N(P_c) \left(1 - \frac{N(P_c)}{K}\right)$$

$$P_1 = P_c(1 - \sqrt{(e/m - A)/(B - e/m)}) < \frac{erK}{4m}$$

$$P_2 = P_c(1 - \sqrt{(e/m - A)/(B - e/m)}) > 0$$

An example of this situation is plotted in Fig. 4.34a. Alternatively, we may require that P_c lies above the increasing part of (4.44), P_1 is sufficiently large and P_2 is sufficiently low yet positive; rigorous conditions are a bit nasty in this case and are not given explicitly. An example of this situation is plotted in Fig. 4.34b.
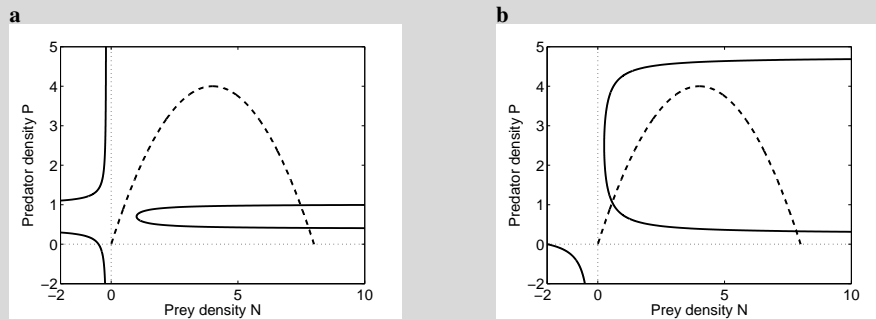
Fig. 4.34 Examples of two co-occurring coexistence equilibria for the functional response with humped h. Solid line = eq. (4.56), dashed line = eq. (4.44). Parameters: (a) $r = 2$, $K = 8$, $e = 1$, $m = 1$, $\lambda = 5$, $A = 0.8$, $B = 2$, $P_c = 0.7$. (b) $r = 2$, $K = 8$, $e = 1$, $m = 1$, $\lambda = 5$, $A = 0.2$, $B = 2$, $P_c = 2.5$

Figure 4.35 exemplifies behavior of the predator-prey system (4.33) and the functional response with humped h, with respect to the trough depth A. Parameter A can here be viewed as a degree of foraging facilitation or predator interference – decreasing (increasing) A means that predator handling time of prey h decreases (increases) for all predator densities P. For $B < e/m$, Fig. 4.35c shows that the system is stable for high A (note that we require $A < B < e/m$) and low to medium K, and for almost any A as soon as K is low. A bistable pattern may occur when A is relatively low and K gets sufficiently high. The bistability regime corresponding to a strong Allee effect among predators occurs for high enough A and low enough K (Fig. 4.35c).

Regarding (de)stabilizing effects of foraging facilitation, the picture is not as straightforward here as in the previous cases. As A decreases, the curve connecting the values of K at which the paradox of enrichment originates does not decline monotonously (Fig. 4.35c). So, for some values of A, as K increases the coexistence equilibrium changes from stable to unstable to stable to again unstable. For other values of A, system dynamics change from demonstrating the strong Allee effect to a unique stable equilibrium to a unique unstable equilibrium. Both these routes hardly describe a destabilizing property of foraging facilitation. For low values of A, however, the paradox-of-enrichment curve has the form expected when foraging fa-

cilitation would be destabilizing. Looked at from another perspective, for low values of *K*, decreasing *A* first stabilizes the system from a strong Allee effect to a unique stable equilibrium and destabilizes it later on from a unique stable equilibrium to a unique unstable equilibrium. For high *K*, on the other hand, we observe a destabilizing route: from a unique stable equilibrium to a unique unstable equilibrium to two unstable equilibria. Hence, the impact of foraging facilitation on dynamics of the predator-prey system (4.33) is ambiguous here.
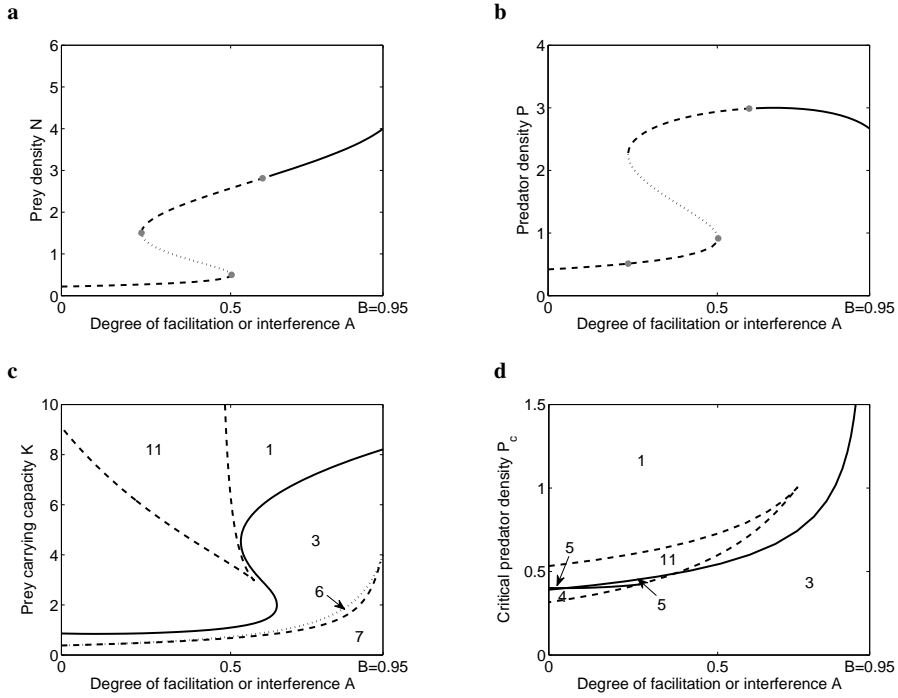
Fig. 4.35 Effects of the functional response with humped *h* on predator-prey dynamics. (a) and (b) Prey and predator equilibrium densities as functions of the degree of foraging facilitation or predator interference. Legend as in Fig. 4.25. Parameters: $r = 2$, $K = 6$, $e = 1$, $m = 1$, $\lambda = 5$, $B = 0.95$, $P_c = 0.6$. (c) and (d) Bifurcation diagrams for selected pairs of model parameters. Legend as in Fig. 4.25, 11 = co-occurrence of two unstable coexistence equilibria. Parameters: $r = 2$, $K = 6$ (d), $e = 1$, $m = 1$, $\lambda = 5$, $B = 0.95$, $P_c = 0.6$ (c)

Quite a different situation arises once $A < e/m$ and $B > e/m$, that is, in the case for which we proved the simultaneous existence of four coexistence equilibria. A snapshot of system dynamics is plotted as Fig. 4.36. Apart from the globally stable prey-only equilibrium observed for high *A* and any *K* or low *K* and any *A* (Fig. 4.36c), all the remaining dynamical regimes that we identified for the selected parameter values involve multiple coexistence equilibria. These include a strong

Allee effect (regimes 2 and 5) and four coexistence equilibria where two stable or unstable equilibria and the stable prey-only equilibrium are interspersed with two saddle points (regimes 9 and 10); see also Fig. 4.36a-b.
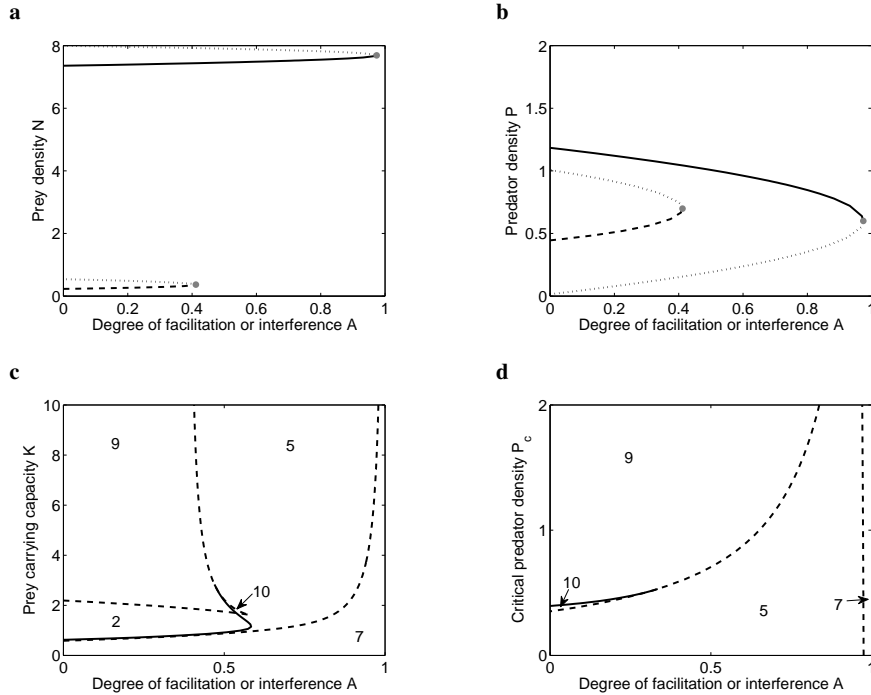

Fig. 4.36 Effects of the functional response with humped h on predator-prey dynamics. (a) and (b) Prey and predator equilibrium densities as functions of the degree of foraging facilitation or predator interference. Legend as in Fig. 4.25. Parameters: $r = 2, K = 8, e = 1, m = 1, \lambda = 5, B = 2, P_c = 0.6$. (c) and (d) Bifurcation diagrams for selected pairs of model parameters. Legend as in Fig. 4.25, 9 = co-occurrence of one stable and one unstable coexistence equilibrium and two saddle points, 9 = co-occurrence of two stable coexistence equilibria and two saddle points. Parameters: $r = 2, K = 8$ (d), $e = 1, m = 1, \lambda = 5, B = 2, P_c = 0.6$ (c)

Summary

This section addresses the previously unexplored question of how foraging facilitation among predators affects predator-prey dynamics. Also, it explores the effects of predator interference, as this requires no extra computational time and makes the resulting picture 'symmetric' and complete. Both foraging facilitation and preda-

tor interference can be modeled as affecting encounter rate between predators and prey or predator handling time of prey. We show that all the common functional responses used to model predator interference can be viewed as arising from encounter rates that decrease with increasing predator density. Therefore, we also account for a novel possibility that the predator handling time of prey might alternatively be affected by foraging facilitation or predator interference.

Several novel and interesting results stem from the performed analysis. Firstly, in systems with the encounter-driven functional response, handling-driven functional response, and functional response where the predator encounter rate with prey first increases and then decreases with increasing predator density, foraging facilitation appears to be destabilizing to predator-prey dynamics. On the contrary, an ambiguity is observed in systems with the functional response where the predator handling time of prey first decreases and then increases with increasing predator density: we can interpret the effects of foraging facilitation on predator-prey dynamics as stabilizing in a portion of the parameter space and as destabilizing in another portion. For a wide range of parameter values, this last way of how foraging facilitation operates can even give rise to four co-occurring coexistence equilibria. The particular way of how foraging facilitation operates (or is modeled) thus significantly affects resulting predator-prey dynamics.

Foraging facilitation is a component Allee effect among predators (Courchamp et al, 2008): an increase in predator population or group size leads to an increase in a fitness component of each of its members. One may therefore be interested in whether at least for some parameter values this component Allee effect gives rise to a strong Allee effect among predators, corresponding to two alternative system steady states: predator extinction and predator persistence. This is indeed the case and we observe quite a wide range of model parameters for which there is a critical predator density below which predators go extinct and prey attain the environmental carrying capacity and above which both species coexist.

We also show that predator interference is stabilizing to predator-prey dynamics once its strength is not too high, and thus corroborate results of others (Rogers and Hassell, 1974; Ruxton et al, 1992; Ruxton, 1995; Huisman and DeBoer, 1997). Contrary to this conventional wisdom, however, the analysis revealed a dynamic regime previously unreported for predator interference: there is quite a wide range of model parameters for which predator interference gives rise to three co-occurring coexistence equilibria. Dynamical behavior around these equilibria depends on specific parameter values: the equilibrium with the highest prey density always appears to be stable while the one with the lowest prey density may be either stable or unstable; the intermediate steady state is always a saddle point. Such a multi-equilibrial regime is rather robust and was observed for all the four functional response types adopted in this article. An interesting topic for future research thus may be to seek for general conditions on the predator functional response that would produce three coexistence steady states in a predator-prey model.

Interestingly, our sample simulations showed that in many cases the unstable equilibria are surrounded by stable limit cycles. Thus, many multi-equilibrial regimes are actually bistability regimes in which either two stable limit cycles or

one stable equilibrium and one stable limit cycle co-occur. Investigation of the limit cycle behavior of our model variants with foraging facilitation and predator interference would certainly be an interesting adventure to be undertaken in the future.

4.5 Conclusions and further research

In this chapter, we explored impacts that Allee effects in the prey or predator populations might have on predator-prey dynamics. For unstructured prey populations, generalist predators with a type II functional response are known to induce an Allee effect in prey (Gascoigne and Lipcius, 2004; Courchamp et al, 2008). We extended this knowledge in two directions. First, we assumed prey themselves are subject to a mate-finding Allee effect even in the absence of predation, and so suffer from a double Allee effect. In addition, these two component Allee effects were supposed to be traded off: as prey mitigate the predation-driven Allee effect by e.g. moving more carefully, they at the same time worsen their mate-finding Allee effect, and vice-versa. Considering a number of mechanisms (and corresponding models) responsible for this coupling, and a number of qualitative forms for such trade-offs (convex, concave), we show that the (relative) population resilience declines with increasing cost of reproduction embodied in a transition from convex to concave reproduction-predation risk trade-offs. In some cases, reproduction can be so costly that the population always goes extinct. In other cases, the population goes extinct only over a certain range of low, intermediate or high levels of reproductive activities. Moreover, we show that predator removal (e.g. in an attempt to save an endangered prey species) has the least effect on populations with low cost of reproduction in terms of predation and, conversely, predator addition (e.g. to eradicate a pest) is most effective for populations with high predation cost of reproduction. Our results indicate that a detailed knowledge of the trade-off can be crucial in applications: for some trade-off shapes, only intermediate levels of reproductive activities might guarantee population survival, while they can lead to extinction for others. We therefore suggest that the fate of populations subject to the two antagonistic Allee effects should be evaluated on a case-by-case basis.

Second, we developed a mathematical model to study dynamics of an age-structured population preyed upon by age-specific, generalist predators. Predation on any age class is either absent, or represented by type II or type III functional responses, in various combinations. We seek for Allee effects or more generally for multiple stable steady states in the prey population, and explore whether predation is more effective on juveniles or adults. One of the key findings we made is the occurrence of predator pit when only one age class is consumed and predators use a type II functional response – this scenario is known to occur for an unstructured prey population consumed through a type III functional response and can never occur for an unstructured prey population consumed through a type II one. In case both age classes are consumed by predators exhibiting a type II functional response strong Allee effects occur frequently, but some parameter combinations give rise to

predator pits and even three stable equilibria (one extinction equilibrium and two interior ones – an Allee effect and a predator pit combined). Multiple stable interior steady states are common if one of the age classes is exploited through a type III functional response – here, in addition to the behaviors mentioned above one may even observe the case of three stable interior equilibria – the 'double' predator pit. Despite intriguing consequences of some these behaviors for population management, our results demonstrate that even consideration of a simple population structure may bring about predictions that are qualitatively different from those based on (frequently used) unstructured models.

In the second part of this chapter, we considered prey populations consumed by specialist predators, that is, predators that numerically responded to prey densities. Since little is known about the impact of prey sexual dimorphism on predator-prey dynamics and the impact of sex-selective harvesting and trophy hunting on long-term stability of exploited species, we first developed and analyzed several simple predator-prey models with sex-selective predation (i.e. predators attacked male and female prey with differing intensities). We show that the consequences of sex-selective predation depend on the interplay of predation bias and prey mating system. Predation on the 'less limiting' prey sex can yield a stable predator-prey equilibrium, while predation on the other sex usually destabilizes the dynamics and promotes population collapses. For prey mating systems that we consider, males are less limiting except for polyandry, and male-biased predation alone on such prey can stabilize otherwise unstable dynamics. On the contrary, female-biased predation on polygynous or monogamous prey requires other stabilizing mechanisms to persist. As a consequence, the observed skew towards male-biased predation might reflect, in addition to sexual selection, the evolutionary history of predator-prey interactions. Our results can also have implications for long-term sustainability of harvesting and trophy hunting of sexually dimorphic species.

Our final model concerned the impacts of foraging facilitation among predators on predator-prey dynamics, showing that these impacts depend on the way this process is modeled. In particular, foraging facilitation destabilizes predator-prey dynamics when it affects the encounter rate between predators and prey. By contrast, it might have a stabilizing effect if the predator handling time of prey is affected. Foraging facilitation is an Allee effect mechanism among predators and we show that for many parameters, it gives rise to a demographic Allee effect or a critical predator density in need to be crossed for predators to persist. We explore also the effects of predator interference, to make the picture 'symmetric' and complete. Predator interference is shown to stabilize predator-prey dynamics once its strength is not too high, and thus corroborates results of others. On the other hand, there is a wide range of model parameters for which predator interference gives rise to three co-occurring coexistence equilibria. Such a multi-equilibrial regime is rather robust as we observe it for all the functional response types we explore. This is a previously unreported phenomenon which we show cannot occur for the Beddington-DeAngelis functional response. An interesting topic for future research thus might be to seek for general conditions on predator functional responses that would produce multiple coexistence equilibria in a predator-prey model.

The issue of impacts of Allee effects on predator-prey dynamics is currently very topical (Boukal et al, 2007; van Voorn et al, 2007; Aguirrea et al, 2009; Verdy, 2010; McLellan et al, 2010; Wang et al, 2011). And still, much remains to be done. One of the promising research avenues is to consider tri-trophic interactions with one or more Allee effects involved, not to speak of larger and more complex food webs. Consider, e.g. a three species chain (such as resource, primary consumer, and carnivore) in which one of the intermediate species may be subject to an Allee effect with respect to the lower species in the chain (such as due to foraging facilitation) and another Allee effect with respect to an upper species in the chain (such as due to an anti-predator behavior). Another situation arises when the intermediate species has an Allee effect that goes beyond this chain, such as a mate-finding one. One might also imagine a predator-prey interaction devoid of Allee effects, when one or the other population are consumed by a generalist predator with a type II functional response. This latter topic is especially interesting given that many models of predator-prey interactions predict coexistence of the two species along a limit cycle. From an empirical perspective, one may imagine a population of trees that aim at attracting pollinators, coupled with a disproportionate predation on resulting seeds, owing to failure to satiate seed predators. Likewise, rare plants can be both pollen limited and subject to herbivore-driven Allee effects, analogous to Allee effects owing to predator satiation. In both these cases, trees or plants are subject to double Allee effects (Berec et al, 2007). Many of these higher trophic interactions can be studied via mathematical models composed of the models examined in this chapter.

Part III
Infectious diseases and pest control

Chapter 5

Double impact of sterilizing pathogens: added value of increased life expectancy on pest control effectiveness

International travel and trade are the major drivers of an unprecedented increase in the rate of non-native species invasions (Mack et al, 2000; Lockwood et al, 2007). While most such invasions turn out to eventually be unsuccessful (Willamson and Fitter, 1996; Simberloff and Gibbons, 2004), those few that succeed impose immense environmental, social and economic damages (Courchamp et al, 2003; Tobin et al, 2009). Need for control of such successful invasive species thus arises, with armies of pest managers equipped with a diversity of weapons, often specific to the focal species (Thacker, 2002; Courchamp et al, 2003).

Generally, control methods aim to enhance species mortality and/or decrease fertility. A substantial intellectual effort has been invested into which of these strategies is more effective. Using an optimal control approach, Stenseth (1981) suggested that fertility reduction should be increasingly preferred the larger is mortality of the uncontrolled population. On the contrary, if mortality of the uncontrolled population is low, the optimal pest control strategy should often aim at increasing mortality as much as possible (Stenseth, 1981). The mating system and the way density dependence operates appear to also play a significant role (Barlow et al, 1997). Reviewing fertility control by chemical or surgical means, Dell'Omo and Palmery (2002) concluded that "an ideal fertility control strategy should induce long-term or permanent sterility without secondary toxic effects such as behavioral alterations, be target-specific, and act on both sexes."

Parallel to this effort, discussions have been under way relating efficacy of the bait delivery and the cost-effectiveness of the operations (Courchamp et al, 2003). Concerns have been raised that areas which are large, difficult to access, or have a low pest density are extremely difficult if not impossible to cover by hunters, traps or poisonous baits. As dissemination of control agents constitutes a major limitation in many control programs, research has focused on biological control. Biological control relies upon self-disseminating natural enemies such as viruses which may have the double advantage of economic viability and high control success. However, use of most pathogens is unethical as they inflict unnecessary suffering before killing the host (Courchamp et al, 2003).

Sterilizing effects are characteristic of a variety of plant pathogens, parasitic castrators of invertebrates, and sexually transmitted diseases (Baudoin, 1975; O'Keefe and Antonovics, 2002; Antonovics, 2009). If no such pathogen is available to a pest species, it could possibly be engineered. Indeed, research effort has recently turned towards virus-vectored immunocontraception (VVIC), a new form of biological control that retains the advantages of self-dissemination of control agents while avoiding the unethical aspects of animal suffering. VVIC is based on a sterilization process that induces the immune system of an individual to attack its own reproductive cells – infecting an individual with a protein derived from the follicular layers activates production of antibodies against its own gametes, thereby blocking fertilization (Tyndale-Biscoe, 1994; Bradley et al, 1997). VVIC agents are viruses that are genetically modified to carry a gene encoding the reproductive protein of a target species (Tyndale-Biscoe, 1994). The use of modified, species-specific viruses thus allows for an efficient dissemination of a control agent through the pest population regardless of its area of distribution, accessibility and density, and combines the advantages of high specificity and optimal dissemination. This potentially powerful technique appears most appropriate for rodents and small herbivores, such as rabbits and possums (Cowan, 1996; McLeod and Twigg, 2006; Rodger, 1997; Smith et al, 1997), yet it could also be very efficient for control of small carnivores such as cats and foxes (Bradley et al, 1997; Courchamp and Cornell, 2000; Pech et al, 1997; Verdier et al, 1999).

Since the publication of seminal review articles by Anderson and May (Anderson and May, 1979, 1981), very many host-parasite models with pathogens inducing reduction of host fertility in general and sterilizing pathogens in particular have been developed. Yet, none of these models has ever accounted for a well-known aspect of life-history theory, namely the cost of reproduction or a trade-off between reproduction and survival – by decreasing the energy outlay on reproduction, individuals with lowered reproduction can live longer. This trade-off predicts that "non-reproducing females have a higher chance of surviving than reproducing females" (Neuhaus and Pelletier, 2001), that there is "a negative relationship between the mean female fecundity and the mean [female] longevity" (Thomas et al, 2000), or that "early reproduction may increase mortality to such an extent that delaying reproduction may increase survival and lifetime reproductive success" (Bennett and Owens, 2002). These trade-offs have indeed been found to occur in birds (Bennett and Owens, 2002), insect parasitoids (Ellers, 1995; Ramesh and Manickavasagam, 2003), mammals (Neuhaus and Pelletier, 2001) and even humans (Thomas et al, 2000).

Sterilizing pathogens thus can have a double impact on their hosts. Not only they depress host reproduction, but by letting the infected individuals live longer, these sterilized animals help spread the pathogen for a longer time which may further increase the control effectiveness. Mathematical models should always form a necessary first step to assess effectiveness of any control technique before it is accepted. Therefore, in this chapter, we develop and analyze a mathematical model to address the question of whether and how much does effectiveness of releasing a sterilizing pathogen into a pest population increase if the cost of reproduction is accounted for.

5.1 Model formulation

We limit ourselves to an SI epidemiological model, assuming that as soon as susceptible individuals (S) get infected, i.e. sterilized, they remain so until they die. This also allows us to assess the full potential of increased longevity due to sterilizing pathogens on pest control effectiveness, since the infection will not be curbed by any latent or immunity period. To keep the model as simple as possible (and to eliminate any confounding factors), we also assume no disease-induced mortality. In fact, sterilizing pathogens may have little or no effect on host mortality (O'Keefe and Antonovics, 2002; Bonds, 2006). Also, we assume no vertical transmission. Although some sexually transmitted infections can also be passed from parents to offspring (Lockhart et al, 1996; Knell and Webberley, 2004), we decided not to consider this additional transmission route here but rather to examine its effect separately. Finally, we assume that the infection does not always lead to sterilization so we distinguish infected individuals that become sterilized due to the disease (I_S) and the remaining infected individuals that are able to spread the virus yet also reproduce (I_F). As the sterilized individuals do not 'waste' resources in reproduction, they are allowed to live longer than the fertile ones.

As a consequence, host dynamics are described by the following model:

$$\frac{dS}{dt} = b(S + I_F) - \Phi(N)\frac{S(I_F + I_S)}{N} - (d + d_1 N)S$$

$$\frac{dI_F}{dt} = (1 - \sigma)\Phi(N)\frac{S(I_F + I_S)}{N} - (d + d_1 N)I_F \qquad (5.1)$$

$$\frac{dI_S}{dt} = \sigma\Phi(N)\frac{S(I_F + I_S)}{N} - (\delta d + d_1 N)I_S$$

We thus assume that both fertile and sterile infectives are able to spread the disease equally. We have σ as the proportion of infected individuals that become sterilized ($0 < \sigma < 1$) and δ as the proportional reduction of the intrinsic mortality rate d in those infected individuals that become sterilized ($0 < \delta < 1$). For the sake of simpler analysis, the host population is assumed here regulated through negative density dependence in the mortality rate, with d_1 being its strength, but one might alternatively consider regulation through the birth rate, or a mixture of the two (Hassell, 1975; Gao and Hethcote, 1992). The function $\Phi(N)$ specifies the way disease is transmitted and covers both the contact rate between individual hosts and the probability of disease transmission upon an adequate contact between infectives and susceptibles. We start with a generic form of $\Phi(N)$, and later on explore the model (5.1) under the standard incidence ($\Phi(N) = \beta$), the mass action incidence ($\Phi(N) = \beta N$), and the asymptotic incidence ($\Phi(N) = \beta N/(c + N)$ for some $c > 0$; e.g. Diekmann and Kretzschmar (1991)) modes of disease transmission.

In the absence of disease, the total host population density N evolves as

$$\frac{dN}{dt} = bN - (d + d_1 N)N \qquad (5.2)$$

Hence, the host population has the intrinsic growth rate $r = b - d$ and attains the environmental carrying capacity $K = (b - d)/d_1$. We assume $b > d$ further on so that the host population is able to persist without the disease. In the presence of disease, we have

$$\frac{dN}{dt} = b(S + I_F) - (d + d_1 N)(S + I_F) - (\delta d + d_1 N)I_S \qquad (5.3)$$

The major question we address in this chapter is how the ability of the disease to suppress the host population changes with δ, the factor that extends the life expectancy of sterilized hosts. This ability, or the control effectiveness, is evaluated here as $E = 1 - N^*/K$ where N^* is the host population density at a stable equilibrium of the model (5.1). It can be $E = 0$ if the disease cannot invade, $0 < E < 1$ if an endemic equilibrium exists, or $E = 1$ if the disease is strong enough to drive the host to extinction.

For $\delta = 1$, i.e. no effect of sterilization on host longevity, the model (5.1) reduces to

$$\begin{aligned}
\frac{dS}{dt} &= b(S + (1 - \sigma)I) - \Phi(N)\frac{SI}{N} - (d + d_1 N)S \\
\frac{dI}{dt} &= \Phi(N)\frac{SI}{N} - (d + d_1 N)I
\end{aligned} \qquad (5.4)$$

See Box 5.1 for the results of an analysis of the model (5.4).

Box 5.1 Case $\delta = 1$: the system (5.4)

For $\delta = 1$, the model (5.1) reduces to the model (5.4). This latter model is a special case of the system analyzed by Zhou and Hethcote (1994, their model (9)). Transforming the model (5.4) to that with state variables $i = I/N$ and $N = S + I$, we get

$$\begin{aligned}
\frac{di}{dt} &= i\left[\Phi(N)(1 - i) - b(1 - \sigma i)\right] \\
\frac{dN}{dt} &= N\left[b(1 - \sigma i) - (d + d_1 N)\right]
\end{aligned} \qquad (5.5)$$

Results of the standard local stability analysis of the system (5.5) are summarized in Table 5.1. Zhou and Hethcote (1994) proved that if the equilibria are locally stable then they are also globally stable.

Equilibrium	Exists	Locally stable	Unstable	E
$(0,0)$	always	–	always $(b > d)$	–
$(K,0)$	always	$R_0 < 1$	$R_0 > 1$	0
$(0,i_0^*)$	AI & MI: feasible only for $\sigma = 1$ for which $i_0^* = 1$	–	exists	–
	SI: $R_0 > 1$, $i_0^* = (\beta - b)/(\beta - \sigma b)$ exists & $i_0^* > 1/(\sigma b/(b-d))$	exists & $i_0^* < 1/(\sigma b/(b-d))$		
(N^*,i^*)	AI & MI: $R_0 > 1$	exists	–	$i^* \sigma b/(b-d)$
	SI: $R_0 > 1$ & $i^* < 1/(\sigma b/(b-d))$	exists	–	$i^* \sigma b/(b-d)$

Table 5.1 Existence and local stability of equilibria of the model (5.4); $R_0 = \Phi(K)/b$, AI = asymptotic incidence, MI = mass action incidence, SI = standard incidence

Alternatively, for $\sigma = 1$, i.e. sterilization of any infected individual, the model (5.1) reduces to

$$\frac{dS}{dt} = bS - \Phi(N)\frac{SI}{N} - (d + d_1 N)S$$
$$\frac{dI}{dt} = \Phi(N)\frac{SI}{N} - (\delta d + d_1 N)I$$
(5.6)

See Box 5.2 for the results of an analysis of the model (5.6).

Box 5.2 Case $\sigma = 1$: the system (5.6)

For $\sigma = 1$, the model (5.1) reduces to the model (5.6). Transforming the model (5.6) to that with state variables $i = I/N$ and $N = S + I$, we get

$$\frac{di}{dt} = i(1-i)\left[\Phi(N) - (b - (1-\delta)d)\right]$$
$$\frac{dN}{dt} = N\left[(b-d)(1-i) - \delta di - d_1 N\right]$$
(5.7)

Results of the standard local stability analysis of the system (5.7) are summarized in Table 5.2. Poincaré-Bendixson theory together with the Dulac criterion (with the multiplying factor $1/[Ni(1-i)]$) can be used to show that also here, if the equilibria are locally stable then they are also globally stable.

Equilibrium	Exists	Locally stable	Unstable	E
$(0,0)$	always	–	always $(b>d)$	–
$(K,0)$	always	$R_0 < 1$	$R_0 > 1$	0
$(0,1)$	always	MI & AI: –	MI & AI: always	–
		SI: $R_0 > 1$	SI: $R_0 < 1$	1
(N^*,i^*)	AI & MI: $R_0 > 1$	AI & MI: exists	AI & MI: –	$0 < E < 1$
	SI: –	SI: –	SI: –	

Table 5.2 Existence and local stability of equilibria of the model (5.6); $R_0 = \Phi(K)/[b-(1-\delta)d]$, AI = asymptotic incidence, MI = mass action incidence, SI = standard incidence

5.2 Model results

Basic reproduction number

As is usual in virtually any study on infectious disease dynamics, we start with calculating the basic reproduction number R_0. Using the next generation matrix approach due to van den Driessche and Watmough (2002), one can show that (see Box 5.3)

$$R_0 = \Phi(K) \left(\frac{1-\sigma}{b} + \frac{\sigma}{b-(1-\delta)d} \right) \qquad (5.8)$$

It is useful to rewrite this term using reciprocals of mortality rates to get its clearer biological interpretation:

$$R_0 = (1-\sigma) \frac{\Phi(K)}{d+d_1 K} + \sigma \frac{\Phi(K)}{\delta d + d_1 K}$$

Here, the first fraction represents the number of secondary infections caused by a reproductive infectious individual introduced into a fully susceptible population, while the second fraction represents the number of secondary infections caused by a sterile infectious individual, with σ the fraction of infectives that become sterilized.

Box 5.3 Basic reproduction number R_0

Using the next generation matrix approach due to van den Driessche and Watmough (2002), we first reshuffle the state variables so that the first two represent infected classes: (I_F, I_S, S). Using the notation of van den Driessche and Watmough (2002), we have

$$\mathscr{F} = \begin{pmatrix} (1-\sigma)\Phi(N)S(I_F+I_S)/N \\ \sigma\Phi(N)S(I_F+I_S)/N \\ 0 \end{pmatrix}$$

comprising all rates of the model (5.1) that describe the appearance of new infections, and

$$\mathscr{V} = \begin{pmatrix} (d+d_1N)I_F \\ (\delta d+d_1N)I_S \\ -b(S+I_F)+\Phi(N)S(I_F+I_S)/N+(d+d_1N)S \end{pmatrix}$$

comprising all remaining rates (with the reverse sign). Setting $x = (I_F, I_S, S)$ and $x_0 = (0, 0, K)$, this implies

$$F = \left[\frac{\partial \mathscr{F}_i}{\partial x_j}(x_0)\right]\bigg|_{1 \le i,j \le 2} = \Phi(K)\begin{pmatrix} 1-\sigma & 1-\sigma \\ \sigma & \sigma \end{pmatrix}$$

and

$$V = \left[\frac{\partial \mathscr{V}_i}{\partial x_j}(x_0)\right]\bigg|_{1 \le i,j \le 2} = \begin{pmatrix} b & 0 \\ 0 & b-(1-\delta)d \end{pmatrix}$$

This implies

$$V^{-1} = \begin{pmatrix} 1/b & 0 \\ 0 & 1/(b-(1-\delta)d) \end{pmatrix}$$

and the next generation matrix thus becomes

$$FV^{-1} = \Phi(K)\begin{pmatrix} (1-\sigma)/b & (1-\sigma)/(b-(1-\delta)d) \\ \sigma/b & \sigma/(b-(1-\delta)d) \end{pmatrix}$$

of which the dominant (in the absolute value) eigenvalue, equal to R_0, is

$$R_0 = \Phi(K)\left(\frac{1-\sigma}{b} + \frac{\sigma}{b-(1-\delta)d}\right) \tag{5.9}$$

The disease thus invades if $R_0 > 1$ or equivalently if

$$\Phi(K) > \frac{b[b-(1-\delta)d]}{b-(1-\sigma)(1-\delta)d} \tag{5.10}$$

R_0 increases with increasing σ (as $\partial R_0/\partial\sigma > 0$ if $b > d$) and, more importantly from our perspective, with decreasing δ (as $\partial R_0/\partial\delta < 0$ for $\sigma > 0$). Indeed, reduction of the intrinsic host mortality rate due to sterilization can revert the outcome of disease invasion – a disease that cannot invade the host population for a high δ might be able to do that for a low δ (Fig. 5.1).
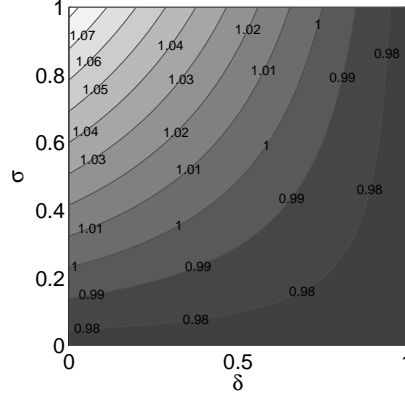
Fig. 5.1 Basic reproduction number R_0 of the model (5.1), as a function of the proportional reduction of the intrinsic mortality rate in those infected individuals that become sterilized (δ) and the proportion of infected individuals that become sterilized (σ). Other parameters values: $\Phi(K) = 1.95$, $b = 2$, $d = 0.2$

System equilibria

We start by going from densities to proportions, thus getting equations for $i_F = I_F/N$ and $i_S = I_S/N$:

$$\frac{di_F}{dt} = (1 - \sigma)\Phi(N)(1 - i_F - i_S)(i_F + i_S) - di_F - i_F[(b - d)(1 - i_S) - \delta d i_S]$$

$$\frac{di_S}{dt} = \sigma\Phi(N)(1 - i_F - i_S)(i_F + i_S) - \delta d i_S - i_S[(b - d)(1 - i_S) - \delta d i_S]$$

(5.11)

As this system contains N, it can be closed with one more equation for the total host population density

$$\frac{dN}{dt} = N[b(1 - i_S) - (d + d_1 N)(1 - i_S) - (\delta d + d_1 N)i_S] \quad (5.12)$$

This system of three differential equations has several equilibrium points (i_F, i_S, N):

- $(0, 0, 0)$ which is an extinction equilibrium
- $(0, 0, K)$ which is the disease-free equilibrium
- $(0, 1, 0)$ which is a disease-induced extinction equilibrium
- $(i_F^*, i_S^*, 0)$ which is another disease-induced extinction equilibrium, feasible only for transmission terms with $\Phi(0) > 0$ (only standard incidence in our case)[1]

---

[1] For $\Phi(0) = 0$ and $0 < \delta < 1$, setting the right-hand sides of both equations of (5.11) to zero leads to two incompatible algebraic equations.

- (i_F^*, i_S^*, N^*) which is an endemic equilibrium; setting the term in square brackets of the right-hand side of (5.12) to zero, we have

$$N^* = \frac{(b-d)(1-i_S^*) - \delta d i_S^*}{d_1} = K - i_S^* \frac{b - (1-\delta)d}{d_1} \qquad (5.13)$$

In the last two cases, i_F^* can be expressed as a function of i_S^* by setting the right-hand sides of both equations of (5.11) to zero, solving both for $\Phi(N)(1 - i_F - i_S)(i_F + i_S)$ and equating the resulting expressions. This gives

$$i_F^* = i_S^* \frac{(1-\sigma)(\delta d + [(b-d)(1-i_S^*) - \delta d i_S^*])}{\sigma(d + [(b-d)(1-i_S^*) - \delta d i_S^*])} = \frac{\delta(1-\sigma)i_S^*(1-i_S^*)}{\sigma[\delta(\alpha - i_S^*) + 1 - \alpha]} \qquad (5.14)$$

where we have denoted

$$\alpha = \frac{1}{1 + \frac{\delta d}{b-d}} \qquad (5.15)$$

Note that $0 < \alpha < 1$ as soon as $b > d$.

We are now going to explore existence, uniqueness and stability of these equilibria for the transmission terms we consider. The underlying calculations are given as proofs of a set of propositions.

Proposition 5.1. *The extinction equilibrium* $(0,0,0)$ *is always unstable.*

Proof. The Jacobian of the system (5.11) and (5.12) evaluated at this equilibrium is

$$J(0,0,0) = \begin{pmatrix} (1-\sigma)\Phi(0) - b & (1-\sigma)\Phi(0) & 0 \\ \sigma\Phi(0) & \sigma\Phi(0) - b + (1-\delta)d & 0 \\ 0 & 0 & b - d \end{pmatrix} \qquad (5.16)$$

As we assume $b > d$, this matrix has at least one eigenvalue with positive real part, hence the extinction equilibrium $(0,0,0)$ is always unstable.

□

Proposition 5.2. *The disease-free equilibrium* $(0,0,K)$ *is locally stable if and only if $R_0 < 1$ and unstable if and only if $R_0 > 1$.*

Proof. The Jacobian of the system (5.11) and (5.12) evaluated at this equilibrium is

$$J(0,0,K) = \begin{pmatrix} (1-\sigma)\Phi(K) - b & (1-\sigma)\Phi(K) & 0 \\ \sigma\Phi(K) & \sigma\Phi(K) - [b - (1-\delta)d] & 0 \\ 0 & -[b - (1-\delta)d]K & -(b-d) \end{pmatrix} \qquad (5.17)$$

As we assume $b > d$, one eigenvalue is always negative and the other two have negative real parts if and only if

$$\Phi(K) < 2b - (1-\delta)d$$

and

$$\Phi(K) < \frac{b[b-(1-\delta)d]}{b-(1-\delta)(1-\sigma)d}$$

Note that the second condition is equivalent to $R_0 < 1$ (5.10) and includes the first one, because

$$2b-(1-\delta)d - \frac{b[b-(1-\delta)d]}{b-(1-\delta)(1-\sigma)d} =$$

$$= \frac{[b-(1-\sigma)(1-\delta)d]^2 + \sigma(1-\sigma)d^2(1-\delta)^2}{b-(1-\delta)(1-\sigma)d} > 0$$

Hence, the disease-free equilibrium $(0,0,K)$ is locally stable if and only if $R_0 < 1$ and unstable if and only if $R_0 > 1$.

$\square$

Proposition 5.3. *The disease-induced extinction equilibrium $(0,1,0)$ is locally stable if and only if $(1-\delta)d - b(1-\sigma) > 0$ and*

$$\Phi(0) > \frac{(1-\delta)d[b-(1-\delta)d]}{(1-\delta)d - b(1-\sigma)}$$

Proof. The Jacobian of the system (5.11) and (5.12) evaluated at this equilibrium is

$$J(0,1,0) = \begin{pmatrix} -\Phi(0)(1-\sigma)-(1-\delta)d & -\Phi(0)(1-\sigma) & 0 \\ -\sigma\Phi(0) & -\sigma\Phi(0)+[b-(1-\delta)d] & 0 \\ 0 & 0 & -\delta d \end{pmatrix} \quad (5.18)$$

One eigenvalue is therefore always negative and the other two have negative real parts if and only if

$$\Phi(0) > b - 2(1-\delta)d$$

$$\Phi(0) > \frac{(1-\delta)d[b-(1-\delta)d]}{(1-\delta)d - b(1-\sigma)}$$

$$(1-\delta)d - b(1-\sigma) > 0$$

Note that the second condition includes the first one since

$$\frac{(1-\delta)d[b-(1-\delta)d]}{(1-\delta)d-b(1-\sigma)} - [b-2(1-\delta)d] = \frac{d[\delta^2(1-\sigma)+\sigma(1-\delta)^2(1-\alpha)^2]}{(1-\alpha)[\sigma(1-\alpha+\delta\alpha)-\delta]}$$

where we used the term (5.15) for α. The numerator is clearly positive. The denominator is also positive since

$$\sigma(1-\alpha+\delta\alpha) - \delta > 0$$

follows from

$$(1-\delta)d - b(1-\sigma) > 0$$

So, the necessary and sufficient condition for local stability of $(0,1,0)$ is

$$(1-\delta)d - b(1-\sigma) > 0$$

and

$$\Phi(0) > \frac{(1-\delta)d[b-(1-\delta)d]}{(1-\delta)d - b(1-\sigma)}$$

However, this is only possible if $\Phi(0) > 0$. So $(0,1,0)$, while it always exists, can be locally stable only under standard incidence (out of the incidence terms we consider).

$\square$

Corollary 5.1. *For both mass action and asymptotic incidences the disease-induced extinction equilibrium $(0,1,0)$ is always unstable, because $\Phi(0) = 0$.*

Under standard incidence, the system of two equations (5.11) is closed, i.e. not containing N. We are now going to explore the existence and uniqueness of its interior equilibrium (i_F^*, i_S^*).

Proposition 5.4. *Under standard incidence, the system (5.11) has a unique, biologically feasible endemic equilibrium, (i_F^*, i_S^*), if and only if one of the following two conditions is satisfied:*

$$(1-\delta)d - (1-\sigma)b > 0 \quad and \quad \frac{b[b-(1-\delta)d]}{b-(1-\delta)(1-\sigma)d} < \beta < \frac{(1-\delta)d[b-(1-\delta)d]}{(1-\delta)d - (1-\sigma)b}$$

or

$$(1-\delta)d - (1-\sigma)b < 0 \quad and \quad \frac{b[b-(1-\delta)d]}{b-(1-\delta)(1-\sigma)d} < \beta$$

Proof. Substituting i_F^* (5.14) into the second equation of (5.11) and using $\Phi(N) = \beta$ we obtain the following equation for i_S^*

$$\frac{1}{\sigma(1-\alpha)[\delta(\alpha - i_S^*)+1-\alpha]^2} i_S^*(i_S^* - 1)[a_2(i_S^*)^2 + a_1 i_S^* + a_0] = 0$$

with

$$a_2 = (\delta d\sigma + \beta(-1+\alpha))\delta^2$$

$$a_1 = 2\sigma\delta(1-\alpha+\delta\alpha)[\beta(1-\alpha)-\delta d] + \beta\delta^2(1-\alpha)(1-\sigma)$$

$$a_0 = \sigma(1-\alpha+\delta\alpha)^2(\delta d - \beta\sigma + \beta\sigma\alpha) - \beta\delta\sigma(1-\sigma)(1-\alpha)(1-\alpha+\delta\alpha)$$

We are interested in solving the quadratic equation

$$A(i_S^*) = a_2(i_S^*)^2 + a_1 i_S^* + a_0 = 0$$

since the roots 0 and 1 correspond to the extinction and disease-free equilibria and the disease-induced extinction equilibrium, respectively. The two roots of this quadratic equation are of the form

$$m \pm n\sqrt{D}$$

with

$$D = 4\,\delta\,\beta\,(1-\alpha)^2\,(1-\sigma)^2\left(d\,(1-\delta)\,(1-\alpha+\alpha\,\delta)\,\sigma + \frac{1}{4}\,\beta\,\delta\right)$$

The existence of real roots of the quadratic equation is equivalent to $D > 0$, that is,

$$d\sigma\,(1-\delta)\,[1-\alpha(1-\delta)] + \frac{1}{4}\,\beta\,\delta > 0$$

which is always true since $0 < \alpha < 1$ and $0 < \delta < 1$.

We first prove the uniqueness of (i_F^*, i_S^*) in the interval $(0,1)$. Let us assume that both the roots $m \pm n\sqrt{D}$ lie in the interval $(0,1)$. This assumption leads to two cases:

(a) $0 < m < \frac{1}{2}$ and $n^2 D < m^2$
(b) $\frac{1}{2} < m < 1$ and $n^2 D < (1-m)^2$

The following quantities will characterize these inequalities:

$$m = \frac{-\beta(1-\alpha)\left[\frac{\delta}{2} + \sigma\left((1-\alpha)(1-\delta) + \frac{\delta}{2}\right)\right] + \sigma\delta d(1-\alpha+\alpha\delta)}{\delta[\sigma\delta d - (1-\alpha)\beta]} \tag{5.19}$$

$$\frac{1}{2} - m = -\frac{\sigma[\delta d - (1-\alpha)\beta]\left[(1-\alpha)(1-\delta) + \frac{\delta}{2}\right]}{\delta[\sigma\delta d - (1-\alpha)\beta]} \tag{5.20}$$

$$1 - m = \frac{(1-\alpha)\left[\beta\left(\sigma\left((1-\alpha)(1-\delta) + \frac{\delta}{2}\right) - \frac{\delta}{2}\right) - \sigma\delta d(1-\delta)\right]}{\delta[\sigma\delta d - (1-\alpha)\beta]} \tag{5.21}$$

$$m^2 - n^2 D = \frac{\sigma(1-\alpha+\delta\alpha)\left[-\beta(1-\alpha)\left((1-\delta)(1-\alpha)\sigma + \delta\right) + \delta d(1-\alpha+\delta\alpha)\right]}{\delta^2[\sigma\delta d - (1-\alpha)\beta]} \tag{5.22}$$

$$(1-m)^2 - n^2 D = -\frac{\sigma(1-\delta)(1-\alpha)^2\left[\beta(\sigma(1-\alpha+\delta\alpha) - \delta) - \delta d(1-\delta)\right]}{\delta^2[\sigma\delta d - (1-\alpha)\beta]} \tag{5.23}$$

First suppose $\sigma\delta d - (1-\alpha)\beta > 0$. This is equivalent to

$$\beta < \frac{\sigma\delta d}{1-\alpha}$$

and also implies that $\delta d - (1-\alpha)\beta > 0$ and hence $\frac{1}{2} - m < 0$. So the case (a) is not possible. To satisfy the case (b) we need $1 - m > 0$, which is equivalent to

$$\sigma\left[(1-\alpha)(1-\delta)+\frac{\delta}{2}\right]-\frac{\delta}{2}>0$$

and

$$\beta>\frac{\sigma\delta d(1-\delta)}{\sigma\left[(1-\alpha)(1-\delta)+\frac{\delta}{2}\right]-\frac{\delta}{2}}$$

Thus we have a lower and upper bound of β that need to satisfy

$$\frac{\sigma\delta d(1-\delta)}{\sigma\left[(1-\alpha)(1-\delta)+\frac{\delta}{2}\right]-\frac{\delta}{2}}<\frac{\sigma\delta d}{1-\alpha}$$

However, this is equivalent (after simplification) to $\sigma>1$ so the case (b) is also not possible.

Similarly, we assume now

$$\sigma\delta d-(1-\alpha)\beta<0,\quad\text{i.e.}\quad\beta>\frac{\sigma\delta d}{1-\alpha}$$

Now $\frac{1}{2}-m>0$ is equivalent to

$$\delta d-(1-\alpha)\beta>0,\quad\text{i.e.}\quad\beta<\frac{\delta d}{1-\alpha}$$

and $m^2-n^2D>0$ is equivalent to

$$\beta>\frac{\delta d(1-\alpha+\delta\alpha)}{(1-\alpha)[(1-\delta)(1-\alpha)\sigma+\delta]}$$

This again leads to the case (a) being not possible since

$$\frac{\delta d(1-\alpha+\delta\alpha)}{(1-\alpha)[(1-\delta)(1-\alpha)\sigma+\delta]}<\frac{\delta d}{1-\alpha}$$

is equivalent to $\sigma>1$.

For the case (b) to hold, we need $1-m>0$ and $(1-m)^2-n^2D>0$. These two inequalities are equivalent to

$$\beta\left[\sigma\left((1-\alpha)(1-\delta)+\frac{\delta}{2}\right)-\frac{\delta}{2}\right]<\sigma\delta d(1-\delta)$$

$$\beta\left[\sigma(1-\alpha+\delta\alpha)-\delta\right]>\delta d(1-\delta)$$

Notice that

$$\left[\sigma\left((1-\alpha)(1-\delta)+\frac{\delta}{2}\right)-\frac{\delta}{2}\right]>\sigma(1-\alpha+\delta\alpha)-\delta$$

since it is equivalent to $\sigma < 1$ and

$$\sigma(1 - \alpha + \delta\alpha) - \delta > 0$$

from the second inequality above. Thus we have again the following bounds for β

$$\frac{\delta d(1 - \delta)}{\sigma(1 - \alpha + \delta\alpha) - \delta} < \beta < \frac{\sigma\delta d(1 - \delta)}{\sigma\left((1 - \alpha)(1 - \delta) + \frac{\delta}{2}\right) - \frac{\delta}{2}}$$

But this is impossible since it implies

$$\sigma(1 - \alpha + \alpha\delta) - \frac{\delta}{2} < 0$$

which contradicts

$$\sigma(1 - \alpha + \alpha\delta) - \delta > 0$$

So the case (b) is also impossible.

Altogether, if an i_S^* exists, it is unique. We are now going to derive conditions for its existence. The existence of a unique biologically feasible real root is equivalent to (also taking into account $0 < i_S^* < 1$)

$$A(0)A(1) < 0 \quad \Leftrightarrow \quad a_0(a_2 + a_1 + a_0) < 0$$

This is equivalent to

$$-\sigma^2(1 - \delta)(1 - \alpha)^2(1 - \alpha + \delta\alpha)B(\beta) < 0$$

or

$$B(\beta) > 0$$

with

$$B(x) = b_2 x^2 + b_1 x + b_0$$

and

$$b_2 = -(1 - \alpha)\left[(1 - \alpha + \delta\alpha)\sigma - \delta\right]\left[(1 - \alpha)(1 - \delta)\sigma + \delta\right]$$

$$b_1 = \left(2\left(\left(1/2 - \alpha + \alpha^2\right)\delta^2 + \left(3\alpha - 1 - 2\alpha^2\right)\delta + (\alpha - 1)^2\right)\sigma - \delta^2\right)d\delta$$

$$b_0 = -\delta^2 d^2(1 - \delta)(1 - \alpha + \delta\alpha) < 0$$

The quadratic equation $B(x) = 0$ has two real roots as follows:

$$x_1 = \frac{\delta d(1 - \alpha + \alpha\delta)}{(1 - \alpha)[\delta + \sigma(1 - \alpha)(1 - \delta)]} > 0$$

and

$$x_2 = \frac{\delta d(1 - \delta)}{\sigma(1 - \alpha + \delta\alpha) - \delta}$$

Note that the signs of x_2 and b_2 are opposite to each other and they are given by $\sigma(1 - \alpha + \delta\alpha) - \delta$. We have the following two sets of conditions for $B(\beta) > 0$

$$\sigma(1 - \alpha + \delta\alpha) - \delta > 0 \quad \text{and} \quad \min\{x_1, x_2\} < \beta < \max\{x_1, x_2\} \qquad (5.24)$$

or

$$\sigma(1 - \alpha + \delta\alpha) - \delta < 0 \quad \text{and} \quad x_1 < \beta \qquad (5.25)$$

Note that in the case of (5.24) both x_1 and x_2 are positive so we need to establish the min and the max of the two. We will show that $x_1 < x_2$ under the assumption in (5.24):

$$x_1 - x_2 = -\frac{2d\delta^2(1-\sigma)\left((\alpha - 1/2)\delta - \alpha + 1\right)}{[(1 - \alpha + \alpha\delta)\sigma - \delta](1 - \alpha)[(1 - \delta)(1 - \alpha)\sigma + \delta]}$$

The sign of this expression depends on the term

$$T = (\alpha - 1/2)\delta - \alpha + 1$$

which, written in terms of the original parameters, is

$$T = \frac{\delta[b + d(1 - \delta)]}{2(b - (1 - \delta)d)} > 0$$

Therefore, $x_1 - x_2 < 0$ and the above conditions now read:

$$(1 - \delta)d - (1 - \sigma)b > 0 \quad \text{and} \quad \frac{b[b - (1 - \delta)d]}{b - (1 - \delta)(1 - \sigma)d} < \beta < \frac{(1 - \delta)d[b - (1 - \delta)d]}{(1 - \delta)d - (1 - \sigma)b}$$
$$(5.26)$$

or

$$(1 - \delta)d - (1 - \sigma)b < 0 \quad \text{and} \quad \frac{b[b - (1 - \delta)d]}{b - (1 - \delta)(1 - \sigma)d} < \beta \qquad (5.27)$$
$$\square$$

   Note that negating the condition for local stability of the disease-induced extinction equilibrium $(0, 1, 0)$ is in agreement with the conditions (5.26) and (5.27). Note also that the lower bound for β in both (5.26) and (5.27) is in fact the condition $R_0 > 1$; see (5.10).

   Concerning the stability of (i_F^*, i_S^*), we obtained the following result:

Proposition 5.5. *The solutions of the system* (5.11) *under standard incidence are globally stable whenever they exist.*

Proof. First denote

$$F(i_F, i_S) = di_F/dt = (1 - \sigma)\beta(1 - i_F - i_S)(i_F + i_S) - di_F - i_F[(b - d)(1 - i_S) - \delta di_S]$$

$$G(i_F, i_S) = di_S/dt = \sigma\beta(1 - i_F - i_S)(i_F + i_S) - \delta di_S - i_S[(b - d)(1 - i_S) - \delta di_S]$$

We use the Poincaré-Bendixson trichotomy that says the following for a planar system: Any trajectory that remains in a closed and bounded region of the plane with

finitely many fixed points has the limit set either (1) an equilibrium, (2) a periodic orbit, (3) a finite set of equilibria and trajectories that emerge in and converge to this finite set of equilibria.

Note that, since we have already proved the uniqueness of (i_F^*, i_S^*) in the rectangle $[0,1] \times [0,1]$, the option (3) is ruled out from the start. What remains is to show that for any initial condition in this rectangle the solution stays inside the rectangle and also to rule out periodic solutions. The original system in S, I_F and I_S is positively invariant. This ensures that the rectangle $[0,1] \times [0,1]$ is invariant for the system of proportions of infectives i_F and i_S. To rule out periodic solutions, consider the following Dulac function

$$\varphi(i_F, i_S) = \frac{1}{i_F + i_S}$$

Then

$$\frac{\partial}{\partial i_F} \left[\varphi(i_F, i_S) F(i_F, i_S) \right] + \frac{\partial}{\partial i_S} \left[\varphi(i_F, i_S) G(i_F, i_S) \right] = -\frac{1}{i_F + i_S} \left\{ \beta i_F + \right.$$

$$\left. + i_S [\beta - (b - (1-\delta)d)] + (b - (1-\delta)d)(1 - i_S) + d(1-\delta) \frac{i_S}{i_F + i_S} \right\} < 0$$

This follows from the existence condition on the interior equilibrium (i_F^*, i_S^*), i.e.

$$\beta > \frac{b[b - (1-\delta)d]}{b - (1-\delta)(1-\sigma)d} > b - (1-\delta)d.$$

Thus periodic solutions are ruled out and the unique interior equilibrium (i_F^*, i_S^*) is globally stable whenever it exists.

$\square$

Proposition 5.6. *Define*

$$B_1 = \frac{b[b - (1-\delta)d]}{b - (1-\delta)(1-\sigma)d}$$

$$B_2 = \frac{\sigma d[b - (1-\delta)d]}{[d - b(1-\sigma)][\delta + (1-\delta)\sigma]}$$

$$B_3 = \frac{(1-\delta)d[b - (1-\delta)d]}{(1-\delta)d - (1-\sigma)b}$$

Then under standard incidence, we have that:

Case 1: $(1-\delta)d - b(1-\sigma) > 0$ *implies* $B_1 < B_2 < B_3$ *and*

- *if* $B_1 < \beta < B_2$ *then* (i_F^*, i_S^*, N^*) *is globally stable*
- *if* $B_2 < \beta < B_3$ *then* $(i_F^*, i_S^*, 0)$ *is globally stable*

Case 2: $(1-\delta)d - b(1-\sigma) < 0$ *implies* $B_1 < B_2$ *and*

- *if* $b(1-\sigma) - d < 0$ *and* $B_1 < \beta < B_2$, *or if* $b(1-\sigma) - d > 0$ *and* $\beta > B_2$ *then* (N^*, i_F^*, i_S^*) *is globally stable*

- *if $b(1-\sigma) - d < 0$ and $\beta > B_2$ then $(0, i_F^*, i_S^*)$ is globally stable*

Proof. From the equation for N (5.12) we know that

- $(i_F^*, i_S^*, 0)$ is globally stable if and only if $i_S^* > \alpha$ if and only if $A(\alpha)A(1) < 0$
- (i_F^*, i_S^*, N^*) is globally stable if and only if $i_S^* < \alpha$ if and only if $A(0)A(\alpha) < 0$

where

$$A(i_S) = a_2(i_S)^2 + a_1 i_S + a_0$$

It is

$$A(\alpha)A(1) = -\frac{d^4 \delta^6 \sigma(1-\delta)T_1 T_2}{[b - (1-\delta)d]^6}$$

where

$$T_1 = [b(1-\sigma) - d][\delta + (1-\delta)\sigma]\beta + \sigma d(b - [1-\delta)d]$$

$$T_2 = [(1-\delta)d - b(1-\sigma)]\beta - d(1-\delta)[b - (1-\delta)d]$$

Taking into account the existence and uniqueness conditions (5.26) and (5.27) for a steady state i_S^* in the interval $(0, 1)$, we conclude that

$$T_2 < 0$$

So $A(\alpha)A(1) < 0$ if and only if $T_1 < 0$. This is equivalent to

$$b(1-\sigma) < d \quad \text{and} \quad \beta > \frac{\sigma d[b - (1-\delta)d]}{[d - b(1-\sigma)][\delta + (1-\delta)\sigma]}$$

This threshold for β is greater than the lower bound for β in the conditions (5.26) and (5.27):

$$\frac{\sigma d[b - (1-\delta)d]}{[d - b(1-\sigma)][\delta + (1-\delta)\sigma]} - \frac{b[b - (1-\delta)d]}{b - (1-\delta)(1-\sigma)d} =$$

$$= \frac{[b - (1-\delta)d](1-\sigma)(b-d)[(1-\delta)(b+d)\sigma + \delta b]}{[\delta + (1-\delta)\sigma][d - b(1-\sigma)][b - d(1-\delta)(1-\sigma)]} > 0$$

Furthermore, if the condition (5.26) is satisfied then this threshold is lower than the upper bound on β (5.26), because

$$\frac{(1-\delta)d[b - (1-\delta)d]}{(1-\delta)d - (1-\sigma)b} - \frac{\sigma d[b - (1-\delta)d]}{[d - b(1-\sigma)][\delta + (1-\delta)\sigma]} =$$

$$= \frac{\delta d(1-\sigma)[b - (1-\delta)d][(1-\delta)[d - b(1-\sigma)] + b\sigma]}{[d(1-\delta) - b(1-\sigma)][d - b(1-\sigma)][\delta + \sigma(1-\delta)]} > 0$$

□

Altogether, in terms of β, we have the following results for standard incidence:
Case 1: $(1-\delta)d - b(1-\sigma) > 0$ implies $B_1 < B_2 < B_3$ and

- if $\beta < B_1$ then $(0, 0, K)$ is locally stable

- if $B_1 < \beta < B_2$ then (i_F^*, i_S^*, N^*) is globally stable
- if $B_2 < \beta < B_3$ then $(i_F^*, i_S^*, 0)$ is globally stable
- if $\beta > B_3$ then $(0, 1, 0)$ is locally stable

Case 2: $(1-\delta)d - b(1-\sigma) < 0$ implies $B_1 < B_2$ and

- if $\beta < B_1$ then $(0, 0, K)$ is locally stable
- if $b(1-\sigma) - d < 0$ and $B_1 < \beta < B_2$ or if $b(1-\sigma) - d > 0$ and $\beta > B_2$ then (N^*, i_F^*, i_S^*) is globally stable
- if $b(1-\sigma) - d < 0$ and $\beta > B_2$ then $(0, i_F^*, i_S^*)$ is globally stable

Proposition 5.7. *Under both mass action incidence and asymptotic incidence, the endemic equilibrium (i_F^*, i_S^*, N^*) exists and is unique if and only if $R_0 > 1$.*

Proof. We carry out the phase plane analysis to prove existence and uniqueness of the endemic equilibrium (i_F^*, i_S^*, N^*). With (5.14), we have

$$i_F^* + i_S^* = i_S^* \left(1 + \frac{\delta(1-\sigma)(1-i_S^*)}{\sigma[\delta(\alpha - i_S^*) + 1 - \alpha]} \right) = i_S^* c(i_S^*)$$

where we defined

$$c(i_S^*) = \frac{\delta(1-\sigma)(1-i_S^*)}{\sigma[\delta(\alpha - i_S^*) + 1 - \alpha]}$$

Inserting this form into the second equation of (5.11) and simplifying, $i_S^* > 0$ and $N^* > 0$ will be solutions of the system

$$\sigma\Phi(N)[1 - i_S c(i_S)]c(i_S) - [b - (1-\delta)d](1-i_S) = 0$$
$$(b-d) - [b - (1-\delta)d]i_S - d_1 N = 0 \tag{5.28}$$

where the second equation follows from (5.12). This second equation implies (recall $K = (b-d)/d_1$)

$$N = K - i_S \frac{b - (1-\delta)d}{d_1} \tag{5.29}$$

so that the N-isocline is a linearly decreasing function of i_S, starting at K for $i_S = 0$ and terminating at $-\delta d/d_1$ for $i_S = 1$. The first equation of (5.28) implies

$$\Phi(N) = \frac{[b - (1-\delta)d](1-i_S)}{\sigma[1 - i_S c(i_S)]c(i_S)} > 0 \tag{5.30}$$

since $c(i_S) > 0$. This can be seen by noting that $\delta(\alpha - i_S) + 1 - \alpha > 0$ if and only if

$$i_S < \frac{1 - \alpha + \alpha\delta}{\delta} = \frac{b}{b - (1-\delta)d} \tag{5.31}$$

if we insert the formula (5.15) for α. As $b/[b - (1-\delta)d] > 1$ the inequality (5.31) is satisfied for any $i_S \in [0, 1]$.

Let us now explore the right-hand side of (5.30) as a function of i_S, say $f(i_S)$,

$$f(i_S) = \frac{[b-(1-\delta)d](1-i_S)}{\sigma[1-i_S c(i_S)]c(i_S)}$$

It is $f(1) = [b-(1-\delta)d]/\sigma$ and $f(0) = [b-(1-\delta)d]/[\sigma c(0)]$. In addition,

$$c(0) = 1 + \frac{\delta(1-\sigma)}{\sigma(\delta\alpha+1-\alpha)} = 1 + \frac{\delta(1-\sigma)[b-(1-\delta)d]}{\sigma\delta b} > 1$$

where we used the formula (5.15) for α. Hence, $f(0) < f(1)$. Differentiating the function $f(i_S)$ with respect to i_S, we get

$$f'(i_S) = \frac{[b-(1-\delta)d]\delta(1-\alpha+\alpha\delta-\delta i_S)(1-\sigma)\sigma}{[\sigma(1-\alpha+\alpha\delta)-\delta i_S]^2[\sigma(1-\alpha)-\delta(1-i_S-\sigma(1-\alpha))]^2} \times$$

$$\times\{\delta[(1-2i_S)(1-\alpha+\alpha\delta)+\delta i_S]+2(1-\alpha)(1-\delta)\sigma(1-\alpha+\alpha\delta)\}$$

Everything off the curled brackets of $f'(i_S)$ is positive, so that we are going to explore the sign of the expression in the curled brackets, which can be rewritten as

$$(1-\alpha+\alpha\delta)[\delta+2(1-\alpha)(1-\delta)\sigma]-i_S\delta[2(1-\alpha+\alpha\delta)-\delta] \qquad (5.32)$$

Setting this expression to zero and solving it for i_S, we have

$$i_S^\circ = \frac{(1-\alpha+\alpha\delta)[\delta+2(1-\alpha)(1-\delta)\sigma]}{\delta[2(1-\alpha+\alpha\delta)-\delta]}$$

Substituting the formula (5.15) for α, we eventually have

$$i_S^\circ = \frac{b+(1-\delta)d\left(\frac{2b\sigma}{b-(1-\delta)d}\right)}{b+(1-\delta)d}$$

Obviously, $i_S^\circ > 0$. In addition, the expression (5.32) is positive for $i_S < i_S^\circ$ and negative for $i_S > i_S^\circ$. Hence, the function $f(i_S)$ is growing for $i_S < i_S^\circ$ and declining for $i_S > i_S^\circ$, and reaches a maximum at $i_S = i_S^\circ$. We note that it might be $i_S^\circ > 1$ for high enough σ, and $f(i_S)$ will then be growing for all $i_S \in [0,1]$.

Now, because N is declining in i_S (5.29) and both $\Phi(N) = \beta N$ (mass action incidence) and $\Phi(N) = \beta N/(c+N)$ (asymptotic incidence) are growing in N, the composite function $\Phi(N(i_S))$ will be declining in i_S. This implies that the necessary and sufficient condition for the existence of an endemic equilibrium is

$$\Phi(K) > f(0)$$

or equivalently, after insertion for $f(0)$ and trivial algebraic manipulations,

$$\Phi(K) > \frac{b[b-(1-\delta)d]}{b-(1-\sigma)(1-\delta)d}$$

This last expression is equivalent to $R_0 > 1$, see (5.10). Finally, because of the shape and endpoints of the involved isoclines, the endemic equilibrium is unique provided it exists.

$\square$

We were not able to rigorously prove local stability (or not) of the endemic equilibrium (i_F^*, i_S^*, N^*) under both mass action incidence and asymptotic incidence. Therefore, we resorted to large-scale numerical simulations. These consisted of randomly generating values of model parameters such that $R_0 > 1$, seeking for endemic equilibria corresponding to these parameter values, evaluating the Jacobian of the model (5.1) at these equilibria, and seeking for eigenvalues of the Jacobian. For both mass action incidence and asymptotic incidence, we made 10^6 such parameter values generations and eigenvalue evaluations, and all of these produced only eigenvalues with negative real parts. So, we make the following conjecture:

Conjecture 5.1. Under both mass action incidence and asymptotic incidence, the endemic equilibrium (i_F^*, i_S^*, N^*) is locally stable if and only if $R_0 > 1$, i.e. whenever it exists.
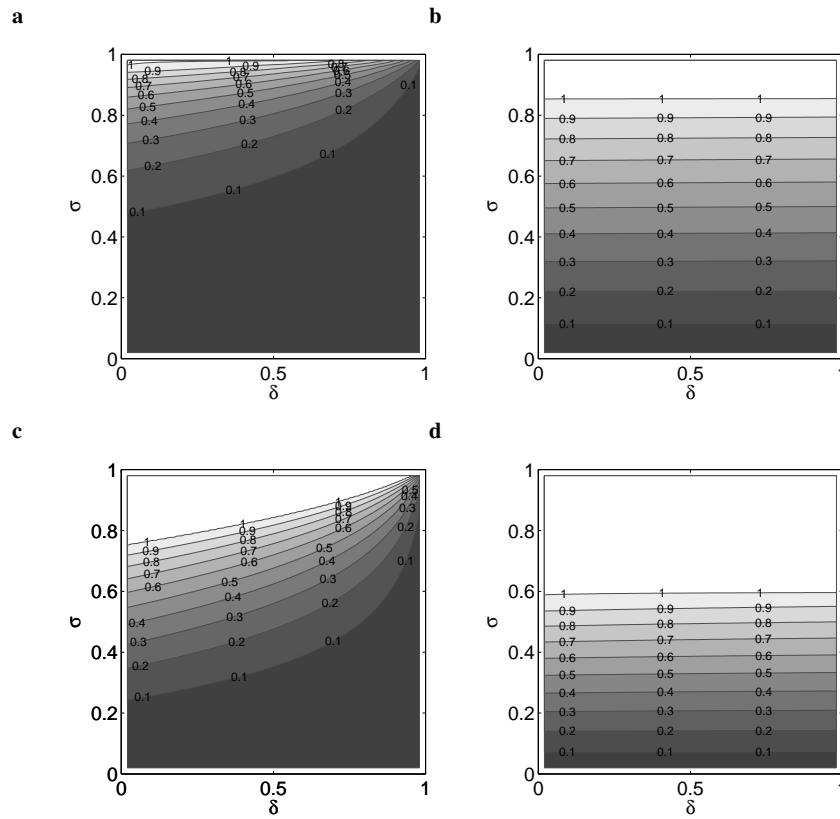
Control effectiveness

In this section, we run the model (5.1) for a variety of parameter sets and evaluate the effectiveness E with which the host population is controlled. Based on these simulations, we aim at identifying the parameter range (i.e. pathogen properties) in which a significant effect of increased lifespan of the sterilized individuals on the pest control effectiveness is observed. Once $R_0 > 1$, the results we present below do not change qualitatively with the strength of negative density dependence d_1.

Standard incidence

For any fixed value of δ, the control effectiveness E increases with increasing σ (Fig. 5.2). For relatively low β, the increase is rather unnoticed for low σ up to a point from which the control effectiveness rapidly increases to 1 (Fig. 5.2a and c). For relatively high β, however, the increase is virtually linear in σ until the maximum value $E = 1$ of the control effectiveness is reached (Fig. 5.2b and d).

Most importantly from our perspective, for any fixed value of σ, the control effectiveness E increases with decreasing δ. However, as Fig. 5.2 suggests, the factor δ that extends life expectancy of the sterilized hosts has a measurable effect only for β close to b, high enough d, and relatively high σ. Indeed, this is confirmed in Figs. 5.3 and 5.4. In such cases, the increase in the control effectiveness can be very dramatic, from virtually 0 to something in between 0.5 and 1 (Fig. 5.2c). Still, an increase in β relative to b appears to have the most substantial effect (Figs. 5.2d and 5.4).
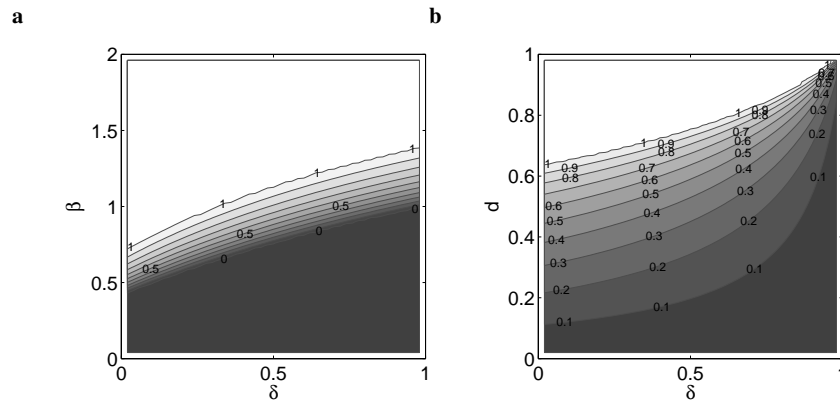
Fig. 5.2 Control effectiveness with standard incidence, as a function of the proportion of infected individuals that become sterilized (σ) and the proportional reduction of the intrinsic mortality rate in those infected individuals that become sterilized (δ). Other parameter values: (a) $\beta = 1$, $b = 1$, $d = 0.2$; (b) $\beta = 3$, $b = 1$, $d = 0.2$. (c) $\beta = 1$, $b = 1$, $d = 0.5$; (d) $\beta = 3$, $b = 1$, $d = 0.5$; all panels: $d_1 = 0.1$

Finally, we explore how the control effectiveness E depends on δ for $\beta = b$. The higher is d with respect to b and the higher is σ, the more rapidly E increases as δ decreases (Fig. 5.5). For example, for $d/b = 0.6$ and $\sigma = 0.8$, the 5% control effectiveness observed for $\delta = 1$ (no increase in longevity due to disease) increases up to about 50% control effectiveness for $\delta = 0.9$ (corresponding to the 10% increase in longevity of sterilized individuals).

Mass action incidence

While the trends identified for standard incidence are maintained also here, the control effectiveness E attains much lower values (Figs. 5.6 and 5.7). Note that we scale

a   **b**

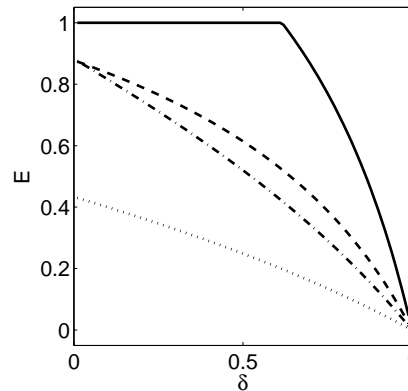**Fig. 5.3** Control effectiveness with standard incidence, as a function of: (a) the disease transmission efficiency β and the proportional reduction of the intrinsic mortality rate in those infected individuals that become sterilized (δ); (b) the intrinsic mortality rate d and the proportional reduction of the intrinsic mortality rate in those infected individuals that become sterilized (δ). Other parameter values: (a) $b = 1$, $d = 0.7$, $\sigma = 0.6$; (b) $b = 1$, $\beta = 1$, $\sigma = 0.6$; all panels: $d_1 = 0.1$
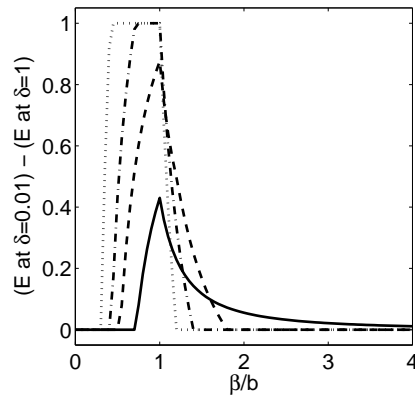
Fig. 5.4 Control effectiveness with standard incidence, as a function of the β/b ratio. Plotted is the difference between control effectiveness at $\delta = 0.01$ and $\delta = 1$, hence the added value of increased life expectancy in the most optimistic case. Line coding: $d = 0.4b$ (solid), $d = 0.6b$ (dashed), $d = 0.7b$ (dash-dot), $d = 0.8b$ (dotted); $\sigma = 0.6$, $b = 1$, $d_1 = 0.1$. The figure is identical for other values of b

here the transmission efficiency β by the environmental carrying capacity of the host K, so as to keep the same basic reproduction numbers R_0 for all adopted disease transmission models.

Fig. 5.5 Control effectiveness with standard incidence, as a function of the proportional reduction of the intrinsic mortality rate in those infected individuals that become sterilized (δ). Line coding: $\sigma = 0.8$, $d = 0.6b$ (solid), $\sigma = 0.8$, $d = 0.4b$ (dashed), $\sigma = 0.6$, $d = 0.6b$ (dash-dot), $\sigma = 0.6$, $d = 0.4b$ (dotted); common parameter values: $b = \beta = 1$, $d_1 = 0.1$

Asymptotic incidence

While the trends identified for the previous two incidence terms are maintained also here, the control effectiveness E attains lower values than standard incidence but higher values than mass action incidence (Figs. 5.8 and 5.9). Note that we scale here the transmission efficiency β by the term $K/(K+c)$, so as to keep the same basic reproduction numbers R_0 for all adopted disease transmission models.

5.3 Discussion

In this chapter, we explored consequences for infection spread and host population suppression of the assumption that sterilizing pathogens preventing reproduction in some infected individuals cause a redistribution of resources and hence increased longevity of sterilized population members. This in turn allows for a more efficient infection spread, as just some of the infectious individuals are those that live longer, and hence for a greater population suppression at endemic equilibrium compared with when no longevity promotion is assumed.

It is not surprising that higher efficiencies of sterilization (larger σ) and higher stretches of longevity (lower δ) promote higher effectiveness of host control by sterilizing pathogens. Much less obvious is under what circumstances these effects are 'measurable' and, in particular, of practical importance for population management. We show that the effect of increased longevity of sterilized individuals increases with (1) decreasing difference between the per capita birth rate (b) and the transmis-
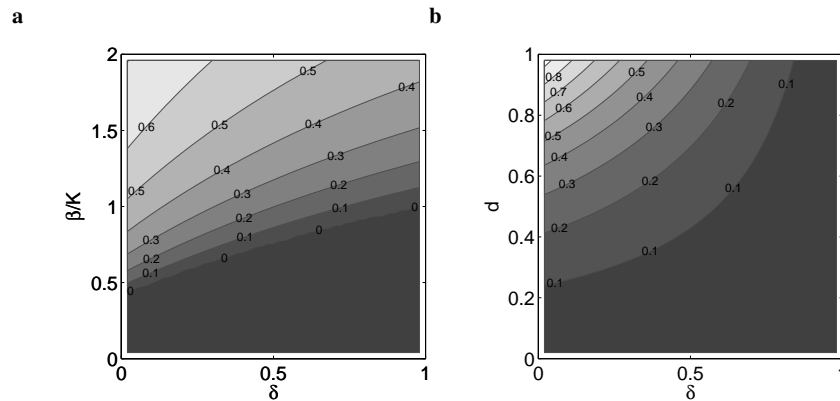
a

b

c

d
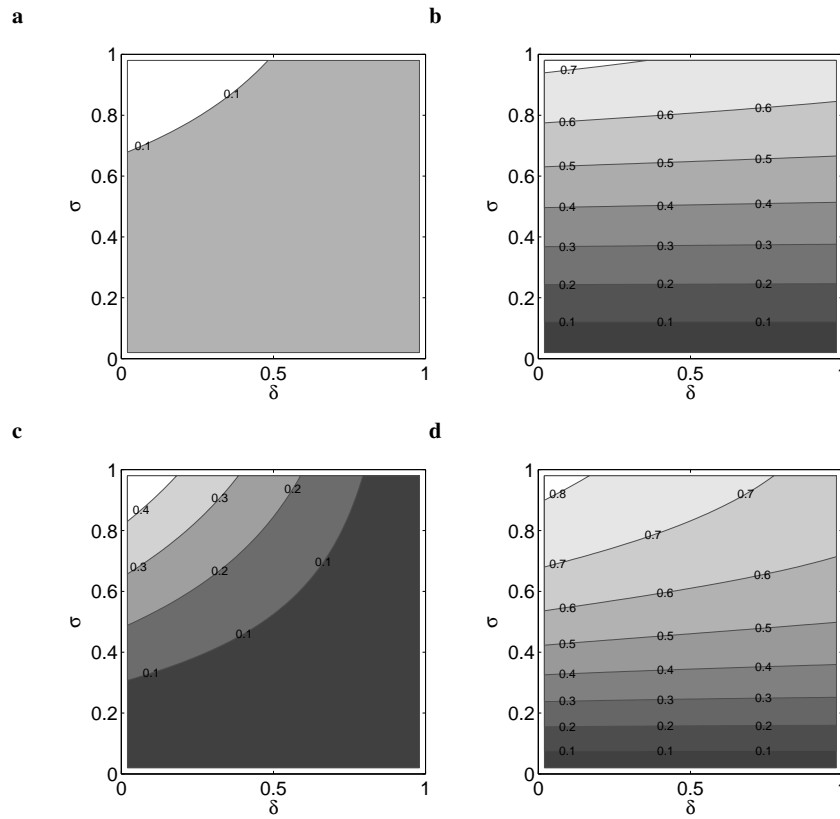
Fig. 5.6 Control effectiveness with mass action incidence, as a function of the proportion of infected individuals that become sterilized (σ) and the proportional reduction of the intrinsic mortality rate in those infected individuals that become sterilized (δ). Other parameter values: (a) $\beta = 1/K, b = 1, d = 0.2$; (b) $\beta = 3/K, b = 1, d = 0.2$. (c) $\beta = 1/K, b = 1, d = 0.5$; (d) $\beta = 3/K$, $b = 1, d = 0.5$; all panels: $d_1 = 0.1, K = (b-d)/d_1$

sion rate between individuals at the carrying capacity ($\phi(K)$), (2) decreasing birth-to-intrinsic-death-rate ratio (i.e. $b/d \rightarrow 1$, recall we assume $b > d$), and (3) increasing sterilization efficiency of the pathogen (σ). This result makes perfect sense since it corresponds to the situation where the natural life expectancy is relatively short and the disease transmission is relatively slow. In this situation, the enhanced life expectancy of the sterilized hosts will have maximal effect in facilitating spread of the pathogen. Interestingly, with no regard to disease-induced sterilization, Stenseth (1981) concluded that "The larger the mortality of the uncontrolled population, the more likely is reproduction to be the optimal pest control."

The qualitative character of transmission is also of high importance – keeping R_0 the same across the transmission models, the largest control efficiencies are generally achieved for standard incidence, followed by asymptotic incidence and eventu-
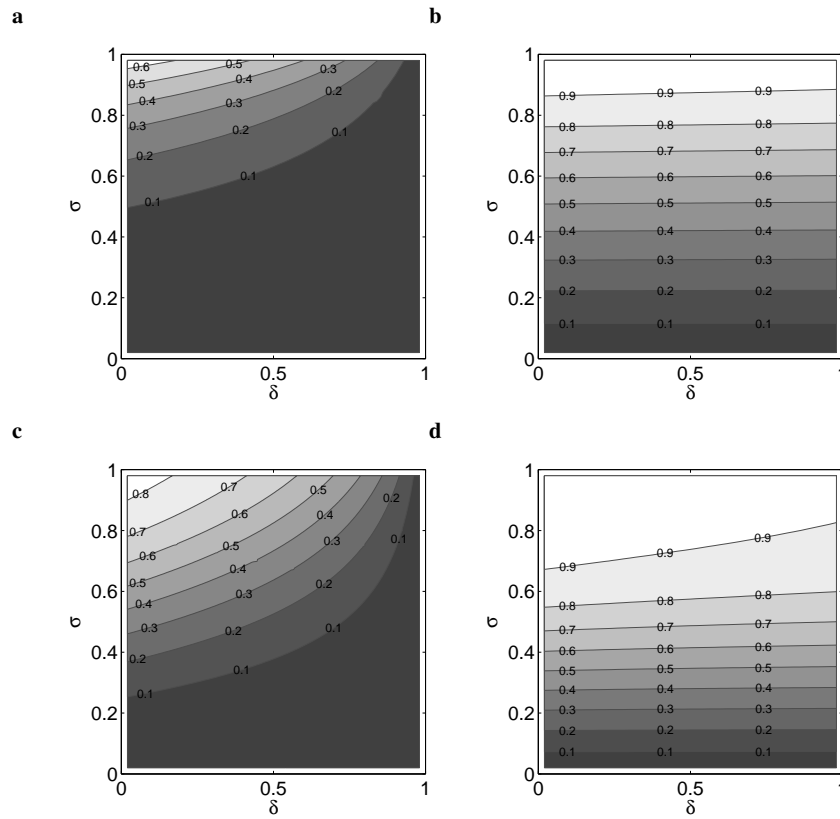
Fig. 5.7 Control effectiveness with mass action incidence, as a function of: (a) the (scaled) disease transmission efficiency β/K and the proportional reduction of the intrinsic mortality rate in those infected individuals that become sterilized (δ); (b) the intrinsic mortality rate d and the proportional reduction of the intrinsic mortality rate in those infected individuals that become sterilized (δ). Other parameter values: (a) $b = 1$, $d = 0.7$, $\sigma = 0.6$; (b) $b = 1$, $\beta = 1/K$, $\sigma = 0.6$; all panels: $d_1 = 0.1$, $K = (b-d)/d_1$

ally mass action incidence. Standard incidence provides the most effective control mainly because this transmission dynamic allows for disease-induced population extinction, which is not the case for the other two transmission dynamics (unless $\delta = \sigma = 1$). This should not concern us much, however, as sterilizing viruses are mostly sexually transmitted (Lockhart et al, 1996) and sexually transmitted diseases most closely fit the standard incidence paradigm (McCallum et al, 2001). If the sterilizing pathogens are to be engineered, on the other hand, we have to carefully consider their transmission mode. Our results have direct implications for the development of effective VVIC agents. In particular, our results indicate how effective, in terms of β and σ, the control agents should be, relative to the life history parameters of a pest species (b, d and δ).

The above results can only be applied, however, when we are able to estimate δ, the factor that extends life expectancy of the sterilized hosts. We expect this might be a problem in many species, mostly in those that are long-lived, but it might on the other hand be relatively easy in short-lived species such as insects or passerine birds or rodents. It is just in these short-lived species where δ can be significantly high, as we do not actually expect high δ in long-lived species. Studies that would allow for an estimate of δ are rare, however; some are listed in Table 5.3. More often, studies of reproduction-survival trade-offs summarize their results in the form of correlations. For example, there is a highly significant negative correlation between egg production and longevity in a wing-dimorphic cricket (Tanaka and Suzuki, 1998). Also, some studies do not present intra-specific variability in fecundity vs. longevity, but rather represent mean evolutionary endpoints at higher units: Bennett and Owens (2002) thus showed that annual fecundity and clutch size were negatively correlated

a   **b**

c   **d**

Fig. 5.8 Control effectiveness with asymptotic incidence, as a function of the proportion of infected individuals that become sterilized (σ) and the proportional reduction of the intrinsic mortality rate in those infected individuals that become sterilized (δ). Other parameter values: (a) $\beta/(K/(c+K)) = 1, b = 1, d = 0.2$; (b) $\beta = 3/(K/(c+K)), b = 1, d = 0.2$. (c) $\beta = 1/(K/(c+K))$, $b = 1, d = 0.5$; (d) $\beta = 3/(K/(c+K)), b = 1, d = 0.5$; all panels: $d_1 = 0.1, c = 1, K = (b-d)/d_1$

to adult survival rate and age at first breeding was positively correlated to adult survival rate, calculated across bird families and orders, while Thomas et al (2000) showed that in humans, a significant negative relationship exists between the mean female fecundity and the mean female longevity, calculated across countries – this result indicates that women in rich countries tend to have fewer children and live longer.

The trade-off between reproduction and survival does not need to be intrinsic to the focal species, i.e. it need not always be driven by changes in energy allocation. Many animals suffer from a conflict between mating success and survival – their mating signals are exploited by their natural enemies (Zuk and Kolluru, 1998). For example, gravid females might be more conspicuous to predators and hence suffer from higher mortality such as in some copepods (Svensson, 1992). As gravid fe-
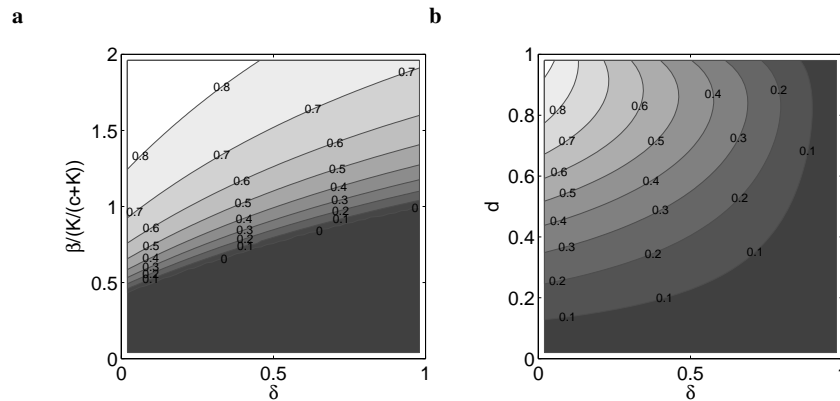
Fig. 5.9 Control effectiveness with asymptotic incidence, as a function of: (a) the (scaled) disease transmission efficiency $\beta/(K/(c+K))$ and the proportional reduction of the intrinsic mortality rate in those infected individuals that become sterilized (δ); (b) the intrinsic mortality rate d and the proportional reduction of the intrinsic mortality rate in those infected individuals that become sterilized (δ). Other parameter values: (a) $b=1$, $d=0.7$, $\sigma=0.6$; (b) $b=1$, $\beta=1/(K/(c+K))$, $\sigma=0.6$; all panels: $d_1=0.1$, $c=1$, $K=(b-d)/d_1$

males, or more generally individuals generating a mating signal, are obviously not sterile, this is yet another mechanism that may increase longevity of sterilized females. So δ might also decrease due to predators or parasitoids, and thus possibly attain relatively low values.

One of our main results is that an increase in longevity of the sterilized infected individuals further enhances their ability to spread the disease. A natural follow-up would be to extend the model to include an indigenous species that is negatively affected by the presence of an invasive species we aim to eradicate with the sterilizing virus. In that case, the lower mortality rate of the sterilized infected individuals can have both a negative and positive effect: on the one hand, they live longer and spread the disease more efficiently, on the other hand, they have more time to cause damage to the indigenous species. It all depends on how fast the invasive species can eliminate the indigenous one. For example, in the Great Lakes, the Asian carp is a huge problem because it is extremely efficient at eradicating plankton, which in turn causes starvation and extinction in native populations (hence a competitive interaction).

If we release a pathogen that sterilizes just males (as can happen, e.g. for VVIC), we invoke a sort of "disease-induced" sterile-male-release technique (Dell'Omo and Palmery, 2002; Dyck et al, 2005). In particular, an increasing fraction of the male population becomes sterile, and females will loose time and opportunities in mating with sterile males. This can create a mate-finding Allee effect (Courchamp et al, 2008) and accelerate the population decline, especially when females mate only once; see also Barlow et al (1997) for the importance of mating systems in effectiveness of fertility control. On the other hand, reduction of host population density

Species	Observation	Estimate of δ	Reference
Parasitoid *Trichogramma brasiliensis*	Adult females survived shorter (10 days) when an unlimited supply of hosts was present, but longer (16 days) when no hosts were provided	$10/16 = 0.625$	Ramesh and Manickavasagam (2003)
Dung beetle *Onthophagus binodis*	Mating is not costly in terms of reduced longevity for female dung beetles; despite a longevity cost of reproduction for males, no evidence was found for differential longevity costs associated with alternative reproductive tactics – quantitative results: males in mixed sex populations = 54.8 ± 2.5 days (mean $\pm$ standard error), males in single sex populations = 62.6 ± 2.7 days, females in mixed sex populations = 55.2 ± 2.7 days, females in single sex populations = 54.7 ± 2.8 days	$54.8/62.6 \sim 0.875$	Kotiaho and Simmons (2003)
Columbian ground squirrel *Spermophilus columbianus*	Reproductive status influenced mortality in females – non-reproducing females had a higher chance of surviving (83.5%) than reproducing females (75.7%)	$16.5/24.3 \sim 0.679$	Neuhaus and Pelletier (2001)

Table 5.3 Some studies of fecundity-longevity or reproduction-survival trade-offs that allow for an estimate of δ

makes it more difficult for pathogens to spread via mass action or asymptotic transmission, as efficiency of that transmission declines with decreasing population density. Fortunately, when an Allee effect creates a demographic extinction threshold, even diseases with mass action or asymptotic transmission can drive host populations to extinction (Hilker et al, 2009). Given also that mating can be costly in terms of reduced longevity for one sex but not the other (Kotiaho and Simmons, 2003), more predictive models should be sexually structured, reflecting sex-specificity of the involved processes and possibility for a mate-finding Allee effect.

5.4 Conclusions and further research

Sterilizing pathogens are commonly assumed not to affect longevity of infected individuals, and if they do then negatively. Examples abound, however, of species in which the absence of reproduction actually increases life expectancy. This happens because by decreasing the energy outlay on reproduction individuals with lowered reproduction can live longer. Alternatively, fertile individuals are more susceptible to predators or parasitoids if the latter can capitalize on mating signals of the former. Here we develop and analyze an SI epidemiological model to explore whether and to what extent does such a life expectancy prolongation due to sterilizing pathogens

affect host dynamics. In particular, we are interested in an added value of increased life expectancy on the possibility of successful pest control, that is, the effect of increased lifespan and hence increased potential of the infected individuals to spread the disease on pest control effectiveness. We show that although the parameter range in which we observe an effect of increased lifespan of the sterilized individuals is not large, the effect itself can be significant. In particular, the increase in pest control effectiveness can be very dramatic when disease transmission efficiency is close to birth rate, mortality rate of susceptible individuals is relatively high (i.e. the species is relatively short-lived), and sterilization efficiency is relatively high. Our results thus characterize pathogens that are promising candidates for an effective pest control and that might possibly be engineered if not occurring naturally.

Among other things, we plan to extend the model studied in this chapter to a two-sex version, due to reasons specified in the final paragraph of the previous section. Actually, development of two-sex models is always a challenge, as it requires consideration of many more processes than classical one-sex models (see Chapter 3). On top of that, there are no standard functional forms for modeling these processes. When it comes to two-sex models, the core element is the mating function or the rate at which males and females meet and mate. When it comes to models of infectious disease dynamics, the core element is the transmission function or the rate at which infected and susceptible individuals meet and the disease is transmitted. So, both these processes have something in common, and when it comes to modeling dynamics of sexually transmitted diseases among males and females that form only ephemeral pair bonds (just to meet, mate, and say goodbye), these two processes of mating and disease transmission have a common base – the way males and females meet and mate. So the mating and transmission functions should at least under some circumstances be structurally consistent.

Let S_M, I_M, S_F and I_F be densities of susceptible males, infected males, susceptible females, and infected females, respectively. Moreover, let ϕ_{SS}, ϕ_{IS}, ϕ_{SI} and ϕ_{II} be the rates at which susceptible males meet and court susceptible females, infected males meet and court susceptible females, susceptible males meet and court infected females, and infected males meet and court infected females, respectively. Assuming no recovery, the corresponding two-sex, SI epidemiological model is as follows (the other symbols used in the model are explained in Table 5.4):

$$\frac{dS_M}{dt} = \mu b w (\chi_{SS}\phi_{SS} + \sigma_{IS}\chi_{IS}\phi_{IS}) + \mu b \xi w (\sigma_{SI}\chi_{SI}\phi_{SI} + \sigma_{II}\chi_{II}\phi_{II}) - \tau_F \chi_{SI}\phi_{SI} - d_M S_M$$

$$\frac{dI_M}{dt} = \mu b (1-\xi) w (\sigma_{SI}\chi_{SI}\phi_{SI} + \sigma_{II}\chi_{II}\phi_{II}) + \tau_F \chi_{SI}\phi_{SI} - (d_M + \alpha_M) I_M$$

$$\frac{dS_F}{dt} = (1-\mu) b w (\chi_{SS}\phi_{SS} + \sigma_{IS}\chi_{IS}\phi_{IS}) + (1-\mu) b \xi w (\sigma_{SI}\chi_{SI}\phi_{SI} + \sigma_{II}\chi_{II}\phi_{II}) - \tau_M \chi_{IS}\phi_{IS} - d_F S_F$$

$$\frac{dI_F}{dt} = (1-\mu) b (1-\xi) w (\sigma_{SI}\chi_{SI}\phi_{SI} + \sigma_{II}\chi_{II}\phi_{II}) + \tau_M \chi_{IS}\phi_{IS} - (d_F + \alpha_F) I_F$$

$$(5.33)$$

What remains to specify is how the encounter rates ϕ_{SS}, ϕ_{IS}, ϕ_{SI}, and ϕ_{II} depend on male and female densities. Let $a_S(S_M + I_M)$ and $a_I(S_M + I_M)$ be the rates at which

Parameter	Meaning
μ	Sex ratio at birth
b	Birth rate
σ	Factors reducing birth rate if any partner is infected
χ	Probabilities of mating of the respective pairs upon encounter
ξ	Probability of the infection being transmitted vertically
d_M (d_F)	Male (female) background mortality rate
α_M (α_F)	Male (female) disease-induced mortality rate
w	Fraction of matings that result in (instant) reproduction
τ_M (τ_F)	Probability of disease transmission from male (female) upon mating

Table 5.4 Parameters used in the model (5.33)

a susceptible female and an infected female, respectively, meet males as a function of total male density $S_M + I_M$. Then,

$$\phi_{SS} = a_S(S_M + I_M)\frac{S_M}{S_M + I_M}S_F$$

$$\phi_{IS} = a_S(S_M + I_M)\frac{I_M}{S_M + I_M}S_F$$

$$\phi_{SI} = a_I(S_M + I_M)\frac{S_M}{S_M + I_M}I_F \qquad (5.34)$$

$$\phi_{II} = a_I(S_M + I_M)\frac{I_M}{S_M + I_M}I_F$$

There are some standard ways of how to model a_S and a_I. One of them includes so-called *mating functions* (also called pair formation functions or marriage functions) that are commonly assumed homogeneous of degree one and define the rate at which males and females mate (e.g. Dietz and Hadeler, 1998). Denoting such a mating function as $\mathscr{M}(S_M + I_M, S_F + I_F)$, we have

$$a(S_M + I_M) = \frac{\mathscr{M}(S_M + I_M, S_F + I_F)}{S_F + I_F} \qquad (5.35)$$

(we give a form common to a_S and a_I here, the two functions may differ by choosing sex-specific parameter values of $\mathscr{M}$). Also, one may assume that the host population is subject to an Allee effect and consider an alternative description of a:

$$a(S_M + I_M) = c\,\frac{S_M + I_M}{S_M + I_M + \theta} \qquad (5.36)$$

The model (5.33) can be used to explore a number of issues, among which are impacts of vertically transmitted male-killing bacteria, by setting to zero the first term of the right-hand side in the equation for I_M; these bacteria can also be simultaneously spread horizontally (Keeling et al, 2003; Hurst and Jiggins, 2000, and references therein). Also, this model can be used to study effects of parasites pro-

moting mating success, by setting, e.g. $\chi_{SS} < \chi_{IS} = \chi_{SI} < \chi_{II}$ (McLachlan, 1999; Knell and Webberley, 2004). We are currently working on the latter topic.

Also, we are currently examining how dynamics of the generic model (5.33) are affected by the form of the mating function $\mathscr{M}$ and an appropriate, consistent transmission function. The preliminary result we have so far is as follows. Consider the following variant of the model (5.33), with a general mating function $\mathscr{M}(N_M, N_F)$:

$$\frac{dS_M}{dt} = \gamma_M Cwb \frac{\mathscr{M}(N_M, N_F)}{N_F}(S_F + \sigma I_F) - \delta C \frac{\mathscr{M}(N_M, N_F)}{N_F} \frac{S_M I_F}{N_M} - (d_M + dN)S_M$$

$$\frac{dI_M}{dt} = \delta C \frac{\mathscr{M}(N_M, N_F)}{N_F} \frac{S_M I_F}{N_M} - (d_M + dN)I_M - \alpha_M I_M$$

$$\frac{dS_F}{dt} = \gamma_F Cwb \frac{\mathscr{M}(N_M, N_F)}{N_F}(S_F + \sigma I_F) - \delta C \frac{\mathscr{M}(N_M, N_F)}{N_F} \frac{S_F I_M}{N_M} - (d_F + dN)S_F$$

$$\frac{dI_F}{dt} = \delta C \frac{\mathscr{M}(N_M, N_F)}{N_F} \frac{S_F I_M}{N_M} - (d_F + dN)I_F - \alpha_F I_F$$

$$\tag{5.37}$$

In addition to the symbols given in Table 5.4, C is the rate at which males and females meet, δ is the probability of disease transmission upon mating, and d is the strength of negative density dependence in host mortality; $N = N_F + N_M$.

Proposition 5.8. *If there is no disease-induced mortality, $\alpha_M = \alpha_F = 0$, the basic reproduction number R_0 of the model* (5.37) *does not depend on the mating function.*

Proof. As in Box 5.3, we use the next generation matrix approach due to van den Driessche and Watmough (2002). We first reshuffle the state variables so that the first two represent infected classes: I_F, I_M, S_F, S_M. Using the notation of van den Driessche and Watmough (2002), we have

$$\mathscr{F} = \begin{pmatrix} \delta C \dfrac{\mathscr{M}(N_M, N_F)}{N_F} \dfrac{S_F I_M}{N_M} \\ \delta C \dfrac{\mathscr{M}(N_M, N_F)}{N_F} \dfrac{S_M I_F}{N_M} \\ 0 \\ 0 \end{pmatrix}$$

comprising all rates of the model (5.37) that describe the appearance of new infections, and

$$\mathscr{V} = \begin{pmatrix} (d_F + dN)I_F + \alpha_F I_F \\ (d_M + dN)I_M + \alpha_M I_M \\ -\dfrac{dS_F}{dt} \\ -\dfrac{dS_M}{dt} \end{pmatrix}$$

comprising all remaining rates (with the reverse sign). Setting $x = (I_F, I_M, S_F, S_M)$ as the system state and $x_0 = (0, 0, N_F^*, N_M^*)$ as the disease-free equilibrium, this implies

$$F = \left[\frac{\partial \mathscr{F}_i}{\partial x_j}(x_0)\right]\Bigg|_{1 \leq i,j \leq 2} = \delta C \mathscr{M}(N_M^*, N_F^*) \begin{pmatrix} 0 & 1/N_M^* \\ 1/N_F^* & 0 \end{pmatrix}$$

and

$$V = \left[\frac{\partial \mathscr{V}_i}{\partial x_j}(x_0)\right]\Bigg|_{1 \leq i,j \leq 2} = \begin{pmatrix} \alpha_F + d_F + d(N_F^* + N_M^*) & 0 \\ 0 & \alpha_M + d_M + d(N_F^* + N_M^*) \end{pmatrix}$$

This implies

$$V^{-1} = \begin{pmatrix} 1/[\alpha_F + d_F + d(N_F^* + N_M^*)] & 0 \\ 0 & 1/[\alpha_M + d_M + d(N_F^* + N_M^*)] \end{pmatrix}$$

and the next generation matrix thus becomes

$$FV^{-1} = \delta C \mathscr{M}(N_M^*, N_F^*) \begin{pmatrix} 0 & \dfrac{1}{N_M^*[\alpha_M + d_M + d(N_F^* + N_M^*)]} \\ \dfrac{1}{N_F^*[\alpha_F + d_F + d(N_F^* + N_M^*)]} & 0 \end{pmatrix}$$

of which the dominant (in the absolute value) eigenvalue equals R_0 (van den Driessche and Watmough, 2002). Therefore,

$$R_0 = \frac{\delta C \mathscr{M}(N_M^*, N_F^*)}{\sqrt{N_F^* N_M^* [\alpha_F + \mu_F + d(N_F^* + N_M^*)][\alpha_M + \mu_M + d(N_F^* + N_M^*)]}} \tag{5.38}$$

In the absence of disease, the model (5.37) simplifies to

$$\begin{aligned} \frac{dN_F}{dt} &= \gamma_F C wb \mathscr{M}(N_M, N_F) - (d_F + dN)N_F \\ \frac{dN_M}{dt} &= \gamma_M C wb \mathscr{M}(N_M, N_F) - (d_M + dN)N_M \end{aligned} \tag{5.39}$$

Setting its right-hand sides to zero, then from the first equation we have for the disease-free equilibrium

$$\frac{\mathscr{M}}{N_F^*} = \frac{d_F + d(N_F^* + N_M^*)}{\gamma_F C wb}$$

and from the second equation, analogously,

$$\frac{\mathscr{M}}{N_M^*} = \frac{d_M + d(N_F^* + N_M^*)}{\gamma_M C wb}$$

So

$$\frac{\mathscr{M}^2}{N_F^* N_M^*} = \frac{[d_F + d(N_F^* + N_M^*)][d_M + d(N_F^* + N_M^*)]}{\gamma_F \gamma_M (C wb)^2}$$

and hence

$$\frac{\mathcal{M}}{\sqrt{N_F^* N_M^*}} = \frac{\sqrt{[d_F + d(N_F^* + N_M^*)][d_M + d(N_F^* + N_M^*)]}}{Cwb\sqrt{\gamma_F \gamma_M}}$$

Substituting this expression into (5.38) we eventually have

$$R_0 = \frac{\delta}{wb\sqrt{\gamma_F \gamma_M}} \times \frac{\sqrt{[d_F + d(N_F^* + N_M^*)][d_M + d(N_F^* + N_M^*)]}}{\sqrt{[\alpha_F + d_F + d(N_F^* + N_M^*)][\alpha_M + d_M + d(N_F^* + N_M^*)]}} \quad (5.40)$$

Hence, if there is no disease-induced mortality, the nominator and denominator of the second fraction cancel out and R_0 does not depend on the mating function $\mathcal{M}$, since

$$R_0 = \frac{\delta}{wb\sqrt{\gamma_F \gamma_M}} \quad (5.41)$$

We note that if there is a disease-induced mortality, R_0 depends on the mating function $\mathcal{M}$ through $N_F^* + N_M^*$, the total population size at the disease-free equilibrium. However, if $d(N_F^* + N_M^*)$ is large relative to both α_F and α_M, we still have a weak dependence of R_0 on the mating function $\mathcal{M}$.

$\square$

References

Abrams PA, Ginzburg LR (2000) The nature of predation: prey dependent, ratio dependent or neither? Trends in Ecology & Evolution 15:337–341

Aguirrea P, González-Olivares E, Sáez E (2009) Two limit cycles in a Leslie-Gower predator-prey model with additive Allee effect. Nonlinear Analysis: Real World Applications 10:1401–1416

Allee WC (1931) Animal aggregations, a study in general sociology. University of Chicago Press, Chicago

Allee WC, Bowen F (1932) Studies in animal aggregations: mass protection against colloidal silver among goldfishes. Journal of Experimental Zoology 61:185–207

Allee WC, Wilder J (1938) Group protection for *Euplanaria dorotocephala* from ultraviolet radation. Physiological Zoology 12:110–135

Allen LJS, Fagan JF, Högnäs G, Fagerholm H (2005) Population extinction in discrete-time stochastic population models with an Allee effect. Journal of Difference Equations and Applications 11:273–293

Almeida RC, Delphim SA, da S Costa MI (2006) A numerical model to solve single-species invasion problems with Allee effects. Ecological Modelling 192:601–617

Anderson RM, May RM (1979) Population biology of infectious diseases. I. Nature 280:361–367

Anderson RM, May RM (1981) The population dynamics of microparasites and their invertebrate hosts. Philosophical Transactions of the Royal Society B: Biological Sciences 291:451–524

Andersson M (1994) Sexual selection. Princeton University Press, Princeton

Anholt BR, Werner EE (1995) Interaction between food availability and predation mortality mediated by adaptive behavior. Ecology 76:2230–2234

Antonovics J (2009) The effect of sterilizing diseases on host abundance and distribution along environmental gradients. Proceedings of the Royal Society B: Biological Sciences 276:1443–1448

van Baalen M, Krivan V, van Rijn PCJ, Sabelis M (2001) Alternative food, switching predators, and the persistence of predator-prey systems. American Naturalist 157:512–524

Babcock R, Keesing J (1999) Fertilisation biology of the abalone *Haliotis laevigata*: laboratory and field studies. Canadian Journal of Fisheries and Aquatic Science 56:1668–1678

Barclay H, Mackauer M (1980) The sterile insect release method for pest control: a density-dependent model. Environmental Entomology 9:810–817

Barkan C, Witham M (1989) Profitability, rate maximization, and reward delay: a test of the simultaneous-encounter model of prey choice with *Parus atricapillus*. American Naturalist 134:254–272

Barlow ND, Kean JM, Briggs CJ (1997) Modelling the relative efficacy of culling and sterilisation for controlling populations. Wildlife Research 24:129–141

Baudoin M (1975) Host castration as a parasitic strategy. Evolution 29:335–352

Beddington JR (1975) Mutual interference between parasites or predators and its effect on searching efficiency. Journal of Animal Ecology 44:331–340

Begon M, Harper JL, Townsend CR (1990) Ecology: individuals, populations and communities (2nd edition). Blackwell Scientific Publications, Oxford

Beisner BE, Haydon DT, Cuddington K (2003) Alternative stable states in ecology. Frontiers in Ecology and the Environment 1:376–382

Bélisle C, Cresswell J (1997) The effects of a limited memory capacity on foraging behavior. Theoretical Population Biology 52:78–90

Bell G (1980) The costs of reproduction and their consequences. American Naturalist 116:45–76

Bennett PM, Owens IPF (2002) Evolutionary ecology of birds. Oxford University Press, Oxford

Berec L (2000) Mixed encounters, limited perception and optimal foraging. Bulletin of Mathematical Biology 62:849–868

Berec L (2002) Techniques of spatially explicit individual-based models: construction, simulation, and mean-field analysis. Ecological Modelling 150:55–81

Berec L (2003) Simultaneous prey encounters by optimally foraging predators: theory and experiments. Comments on Theoretical Biology 8:1–36

Berec L (2010) Impacts of foraging facilitation among predators on predator-prey dynamics. Bulletin of Mathematical Biology 72:94–121

Berec L, Boukal DS (2004) Implications of mate search, mate choice and divorce rate for population dynamics of sexually reproducing species. Oikos 104:122–132

Berec L, Křivan V (2000) A mechanistic model for partial preferences. Theoretical Population Biology 58:279–289

Berec L, Boukal DS, Berec M (2001) Linking the Allee effect, sexual reproduction and temperature-dependent sex determination via spatial dynamics. American Naturalist 157:217–230

Berec L, Angulo E, Courchamp F (2007) Multiple Allee effects and population management. Trends in Ecology & Evolution 22:185–191

Berec L, Eisner J, Křivan V (2010) Adaptive foraging does not always lead to more complex food webs. Journal of Theoretical Biology 266:211–218

Berec M, Křivan V, Berec L (2003) Are great tits (*Parus major*) really optimal foragers? Canadian Journal of Zoology 81:780–788

Berryman AA (1992) The origins and evolution of predator-prey theory. Ecology 73:1530–1535

Bessa-Gomes C, Legendre S, Clobert J (2004) Allee effects, mating systems and the extinction risk in populations with two sexes. Ecology Letters 7:802–812

Bonds MH (2006) Host life-history strategy explains pathogen-induced sterility. American Naturalist 168:281–293

Boots M, Knell RJ (2002) The evolution of risky behaviour in the presence of a sexually transmitted disease. Proceedings of the Royal Society B: Biological Sciences 269:585–589

Boukal DS, Berec L (2002) Single-species models of the Allee effect: extinction boundaries, sex ratios and mate encounters. Journal of Theoretical Biology 218:375–394

Boukal DS, Berec L (2009) Modelling mate-finding Allee effects and populations dynamics, with applications in pest control. Population Ecology 51:445–458

Boukal DS, Sabelis MW, Berec L (2007) How predator functional responses and Allee effects in prey affect the paradox of enrichment and population collapses. Theoretical Population Biology 72:136–147

Boukal DS, Berec L, Krivan V (2008) Does sex-selective predation stabilize or destabilize predator-prey dynamics? PLoS ONE 3(7):e2687

Bradley MP, Hinds LA, Bird PH (1997) A bait-delivered immunocontraceptive vaccine for the European red fox (*Vulpes vulpes*) by the year 2002? Reproduction, Fertility and Development 9:111–116

Case TJ (2000) An illustrated guide to theoretical ecology. Oxford University Press, New York and Oxford

Caswell H (2001) Matrix population models. Construction, analysis, and interpretation. Second Edition. Sinauer Associates, Sunderland, Massachusetts

Caswell H, Weeks EE (1986) Two-sex models: chaos, extinction, and other dynamic consequences of sex. American Naturalist 128:707–735

Charnov EL (1976) Optimal foraging: attack strategy of a mantid. American Naturalist 110:141–151

Charnov EL, Bull J (1977) When is sex environmentally determined? Nature 266:828–830

Choudhury S (1995) Divorce in birds: a review of the hypotheses. Animal Behavior 50:413–429

Christiansen JL, Burken RR (1979) Growth and maturity of the snapping turtle (*Chelydra serpentina*) in Iowa. Herpetologica 35:261–266

Clark CW (1990) Mathematical bioeconomics: optimal management of renewable resources. Wiley, Hoboken

Cosner C, DeAngelis D, Ault JS, Olson DB (1999) Effects of spatial grouping on the functional response of predators. Theoretical Population Biology 56:65–75

Courchamp F, Cornell SJ (2000) Virus-vectored immunocontraception to control feral cats on islands: a mathematical model. Journal of Applied Ecology 37:903–913

Courchamp F, Clutton-Brock TH, Grenfell BT (1999) Inverse density dependence and the Allee effect. Trends in Ecology & Evolution 14:405–410

Courchamp F, Clutton-Brock T, Grenfell B (2000) Multipack dynamics and the Allee effect in the African wild dog, *Lycaon pictus*. Animal Conservation 3:277–285

Courchamp F, Chapuis JL, Pascal M (2003) Mammal invaders on islands: impact, control and control impact. Biological Reviews of the Cambridge Philosophical Society (London) 78:347–383

Courchamp F, Angulo E, Rivalan P, et al (2006) Rarity value and species extinction: the anthropogenic Allee effect. PLoS Biology 4:2405–2410

Courchamp F, Berec L, Gascoigne J (2008) Allee effects in ecology and conservation. Oxford University Press, Oxford

Cowan PE (1996) Possum biocontrol: prospects for fertility regulation. Reproduction, Fertility and Development 8:655–660

Davis HG, Taylor CM, Lambrinos JG, Strong DR (2004) Pollen limitation causes an Allee effect in a wind-pollinated invasive grass (*Spartina alterniflora*). Proceedings of the National Academy of Sciences of the United States of America 101:13,804–13,807

Dawson JW, Mannan RW (1991) The role of territoriality in the social organization of Harris' hawks. Auk 108:661–672

DeAngelis DL, Goldstein RA, O'Neill RV (1975) A model for trophic interaction. Ecology 56:881–892

Dell'Omo G, Palmery M (2002) Fertility control in vertebrate pest species. Contraception 65:273–275

Dennis B (1989) Allee effects: population growth, critical density, and the chance of extinction. Natural Resource Modeling 3:481–538

Dennis B (2002) Allee effects in stochastic populations. Oikos 96:389–401

Deredec A, Courchamp F (2007) Importance of the Allee effect for reintroductions. Ecoscience 14:440–451

Deredec A, Berec L, Boukal DS, Courchamp F (2008) Are non-sexual models appropriate for predicting the impact of virus-vectored immunocontraception? Journal of Theoretical Biology 250:281–290

Dhooge A, Govaerts W, Kuznetsov YA (2003) Matcont: a Matlab package for numerical bifurcation analysis of ODEs. ACM Transactions on Mathematical Software 29:141–164

Dieckmann U, Law R, Metz JAJ (2000) The geometry of ecological interactions: simplifying spatial complexity. Cambridge University Press, Cambridge

Diekmann O, Kretzschmar M (1991) Patterns in the effects of infectious diseases on population growth. Journal of Mathematical Biology 29:539–570

Dietz K, Hadeler KP (1998) Epidemiological models for sexually transmitted diseases. Journal of Mathematical Biology 26:1–25

Drake JM (2004) Allee effects and the risk of biological invasion. Risk Analysis 24:795–802

Drake JM, Lodge DM (2006) Allee effects, propagule pressure and the probability of establishment: risk analysis for biological invasions. Biological Invasions 8:365–375

van den Driessche P, Watmough J (2002) Reproduction numbers and sub-threshold endemic equilibria for compartmental models of disease transmission. Mathematical Biosciences 180:29–48

Dubois F, Cézilly F, Pagel M (1998) Mate fidelity and coloniality in waterbirds: a comparative analysis. Oecologia 116:433–440

Duellman WE, Trueb L (1986) Biology of amphibians. McGraw-Hill, New York

Durrett R (1995) Ten lectures on particle systems. In: Dold FTA (ed) Lecture Notes in Mathematics, vol. 1068, Springer, New York, pp 97–201

Dyck VA, Hendrichs J, Robinson AS (2005) Sterile insect technique: principles and practice in area-wide integrated pest management. Springer, Dordrecht, The Netherlands

Ellers J (1995) Fat and eggs: an alternative method to measure the trade-off between survival and reproduction in insect parasitoids. Netherlands Journal of Zoology 46:227–235

Emlen JM (1966) The role of time and energy in food preferences. American Naturalist 100:611–617

Engen S, Stenseth NC (1984a) An ecological paradox: a food type may become more rare in the diet as a consequence of being more abundant. American Naturalist 124:352–359

Engen S, Stenseth NC (1984b) A general version of optimal foraging theory: the effect of simultaneous encounters. Theoretical Population Biology 26:192–204

Engen S, Lande R, Saether BE (2003) Demographic stochasticity and Allee effects in populations with two sexes. Ecology 84:2378–2386

Ewen JG, Clarke RH, Moysey E, et al (2001) Primary sex ratio bias in an endangered cooperatively breeding bird, the black-eared miner, and its implications for conservation. Biological Conservation 101:137–145

Farnsworth KD, Illius AW (1998) Optimal diet choice for large herbivores: an extended contingency model. Functional Ecology 12:74–81

Fowler MS, Ruxton GD (2002) Population dynamic consequences of Allee effects. Journal of Theoretical Biology 215:39–46

Fryxell JM, Lundberg P (1994) Diet choice and predator-prey dynamics. Evolutionary Ecology 8:407–421

Fryxell JM, Lundberg P (1998) Individual behavior and community dynamics. Chapman & Hall, London

Gao LQ, Hethcote HW (1992) Disease transmission models with density-dependent demographics. Journal of Mathematical Biology 30:717–731

Gascoigne J, Berec L, Gregory S, Courchamp F (2009) Dangerously few liaisons: a review of mate-finding Allee effects. Population Ecology 51:355–372

Gascoigne JC, Lipcius RN (2004) Allee effects driven by predation. Journal of Applied Ecology 41:801–810

Girondot M (1999) Statistical description of temperature-dependent sex determination using maximum likelihood. Evolutionary Ecology Research 1:479–486

Girondot M, Pieau C (1993) Effects of sexual differences of age at maturity and survival on population sex ratio. Evolutionary Ecology 7:645–650

Gleeson SR, Wilson DS (1986) Equilibrium diet: optimal foraging and prey coexistence. Oikos 46:139–144

Goodman LA (1953) Population growth of the sexes. Biometrics 9:212–225

Grevstad FS (1999) Factors influencing the chance of population establishment: implications for release strategies in biocontrol. Ecological Applications 9:1439–1447

Grimm V, Railsback SF (2005) Individual-based modeling and ecology. Princeton University Press, Princeton and Oxford

Hadjiavgousti D, Ichtiaroglou S (2004) Existence of stable localized structures in population dynamics through the Allee effect. Chaos, Solitons & Fractals 21:119–131

Hajek A (2004) Natural enemies. Cambridge University Press, Cambridge

Hassell MP (1975) Density-dependence in single-species populations. Journal of Animal Ecology 44:283–295

Hassell MP, Lawton JH, Beddington JR (1976) The components of arthropod predation. 1. The prey death rate. Journal of Animal Ecology 45:135–164

Hastings A (1983) Age-dependent predation is not a simple process, I. Continuous time models. Theoretical Population Biology 23:347–362

Hastings A (1984a) Age-dependent predation is not a simple process, II. Wolves, ungulates and a discrete time model for predation on juveniles with a stabilizing tail. Theoretical Population Biology 26:271–282

Hastings A (1984b) Delays in recruitment at different trophic levels: effects on stability. Journal of Mathematical Biology 21:35–44

Hastings A (1984c) Simple models for age dependent predation. In: Levin SA, Hallam TG (eds) Mathematical ecology, Lecture Notes in Biomathematics, Springer-Verlag, pp 114–119

Hilker FM, Langlais M, Malchow H (2009) The Allee effect and infectious diseases: extinction, multistability, and the (dis-)appearance of oscillations. American Naturalist 173:72–88

Hirvonen H, Ranta E, Rita H, Peuhkuri N (1999) Significance of memory properties in prey choice decisions. Ecological Modelling 115:177–189

Hobday AJ, Tegner MJ, Haaker PL (2001) Over-exploitation of a broadcast spawning marine invertebrate: decline of the white abalone. Reviews in Fish Biology and Fisheries 10:493–514

Hoelmer KA, Kirk AA (2005) Selecting arthropod biological control agents against arthropod pests: can the science be improved to decrease the risk of releasing ineffective agents? Biological Control 34:255–264

Holling CS (1959) Some characteristics of simple types of predation and parasitism. Canadian Entomologist 91:385–398

Hoogland JL, Cannon KE, DeBarbieri LM, Manno TG (2006) Selective predation on Utah prairie dogs. American Naturalist 168:546–552

Hoppensteadt F (1974) Asymptotic stability in singular perturbation problems. II: Problems having matched asymptotic expansion solutions. Journal of Differential Equations 15:510–521

Hopper KR, Roush RT (1993) Mate finding, dispersal, number released, and the success of biological-control introductions. Ecological Entomology 18:321–331

Houston A, Krebs J, Erichsen J (1980) Optimal prey choice and discrimination time in the great tit (*Parus major* L.). Behavioral Ecology and Sociobiology 6:169–175

Hoyle A, Bowers RG, White A, Boots M (2008) The influence of trade-off shape on evolutionary behaviour in classical ecological scenarios. Journal of Theoretical Biology 250:498–511

Hughes RN (1979) Optimal diets under the energy maximization premise: the effects of recognition time and learning. The American Naturalist 113:209–221

Huisman G, DeBoer RJ (1997) A formal derivation of the "Beddington" functional response. Journal of Theoretical Biology 185:389–400

Hunter ML, Gibbs JP (2007) Fundamentals of conservation biology. Blackwell Publishing

Hurst GDD, Jiggins FM (2000) Male-killing bacteria in insects: mechanisms, incidence, and implications. Emerging Infectious Diseases 6:329–336

Hutchings JA (2001) Influence of population decline, fishing, and spawner variability on the recovery of marine fishes. Journal of Fish Biology 59 (Supplement A):306–322

Iannelli M, Martcheva M, Milner FA (2005) Gender-structured population modeling. SIAM, Philadelphia, PA

Iverson JB (1991) Pattern of survivorship in turtles (order Testudines). Canadian Journal of Zoology 69:385–391

Jang SR (2007) Allee effects in a discrete-time host parasitoid model with stage structure in the host. Discrete and Continuous Synamical Systems – Series B 8:145–159

Jang SR (2010) Discrete host-parasitoid models with Allee effects and age structure in the host. Mathematical Biosciences and Engineering 7:67–81

Janzen FJ, Paukstis GL (1991) Environmental sex determination in reptiles: ecology, evolution, and experimental design. Quarterly Review of Biology 66:149–179

Jeschke JM, Kokko H (2008) Mortality and other determinants of bird divorce rate. Behavioral Ecology and Sociobiology 63:1–9

Jeschke JM, Kopp M, Tollrian R (2002) Predator functional responses: discriminating between handling and digesting prey. Ecological Monographs 72:95–112

Johnson DM, Liebhold AM, Tobin PC, Bjørnstad ON (2006) Allee effects and pulsed invasion by the gypsy moth. Nature 444:361–363

Jost C (1998) Comparing predator-prey models qualitatively and quantitatively with ecological time-series data. Dissertation. Institut National Agronomique, Paris-Grignon, France

Jost C, Arino O, Arditi R (1999) About deterministic extinction in ratio-dependent predator-prey models. Bulletin of Mathematical Biology 61:19–32

Kat PW, Alexander KA, Smith JS, Munson L (1995) Rabies and African wild dogs in Kenya. Proceedings of the Royal Society B: Biological Sciences 262:229–233

Kear J, Berger AJ (1980) The Hawaiian goose: an experiment in conservation. Buteo Books, Vermillion, South Dakota

Keeling MJ, Rohani P (2008) Modeling infectious diseases in humans and animals. Princeton University Press, Princeton, NJ, and Oxford

Keeling MJ, Jiggins FM, Read JM (2003) The invasion and coexistence of competing *Wolbachia* strains. Heredity 91:382–388

Kendall DG (1949) Stochastic processes and population growth. Journal of the Royal Statistical Society B 11:230–282

Kermack WO, McKendrick AG (1927) A contribution to the mathematical theory of epidemics. Proceedings of the Royal Society of London Series A, Containing Papers of a Mathematical and Physical Character 115:700–721

Kermack WO, McKendrick AG (1932) Contributions to the mathematical theory of epidemics. II. The problem of endemicity. Proceedings of the Royal Society of London Series A, Containing Papers of a Mathematical and Physical Character 138:55–83

Kermack WO, McKendrick AG (1933) Contributions to the mathematical theory of epidemics. III. Further studies of the problem of endemicity. Proceedings of the Royal Society of London Series A, Containing Papers of a Mathematical and Physical Character 141:94–122

Kindvall O, Vessby K, Berggren A, Hartman G (1998) Individual mobility prevents an Allee effect in sparse populations of the bush cricket *Metrioptera roeseli*: an experimental study. Oikos 81:449–457

Knell RJ, Webberley KM (2004) Sexually transmitted diseases of insects: distribution, evolution, ecology and host behaviour. Biological Reviews 79:557–581

Knipling EF (1955) Possibilities of insect control or eradication through the use of sexually sterile males. Journal of Economic Entomology 48:459–462

Kokko H, Ranta E, Ruxton G, Lundberg P (2002) Sexually transmitted diseases and the evolution of mating systems. Evolution 56:1091–1100

Kooi BW, Poggiale JC, Auger P, Kooijman SALM (2002) Aggregation methods in food chains with nutrient recycling. Ecological Modelling 157:69–86

Kot M (2001) Elements of mathematical ecology. Cambridge University Press, Cambridge

Kot M, Lewis MA, van den Driessche P (1996) Dispersal data and the spread of invading organisms. Ecology 77:2027–2042

Kotiaho J, Alatalo RV, Mappes J, Parri S, Rivero A (1998) Male mating success and risk of predation in a wolf spider: balance between sexual and natural selection? Journal of Animal Ecology 67:287–291

Kotiaho JS, Simmons LW (2003) Longevity cost of reproduction for males but no longevity cost of mating or courtship for females in the male-dimorphic dung beetle *Onthophagus binodis*. Journal of Insect Physiology 49:817–822

Krafsur ES (1998) Sterile insect technique for suppressing and eradicating insect populations: 55 years and counting. Journal of Agricultural Entomology 15:303–317

Kramer AM, Dennis B, Liebhold AM, Drake JM (2009) The evidence for Allee effects. Population Ecology 51:341354

Krebs CJ (2001) Ecology (5th edition). Benjamin Cummings, San Francisco

Krebs JR, Davies NB (1987) An introduction to behavioural ecology. Blackwell Scientific Publications, Oxford

Krebs JR, McCleery RH (1984) Behavioural adaptations and life history. In: Krebs JR, Davies N (eds) Behavioural Ecology, An Evolutionary Approach, Blackwell Scientific Publications, Oxford, pp 91–121

Krebs JR, Erichsen JT, Webber MI, Charnov EL (1977) Optimal prey selection in the great tit (*Parus major*). Animal Behaviour 25:30–38

Kuang Y, Beretta E (1998) Global qualitative analysis of a ratio-dependent predator-prey system. Journal of Mathematical Biology 36:389–406

Kuussaari M, Saccheri L, Camara M, Hanski I (1988) Allee effect and population dynamics in the Glanville fritillary butterfly. Oikos 82:384–392

Kuznetsov YA (1998) CONTENT - integrated environment for analysis of dynamical systems. Tutorial. Ecole Normale Superieure de Lyon, Rapport de Recherche UPMA-98-224, ftp://ftp.cwi.nl/pub/CONTENT

Křivan V (1996) Optimal foraging and predator-prey dynamics. Theoretical Population Biology 49:265–290

Křivan V (1997) Dynamic ideal free distribution: effects of optimal patch choice on predator-prey dynamics. American Naturalist 149:164–178

Křivan V (2007) The Lotka-Volterra predator-prey model with foraging-predation risk trade-offs. American Naturalist 170:771–782

Křivan V (2011) On the Gause predator-prey model with a refuge: a fresh look at the history. Journal of Theoretical Biology 274:67–73

Křivan V, Sikder A (1999) Optimal foraging and predator-prey dynamics II. Theoretical Population Biology 55:111–126

Lamberson RH, McKelvey R, Noon BR, Voss C (1992) A dynamic analysis of northern spotted owl viability in a fragmented forest landscape. Conservation Biology 6:502–512

Lewis MA, van den Driessche P (1993) Waves of extinction from sterile insect release. Mathematical Biosciences 116:221–247

Lewis MA, Kareiva P (1993) Allee dynamics and the spread of invading organisms. Theoretical Population Biology 43:141–158

Liebhold AM, Bascompte J (2003) The Allee effect, stochastic dynamics and the eradication of alien species. Ecology Letters 6:133–140

Liebhold AM, Tobin PC (2008) Population ecology of insect invasions and their management. Annual Review of Entomology 53:387–408

Lockhart AB, Thrall PH, Antonovics J (1996) Sexually transmitted diseases in animals: ecological and evolutionary implications. Biological Reviews of the Cambridge Philosophical Society (London) 71:415–471

Lockwood JL, Hoopes M, Marchetti M (2007) Invasion ecology. Blackwell Publishing Ltd., Malden

Lotka AJ (1926) Elements of physical biology. Williams and Wilkins, Baltimore

MacArthur RH, Pianka ER (1966) On optimal use of a patchy environment. American Naturalist 100:603–609

Mack RN, Simberloff D, Lonsdale WM, Evans H, Clout M, Bazzaz FA (2000) Biotic invasions: causes, epidemiology, global consequences, and control. Ecological Applications 10:689–710

Maiti A, Patra B, Samanta GP (2006) Sterile insect release method as a control measure of insect pests: a mathematical model. Journal of Applied Mathematics and Computing 22:71–86

Mangel M (2006) The theoretical biologist's toolbox. Cambridge University Press, New York

Mangel M, Roitberg B (1989) Dynamic information and host acceptance by a tephritid fruit fly. Ecological Entomology 14:181–189

May RM (1974) Biological populations with nonoverlapping generations: stable points, stable cycles, and chaos. Science 186:645–647

May RM (1977) Thresholds and breakpoints in ecosystems with a multiplicity of stable states. Nature 269:471–477

McCallum H, Barlow N, Hone J (2001) How should pathogen transmission be modelled? Trends in Ecology & Evolution 16:295–300

McCarthy MA (1997) The Allee effect, finding mates and theoretical models. Ecological Modelling 103:99–102

McCauley E, Wilson WG, de Roos AM (1993) Dynamics of age-structured and spatially structured predator-prey interactions: individual-based models and population-level formulations. American Naturalist 142:412–442

McLachlan A (1999) Parasites promote mating success: the case of a midge and a mite. Animal Behaviour 57:1199–1205

McLellan BN, Serrouya R, Wittmer HU, Boutin S (2010) Predator-mediated Allee effects in multi-prey systems. Ecology 91:286–292

McLeod SR, Twigg LE (2006) Predicting the efficacy of virally-vectored immunocontraception for managing rabbits. New Zealand journal of Ecology 30:103–120

McNair JN (1979) A generalized model of optimal diets. Theoretical Population Biology 15:159–170

McNamara JM, Forslund P (1996) Divorce rates in birds: predictions from an optimization model. American Naturalist 147:609–640

McNamara JM, Houston AI (1987) Partial preferences and foraging. Animal Behaviour 35:1084–1099

Miller MR, White A, Wilson K, Boots M (2007) The population dynamical implications of male-biased parasitism in different mating systems. PLoS ONE 2(7):e624

Milner JM, Nielsen EB, Andreassen HP (2006) Demographic side effects of selective hunting in ungulates and carnivores. Conservation Biology 21:36–47

Mitchell WA (1989) Informational constraints on optimally foraging himmingbirds. Oikos 55:145–154

Møller AP, Legendre S (2001) Allee effect, sexual selection and demographic stochasticity. Oikos 92:27–34

Mooring MS, Fitzpatrick TA, Nishihira TT, Reisig DD (2004) Vigilance, predation risk, and the Allee effect in desert bighorn sheep. Journal of Wildlife Management 68:519–532

Murdoch WW, Oaten A (1975) Predation and population stability. In: Macfadyen A (ed) Advances in Ecological Research, Academic Press, pp 1–131

Murdoch WW, Nisbet RM, McCauley E, de Roos AM, Gurney WSC (1998) Plankton abundance and dynamics across nutrient levels: tests of hypotheses. Ecology 79:1339–1356

Murray JD (1993) Mathematical biology. Springer, Berlin, Heidelberg

Neuhaus P, Pelletier N (2001) Mortality in relation to season, age, sex, and reproduction in Columbian ground squirrels (*Spermophilus columbianus*). Canadian Journal of Zoology 79:465–470

Novák B, Tyson JJ (2004) A model for restriction point control of the mammalian cell cycle. Journal of Theoretical Biology 230:563–579

Obst FJ (1986) Turtles, tortoises and terrapins. Edition, Leipzig

O'Keefe KJ, Antonovics J (2002) Playing by different rules: the evolution of virulence in sterilizing pathogens. American Naturalist 159:597605

Olsen JB, Miller SJ, Harper K, Nagler JJ, Wenburg JK (2006) Contrasting sex ratios in juvenile and adult chinook salmon *Oncorhynchus tshawytscha* (Walbaum) from south-west Alaska: sex reversal or differential survival? Journal of Fish Biology 69 (Supplement A):140–144

O'Malley RE (1991) Singular perturbation methods for ordinary differential equations. Springer-Verlag, New York

Oostermeijer JGB (2000) Population viability analysis of the rare *Gentiana pneumonanthe*: importance of genetics, demography, and reproductive biology. In: Young AG, Clarke GM (eds) Genetics, demography and viability of fragmented populations, Cambridge University Press, Cambridge, pp 313–334

Paukstis GL, Janzen FJ (1990) Sex determination in reptiles: summary of effects of constant temperatures of incubation on sex ratios of offspring. Smithsonian Herpetological Information Service 83:1–28

Pavlova V, Berec L, Boukal DS (2010) Caught between two Allee effects: trade-off between reproduction and predation risk. Journal of Theoretical Biology 264:787–798

Pech R, Hood GM, McIlroy J, Saunders G (1997) Can foxes be controlled by reducing their fertility? Reproduction, Fertility and Development 9:41–50

Perrin N, Mazalov V (2000) Local competition, inbreeding, and the evolution of sex-biased dispersal. American Naturalist 155:116–127

Petrovskii SV, Li BL (2003) An exactly solvable model of population dynamics with density-dependent migrations and the Allee effect. Mathematical Biosciences 186:79–91

Pierce GJ, Ollason JG (1987) Eight reasons why optimal foraging theory is a complete waste of time. Oikos 49:111–125

Preece T, Mao Y (2009) Sustainability of dioecious and hermaphrodite populations on a lattice. Journal of Theoretical Biology 261:336–340

Pulliam HR (1974) On the theory of optimal diets. American Naturalist 108:57–74

Pulliam HR (1975) Diet optimization with nutrient constraints. American Naturalist 109:765–768

Ramesh B, Manickavasagam S (2003) Tradeoff between longevity and fecundity in relation to host availability in a thelytokous oophagous parasitoid, *Trichogramma brasiliensis* Ashmead (Trichogrammatidae: Hymenoptera). Insect Science and Its Application 23:207–210

Raymond B, Vanbergen A, Watt A (2002) Escape from pupal predation as a potential cause of outbreaks of the winter moth, *Operoptera brumata*. Oikos 98:219–228

Rechten C, Krebs JR, Houston AI (1981) Great tits and conveyor belts: a correction for non-random prey distribution. Animal Behaviour 29:1276–1277

Rechten C, Avery M, Stevens A (1983) Optimal prey selection: why do great tits show partial preferences? Animal Behaviour 31:576–584

Rice WR (1983) Sensory modality: an example of its effect on optimal foraging behavior. Ecology 64:403–406

Riley S, Fraser C, Donnelly CA, Ghani AC, Abu-Raddad LJ, Hedley AJ, Leung GM, Ho LM, Lam TH, Thach TQ, Chau P, Chan KP, Lo SV, Leung PY, Tsang T, Ho W, Lee KH, Lau EMC, Ferguson NM, Anderson RM (2003) Transmission dynamics of the etiological agent of SARS in Hong Kong: impact of public health interventions. Science 300:1961–1966

Rodger JC (1997) Likely targets for immunocontraception in marsupials. Reproduction, Fertility and Development 9:131–136

Rogers DJ, Hassell MP (1974) General models for insect parasite and predator searching behaviour: interference. Journal of Animal Ecology 43:239–253

de Roos AM, McCauley E, Wilson WG (1991) Mobility versus density-limited predator-prey dynamics on different spatial scales. Proceedings of the Royal Society B: Biological Sciences 246:117–122

de Roos AM, Persson L, Thieme HR (2003) Emergent Allee effects in top predators feeding on structured prey populations. Proceedings of the Royal Society of London B 270:611–619

Rosenzweig ML (1971) Paradox of enrichment: destabilization of exploitation ecosystems in ecological time. Science 171:385–387

Ross R (1911) Some quantitative studies in epidemiology. Nature 87:466–467

Rowe S, Hutchings JA (2003) Mating systems and the conservation of commercially exploited marine fish. Trends in Ecology & Evolution 18:567–572

Rueffler C, Dooren TJMV, Metz JAJ (2004) Adaptive walks on changing landscapes: Levins' approach extended. Theoretical Population Biology 65:165–178

Ruxton GD (1995) Short term refuge use and stability of predator-prey models. Theoretical Population Biology 47:1–17

Ruxton GD, Gurney WSC, Roos AMD (1992) Interference and generation cycles. Theoretical Population Biology 42:235–253

Saether BE (1986) Life history correlates of promiscuous mating systems: when to be a good father. Oikos 47:125–127

Scheuring I (1999) Allee effect increases the dynamical stability of populations. Journal of Theoretical Biology 199:407–414

Schmidt K (1998) The consequences of partially directed search effort. Evolutionary Ecology 12:263–277

Schmitz OJ (1997) Commemorating 30 years of optimal foraging theory. Evolutionary Ecology 11:631–632

Schmitz OJ, Cohon JL, Rothley KD, Beckerman AP (1998) Reconciling variability and optimal behaviour using multiple criteria in optimization models. Evolutionary Ecology 12:73–94

Schoener TW (1971) Theory of feeding strategies. Annual Review of Ecology and Systematics 11:369–404

Schreiber SJ (2003) Allee effects, extinctions, and chaotic transients in simple population models. Theoretical Population Biology 64:201–209

Schreiber SJ (2004) On Allee effects in structured population. Proceedings of the American Mathematical Society 132:3047–3053

Shi JP, Shivaji R (2006) Persistence in reaction diffusion models with weak Allee effect. Journal of Mathematical Biology 52:807–829

Shuster SM, Wade MJ (2003) Mating systems and strategies. Princeton University Press, Princeton

Simberloff D, Gibbons L (2004) Now you see them, now you don't! - Population crashes of established introduced species. Biological Invasions 6:161–172

Sinclair ARE, Pech RP, Dickman CR, et al (1998) Predicting effects of predation on conservation of endangered prey. Conservation Biology 12:564–575

Skalski GT, Gilliam JF (2001) Functional responses with predator interference: viable alternatives to the Holling type II model. Ecology 82:3083–3092

Smith G, Walmsley A, Polkinghorne I (1997) Plant-derived immunocontraceptive vaccines. Reproduction, Fertility and Development 9:85–89

Solomon ME (1949) The natural control of animal populations. Journal of Animal Ecology 18:1–35

Solomon MG, Cross JV, Fitzgerald JD, et al (2000) Biocontrol of pests of apples and pears in northern and central Europe – 3. Predators. Biocontrol Science and Technology 10:91–128

Stenseth NC (1981) How to control pest species: application of models from the theory of island biogeography in formulating pest control strategies. Journal of Applied Ecology 18:773–794

Stephan T, Wissel C (1994) Stochastic extinction models discrete in time. Ecological Modelling 75/76:183–192

Stephens DW, Charnov EL (1982) Optimal foraging: some simple stochastic models. Behavioral Ecology and Sociobiology 10:251–263

Stephens DW, Krebs JR (1986) Foraging theory. Princeton University Press, Princeton, NJ, USA

Stephens DW, Lynch JF, Sorensen AE, Gordon C (1986) Preference and profitability: theory and experiment. American Naturalist 127:533–553

Stephens PA, Sutherland WJ (1999) Consequences of the Allee effect for behaviour, ecology and conservation. Trends in Ecology & Evolution 14:401–405

Stephens PA, Sutherland WJ, Freckleton R (1999) What is the Allee effect? Oikos 87:185–190

Stillman RA, Goss-Custard JD, Caldow RWG (1997) Modelling interference from basic foraging behaviour. Journal of Animal Ecology 66:692–703

Sun YG, Saker SH (2005) Existence of positive periodic solutions of nonlinear discrete model exhibiting the Allee effect. Applied Mathematics and Computation 168:1086–1097

Svensson GP, Löefsted C, Skals N (2004) The odour makes the difference: male moths attracted by sex pheromones ignore the threat by predatory bats. Oikos 104:91–97

Svensson GP, Löefsted C, Skals N (2007) Listening in pheromone plumes: disruption of olfactory-guided mate attraction in a moth by a bat-like ultrasound. Journal of Insect Science 7(59)

Svensson JE (1992) The influence of visibility and escape ability on sex-specific susceptibility to fish predation in *Eudiaptomus gracilis* (Copepoda, Crustacea). Hydrobiologia 234:143–150

Svensson JE (1997) Fish predation on *Eudiaptomus gracilis* in relation to clutch size, body size, and sex: a field experiment. Hydrobiologia 344:155–161

Tanaka S, Suzuki Y (1998) Physiological trade-off between reproduction, flight capability and longevity in a wing-dimorphic cricket, *Modicogryllus confirmatus*. Journal of Insect Physiology 44:121–129

Taylor CM, Hastings A (2005) Allee effects in biological invasions. Ecology Letters 8:895–908

Taylor CM, Davis HG, Civille JC, Grevstad FS, Hastings A (2004) Consequences of an Allee effect in the invasion of a Pacific estuary by *Spartina alterniflora*. Ecology 85:3254–3266

Thacker JRM (2002) An introduction to arthropod pest control. Cambridge University Press, Cambridge

Thomas F, Teriokhin AT, Renaud F, Meeus TD, Guegan JF (2000) Human longevity at the cost of reproductive success: evidence from global data. Journal of Evolutionary Biology 13:409–414

Tilman D, Lehman CL, Kareiva P (1997) Population dynamics in spatial habitats. In: Tilman D, Kareiva P (eds) Spatial ecology: the role of space in population dynamics and interspecific interactions (Monographs in Population Biology, No 30), Princeton University Press, Princeton, NJ, pp 3–20

Tobin PC, Whitmire SL, Johnson DM, Bjørnstad ON, Liebhold AM (2007) Invasion speed is affected by geographical variation in the strength of Allee effects. Ecology Letters 10:36–43

Tobin PC, Robinet C, Johnson DM, Whitmire SL, Bjørnstad ON, Liebhold AM (2009) The role of Allee effects in gypsy moth, *Lymantria dispar* (L.), invasions. Population Ecology 51:373–384

Tobin PC, Berec L, Liebhold AM (2011) Exploiting Allee effects for managing biological invasions. Ecology Letters 14:615–624

Trochine C, Modenutti B, Balseiro E (2005) When prey mating increases predation risk: the relationship between the flatworm *Mesostoma ehrenbergii* and the copepod *Boeckella gracilis*. Archiv für Hydrobiologie 163:555–569

Tyndale-Biscoe CH (1994) Virus-vectored immunocontraception of feral mammals. Reproduction, Fertility and Development 6:281–287

Veit RR, Lewis MA (1996) Dispersal, population growth, and the Allee effect: dynamics of the house finch invasion of eastern North America. American Naturalist 148:255–274

Vercken E, Kramer AM, Tobin PC, Drake JM (2011) Critical patch size generated by Allee effect in gypsy moth, *Lymantria dispar* (L.). Ecology Letters 14:179–186

Verdier Y, Chaffaux S, Artois M, Boue F (1999) Characterization of sperm antigens for use as a target for immunocontraception in the red fox (*Vulpes vulpes*). Human Reproduction 14:R112

Verdy A (2010) Modulation of predator-prey interactions by the Allee effect. Ecological Modelling 221:1098–1107

Volterra V (1926) Fluctuations in the abundance of a species considered mathematically. Nature 118:558–560

van Voorn GAK, Hemerik L, Boer MP, Kooi BW (2007) Heteroclinic orbits indicate overexploitation in predator-prey systems with a strong Allee effect. Mathematical Biosciences 209:451–469

Waddington K, Holden L (1979) Optimal foraging: on flower selection by bees. American Naturalist 114:179–196

Wang J, Shi J, Wei J (2011) Predator-prey system with strong Allee effect in prey. Journal of Mathematical Biology 62:291–331

Wang MH, Kot M (2001) Speeds of invasion in a model with strong or weak Allee effects. Mathematical Biosciences 171:83–97

Wang MH, Kot M, Neubert MG (2002) Integrodifference equations, Allee effects, and invasions. Journal of Mathematical Biology 44:150–168

Werner EE, Hall DJ (1974) Optimal foraging and the size selection of prey by the bluegill sunfish (*Lepomis macrochirus*). Ecology 55:1042–1052

Wickman PO, Rutowski RL (1999) The evolution of mating dispersion in insects. Oikos 84:463–472

Widén B (1993) Demographic and genetic effects on reproduction as related to population size in a rare, perennial herb, *Senecio integrifolius* (Asteraceae). Biological Journal of the Linnean Society 50:179–195

Wikan A (2001) From chaos to chaos. An analysis of a discrete age-structured prey-predator model. Journal of Mathematical Biology 43:471–500

Willamson M, Fitter A (1996) The varying success of invaders. Ecology 77:1661–1666

Wilson WG, de Roos AM, McCauley E (1993) Spatial instabilities within the diffusive Lotka-Volterra system: individual-based simulation results. Theoretical Population Biology 43:91–127

Winfield IJ, Townsend CR (1983) The cost of copepod reproduction: increased susceptibility to fish predation. Oecologia 60:406–411

Xiao D, Ruan S (2001) Global dynamics of a ratio-dependent predator-prey system. Journal of Mathematical Biology 43:268–290

Yamanaka T (2007) Mating disruption or mass trapping? Numerical simulation analysis of a control strategy for lepidopteran pests. Population Ecology 49:75–86

Zhou J, Hethcote HW (1994) Population size dependent incidence in models for diseases without immunity. Journal of Mathematical Biology 32:809–834

Zuk M, Kolluru GR (1998) Exploitation of sexual signals by predators and parasitoids. Quarterly Review of Biology 73:415–438